ISSN: 2958-8995. 2958-8987
Doi: 10.59799/APPP6605
No:10 Val:1/ December / 2025

Journal of Natural and Applied Sciences URAL

A Quarterly Multidisciplinary Scientific Journal Issued by European Academy for Development and Research / Brussels and Center of Research and Human Resources Development Ramah- Jordan

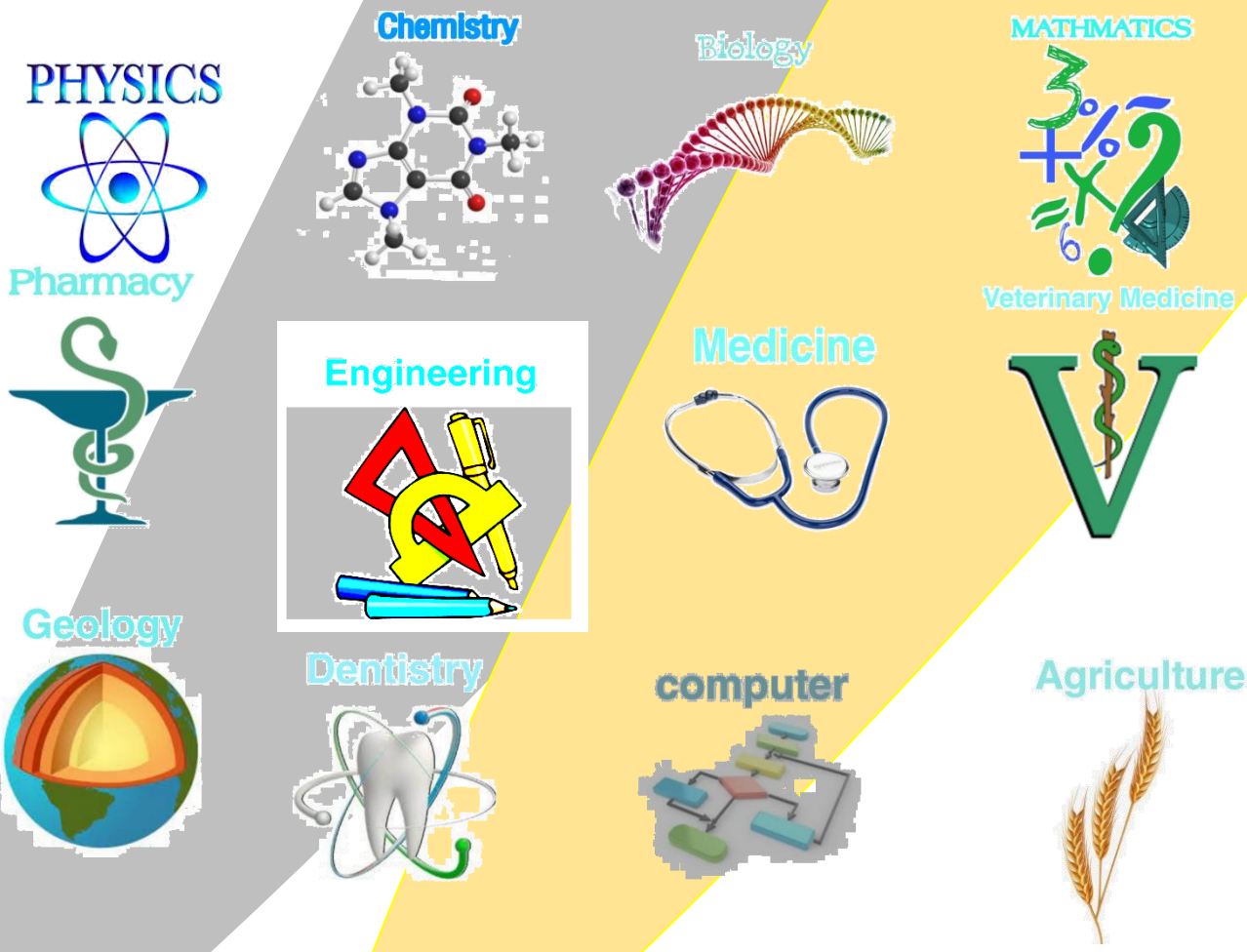

Focus & Scope:

Journal of Natural and Applied Sciences URAL

Journal welcomes high quality contributions investigating topics in the fields of Biology, physics, computer science, Engineering, chemistry, Geology, Agriculture, Medicine, Mathematics, Pharmacy, Veterinary, Nursing, Dentistry, and Environment.

Publication specializations in the journal	
Biology	**Chemistry**
Physics	**Geology**
Computer	**Agriculture**
Engineering	**Mathematics**
Medicine	**Pharmacy**
Veterinary	**Dentistry Veternity,**
Environment	**Nursing**

The Journal is Published in English and Arabic

General Supervisor of the Journal

Prof. Dr. Khalid Ragheb Ahmed Al-Khatib

Head of the Center for Research and Human

Resources Development Ramah – Jordan

Managing Director:

Dr. Mosaddaq Ameen Ateah AL – Doori

Linguistic Reviewer Team

Prof. Dr. Lamiaa Ahmed Rasheed

Tikrit University/College of Education for Women

Asst. Prof. Ahmed Khalid Hasoon

Tikrit University/ College of Education for Women

Asst. Prof. Dr. Mohammad Burjess

Tikrit University/ College of Education

Administrative Title of the Journal:

Amman\ Jordan\ Wasfi Al-Tal \ Gardens

Phone: +962799424774

Index

Solving Multi-Objective Linear Programming Problem by Using Revised Simplex Method and N.S. Advanced Approach

Nejmaddin A. Sulaiman[(1)]

Shaida O. Muhammed[(2)]

1) Department of Mathematics, Faculty of Science , Sulaimani University – Sulaimani, Kurdistan Region,Iraq.

2) Department of Mathematics, College of Education, Salahaddin University – Erbil, Kurdistan Region,Iraq.

*Corresponding author e-mail: shaida.omer88@gmail.com

Solving Multi-Objective Linear Programming Problem by Using Revised Simplex Method and N.S. Advanced Approach

Nejmaddin A. Sulaiman[(1)]

Shaida O. Muhammed[(2)]

1) Department of Mathematics, Faculty of Science , Sulaimani University – Sulaimani, Kurdistan Region,Iraq.

2) Department of Mathematics, College of Education, Salahaddin University – Erbil, Kurdistan Region,Iraq.

*Corresponding author e-mail: shaida.omer88@gmail.com

Abstract

This study introduces a Revised Simplex approach for solving linear programming problems (SLPP) and proposes the S.N. Advanced Technique, which converts multi-objective linear programming problems (MOLPP) into single-objective linear programming problems (SOLPP). An algorithm was developed specifically for the S.N. Advanced Technique to address MOLPPs, and an updated version of Chandra Sen's method was integrated with a new algorithm for solving such problems. The proposed methods were validated through extensive numerical testing, demonstrating their effectiveness and competitiveness compared to existing approaches, highlighting their practicality and efficiency in addressing complex optimization challenges.

Keyword: Revised simplex method , S.N.Advanced technique , Multi objective function.

1. Introduction

Linear programming, first introduced in the late 1940s, has become a fundamental technique for optimization in fields such as economics, engineering, logistics, and communications. The development of the Simplex Method marked a significant milestone, revolutionizing

optimization practices. However, the classical Simplex Method encountered limitations in computational efficiency and numerical stability, particularly for large-scale problems.

To address these challenges, Fiasco and McCormick proposed the Revised Simplex Method (RSM) in 1965 [1]. By 1983, multi-objective optimization (MOO) had been developed as a effective approach to addressing problems which have several objectives. Its principles and applications have been thoroughly investigated [2]. However, MOO is a computational expensive approach and the computational complexity increases with the number of objectives. For the above reasons, numerous solution techniques have been proposed [4] – [15]. RSM was developed to improve the classical simplex algorithm to include more sophisticated characteristics such as the rotational updates and the sparse matrix techniques for large systems without sacrificing the ability to find optimal solutions at polyhedron vertices.

In 2006, a new approach was proposed to transform (MOLPP) problems into (SOLPP) [4]. This was followed by further developments, including the use of mean and median values in 2010 [6]. The research has been carried out to investigate both theoretical and applied aspects of solution methods. Some other methods of solving multi-objective linear programming problems (MOLPP) include Sulaiman and Sadiq proposed Mean and Median Method [4], Sulaiman & Ameen applied Optimal Transformation Technique [7], Harmonic Mean Method introduced by Sulaiman and Mustafa [8], and Nahar and Alimin proposed New Statistical Average Method [10].

As problem sizes increase, shortcomings in solution generation and slower algorithmic convergence become more apparent. To address these problems, this paper proposes an improved transformation strategy for MOLPP. The proposed method is compared with other methods such as Chandra Sen’s method and other transformation methods to show that it is more efficient and simpler.

This paper proposes the use of the Revised Simplex Method to solve MOLPP by converting multi-objective problems into single-objective problems. This approach has been improved over the years, and the most recent contributions are those of Nejmaddin A. Sulaiman and Shaida O. Muhammad in 2024 [18]. The newly suggested S.N. Advanced Transformation Technique provides a very fast solution that can be used for a wide range of problems. Detailed

comparisons, physical interpretations, and data analyses underscore the method's practicality and effectiveness, confirming its potential as a valuable tool for optimization.

2. Multi-Objective Linear Programming Problem (MOLPP)

MOLPP is a branch of numerous criteria decision-making that focuses on mathematical OP where more than one goal function needs to be enhanced at the same time.

Mathematically **(MOLPP)** defined as follow:

$$\text{Max or Min } f_i = C_i^T x$$

Subject to

$$Ax \begin{bmatrix} \leq \\ = \\ \geq \end{bmatrix} B$$

$$x \geq 0$$

$i = 1, \dots, r$ for max. and $i = r+1, \dots, s$ for min.

where $x = \{x_1, x_2, x_3, \dots x_n\}$ of decision variables, P is $a\ (n \times n)$ symmetrical matrix of constants. A is $(m \times n)$ matrix of constants, B = mx1 matrix and $C = 1 \times n$ matrix are n dimensional vectors' of coefficients[6].

3. Shaida, Nejmaddin, Advanced (S. N. Advanced Technique)

(S.N.Advanced) this is one of the new methods that no one has used yet and we are the first to work on it. Therefore,the name advanced is a change in his work and a way forward and the latest way to analyze Multi-Objective Optimization Problem.

The different idea of using this function is that the optimal point is different from the others.

4. Approaches for solving MOLPP

4.1. Sen's, Ch. Method

A multi-objective programming is structured and enhanced subject to shared restraints.

The mathematical representation given as:

Optimize Z= [Max z_1, Max z_2,…,Max z_r,Min z_{r+1},…,Min z_s]

Subject to

$$Ax \begin{bmatrix} \leq \\ = \\ \geq \end{bmatrix} b$$

$$x \geq 0 \qquad \text{.....(*)}$$

In this approach, each objective function must be either maximized or minimized independently using the Simplex method or another technique. This process results in finding the optimal values for each goal function individually as:

$$Z_{\text{optima}} = \{\alpha_1, \alpha_2, \dots, \alpha_s\}$$

The ideal value of the goal function $\alpha_i (i = 1,2, \dots, s)$ may be positive or negative.

These values are combined to create a single goal function by addition (the supreme values) and deducting (the smallest values) for each outcome, then separating each z_i by α_i . The function is expressed as:

$$\text{Max } Z = \sum_{i=1}^{r} \frac{z_i}{|\alpha_i|} - \sum_{i=r+1}^{s} \frac{z_i}{|\alpha_i|}$$

Subject to

$$Ax \begin{bmatrix} \leq \\ = \\ \geq \end{bmatrix} b$$

$$x \geq 0$$

$\alpha_i \neq 0$ for i=1, 2,⋯, s .

where, α_i is the optimum value of ith goal function.

The resulting single-objective optimization problem is then answered using the Revised simplex technique, a technique identified as Chandra Sen's method.

4.2. S. N. Advanced Transformation Approach

A multi-objective linear programming problems can be defined as:

$$\text{Max or Min } [z_1, z_2, \dots, z_s]$$

S. to

$$Ax\{\geq, =, \leq\}b, x \geq 0 \qquad \text{……..(**)}$$

Imagine we optimize each objective function separately and acquire the corresponding values:

$$\text{Max } z_1 = \alpha_1$$

$$\text{Max } z_2 = \alpha_2$$

.
.
.

$$\text{Min } z_{r+1} = \alpha_{r+1}$$

.
.
.

$$\text{Min } z_s = \alpha_s$$

Wherever α_i are the values of goal functions.

We need a combination of different decision criteria to represent the best consensus solution. The identified set of different choice variables can be determined using the following objective function.

Using our transformation algorithm above, we can gain a single goal function like this:

$$\text{Max Z} = \frac{\sum_{i=1}^{r} z_i - \sum_{i=r+1}^{s} z_i}{O_{AT}}$$

Where $O_{AT} = \frac{1}{1/m}$ and

$m = \min\{m_1, m_2, \dots, m_r, m_{r+1}, \dots, m_s\}$; where $m_i = |\alpha_i|$, i=1,…,s

Under the same constraints as outlined in (**).

5. Algorithms

5.1 Algorithm for Chandra Sen's Approach

Step--1: Determine the value of each goal function that needs to be either max. or min.

Step--2: Solve the 1st goal function using Revised simplex technique.

Step--3: Label the optimal value of the 1st objective function $z_1$by α_1.

Step--4: Replication step-2 for i=2,3,…,s .

Step--5: Determine Optimal Z= [Max z_1, Max z_2,…,Max z_r,Min z_{r+1},…,Min z_s].

Step--6: Select Z optima = $\{\alpha_1, \alpha_2, \dots, \alpha_s\}$.

Step--7: Optimize the collective purposes function as:

$$\text{Max Z} = \sum_{i=1}^{r} \frac{z_i}{\alpha_i} - \sum_{i=r+1}^{s} \frac{z_i}{\alpha_i}$$

Below the same restraints by repetition Steps 2 & 3.

5.2 Algorithm for S. N. Advanced Technique

Step--1: Determine the value of individually goal function that needs to be either max. or min.

Step--2: Solve the 1st goal function using RSM.

Step--3: Label the optimal value of the first goal function z_1 by α_1.

Step--4: Replication step-2 for i=2,3,…,s .

Step--5: Choice m=min $\{m_1, m_2, \dots, m_r, m_{r+1}, \dots, m_s\}$, where $m_i = |\alpha_i|$, i=1,…, s

Step--6: Choice m=min $\{m_1, m_2, \dots, m_r, m_{r+1}, \dots, m_s\}$ and calculate $O_{AT} = \frac{1}{1/m}$.

Step--7: Optimize the combined goal function as

$$\text{Max Z} = \frac{\sum_{i=1}^{r} z_i - \sum_{i=r+1}^{s} z_i}{O_{AT}}$$

Below the same restraints by repetition Steps 2 & 3.

5. Example:

Assume the following Multi-Objective Linear Programming problem:

$$\text{Max } Z_1 = 5x_1 + 3x_2$$

$$\text{Max } Z_2 = 9x_1 + 5x_2$$

$$\text{Max } Z_3 = 3x_1 - 4x_2$$

$$\text{Max } Z_4 = 3x_1 + 2x_2$$

Subject to

$$x_1 + x_2 \leq 3$$

$$2x_1 + x_2 \leq 5$$

$$x_1 \leq 2$$

$$x_1 , x_2 \geq 0$$

Solution:

1- The given problematic in the revised simplex method for first objective function form may be expressed by presenting the slack variables s_1, s_2 and s_3 as:

$$\text{Max } Z_1 = 5x_1 + 3x_2$$

Subject to

$$x_1 + x_2 \leq 3$$

$$2x_1 + x_2 \leq 5$$

$$x_1 \leq 2$$

$$x_1 , x_2 \geq 0$$

$$\text{Max } Z = 5x_1 + 3x_2 + 0s_1 + 0s_2 + 0s_3$$

s.t.

$$x_1 + x_2 + s_1 = 3$$

$$2x_1 + x_2 + s_2 = 5$$

$$x_1 + s_3 = 2$$

$$x_1 , x_2 , s_1 , s_2 , s_3 \geq 0$$

And

$$Z - 5x_1 - 3x_2 + 0s_1 + 0s_2 + 0s_3 = 0$$

$$x_1 + x_2 + s_1 = 3$$

$$2x_1 + x_2 + s_2 = 5$$

$$x_1 + s_3 = 2$$

$$x_1 , x_2 , s_1 , s_2 , s_3 \geq 0$$

The constraint equations of the system represented by the following matrix form:

$$\begin{bmatrix} 1 & -5 & -3 & 0 & 0 & 0 \\ 0 & 1 & 1 & 1 & 0 & 0 \\ 0 & 2 & 1 & 0 & 1 & 0 \\ 0 & 1 & 0 & 0 & 0 & 1 \end{bmatrix} * \begin{bmatrix} Z \\ x_1 \\ x_2 \\ s_1 \\ s_2 \\ s_3 \end{bmatrix} = \begin{bmatrix} 0 \\ 3 \\ 5 \\ 2 \end{bmatrix}$$

Determine to first table in Revised simplex method (RSM):

Basic variable	B_0	B_1	B_2	B_3	x_B	x_k	Ratio x_B/x_k	a_1	a_2
Z	1	0	0	0	0	-5	-	-5	-3
s_1	0	1	0	0	3	1	3	1	1
s_2	0	0	1	0	5	2	2.5	2	1
← s_3	0	0	0	1	2	1	2←	1	0

$$Z=(1,0,0,0) * \begin{bmatrix} -5 & -3 \\ 1 & 1 \\ 2 & 1 \\ 1 & 0 \end{bmatrix} = \min\{-5,-3\}=-5$$

Final table in Revised simplex method (RSM):

Basic variable	B_0	B_1	B_2	B_3	x_B	x_k	Ratio x_B/x_k	a_1	a_2
Z	1	3	0	2	13			0	0
x_2	0	1	0	-1	1			0	1
s_2	0	-1	1	-1	0			0	0
← x_1	0	0	0	1	2			1	0

Z=(1,3,0,2) * $\begin{bmatrix} 0 & 0 \\ 0 & 1 \\ 0 & 0 \\ 1 & 0 \end{bmatrix}$ = min{2, 3} $\geq$ 0 . It is optimal solution.

$x_1 = 2$, $x_2 = 1$ and $Z_1=Q_1=13$

Thus Max $Z_1 = 13$ at (2, 1).

- After discovery the value of apiece of individual goal function by using Revised simplex method (RSM), the numerical outcomes are given in **Table 1**.

Table1. Numerical results for given example.

I	Z_i	$x_i(x_1,x_2)$	Q_i	OA_i
1	13	(2,1)	13	13
2	23	(2,1)	23	23
3	6	(2,,0)	6	6
4	8	(2,1)	8	8

Table1

- **Applied Sen's,Ch. Approach of this example :**

By Sen's,Ch. Approach, and by Table 1.

$$\text{Max } Z = \sum_{k=1}^{2} \frac{Z_k}{|Q_k|} - \sum_{k=3}^{4} \frac{Z_k}{|Q_k|}$$

$$\text{Max } Z = \frac{Z_1}{Q_1} + \frac{Z_2}{Q_2} - \frac{Z_3}{Q_3} - \frac{Z_4}{Q_4}$$

$$= \frac{5x1 + 3x2}{13} + \frac{9x1 + 5x2}{23} - \frac{3x1 - 4x2}{6} - \frac{3x_1+2x_2}{8} = 1.64\, x_1 + 0.04\, x_2$$

Using Sen's, Ch. Approach, the structure converts,

Max Z = 1.64 x_1 + 0.04 x_2

Subject to

$x_1 + x_2 \leq 3$

$2x_1 + x_2 \leq 5$

$x_1 \leq 2$

$x_1 , x_2 \geq 0$

Solving by Revised simplex method (RSM):

Max $Z = 1.64x_1 + 0.04x_2 + 0s_1 + 0s_2 + 0s_3$

s.t. $x_1 + x_2 + s_1 = 3$

$2x_1 + x_2 + s_2 = 5$

$x_1 + s_3 = 2$

$x_1 , x_2 , s_1 , s_2 , s_3 \geq 0$

And $Z - 1.64x_1 - 0.04x_2 + 0s_1 + 0s_2 + 0s_3 = 0$

$x_1 + x_2 + s_1 = 3$

$2x_1 + x_2 + s_2 = 5$

$x_1 + s_3 = 2$

$x_1 , x_2 , s_1 , s_2 , s_3 \geq 0$

The system of constraint equations represented in the following matrix form:

$$\begin{bmatrix} 1 & -1.64 & -0.04 & 0 & 0 & 0 \\ 0 & 1 & 1 & 1 & 0 & 0 \\ 0 & 2 & 1 & 0 & 1 & 0 \\ 0 & 1 & 0 & 0 & 0 & 1 \end{bmatrix} * \begin{bmatrix} Z \\ x_1 \\ x_2 \\ s_1 \\ s_2 \\ s_3 \end{bmatrix} = \begin{bmatrix} 0 \\ 3 \\ 5 \\ 2 \end{bmatrix}$$

Determine to first table in Revised simplex method (RSM):

Basic variable	B_0	B_1	B_2	B_3	x_B	x_k	Ratio x_B/x_k	a_1	a_2
Z	1	0	0	0	0	-1.64	-	-1.64	-0.04
s_1	0	1	0	0	3	1	3	1	1
s_2	0	0	1	0	5	2	2.5	2	1
← s_3	0	0	0	1	2	1	2←	1	0

$$Z=(1,0,0,0) * \begin{bmatrix} -1.64 & -0.04 \\ 1 & 1 \\ 2 & 1 \\ 1 & 0 \end{bmatrix} = \min\{-1.64,-0.04\} = -1.64$$

Final table in Revised simplex method (RSM):

Basic variable	B_0	B_1	B_2	B_3	x_B	x_k	Ratio x_B/x_k	a_1	a_2
Z	1	0.04	0	1.6	3.32			0	0
x_2	0	1	0	-1	1			0	1
s_2	0	0	1	-1	0			0	0
← x_1	0	0	0	1	2			1	0

$$Z=(1,0.04,0,1.6) * \begin{bmatrix} 0 & 0 \\ 0 & 1 \\ 0 & 0 \\ 1 & 0 \end{bmatrix} = \min\{1.6, 0.04\} \geq 0 \text{ . It is optimal solution .}$$

Max $Z_{Optimal} = 3.32$ at (2,1)

- **AppliedS.N.Advanced Technique of this example :**

Using proposed Technique , and by Table 1.

m_i =min$|\alpha_i|$ where i=1,…,4

m=min $\{Q_1, Q_2, Q_3, Q_4\}$

m= min $\{13,23,6,8\}$ = 6

$O_{AT} = \frac{1}{1/m} = \frac{1}{1/6} = 6$

Max Z = $\frac{\sum_{i=1}^{4} z_i}{O_{AT}} = \frac{5x1 + 3x2 + 9x1 + 5x2 + 3x1 - 4x2 + 3x1 + 2x2}{6} = 3.33\, x_1 + x_2$

Max Z = 3.33 $x_1 + x_2$

Subject to

$x_1 + x_2 \leq 3$

$2x_1 + x_2 \leq 5$

$x_1 \leq 2$

$x_1 , x_2 \geq 0$

Solving by Revised simplex method (RSM):

Max Z = $3.33x_1 + x_2 + 0s_1 + 0s_2 + 0s_3$

s.t. $x_1 + x_2 + s_1 = 3$

$2x_1 + x_2 + s_2 = 5$

$x_1 + s_3 = 2$

$x_1 , x_2 , s_1 , s_2 , s_3 \geq 0$

And $Z - 3.33x_1 - x_2 + 0s_1 + 0s_2 + 0s_3 = 0$

$x_1 + x_2 + s_1 = 3$

$2x_1 + x_2 + s_2 = 5$

$x_1 + s_3 = 2$

$$x_1 , x_2 , s_1 , s_2 , s_3 \geq 0$$

The system of constraint equations represented in the following matrix form:

$$\begin{bmatrix} 1 & -3.33 & -1 & 0 & 0 & 0 \\ 0 & 1 & 1 & 1 & 0 & 0 \\ 0 & 2 & 1 & 0 & 1 & 0 \\ 0 & 1 & 0 & 0 & 0 & 1 \end{bmatrix} * \begin{bmatrix} Z \\ x_1 \\ x_2 \\ s_1 \\ s_2 \\ s_3 \end{bmatrix} = \begin{bmatrix} 0 \\ 3 \\ 5 \\ 2 \end{bmatrix}$$

Determine to first table in Revised simplex method (RSM):

Basic variable	B_0	B_1	B_2	B_3	x_B	x_k	Ratio x_B/x_k	a_1	a_2
Z	1	0	0	0	0	-3.33	-	-3.33	-1
s_1	0	1	0	0	3	1	3	1	1
s_2	0	0	1	0	5	2	2.5	2	1
← s_3	0	0	0	1	2	1	2←	1	0

$$Z=(1,0,0,0) * \begin{bmatrix} -3.33 & -1 \\ 1 & 1 \\ 2 & 1 \\ 1 & 0 \end{bmatrix} = \min\{-3.33,-1\} = -3.33$$

Final table in Revised simplex method (RSM):

Basic variable	B_0	B_1	B_2	B_3	x_B	x_k	Ratio x_B/x_k	a_1	a_2
Z	1	1	0	2.33	7.66			0	0
x_2	0	1	0	-1	1			0	1
s_2	0	-1	1	-1	0			0	0
← x_1	0	0	0	1	2			1	0

$Z=(1,1,0,2.33) * \begin{bmatrix} 0 & 0 \\ 0 & 1 \\ 0 & 0 \\ 1 & 0 \end{bmatrix} = \min\{2.33, 1\} \geq 0$. It is optimal solution .

Max $Z_{Optimal} = 7.66$ at (2,1)

6. Results:

Because the path to analyzing reservations is very long, we have only emphasized one multi-example, including the oldest and the latest the path in my name is (S.N.Advanced Technique). If we look closely, both approaches become optimal at the same point, but the difference is in the maximum price.

We got very good results with a very clear and beautiful difference between them.

As shown in the **table 2.** below.

7. Results comparation between Chandra Sen's Techniques and S.N.Advanced Technique

Example	Chandra Sen's Techniques	N.S.Advanced Technique
Example	$Z_{opt.} = 3.33$ $x_1 = 2$ $x_2 = 1$	Z opt. = 7.66 $x_1 = 2$ $x_2 = 1$

Table 2

8. Conclusion:

The study revealed that the results from the numerical examples were identical for both the traditional Chandra Sen Techniques and the S.N. Advanced Techniques, as shown in Table 2. However, the results from the S.N. Advanced Techniques were achieved in less time compared to the traditional methods. Therefore, we conclude that the S.N. Advanced Techniques are more efficient for application.

References:

[1] Fiasco, A. & McCormick, B., 1965. Advancements in Computational Techniques for Optimization. Operations Research, 13(4), pp. 589-602.

[2] Sen, C., 1983. A New Approach for Multi Objective Rural Development Planning. The Indian Economic Journal, 30, pp. 91-96.

[3] Sharma, S., 1988. Operation Research. Meerut, India: Kedar Nath Ram Nath BCO.

[4] Sulaiman, N.A. & Sadiq, G.W., 2006. Solving the Linear Multi-Objective Programming Problems: Using Mean and Median Value. Al-Rafiden Journal of Computer Sciences and Mathematics, University of Mosul, 3, pp. 69-83.

[5] Caramia, M. & Dell'Olmo, P., 2008. Multi-Objective Management in Freight Logistics. London: Springer-Verlag.

[6] Sulaiman, N.A. & Salih, A.D., 2010. Using mean and median values to solve linear fraction multi objective programming problem. Zanco Journal for Pure and Applied Science, 22(5). Salahaddin University – Erbil, Iraq.

[7] Sulaiman, N.A. & Hamadameen, 2008. Optimal Transformation Technique to Solve Multi Objective Linear Programming Problem. Journal of Kirkuk University-Scientific Studies, 3, pp. 96-106.

[8] Sulaiman, N.A. & Mustafa, R.B., 2016. Using Harmonic Mean to Solve Multi Objective Linear Programming Problem. American Journal of Operation Research, 6, pp. 25-30.

[9] Sulaiman, N.A., Abdullah, R.M. & Abdull, S.O., 2016. Using Optimal Geometric Average Technique to solve Extreme Point Multi-Objective Quadratic Programming Problem. Journal of Zankoy Sulaimani-Part A, 18, pp. 63-72.

[10] Nahar, S. & Alim, A., 2017. A New Statistical Average Method to Solve Multi Objective Linear Programming Problem. International Journal of Science and Research, 6, pp. 623-629.

[11] Sulaiman, N.A. & Mahmood, Z.M., 2022. A new transformation technique to solve multi-objective linear programming problem TICMA. Zanco Journal for Pure and Applied Science. Salahaddin University – Erbil, Iraq.

[12] Sulaiman, N.A. & Mustafa, R.B., 2016. Transform Extreme Point Multi Objective Linear Programming Problem to Extreme Point Single Objective Linear Programming Problem Using Harmonic Mean. Applied Mathematics, 6, pp. 95-99.

[13] Hamad-Amin, A.O., 2008. An Adaptive Arithmetic Average Transformation Technique for Solving MOOPP. MSc. Thesis, University of Koya, Koya.

[14] Nahar, S. & Alim, A., 2017. A New Statistical Average Method to Solve Multi Objective Linear Programming Problem. International Journal of Science and Research, 6, pp. 623-629.

[15] Sohag, Z.I. & Asadujjaman, M., 2018. A Proposed New Average Method for Solving Multi Objective Linear Programming Problem Using Various Kinds of Mean Technique. Mathematics Letter, 4, pp. 25-33.

[16] Sen, C., 2018. Sen's Multi Objective Programming Method and Comparison with Other Techniques. American Journal of Operation Research, 8, pp. 10-13.

[17] Yesmin, M. & Alim, M.A., 2021. Advanced transformation technique to solve multi-objective optimization problem. American Journal of Operation Research, 11, pp.166-180.

[18] Nejmaddin A. Sulaiman and Shaida O. Muhammed. (2024) 'Comparison between revised simplex and usual simplex methods for solving linear programming problems', *Journal of Computational Analysis and Applications*, 33(6), pp. 899-905.

[19] Suleiman, N.A. and Nawkhass, M.A. (2013) 'Transforming and solving multi-objective quadratic fractional programming problems by optimal average of maximin & minimax techniques', American Journal of Operational Research, 3(3), pp. 92-98.

Neutrosophic Hybrid Weibull Inverse Weibull distribution: Mathematical Properties with simulation and Neutrosophic Real Data Application

Kamal N. Abdullah[1]
Mundher A. Khaleel [2]
[1,1] Mathematics Departments, College of Computer Science and Mathematics, Tikrit University, Iraq
[1,2] Mathematics Departments, College of Computer Science and Mathematics, Tikrit University, Iraq
[1,1] kn230022pcm@st.tu.edu.iq

[1,2] mun880088@tu.edu.iq

Neutrosophic Hybrid Weibull Inverse Weibull distribution: Mathematical Properties with simulation and Neutrosophic Real Data Application

Kamal N. Abdullah[1]
, Mundher A. Khaleel [2]
[1,1] Mathematics Departments, College of Computer Science and Mathematics, Tikrit University, Iraq
[1,2] Mathematics Departments, College of Computer Science and Mathematics, Tikrit University, Iraq
[1,1] kn230022pcm@st.tu.edu.iq [1,2] mun880088@tu.edu.iq

Abstract:

This study is concerned with finding a statistical distribution that deals with a Neutrosophic random variable and Neutrosophic parameters called Neutrosophic Hybrid Weibull Inverse Weibull (NHWIW) distribution. The basic functions of proposed distribution are found, as well as many statistical properties of distribution with an estimation of the model parameters in three different techniques, with a Monte Carlo simulation to determine the estimation efficiency of NHWIW distribution, with a comparison with three measures to determine the best method for estimation. A practical application is also conducted on two types of Neutrosophic real data, the first represented by mortality data for children under five years of age, and the second is COVID-19 in Netherlands for thirty days, where the analysis efficiency of the NHWIW distribution is determined by comparing it with six other distributions using 4 information criteria and 4 statistical measures, which showed the efficiency and flexibility of NHWIW distribution.

Keywords: HWG-family, Neutrosophic data, Bias, Cramér-von Mises, and flexibility.

1. Introduction:

Probability distributions are a fundamental tool in statistical modeling used to describe and analyze various phenomena in many fields. One of the most prominent methods recently developed to expand the scope of basic distributions is the T-X method, which provides a flexible framework for creating new distributions with improved mathematical properties, making them more accurate in representing real-world data. The methods is based on forming a family of complex distributions using transformation functions, which contributes to enhancing the flexibility and ability to deal with complex properties, such as heterogeneous or asymmetrically distributed data [1]. Examples of this method include: BIIIEE-X family [2], NOGEE−G family [3], WEE-X Family [4], OLG family [5], NGOF-G Family [6], EOIW-G Family [7], GOM-G family [8], and HOE-Φ family [9]. This study based on HWG family which was has a CDF function by form [10]:

$$F_{HWG}(x,a,b,\zeta) = 1 - e^{\left(-a\left[-\mathcal{G}(x;\varepsilon).log\left(1-\mathcal{G}(x;\varepsilon)\right)\right]^{b}\right)}, \qquad x \geq 0, a, b > 0 \tag{1}$$

And PDF function by form:

$$f_{HWG}(x,a,b,\zeta) = ab\ g(x;\varepsilon)\left[\frac{\mathcal{G}(x;\varepsilon)}{1-\mathcal{G}(x;\varepsilon)} - log\left(1-\mathcal{G}(x;\varepsilon)\right)\right] \tag{2}$$

$$\times\left[-\mathcal{G}(x;\varepsilon).log\left(1-\mathcal{G}(x;\varepsilon)\right)\right]^{b-1}e^{\left(-a\left[-\mathcal{G}(x;\varepsilon).log\left(1-\mathcal{G}(x,\varepsilon)\right)\right]^{b}\right)}$$

Where $\mathcal{G}(x;\varepsilon)$, and $g(x;\varepsilon)$ are CDF and PDF functions for any baseline distribution and $a,b \geq 0$ are shapes parameters for HWG family.

On other hand, the Neutrosophic logic (N.L) is a recent development in the field of fuzzy and uncertain data analysis. This logic aims to address ambiguity and uncertainty in data by introducing three main dimensions: Truth (T), falsehood (F), and indeterminacy (I). this framework provides an effective way to model data that cannot be conclusively characterized using traditional methods. There are two types of N.L: the traditional method, in which the data is divided into three parts and then dealt with by using, for example, the triangular function, in which the peaks represent the T values and the troughs represent F values and what is an between represents I values, or trapezoidal function in the same manner. As for the second method, which depends on the values of intervals and contains all parts of N.L, which called the direct method, and it's the method used in forming the proposed distribution.

Focuses on finding a statistical distribution that deals with a Neutrosophic variables and parameters. The main gap is the lack of previous research that integrates Neutrosophic data with complex distributions such as a distribution based on a hybrid family of Weibull distribution and a hybrid integral limit. Existing studies often focus on traditional data or on specific distributions without considering Neutrosophic data of an uncertain or ambiguous nature. The aim of the study is to develop a " Neutrosophic Hybrid Weibull Inverse Weibull" and test its efficiency and flexibility on real Neutrosophic data using multiple estimation methods, and compare with other distributions to determine the efficiency and flexibility in dealing with Neutrosophic data.

2. Neutrosophic Hybrid Weibull Inverse Weibull (NHWIW) distribution

Let X be a random variable, then the CDF and PDF functions for Inverse Weibull distribution has a forms [11]:

$$\mathcal{G}(x;q,p) = e^{-qx^{-p}} \quad ,q,p,x>0 \tag{3}$$

$$g(x;q,p) = qpx^{-(p+1)}e^{-qx^{-p}} \quad ,q,p,x>0 \tag{4}$$

Where q,p are shape parameters for Inverse Weibull distribution.

To get the CDF function for Hybrid Weibull Inverse Weibull we combine equation (1) with equation (3) by form:

$$F(x) = 1-e^{\left(-a\left[-e^{-qx^{-p}}.log\left(1-e^{-qx^{-p}}\right)\right]^{b}\right)}, \qquad x\ a,b,q,p>0 \tag{5}$$

The PDF function for Hybrid Weibull Inverse Weibull (HWIW) we combine equation (2) with equation (3) and (4) to get it by form:

$$f(x) = ab\ qpx^{-(p+1)}e^{-qx^{-p}}\left[\frac{e^{-qx^{-p}}}{1-e^{-qx^{-p}}}-log\left(1-e^{-qx^{-p}}\right)\right] \times\left[-e^{-qx^{-p}}.log\left(1-e^{-qx^{-p}}\right)\right]^{b-1}e^{\left(-a\left[-e^{-qx^{-p}}.log\left(1-e^{-qx^{-p}}\right)\right]^{b}\right)} \tag{6}$$

In order to integrate the HWIW distribution with N.L, the random variable and parameters of HWIW distribution are converted to Neutrosophic random variable and Neutrosophic parameters as follows:

Let $X_N = d+tI,\ tI\in[X_L,X_U]$, where X_L, X_U are lower and upper values of the neutrosophic random variable having determined part d and indeterminate part tI, $tI\in[I_L,I_U]$.

Note that the NHWIW distribution reduces to classical HWIW distribution when $X_L = X_U$. The neutrosophic cumulative density function (NCDF) of NHWIW has a Neutrosophic shape parameters $a_N \in [a_L, a_U]$, $b_N \in [b_L, b_U]$, $q_N \in [q_L, q_U]$, and $p_N \in [p_L, p_U]$, has the form:

$$F(x_N) = 1 - e^{\left(-a_N\left[-e^{-q_N x_N^{-p_N}}.log\left(1-e^{-q_N x_N^{-p_N}}\right)\right]^{b_N}\right)}, \qquad x_N\, a_N, b_N, q_N, p_N > 0 \tag{7}$$

To obtain the nature of NCDF, the function is plotted with different intervals of parameters and in 2-dimentional and 3-dimensional forms as follows:

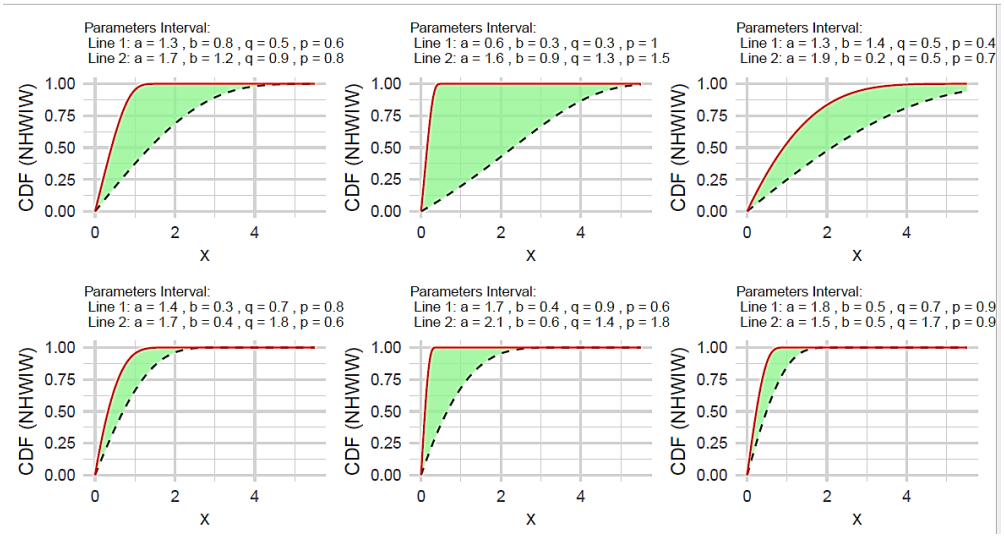

Figure 1. plot of NCDF for NHWIW distribution

And the probability density function (NCDF) of NHWIW has a form:

$$f(x_N) = q_N p_N x_N^{-(p_N+1)} e^{-q_N x_N^{-p_N}} \left[\frac{e^{-q_N x_N^{-p_N}}}{1-e^{-q_N x_N^{-p_N}}} - log\left(1-e^{-q_N x_N^{-p_N}}\right)\right]$$
$$\times\left[-e^{-q_N x_N^{-p_N}}.log\left(1-e^{-q_N x_N^{-p_N}}\right)\right]^{b_N-1} e^{\left(-a_N\left[-e^{-q_N x_N^{-p_N}}.log\left(1-e^{-q_N x_N^{-p_N}}\right)\right]^{b_N}\right)} \tag{8}$$

To obtain the nature of NCDF, the function is plotted with different intervals of parameters and in 2-dimentional and 3-dimensional forms as follows:

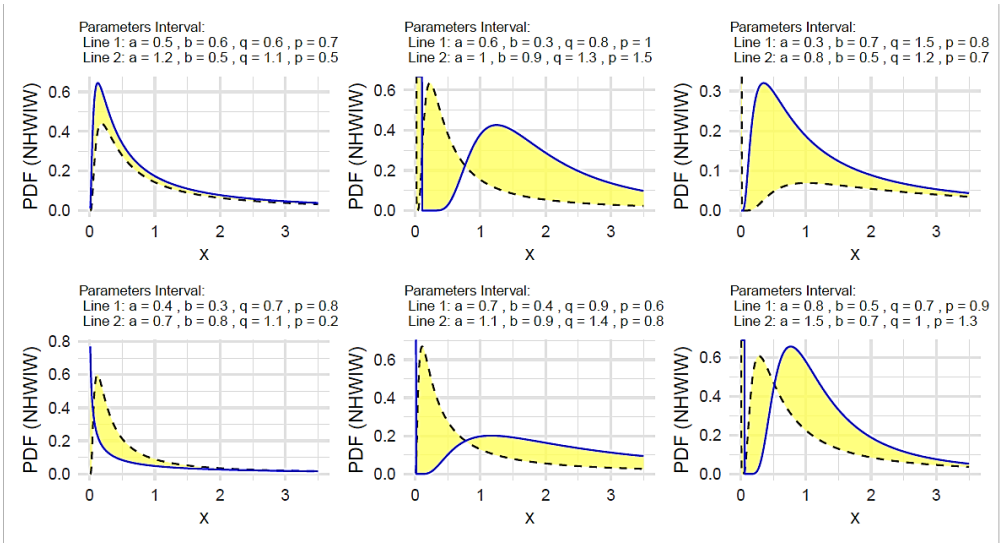

Figure 2. plot of NPDF for NHWIW distribution

While the survival function foe NHWIW distribution given by formula [12]:

$$S(x_N) = e^{\left(-a_N\left[-e^{-q_N x_N^{-p_N}}.log\left(1-e^{-q_N x_N^{-p_N}}\right)\right]^{b_N}\right)} \quad (9)$$

And the hazard function has a formula:

$$h(x_N) = \frac{q_N p_N x_N^{-(p_N+1)} e^{-q_N x_N^{-p_N}} \left[\frac{e^{-q_N x_N^{-p_N}}}{1-e^{-q_N x_N^{-p_N}}} - log\left(1-e^{-q_N x_N^{-p_N}}\right)\right]}{\left[-e^{-q_N x_N^{-p_N}}.log\left(1-e^{-q_N x_N^{-p_N}}\right)\right]^{1-b_N}} \quad (10)$$

3. Properties for NHWIW distribution

In this section we will prove some statistical properties for NHWIW distribution, and show what changing of classical IW distribution.

3.1 NCDF and NPDF expansion

Due to the difficulty of NCDF and NPDF functions in equations (7) and (8) respectively, these functions are simplified in order to simplify the proof of NHWIW distribution properties. This is done using binomial expansion, the exponential function expansion, and the logarithm expansion. Therefore, the simplified NCDF function is obtained as follows:

$$F(x_N) = 1 - \psi\left(e^{-q_N x_N^{-p_N}}\right)^{j+2ib_N} \quad (11)$$

Where $\psi = \sum_{i=j=0}^{\infty} \frac{(-1)^{i+ib_N+j}}{i!} a_N{}^i d_{ib_N,j}$, and

$d_{ib_N,j} = j^{-1}\sum_{m=1}^{j} \frac{m(ib_N+1)-j}{m+1}$ $for\ j \geq 0\ and\ d_{ib_N,0} = 1$

By same way we can expansion NPDF function to get a form:

$$f(x_N) = Mx_N^{-(p_N+1)} e^{-(2ib_N+2b_N+j+k)q_N x_N^{-p_N}} - Nx_N^{-(p_N+1)} e^{-(2ib_N+2b_N+j+z)q_N x_N^{-p_N}} \quad (12)$$

Where $M = \sum_{i=j=k=0}^{\infty} \frac{(-1)^{i+ib_N+b_N-1+j+k}}{i!} a_N{}^{i+1} d_{ib_N+b_N-1,j}\, b_N\, q_N p_N$

And $N = \sum_{i=j=z=0}^{\infty} \frac{(-1)^{i+ib_N+b_N-1+j}}{i!} a_N{}^{i+1} d_{ib_N+b_N-1,j} d_{1,z}\, b_N\, q_N p_N$

As $d_{1,z} = z^{-1}\sum_{m=1}^{j}\frac{2m-j}{m+1} \quad for\ z \geq 0 \quad and\ d_{1,0} = 1$ and

$d_{ib_{N+}b_N-1,j} = j^{-1}\sum_{m=1}^{j}\frac{m(ib_{N+}b_N)-j}{m+1} \quad for\ j \geq 0 \quad and\ d_{ib_{N+}b_N-1,0} = 1$

3.2 Moment

Let X_N be any Neutrosophic random variable, then the n^{th} moment for NHWIW distribution is given by form [13], [14], [15], [16]

$$\mu_n = E(x_N^n)_{NHWIW} = \int_{-\infty}^{\infty} x_N^n f(x_N) dx_N \tag{13}$$

By putting equation (12) in equation (13) we have got a form:

$$\mu_n = \mathrm{M}\int_0^{\infty} \mathrm{x_N}^{n-(p_N+1)} \mathrm{e}^{-(2ib_{N+}2b_N+j+k)q_N x_N^{-p_N}} - N\int_0^{\infty} x_N^{n-(p_N+1)} e^{-(2ib_{N+}2b_N+j+z)q_N x_N^{-p_N}}\, dx_N$$

To get a final form:

$$\mu_n = \frac{\Gamma\left(\frac{n-p_N}{p_N}\right)}{p_N q_N^{\frac{n-p_N}{p_N}}}\left[\frac{M}{(2ib_{N+}2b_N+j+k)^{\frac{n-p_N}{p_N}}} - \frac{N}{(2ib_{N+}2b_N+j+z)^{\frac{n-p_N}{p_N}}}\right] \tag{14}$$

The first four moments are found by substituting the value of n and as follows:

$$\mu_1 = \frac{\Gamma\left(\frac{1-p_N}{p_N}\right)}{p_N q_N^{\frac{1-p_N}{p_N}}}\left[\frac{M}{(2ib_{N+}2b_N+j+k)^{\frac{1-p_N}{p_N}}} - \frac{N}{(2ib_{N+}2b_N+j+z)^{\frac{1-p_N}{p_N}}}\right] \tag{15}$$

$$\mu_2 = \frac{\Gamma\left(\frac{2-p_N}{p_N}\right)}{p_N q_N^{\frac{2-p_N}{p_N}}}\left[\frac{M}{(2ib_{N+}2b_N+j+k)^{\frac{2-p_N}{p_N}}} - \frac{N}{(2ib_{N+}2b_N+j+z)^{\frac{2-p_N}{p_N}}}\right] \tag{16}$$

$$\mu_3 = \frac{\Gamma\left(\frac{3-p_N}{p_N}\right)}{p_N q_N^{\frac{3-p_N}{p_N}}}\left[\frac{M}{(2ib_{N+}2b_N+j+k)^{\frac{3-p_N}{p_N}}} - \frac{N}{(2ib_{N+}2b_N+j+z)^{\frac{3-p_N}{p_N}}}\right] \tag{17}$$

$$\mu_4 = \frac{\Gamma\left(\frac{4-p_N}{p_N}\right)}{p_N q_N^{\frac{4-p_N}{p_N}}}\left[\frac{M}{(2ib_{N+}2b_N+j+k)^{\frac{4-p_N}{p_N}}} - \frac{N}{(2ib_{N+}2b_N+j+z)^{\frac{4-p_N}{p_N}}}\right] \tag{18}$$

From it, we can obtain the skewness and Kurtosis of NHWIW distribution respectively as follows [16]:

$$SK_{NHWIW} = \frac{\frac{\Gamma\left(\frac{3-p_N}{p_N}\right)}{p_N q_N^{\frac{3-p_N}{p_N}}}\left[\frac{M}{(2ib_{N+}2b_N+j+k)^{\frac{3-p_N}{p_N}}} - \frac{N}{(2ib_{N+}2b_N+j+z)^{\frac{3-p_N}{p_N}}}\right]}{\left(\frac{\Gamma\left(\frac{2-p_N}{p_N}\right)}{p_N q_N^{\frac{2-p_N}{p_N}}}\left[\frac{M}{(2ib_{N+}2b_N+j+k)^{\frac{2-p_N}{p_N}}} - \frac{N}{(2ib_{N+}2b_N+j+z)^{\frac{2-p_N}{p_N}}}\right]\right)^{\frac{3}{2}}} \tag{19}$$

$$KU_{NHWIW} = \frac{\frac{\Gamma\left(\frac{4-p_N}{p_N}\right)}{p_N q_N^{\frac{4-p_N}{p_N}}}\left[\frac{M}{(2ib_{N+}2b_N+j+k)^{\frac{4-p_N}{p_N}}} - \frac{N}{(2ib_{N+}2b_N+j+z)^{\frac{4-p_N}{p_N}}}\right]}{\left(\frac{\Gamma\left(\frac{2-p_N}{p_N}\right)}{p_N q_N^{\frac{2-p_N}{p_N}}}\left[\frac{M}{(2ib_{N+}2b_N+j+k)^{\frac{2-p_N}{p_N}}} - \frac{N}{(2ib_{N+}2b_N+j+z)^{\frac{2-p_N}{p_N}}}\right]\right)^{2}} - 3 \tag{20}$$

To know the change in the moments of NHWIW distribution with change in intervals of Neutrosophic parameters, table 1 shows a set of moments with variance, skewness, and Kurtosis as follows:

Table.*1* some intervals of moments for NHWIW

a_N	b_N	q_N	p_N	$\grave{\mu}_{1\,N}$	$\grave{\mu}_{2\,N}$	$\grave{\mu}_{3\,N}$	$\grave{\mu}_{4\,N}$	σ_N^2	S_N	K_N
[1.8,2.8]	[1.6,2.6]	[1.4, 2.4]	[1.1,2.1]	[2.146064, 2.857927]	[4.723157, 10.57421]	[10.64869, 52.02946]	[24.5692,354.4007]	[0.117566, 2.406463]	[1.037403, 1.513134]	[1.101352, 3.169558]
			[1.2,2.2]	[2.0717, 2.593549]	[4.391856, 8.343002]	[9.518114, 33.94803]	[21.06914, 179.7407]	[0.099915, 1.616506]	[1.034139, 1.408741]	[1.092322, 2.58227]
		[1.6, 2.6]	[1.3,2.3]	[2.077192, 2.651157]	[4.406707, 8.434903]	[9.540035, 32.68622]	[21.05919, 157.4864]	[0.09198,1.40627]	[1.031285, 1.334273]	[1.084459, 2.213517]
			[1.4,2.4]	[2.014016, 2.458261]	[4.135742, 7.066473]	[8.652692, 24.02667]	[18.43118, 98.13544]	[0.079482, 1.023426]	[1.028777, 1.279056]	[1.077572, 1.965262]
	[1.9,2.9]]	[1.8, 2.8]	[1.5,2.5]	[2.047589, 2.552581]	[4.257436, 7.198049]	[8.983496, 22.42205]	[19.22557, 77.17473]	[0.064815, 0.682379]	[1.022641, 1.161056]	[1.060677, 1.489517]
			[1.6,2.6]	[1.991347, 2.400354]	[4.022199, 6.28886]	[8.235853, 17.98276]	[17.08652, 56.13042]	[0.056736, 0.527161]	[1.020971, 1.140246]	[1.056152, 1.419235]
		[1.9,2.9]	[1.7,2.7]	[1.966076, 2.347823]	[3.916789, 5.956809]	[7.902665, 16.33094]	[16.14081, 48.38371]	[0.051334, 0.444536]	[1.019479, 1.123287]	[1.052119, 1.363552]
			[1.8,2.8]	[1.894836, 2.153215]	[3.634783, 5.001715]	[7.055468, 12.54589]	[13.85253, 34.02125]	[0.04438,0.36538]	[1.018141, 1.121561]	[1.048509, 1.359917]

Table 1 presents the different values of statistical moments (mean, variance, skewness, kurtosis) for the NHWIW distribution with changes in the upper and lower boundary parameters of the unspecified variables. The values show that the moments of the distribution change significantly when the boundaries are modified. Skewness and kurtosis are used to assess the shape of the distribution. The mean expresses the expected center of the distribution and changes with the variation of the ambiguous parameters. The variance. High values indicate that the distribution can handle disparate and scattered data, while it indicates the level of concentration in the values. Low values indicate that the distribution can handle data with a wide range. Low values indicate that the distribution is balanced, which enhances its suitability to realistic data.

3.3 Moment Generating Function

Let X_N be any Neutrosophic random variable, then the Moment Generating Function (MGF) for NHWIW distribution is given by form [17] , [18] :

$$M_x(t) = E(e^{tx}) = \int_{-\infty}^{\infty} e^{tx} f(x_N) dx$$

From equation (14) and using exponential expansion we get a final form:

$$M_x(t) = \sum_{r=0}^{\infty} \frac{t^r}{r!} \left[\frac{\Gamma(\frac{n-p_N}{p_N})}{p_N q_N^{\frac{n-p_N}{p_N}}} \left[\frac{M}{(2ib_N+2b_N+j+k)^{\frac{n-p_N}{p_N}}} - \frac{N}{(2ib_N+2b_N+j+z)^{\frac{n-p_N}{p_N}}} \right] \right] \quad (21)$$

3.4 Quantile function of NHWIW distribution

The Quantile function has a major role in application of Monte Carlo simulation and represents the inverse of NCDF function $Q(u) = F^{-1}(u)$ [19], which is obtained for the NHWIW distribution as follows:

$$Q(u) = \left[\frac{log\left[\frac{\Theta}{(\Theta + W_{-1}(\Theta) e^{\Theta})}\right]}{q_N} \right]^{\frac{-1}{b_N}}, \Theta = \left[\frac{-log(1-u)}{a_N} \right]^{\frac{1}{b_N}} \quad (22)$$

Table 2 expresses a set of intervals of the Quintile function values of NHWIW for different intervals as follow:

Table 2: Quintile function values of NHWIW for different intervals

s_N	(a_N, b_N, q_N, p_N)				
	[0.4, 0.8],[1.1, 1.9] [0.4, 1.4],[1.2, 1.7]	[0.6, 1.6],[1, 1.5] [0.4, 1.4],[1, 1.5]	[0.5,1.5],[1.1.1,6] [0.51.5],[1.1,1.6]	[1.2,1.7],[1,1.5] [0.8,1.8],[1.2,1.7]	[1.1,1.7],[1.9,1.9] [0.7,1.7],[1.5,2]
0.1	[0.5880204,1.50829]	[0.407121, 1.194348]	[0.622559, 1.33252]	[0.669702, 3.3304]	[0.9420654, 3.28916]
0.2	[0.8511505,1.75326]	[0.6020268, 1.40746]	[0.898051, 1.54565]	[0.86103, 1.38635]	[1.1027903, 1.56190]
0.3	[1.1616532, 1.95887]	[0.8308531, 1.59006]	[1.214072, 1.72384]	[1.047516, 1.5928]	[1.2370894, 1.68682]
0.4	[1.5748618, 2.15671]	[1.1324191, 1.76916]	[1.621220, 1.89484]	[1.253187, 1.7644]	[1.3657090, 1.80121]
0.5	[2.1794962, 2.36248]	[1.5680264, 1.95911]	[2.07237,2.194616]	[1.499006, 1.9283]	[1.4988826, 1.91481]
0.6	[2.590992,3.165274]	[2.174631,2.267291]	[2.26927,3.086756]	[1.816802, 2.0979]	[1.6459544, 2.03529]
0.7	[2.863979,5.033473]	[2.43857,3.5705340]	[2.50435,4.680039]	[2.270645, 2.2853]	[1.8204959, 2.17226]
0.8	[3.226530,9.576866]	[2.800418,6.695981]	[2.816750,8.25737]	[2.50855,3.02963]	[2.0505678, 2.34410]
0.9	[3.821119,28.62166]	[3.423055,19.87242]	[3.33042,21.51546]	[2.80425,4.80523]	[2.4236659, 2.60524]

Table 2 presents the values of the quantile function for the NHWIW distribution for different probability intervals. The different values reflect changes in the range of the data distribution based on the probability. Narrower intervals show greater accuracy in representing the data, while wider intervals reflect greater flexibility. Small values indicate the distribution's ability to provide accurate boundaries for the intervals.

3.5 Renyi entropy

The Renyi entropy is given by form [20], [21] :

$$I_R(c)_{NHWIW} = \frac{1}{1-c} log \int_0^{\infty} f(x_N)^c dx$$

$$I_R(c)_{NHWIW} = \frac{1}{1-c} log \int_0^{\infty} (M x_N^{-(p_N+1)} e^{-(2ib_{N+}2b_N+j+k)q_N x_N^{-p_N}} - N x_N^{-(p_N+1)} e^{-(2ib_{N+}2b_N+j+z)q_N x_N^{-p_N}})^c dx$$

Then the final form:

$$II_R(c)_{NHWIW} = \frac{1}{1-c} \log\left[R.\Gamma\left(\frac{1-c(p_N+1)}{p_N}\right)\right]$$

$$R = \sum_{n=0}^{c} (-1)^n \binom{c}{n} M^{c-n} N^n \frac{1}{p_N q^{\frac{-c(p_N+1)}{p_N}+\frac{1}{p_N}} (2ic b_{N+} 2cb_N + cj + ck - nk + nz)^{\frac{-c(p_N+1)}{p_N}+\frac{1}{p_N}}} \quad (23)$$

4. Estimation

4.1maximum likelihood estimation

The NHWIW distribution parameters are determine using maximum likelihood estimation approach. For sample $x_{N_1}, x_{N_2}, \dots, x_{N_m}$ the random sample [22], [23], [24], [25], [26] The NHWIW distribution NPDF is followed:

$$L(\theta_N, x_{N_i}) = \prod_{i=1}^{m} q_N p_N x_{N_i}^{-(p_N+1)} e^{-q_N x_{N_i}^{-p_N}} \left[\frac{e^{-q_N x_{N_i}^{-p_N}}}{1-e^{-q_N x_{N_i}^{-p_N}}} - log\left(1-e^{-q_N x_{N_i}^{-p_N}}\right)\right]$$

$$\times \left[-e^{-q_N x_{N_i}^{-p_N}} . log\left(1-e^{-q_N x_{N_i}^{-p_N}}\right)\right]^{b_N-1} e^{\left(-a_N\left[-e^{-q_N x_{N_i}^{-p_N}} . log\left(1-e^{-q_N x_{N_i}^{-p_N}}\right)\right]^{b_N}\right)}$$

we compute the log- likelihood:

$$L = mlog(q_N) + mlog(p_N) - (p_N - 1)\sum_{i=1}^{m} \log(x_{N_i}) - \sum_{i=1}^{m} q_N x_{N_i}^{-p_N}$$

$$+ \sum_{i=1}^{m} \log\left[\frac{e^{-q_N x_{N_i}^{-p_N}}}{1-e^{-q_N x_{N_i}^{-p_N}}} - log\left(1-e^{-q_N x_{N_i}^{-p_N}}\right)\right]$$

$$+ (b_N - 1)\sum_{i=1}^{m} \log\left[-e^{-q_N x_{N_i}^{-p_N}} . log\left(1-e^{-q_N x_{N_i}^{-p_N}}\right)\right] \quad (24)$$

$$-a_N \sum_{i=1}^{m} \left[-e^{-q_N x_{N_i}^{-p_N}} . log\left(1-e^{-q_N x_{N_i}^{-p_N}}\right)\right]^{b_N}$$

4.2Least square estimation

The following formula can be used to estimate a parameters using the Least square estimation (LSE) method [27], [28]:

$$\varphi(\theta_N) = \sum_{i=1}^{m}\left[1 - e^{\left(-a_N\left[-e^{-q_N x_{N_i}^{-p_N}}.log\left(1-e^{-q_N x_{N_i}^{-p_N}}\right)\right]^{b_N}\right)} - \frac{1}{n+1}\right]^2 \quad (25)$$

4.3Weighted Least square estimation

The following formula can be used to estimate a parameters using the Weighted Least square estimation (WLSE) method [29]:

$$W(\theta_N) = \sum_{i=1}^{m}\frac{(n+1)^2(n+2)}{i(n-i+1)}\left[1 - e^{\left(-a_N\left[-e^{-q_N x_{N_i}^{-p_N}}.log\left(1-e^{-q_N x_{N_i}^{-p_N}}\right)\right]^{b_N}\right)} - \frac{i}{n+1}\right]^2 \quad (26)$$

Estimates of the parameters for the three previously described methods may be obtained by finding the partial derivative of four parameters and setting it to zero. Computer technologies such as the R language are used since it is difficult to find these values in numerical solutions.

5. Simulation

To demonstrate the efficieny of the estimation of NHWIW distribution, a Monte Carlo simulation is conducted for the three methods presented in a fourth section, where the sizes of generated samples were relied upon at n=50, 100, 150, and 200, to 1000 with the calculation of the values of mean square error (MSE), and its root (RMSE) [30], and the calculation of the bias in the estimated parameters, where Table 3 shows the simulation values as follows:

Table 3 : Monte Carlo simulations conducted for the NHWIW

$r_N = [0.4,1.4]$, $u_N = [0.5,1.5]$, $b_N = [0.7,1.7]$, $c_N = [0.8,1.8]$					
N	**Est.**	**Ess. Par.**	**MLE**	**LSE**	**WLSE**
50	**Mean**	$\widehat{a_N}$	[2.71415, 3.8807]	[1.81833, 2.2308]	[2.18454, 2.62480]
		$\widehat{b_N}$	[2.14886, 3.4619]	[2.00585, 2.14894]	[2.28999, 2.41772]
		$\widehat{q_N}$	[1.98333, 2.030004]	[1.68494, 2.65528]	[1.49501, 2.36023]
		$\widehat{p_N}$	[1.78887, 2.01288]	[1.74966, 2.63342]	[1.46794, 2.40224]
	MSE	$\widehat{a_N}$	[22.2105,25.1223]	[1.40892, 1.91622]	[2.77863, 3.67925]
		$\widehat{b_N}$	[2.20026, 5.72680]	[0.44948,1.0952]	[0.98082,1.91795]
		$\widehat{q_N}$	[3.88680, 5.14601]	[0.96725, 2.38973]	[1.04593, 2.03972]
		$\widehat{p_N}$	[1.26702, 2.03484]	[0.96801, 1.11202]	[0.64689, 0.95739]
	RMSE	$\widehat{a_N}$	[4.7128,5.01222]	[1.18698, 1.38427]	[1.66692, 1.91813]
		$\widehat{b_N}$	[1.48332, 2.3930]	[0.67043,1.04654]	[0.99036,1.38490]
		$\widehat{q_N}$	[1.97149, 2.26848]	[0.98348, 1.54587]	[1.02270, 1.42818]
		$\widehat{p_N}$	[1.12562, 1.42648]	[0.98387, 1.05452]	[0.80430, 0.97846]
	Bias	$\widehat{a_N}$	[1.314151, 1.9807]	[0.33082,0.41833]	[0.72480,0.78454]
		$\widehat{b_N}$	[0.64886, 1.4619]	[0.14894,0.50585]	[0.41772,0.78999]
		$\widehat{q_N}$	[0.26999,0.28333]	[0.015057, 0.35528]	[0.06023,0.20498]
		$\widehat{p_N}$	[0.01112, 0.48711]	[0.05033, 0.13342]	[0.33205, 0.09775]
100	**Mean**	$\widehat{a_N}$	[2.31534, 3.4201]	[1.85065, 2.25892]	[1.96960, 2.52434]
		$\widehat{b_N}$	[1.6431, 2.78082]	[1.95885, 2.19012]	[1.95962, 2.37243]

		$\widehat{q_N}$	[2.04081,2.10196]	[1.54758, 2.51858]	[1.44971, 2.36524]
		$\widehat{p_N}$	[1.80824, 2.09797]	[1.62019, 2.56520]	[1.48308, 2.427468]
	MSE	$\widehat{a_N}$	[6.10985, 16.8563]	[1.28531, 1.92259]	[1.61472, 2.84221]
		$\widehat{b_N}$	[0.52321, 2.10325]	[0.42942,0.75540]	[0.67244, 0.73143]
		$\widehat{q_N}$	[1.90643, 2.19297]	[0.51869, 1.71932]	[0.362008, 1.65003]
		$\widehat{p_N}$	[0.70767,0.72883]	[0.52677, 0.82273]	[0.32772, 0.84436]
	RMSE	$\widehat{a_N}$	[2.47181, 4.10565]	[1.13371, 1.38657]	[1.27071, 1.68588]
		$\widehat{b_N}$	[0.72333, 1.45026]	[0.65530,0.86914]	[0.82002, 0.85523]
		$\widehat{q_N}$	[1.38073, 1.48086]	[0.72020, 1.31123]	[0.60167, 1.28453]
		$\widehat{p_N}$	[0.84123,0.85372]	[0.72579, 0.90704]	[0.57247, 0.91889]
	Bias	$\widehat{a_N}$	[0.91534, 1.52011]	[0.35892,0.45065]	[0.56960, 0.62434]
		$\widehat{b_N}$	[0.14319, 0.78082]	[0.19012,0.45885]	[0.37243,0.45962]
		$\widehat{q_N}$	[0.25918,0.40196]	[0.15241, 0.21858]	[0.06524,0.25028]
		$\widehat{p_N}$	[0.00824, 0.40202]	[0.065207,0.17980]	[0.07253,0.31691]
150	**Mean**	$\widehat{a_N}$	[2.39295, 2.59663]	[1.69799, 2.28928]	[1.84874, 2.51742]
		$\widehat{b_N}$	[1.48475, 2.38927]	[1.84251, 2.22170]	[1.82141, 2.36527]
		$\widehat{q_N}$	[2.32242, 2.26305]	[1.56125, 2.38488]	[1.55411, 2.22098]
		$\widehat{p_N}$	[1.83872, 2.33146]	[1.62906, 2.47499]	[1.61889, 2.31876]
	MSE	$\widehat{a_N}$	[5.19190,6.34498]	[0.76663, 1.61336]	[1.38675, 2.57476]
		$\widehat{b_N}$	[0.36447, 0.76441]	[0.41032,0.45602]	[0.17093, 0.63993]
		$\widehat{q_N}$	[1.85714,2.85060]	[0.39942, 0.41032]	[0.39838, 1.05506]
		$\widehat{p_N}$	[0.30307, 0.49069]	[0.29310, 1.01496]	[0.40961, 0.52287]
	RMSE	$\widehat{a_N}$	[2.27857,2.51892]	[0.87557, 1.27018]	[0.27180, 1.60460]
		$\widehat{b_N}$	[0.60371, 0.8743]	[0.64056,0.67529]	[0.63118, 0.79996]
		$\widehat{q_N}$	[1.36277,1.68837]	[0.63200, 1.00745]	[0.64001, 1.02716]
		$\widehat{p_N}$	[0.55052, 0.70049]	[0.54139, 0.75893]	[0.52135, 0.72310]
	Bias	$\widehat{a_N}$	[0.69663,0.99295]	[0.38928,1.17760]	[0.44874, 0.61742]
		$\widehat{b_N}$	[0.015245, 0.38927]	[0.22170,0.29799]	[0.32141, 0.36527]
		$\widehat{q_N}$	[0.036943,0.62242]	[0.08488,0.34251]	[0.07901,0.14588]
		$\widehat{p_N}$	[0.03872, 0.16853]	[0.025003,0.13874]	[0.18110, 0.18123]
200	**Mean**	$\widehat{a_N}$	[2.56066, 2.69271]	[1.65731, 2.22683]	[1.74361, 2.39868]
		$\widehat{b_N}$	[1.428845, 2.33717]	[1.77586, 2.16486]	[1.70362, 2.29352]
		$\widehat{q_N}$	[2.19764,2.30402]	[1.61052, 2.37936]	[1.65621, 2.25097]
		$\widehat{p_N}$	[1.77657, 2.30401]	[1.68037, 2.492011]	[1.66439, 2.36508]
	MSE	$\widehat{a_N}$	[6.98059,8.23299]	[0.73184, 1.36073]	[0.941745, 2.21622]
		$\widehat{b_N}$	[0.25652, 0.56396]	[0.31173,0.35832]	[0.28724, 0.46309]
		$\widehat{q_N}$	[1.12979,2.25599]	[0.351277, 0.86185]	[0.39563, 1.00733]
		$\widehat{p_N}$	[0.15658, 0.33635]	[0.29343, 0.49330]	[0.19297, 0.43221]
	RMSE	$\widehat{a_N}$	[2.64208,2.86931]	[0.85547, 1.16650]	[0.97043, 1.48869]
		$\widehat{b_N}$	[0.506478, 0.75097]	[0.55833,0.59860]	[0.53595, 0.68050]
		$\widehat{q_N}$	[1.06291,1.50199]	[0.59268, 0.92836]	[0.62899, 1.00366]
		$\widehat{p_N}$	[0.39571, 0.57996]	[0.54169, 0.70235]	[0.43929, 0.65742]
	Bias	$\widehat{a_N}$	[0.79271,1.16066]	[0.25731, 0.32683]	[0.34361, 0.49868]
		$\widehat{b_N}$	[0.071154, 0.33717]	[0.16486,0.27586]	[0.20362, 0.29352]
		$\widehat{q_N}$	[0.10235,0.60402]	[0.07936,0.08947]	[0.043784, 0.04902]

		$\widehat{p_N}$	[0.023423, 0.19598]	[0.00798,0.11962]	[0.13491,0.13560]

Table 3 shows the lowest MSE and RMSE values for the MLE method, indicating that it is the most accurate. Bias is low in all methods, reflecting the quality of the estimates. MLE (Maximum Likelihood Estimation) showed superior performance, especially with large sample sizes, making it the best fit for the distribution. LSE and WLSE perform well with small sample sizes but are less accurate as the size increases.

6. Application

To demonstrate the extent of the quality of the distribution and its efficiency in practical applications, the practical aspect is an important aspect to show this, as in this part a practical applications is conducted on real neutrosophic data that is used [31], with a comparison of the results obtained between the proposed distribution and six other distribution represented by:

- Neutrosophic beta inverse Wiebull (NBeIW)
- Neutrosophic Kumaraswamy inverse Wiebull (NKuIW)
- Neutrosophic Exponeted generalized inverse Wiebull (NEGIW)
- Neutrosophic log-Gamma inverse Wiebull (NLGamIW)
- Neutrosophic Gompertz inverse Wiebull (NGoIW)
- Neutrosophic inverse Wiebull (NIW)

This comparision required the use of four information criteria, which are (AIC [19], CAIC [32], [33], HQIC [34], [35], , and BIC [36]) in addition to four statistical measures, which are (Kolmogorov-Smirnov (KS), Anderson- Darling (A), Cramér-von Mises (W), and p-value [37], [38]).

Data set-1

The first represented by mortality data for children under five years of age [31]**.**

Var	N	Mean	SD	Median	Trimmed	Mad	Min	Max	Range	SK	KU	Se
1	**26**	**[15.76, 16.76]**	**[7.27, 7.37]**	**[14.21, 15.32]**	**[15.22, 16.26]**	**[7.87, 8.27]**	**[6.81, 7.98]**	**[31.53, 31.81]**	**[23.83, 24.72]**	**0.56**	**[-0.96, -0.93]**	**[1.43, 1.45]**

The results of the criteria for the distributions were displayed in Table 4, while Table 5 expressed the value of the statistical measures, while Table 6 displayed the values of the estimated parameters for each distribution.

Table 4. results of the criteria for the distributions

Dist.	-2L	AIC	CAIC	BIC	HQIC
HWIW	[85.40969,85.5326]	[178.8194,179.06]	[180.7241,180.97]	[183.851,184.097]	[180.268,180.514]
BeIW	[86.0416, 87.6206]	[180.089, 183.302]	[181.994, 185.207]	[185.122, 188.334]	[181.538, 184.751]
KuIW	[86.1110, 86.5381]	[180.234, 181.085]	[182.139, 182.990]	[185.267, 186.118]	[181.683, 182.535]
EGIW	[86.2713,86.31197]	[180.564,180.649]	[182.469,182.554]	[185.597,185.681]	[182.014,182.098]
LGamIW	[85.63031,85.8919]	[179.260,179.785]	[181.165,181.690]	[184.293,184.818]	[180.709,181.235]
GoIW	[87.0561, 87.2476]	[182.112, 182.495]	[184.017, 184.400]	[187.144, 187.527]	[183.561, 183.944]
IW	[96.1148, 104.916]	[196.24, 213.9324]	[196.761, 214.454]	[198.756, 216.448]	[196.9645, 214.65]

From Table 4, NHWIW achieved the lowest values for most of the criteria, indicating its high fit to the data. The IW distribution was the least efficient due to its high values, as low

values of the criteria enhance the stability of the distribution when comparing models with different complexities .

Table 5. value of the statistical measures

Dist.	W	A	K-S	p-value
HWIW	[0.03774283,0.0473640]	[0.313303,0.341763]	[0.103911, 0.106321]	[0.900544,0.9142441]
BeIW	[0.04349193,0.0582771]	[0.3464307,0.40208]	[0.088246, 0.119375]	[0.8107124,0.9765447]
KuIW	[0.04234476,0.0551776]	[0.341253,0.386771]	[0.081400, 0.094516]	[0.9572919,0.9896749]
EGIW	[0.04774075,0.0614708]	[0.370513,0.420625]	[0.082911, 0.090155]	[0.9714649,0.9874063]
LGamIW	[9.373411,9.426508]	[52.44084, 52.46839]	[0.9483765, 0.94545]	5.551115e-16
GoIW	[0.0627775,0.06469447]	[0.461921, 0.464890]	[0.12449, 0.1460138]	[0.5858848,0.7699224]
IW	[0.04225913,0.0575322]	[0.339643,0.397695]	[0.227421, 0.364774]	[0.001313552,0.1155558]

Table 5 shows that NHWIW achieved the highest p-value and lowest W and A values, reflecting its high fit to the data. Other distributions showed poorer performance compared to NHWIW .

Table 6. Estimator value interval for parameters by MLE

Dist.	$\hat{a}_N$	$\hat{b}_N$	$\hat{q}_N$	$\hat{p}_N$
HWIW	[0.013462, 0.0280360]	[3.3452479,3.5492839]	[7.5562016, 12.242277]	[1.918304,1.948398]
BeIW	[5.941547,6.880572]	[3.479567, 3.568686]	[6.136480,7.531162]	[0.966692,1.129877]
KuIW	[5.85491, 5.858095]	[4.048258,4.141243]	[6.026946, 6.382458]	[1.111050,1.119379]
EGIW	[3.8376168, 4.5794689]	[6.6182216, 7.6331922]	[7.205414,7.2723604]	[0.789913,0.848330]
LGamIW	[7.337486, 8.415236]	[5.380997, 6.665243]	[7.4194373, 8.495675]	[1.17855,1.194137]
GoIW	[0.006215729,0.00781413]	[1.4543039, 1.4894439]	[1.9634420,1.9943284]	[1.486703,1.493761]
IW	---	---	[6.1610960,13.242297]	[0.8713852,1.14196]

Table 6 shows the estimated intervals of the main parameters of the NHWIW distribution compared to other distributions (such as BeIW, KuIW, etc.) using the maximum likelihood estimation (MLE) method for the first dataset. The NHWIW distribution showed narrow intervals of the parameters, indicating the stability of the estimates, while other distributions such as BeIW and KuIW showed greater variation in the intervals of the parameters, which may indicate their poor efficiency compared to NHWIW.

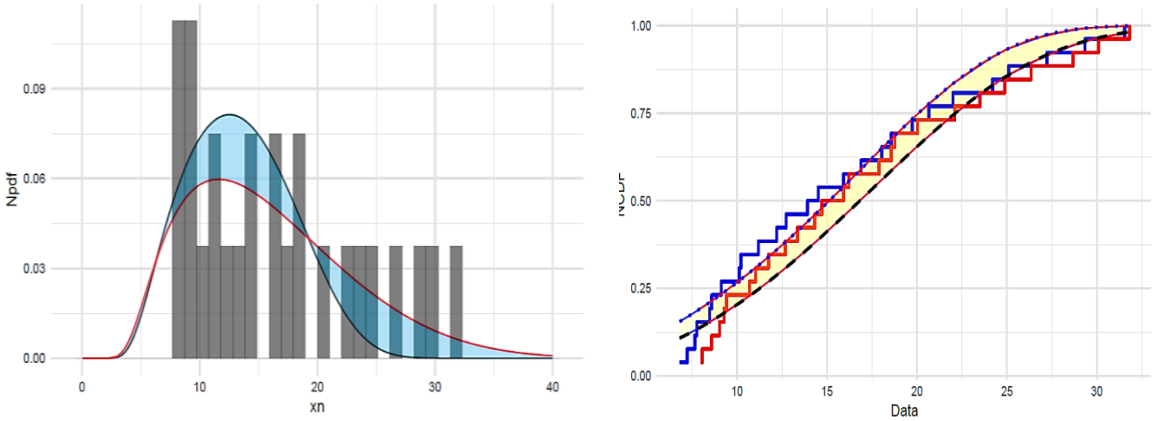

(a) (b)

Figure 3: (a) Fitting pdfs NHWIW with histogram data set, (b) Empirical Fitted CDFs NHWIW with data set

Figure 3 (a) shows how well the probability density function (PDF) of the NHWIW distribution matches the actual data for the first set. The distribution shows a strong fit with the structural distribution of the data, with the curve following the shape of the experimental data.

This indicates the ability of NHWIW to accurately and flexibly represent real data. Figure 3 (b) shows the empirical CDF compared with the theoretical CDF. The strong fit between the distributions reflects the efficiency of NHWIW in representing the cumulative probability of the data.

Data set-2

The second is COVID-19 in Netherlands for thirty days [39]

Var	N	Mean	SD	Median	Trimmed	Mad	Min	Max	Range	SK	KU	Se
1	30	[6.14, 6.36]	[3.51, 3.56]	[5.37, 5.64]	[5.79, 6]	[2.72, 2.85]	[1.27, 1.34]	[14.92, 15.66]	[13.64, 14.33]	[0.8, 0.82]	[-0.18, 0.03]	[0.64, 0.65]

Table 7. results of the criteria for the distributions

Dist.	-2L	AIC	CAIC	BIC	HQIC
HWIW	[76.43589,77.09943]	[160.8718, 162.1989]	[162.4718,163.7989]	[166.4766,167.8036]	[162.6648,163.9919]
BeIW	[76.48142,77.32048]	[160.9628, 162.641]	[162.5628,164.241]	[166.5676,168.2457]	[162.7559,164.434]
KuIW	[76.59179, 77.27442]	[161.1836, 162.5488]	[162.7836,164.1488]	[166.7884,168.1536]	[162.9766,164.3419]
EGIW	[78.25885, 79.37512]	[164.5248, 166.7519]	[166.1248,168.3519]	[170.1296,172.3567]	[166.3179,168.545]
LGamIW	[76.56406, 77.31349]	[161.1281, 162.627]	[162.7281,164.227]	[166.7329,168.2318]	[162.9211,164.42]
GoIW	[77.94244, 79.25779]	[163.9185, 166.5239]	[165.5185,168.1239]	[169.5233,172.1287]	[165.7115,168.3169]
IW	[80.90795, 81.86503]	[165.8159, 167.7301]	[166.2603,168.1745]	[168.6183,170.5325]	[166.7124,168.6266]

Table 7 compares NHWIW with other distributions using informative criteria such as AIC, BIC, CAIC, and HQIC for the second dataset. NHWIW distribution had the lowest values for all criteria compared to other distributions. Other distributions, such as IW and GoIW, showed high values, indicating their poor performance in fitting the data.

Table 8. value of the statistical measures

Dist.	W	A	K-S	p-value
HWIW	[0.0233792, 0.0241559]	[0.1664448, 0.1756536]	[0.070432, 0.0770078]	[0.9881955, 0.99588]
BeIW	[0.02499, 0.02863132]	[0.185047, 0.2137449]	[0.08221554,0.085797]	[0.96637, 0.977128]
KuIW	[0.0217852, 0.0257614]	[0.1728076, 0.1938708]	[0.0685944, 0.076441]	[0.9891058,0.9971004]
EGIW	[0.0612384, 0.082723]	[0.4535322, 0.57210]	[0.1106459, 0.114588]	[0.784162,0.8173854]
LGamIW	[9.976712,10.01212]	[60.25735,60.30363]	[0.9854649, 0.987072]	1.221245e-15
GoIW	[0.0474965, 0.0719870]	[0.3674051, 0.5081394]	[0.0990987, 0.105585]	[0.8571036,0.9018158]
IW	[0.1411036, 0.1590753]	[0.940501, 1.032139]	[0.1517456, 0.153257]	[0.4380138,0.4503734]

Table 8 NHWIW had the highest p-value and the lowest values for W, A, and K-S, indicating that this distribution is superior to other distributions and provides an excellent fit to the data and there is no evidence to reject the hypothesis of the distribution. Distributions such as IW showed high values for the criteria, reflecting their poor representation of the data.

Table 9. Estimator value interval for parameters by MLE

Dist.	$\hat{a}_N$	$\hat{b}_N$	$\hat{q}_N$	$\hat{p}_N$
HWIW	[5.837801, 6.1923656]	[4.02133, 4.2564547]	[0.8979603,0.91083]	[0.3596752,0.37002]
BeIW	[0.326699, 0.5555232]	[23.3992253,26.28143]	[13.330017,19.726555]	[0.642861,0.746774]
KuIW	[3.5882782,9.1795205]	[65.592337, 74.372615]	[1.0179446, 2.7114185]	[0.421744,0.426545]
EGIW	[4.458458,5.3694787]	[2.5368242, 2.864744]	[3.8798198,4.1462443]	[0.652446,0.696044]
LGamIW	[0.4306123, 0.5999024]	[21.714107, 25.562351]	[12.796964,15.607732]	[0.624186,0.698871]
GoIW	[7.8853573,8.9050606]	[0.9466685, 1.2100697]	[7.3119639,8.3552368]	[0.706303,0.712820]
IW	---	---	[7.869781, 8.576315]	[1.553003, 1.564124]

Table 9 NHWIW distribution showed more accurate and stable estimation intervals compared to other distributions. Distributions such as GoIW and BeIW showed wide variations in estimates.

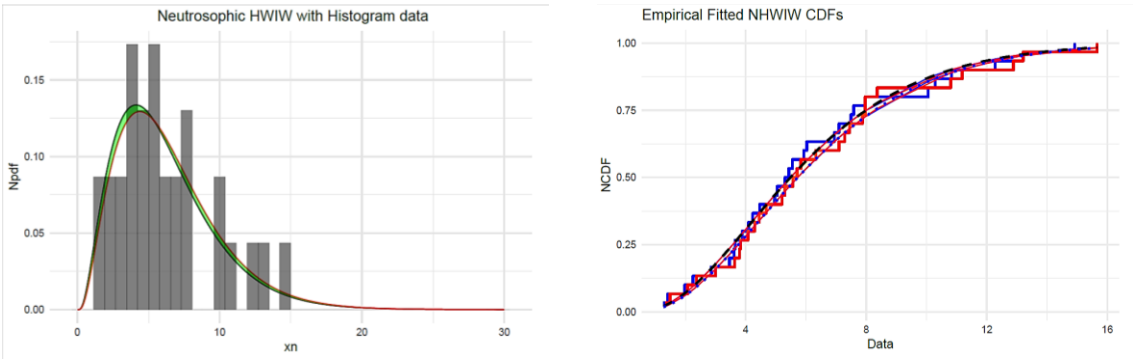

(a) (b)

Figure 4: (a) Fitting pdfs NHWIW with histogram data set2, (b) Empirical Fitted CDFs NHWIW with data set2

Figure 4 (a) shows how well the PDF of the NHWIW distribution fits the real data of the second group (COVID-19 data). The curve shows that NHWIW captures the main characteristics of the data. The good fit indicates the flexibility of the distribution in dealing with different types of data. Figure 4 (b) compares the empirical CDF with the theoretical NHWIW CDF for the second group of data. The close fit between the two curves reflects the accuracy of NHWIW in predicting the cumulative probabilities of the data. This enhances the reliability of the distribution and its relevance to real-world data such as COVID-19.

Conclusion

The NHWIW distribution showed high efficiency in representing real data compared to 6 other distributions. NHWIW outperformed in information criteria (AIC, BIC, CAIC, HQIC) and statistical criteria (K-S, W, A, p-value). The distribution has great flexibility that enables it to adapt to uncertain or ambiguous data using neutrosophic parameters. The maximum likelihood method (MLE) was the most accurate in estimating the parameters, indicating the stability of the model. Simulations proved that NHWIW provides accurate estimates even with small or medium sample sizes. The distribution is suitable for representing real data such as under-five mortality and COVID-19 data in the Netherlands. NHWIW showed high agreement with experimental data as shown in the figures. NHWIW represents an important step in applying neutrosophic logic in statistical modeling and bridges the research gap in integrating ambiguous data with complex mathematical distributions.

References

[1] A. Alzaatreh, C. Lee and F. Famoye, "A new method for generating families of continuous distributions," *Metron*, p. 63–79, 71 2013.

[2] S. Hussain, M. U. Hassan, M. S. Rashid and R. Ahmed, "Families of Extended Exponentiated Generalized Distributions and Applications of Medical Data Using Burr III Extended Exponentiated Weibull Distribution," *Mathematics*, p. 3090, 14 11 2023.

[3] A. B. Odeyale, S. U. Gulumbe, U. Umar and K. O. Aremu, "New New Odd Generalized Exponentiated Exponential-G Family of Distributions," *UMYU Scientifica*, pp. 56-64, 4 2 2023.

[4] S. Hussain, M. U. Hassan, M. S. Rashid and R. Ahmed, "Families of Extended Exponentiated Generalized Distributions and Applications of Medical Data Using Burr III Extended Exponentiated Weibull Distribution," *Mathematics*, p. 3090, 14 11 2023.

[5] N. A. Noori, A. A. Khalaf and M. A. Khaleel, "A New Generalized Family of Odd Lomax-G Distributions Properties and Applications," *Advances in the Theory of Nonlinear Analysis and Its Application*, pp. 1-16, 4 7 2023.

[6] I. A. Sadiq, S. I. Doguwa, A. Yahaya and J. Garba, "New Generalized Odd Fréchet-G (NGOF-G) Family of Distribution with Statistical Properties and Applications," *UMYU Scientifica*, pp. 100-107, 3 2 2023.

[7] Y. Y. Abdelall, A. S. Hassan and E. M. Almetwally, "A new extention of the odd inverse Weibull-G family of distributions: Bayesian and non-Bayesian estimation with engineering applications," *Computational Journal of Mathematical and Statistical Sciences* , pp. 359-388, 2 3 2024.

[8] A. I. Ishaq, U. Panitanarak, A. A. Alfred , A. A. Suleiman and H. Daud, "The Generalized Odd Maxwell-Kumaraswamy Distribution: Its Properties and Applications," *Contemporary Mathematics*, pp. 711-742, 2024.

[9] G. A. Mahdi, M. A. Khaleel, A. M. Gemeay, M. Nagy , A. H. Mansi, M. M. Hossain and E. Hussam, "A new hybrid odd exponential-Φ family: Properties and applications," *AIP Advances*, 4 14 2024.

[10] N. A. Noori and M. A. khaleel, "Estimation and Some Statistical Properties of the hybrid Weibull Inverse Burr Type X Distribution with Application to Cancer Patient Data," *Iraqi Statisticians Journal*, pp. 8-29, 2 1 2024.

[11] N. A. Noori, A. A. Khalaf and M. A. Khaleel, "A new expansion of the Inverse Weibull Distribution: Properties with Applications," *Iraqi Statistians Journal*, pp. 52-62, 1 1 2024.

[12] N. A. Noori, "Exploring the Properties, Simulation, and Applications of the Odd Burr XII Gompertz Distribution," *Advances in the Theory of Nonlinear Analysis and Its Application*, pp. 60-75, 4 7 2023.

[13] A. L. Solomon Sarpong and S. Nasiru, "Odd Chen-G family of distributions," *Annals of Data Science*, pp. 369-391, 2 9 2022.

[14] M. M. Alanaz and Z. Y. Algamal, "Neutrosophic exponentiated inverse Rayleigh distribution: Properties and Applications," *International Journal of Neutrosophic Science*, pp. 36-43, 4 21 2023.

[15] M. M. Alanaz, M. Y. Mustafa and Z. Y. Algamal, "Neutrosophic Lindley distribution with application for Alloying Metal Melting Point," *International Journal of Neutrosophic Science*, pp. 65-71, 4 21 2023.

[16] A. A. Khalaf, M. Q. Ibrahim and N. A. Noori, "[0,1]Truncated Exponentiated Exponential Burr type X Distributionwith Applications," *Iraqi Journal of Science*, pp. 4428-4440, 8 65 2024.

[17] H. J. Gómez, K. I. Santoro, I. B. Chamorro, O. Venegas, D. I. Gallardo and H. W. Gómez, "A Family of Truncated Positive Distributions," *Mathematics*, p. 4431, 21 11 2023.

[18] A. A. Khalaf and M. khaleel, "The New Strange Generalized Rayleigh Family: Characteristics and Applications to COVID-19 Data," *Iraqi Journal For Computer Science and Mathematics*, vol. 5, no. 3, pp. 92-107, 2024.

[19] M. A. Khaleel, P. E. Oguntunde, J. N. Al Abbasi, N. A. Ibrahim and M. H. AbuJarad, "The Marshall-Olkin Topp Leone-G family of distributions: A family for generalizing probability models," *Scientific African*, p. e00470, 8 2020.

[20] K. H. Al-Habib, M. A. Khaleel and H. Al-Mofleh, "A new family of truncated nadarajah-haghighi-g properties with real data applications," *Tikrit Journal of Administrative and Economic Sciences*, p. 2, 61 19 2023.

[21] L. Handique, M. A. ul Haq and C. Subrata, "Generalized Modified exponential-G family of distributions: its properties and applications," *International Journal of Mathematics and Statistics*, pp. 1-17, 1 21 2020.

[22] A. Z. Afify , H. Yousof and S. Nadarajah, "The beta transmuted-H family for lifetime data," *Statistics and its Interface*, pp. 505-520, 3 10 2017.

[23] F. Chipepa, B. O. Oluyede and B. Makubate, "A New Generalized Family of Odd Lindley-G Distributions With Application," *International Journal of Statistics and Probability*, pp. 1-23, 6 8 2019.

[24] F. A. Bhatti, G. G. Hamedani, M. C. Korkmaz, G. M. Cordeiro, H. M. Yousof and M. Ahmad , "On Burr III Marshal Olkin family: development, properties, characterizations and applications," *Journal of Statistical Distributions and Applications*, pp. 1-21, 6 2019.

[25] K. H. Habib , M. A. Khaleel, H. Al-Mofleh, P. E. Oguntunde and S. J. Adeyeye, "Parameters Estimation for the [0, 1] Truncated Nadarajah Haghighi Rayleigh Distribution," *Scientific African*, p. e02105, 2024.

[26] J. Farrukh, M. A. Nasir, M. H. Tahir and N. H. Montazeri, "The odd Burr-III family of distributions," *Journal of Statistics Applications and Probability*, pp. 105-122, 1 6 2017.

[27] N. S. Khalaf, A. Hameed, K. Moudher , M. A. Khaleel and Z. M. Abdullah, "the Topp Leone flexible Weibull distribution: an extension of the flexible Weibull distribution," *International Journal of Nonlinear Analysis and Applications*, pp. 2999-3010, 1 13 2022.

[28] A. Khaoula, N. Seddik-Ameur, A. A. Abd El-Baset and M. A. Khaleel, "The Topp-Leone Extended Exponential Distribution: Estimation Methods and Applications," *Pakistan Journal of Statistics and Operation Research*, pp. 817-836, 4 18 2022.

[29] H. Sharqa , M. Ahsan-ul-Haq, J. Zafar and M. A. Khaleel, "Unit Xgamma Distribution: Its Properties, Estimation and Application: Unit-Xgamma Distribution," *Proceedings of the Pakistan Academy of Sciences: A. Physical and Computational Sciences*, pp. 15-28, 1 59 2022.

[30] S. Naz, L. A. Al-Essa, H. S. Bakouch and C. Chesneau, "A transmuted modified power-generated family of distributions with practice on submodels in insurance and reliability," *Symmetry* , p. 1458, 7 15 2023.

[31] Z. Khan, M. M. A. Almazah, O. H. Odhah and H. M. Alshanbari, "Generalized Pareto Model: Properties and Applications in Neutrosophic Data Modeling," *Mathematical Problems in Engineering*, p. 3686968, 1 2022.

[32] M. M. Rahman, A. M. Gemeay, M. A. I. Khan, M. A. Meraou, M. E. Bakr, A. H. Muse, E. Hussam and O. S. Balogun, "A new modified cubic transmuted-G family of distributions: Properties and different methods of estimation with applications to real-life data," *AIP Advances*, p. 095025, 9 13 2023.

[33] P. E. Oguntunde, M. A. Khaleel, H. I. Okagbue and O. A. Odetunmibi, " the Topp–Leone Lomax (TLLo) distribution with applications to airbone communication transceiver dataset," *Wireless Personal Communications*, pp. 349-360, 2019.

[34] G. M. Cordeiro, M. Alizadeh, T. G. Ramires and E. M. M. Ortega, "The generalized odd half-Cauchy family of distributions: Properties and applications," *Communications in Statistics-Theory and Methods*, pp. 5685-5705, 11 46 2017.

[35] S. Abid and R. Abdulrazak, "[0, 1] truncated Frechet-Weibull and Frechet distributions," *International Journal of Research in Industrial Engineering*, pp. 106-135, 1 7 2018.

[36] M. Aboraya, "A new one-parameter G family of compound distributions: copulas, statistical properties and applications," *Statistics, Optimization & Information Computing, forthcoming*, p. 942–962, 9 2021.

[37] O. E. Al-Saqal, Z. A. Hadied and Z. Y. Algamal, "Modeling bladder cancer survival function based on neutrosophic inverse Gompertz distribution," *International Journal of Neutrosophic Science*, pp. 75-5, 1 25 2025.

[38] N. A. Noori, A. A. Khalaf and M. A. Khaleel, "A new expansion of the Inverse Weibull Distribution: Properties with Applications," *Iraqi Statistians Journal*, pp. 52-62, 1 1 2024.

[39] H. M. Almongy, E. M. Almetwally, H. M. Aljohani, A. S. Alghamdi and E. H. Hafez, "A new extended Rayleigh distribution with applications of COVID-19 data," *Results in Physics*, p. 104012, 23 2021.

Machine Scheduling Problem for Solving Tri-Objective Function Using Local Search Algorithm

Mohammed Muter [1]

Iraq T. Abbas[2,a)]

[1] *University of Baghdad, Baghdad, College of Education for Pure Science Ibn-Al-Haitham, Department of Mathematics, Iraq, mohammed.juru2303p@ihcoedu.uobaghdad.edu.iq*

[2] *University of Baghdad, Department of Mathematics, Baghdad, Iraq, College of Science,*
[a)]*Iraq.t@sc.uobaghdad.edu.iq*

Machine Scheduling Problem for Solving Tri-Objective Function Using Local Search Algorithm

Mohammed Muter [1]

Iraq T. Abbas[2,a)]

[1] *University of Baghdad, Baghdad, College of Education for Pure Science Ibn-Al-Haitham, Department of Mathematics, Iraq, mohammed.juru2303p@ihcoedu.uobaghdad.edu.iq*

[2] *University of Baghdad, Department of Mathematics, Baghdad, Iraq, College of Science,* [a)]*Iraq.t@sc.uobaghdad.edu.iq*

Abstract.

This study introduces the multi-objective single-machine approach. Reducing the three criteria of maximum earliest time E_{max}, tardiness (ΣT_j), and total completion time (ΣC_j) will solve the machine scheduling problem (MSP). It is an NP-hard problem.

In this paper's theoretical section, we give the mathematical formulation of. Next, we'll look at how the dominance rule may help you make the most informed decisions. In the practical part, the Branch and Bound method is one of the most important exact approaches. A collection of optimal determination issues for $1//F(\Sigma C_j + \Sigma T_j + E_{max})$ are generated, and the provided MSP goal is solved. In a fair amount of time, the BAB approach finds the best resolution issues to the problem. In addition, we provide two heuristic methods to address the Issue and provide appropriate estimates. The two suggested determination issues work well, according to the results of the practical investigation.

Keywords. Branch and Bound, Multi-Objective, Total Completion Time, Heuristic Approaches.

المستخلص

تُقدّم هذه الدراسة نهج الآلة الواحدة متعدد الأهداف. سيؤدي تقليل المعايير الثلاثة لأقصى وقت مبكر E_{max} ، والتأخير(ΣT_j) ، وإجمالي وقت الإكمال (ΣT_j) إلى حل مشكلة جدولة الآلة .(MSP) وهي مشكلة من نوع.NP-hard

في القسم النظري من هذه الورقة، نُقدّم الصياغة الرياضية لـ. بعد ذلك، سننظر في كيفية مساعدة قاعدة الهيمنة في اتخاذ القرارات الأكثر استنارة. في الجزء العملي، تُعد طريقة الفرع والحد واحدة من أهم الطرق الدقيقة. يتم توليد مجموعة من مشكلات التحديد الأمثل لـ$1//F(\Sigma C_j + \Sigma T_j + E_{max})$ ، ويتم حل هدف MSP المُقدّم. في فترة زمنية معقولة، يجد نهج BABأفضل مشكلات الحل للمشكلة. بالإضافة إلى ذلك، نُقدّم طريقتين استدلاليتين لمعالجة المشكلة وتقديم تقديرات مناسبة. تعمل مشكلتا التحديد المقترحتان بشكل جيد، وفقًا لنتائج البحث العملي.

1-Introduction

The difficulty of allocating a group of tasks to a group of machines under a specific time constraint is known as the scheduling Issue [1-3]. A given number of jobs, n, each requiring a set number of operations to be planned on one or more machines over a particular amount of time about a specific target to be lowered, may be characterized as the machine scheduling Issue (MSP) [4] and [16].

A single objective Issue has been the focus of most research until the late 1980s. Actually, in order to provide decision makers about more practical options, scheduling choices should consider a number of elements. Modeling and solving scheduling Issues (SP) becomes more difficult when several objectives (criteria) are required. In many cases, using the same choice variables won't optimize several goals. There is hence a trade-off between several goals. A Multi Objective Scheduling Issue (MOSP) is the term for this type of Issue [5, 6].

The multicriteria goal's function $1//(\sum C_j + R_L + T_{max})$ is used to solve the Tricriteria Machine Scheduling Issue (SMSP), which is done about BAB and a few heuristic strategies [7]. Effective determination Issues to the Issues at hand are demonstrated in a number of particular examples. To find good or optimal determination Issues, they employed both heuristic and exact techniques to address the $1//(\sum C_j + R_L + T_{max})$ Issue [8].

Determine the sequence that minimizes this MOF by investigating the $1//(\sum(E_j + T_j + C_j + U_j + V_j)$ Issue [9] and [16]. They give a BAB determination Issue for this issue. Additionally, they employ fast LSMs, yielding almost perfect Outcomes. They report on computation experience and evaluate the performance of exact and LSMs on a variety of test Issues.

In order to decrease a multi-objective function, this article discusses arranging the number of tasks (n) on one machine. This may be expressed as follows: A separate machine, capable of performing one job at a time, will manage the whole load. A processing time and a due date are assigned to every job. All tasks are completed and prepared for execution at time zero. The objective is to resolve the $1//F(\Sigma C_j + \Sigma T_j + E_{max})$ issue.

Section two demonstrates various machine scheduling Issue (MSP) principles. Section 3 will cover the mathematical formulation of $1//F(\Sigma C_j + \Sigma T_j + E_{max})$. Section 4 presents special cases. Section 5 illustrates our proposed determination Issues. Section six discusses the practical and comparative outcomes. In section seven, we shall present the most important conclusions and recommendations.

1- Machine Schedule Issue Concept

2.1 Important Notations

This research employs many notations:

This research employs many notations:

n: number of jobs.
p_j: processing time of jobs j.
d_j: due date of jobs j.
C_j: completion time of job j, where $C_j = \Sigma_{k=1}^{j} p_k$
ΣC_j: total completion time.
L_j: lateness of job j, $L_j = C_j - d_j$.
T_j: tardiness of job j, $T_j = \max\{L_j, 0\}$.

2.2 Important Definition Machine Scheduling Issue

A number of terms are necessary in this study:

Shortest Processing Time [10]**:** Using a non-decreasing order of processing time (p_j). The Issue $1 // \Sigma C_j$ is resolved by using this process.

Minimum Slack Time [11]*:* Jobs are arranged according to the slack time $s_j = d_i - p_j$, which means that $(s_1 \leq s_2 \leq s_3 \leq \cdots \leq s_n)$,in non − decreasing order.Applying this rule will minimize E_{max}.

Definition (1) [12] and [14]*:* The matrix A(G) represents the adjacency matrix of an n-vertices graph, whose i, j^{th} element is 1 in the instance that V_i and V_j have a minimum one edge, and nothing else.

Emmon's Theorem (1) [13]: For the $1/\,/(\Sigma C_j, \Sigma T_j)$ issue, if $p_i \leq p_j$ and $d_i \leq d_j$, then task i occurs first.

2- Mathematical Formulation of Multi-Objectives Function

The following is the formulation of the suggested Issue: When considering a particular schedule, $\sigma = (1,2,\ldots,n)$, where n is how many tasks SCSTEP completed.

$$V = \min\left(\sum_{j=1}^{n} C_{\sigma(j)} + \sum_{j=1}^{n} T_{\sigma(j)} + E_{max}\right)$$

S.t:

$C_1 = p_{\sigma(1)}$,

$C_j = C_{(j-1)} - p_{\sigma(j)}, j = 2,3,\ldots,n$

$$L_j = C_j - d_{\sigma(j)}, j = 1,2,\dots.,n \qquad \dots(\text{SCSTEP})$$

$$T_j \geq C_j - d_{\sigma(j)}\ , j = 1,2,\dots.,n$$

$$E_j \geq d_{\sigma(j)} - C_j, j = 1,2,\dots.,n$$

$$E_{max} \geq \max\{d_{\sigma(j)} - C_j, 0\}, j = 1,2,\dots.,n$$

$$C_j, T_j \geq 0\ , E_j \geq 0\ , j = 1,2,\dots.,n$$

The SCSTEP challenge aims to minimize the overall number of completion times, total tardiness and maximum Earliest$\left(\sum_{j=1}^{n} C_{\sigma(j)} + \sum_{j=1}^{n} T_{\sigma(j)} + E_{max}\right)$ by scheduling the tasks on one machine. $\sigma \in S$ (S represents a set of all possible determination Issues), is the Issue's objective. As a result, the complexity of our issue is n! due to the ΣT_j function, it is considered an NP-hard issue.

3- Special Cases for SCSTEP -Issue

Case (1): For Issue (SCSTEP) if $p_j = p$ and $d_j = d\ , \forall j$ if so, we offer a special determination Issue:

1- $d \leq C_j\ , \forall j$ then $(\Sigma C_j + \Sigma T_j + E_{max}) = n(p(n+1) - d)$

2- $d > C_j\ , \forall j$ then $(\Sigma C_j + \Sigma T_j + E_{max}) = p\frac{n^2+n-2}{2} + d$

Proof: due to $p_j = p$, then $C_j = jp$, then

$$\Sigma C_j = p\frac{n(n+1)}{2} \qquad \dots(1)$$

For $d_j = d$ if :

1- $d \leq C_j\ , \forall j$ that's mean all jobs are tardy and $L_j = C_j - d = jp - d$, then

$$T_j = \max\{jp - d, 0\} = jp - d$$

$$\Sigma T_j = \Sigma jp - \Sigma d = p\frac{n(n+1)}{2} - nd \qquad \dots(2)$$

$$E_j = \max\{d - C_j, 0\} = 0\ , \forall j$$

$$\therefore E_{max} = 0 \qquad \dots(3)$$

From (1), (2) and (3) we obtain:

$$\Sigma C_j + \Sigma T_j + E_{max} = p\frac{n(n+1)}{2} + p\frac{n(n+1)}{2} - nd + 0 = pn(n+1) - nd = n(p(n+1) - d)$$

2 − $d > C_j\ , \forall j$ that's mean all jobs are early then $T_j = \max\{jp - d, 0\} = 0\ , \forall j$ then :

$$\Sigma T_j = 0 \qquad \dots(4)$$

$$E_j = \max\{d - C_j, 0\} = d - C_j = d - jp$$

$$E_{max} = d - p \qquad \dots(5)$$

From (1), (4) and (5) we obtain:

$$\Sigma C_j + \Sigma T_j + E_{max} = \left(p\frac{n(n+1)}{2} + 0 + d - p\right) = p\frac{n^2+n-2}{2} + d$$

Case (2): For the Issue (SCSTEP):

1- If $d_j > C_j \ , \forall j$, then the Issue changed to $(\Sigma C_j + E_{max})$,this Issue has just one determination Issue if SPT and MST are the same.
2- If $d_j < C_j \ , \forall j \in N$ then the Issue changed to $(\Sigma C_j , +\Sigma T_j)$,this Issue has just one determination Issue if SPT and EDD are the same.
3- If $d_j = C_j \ , \forall j \in N$ then the Issue changed to (ΣC_j) ,this Issue has a unique determination Issue according to the SPT rule.

Proof:

1- due to $d_j > C_j$, $\forall j$, then all jobs are early $T_j = 0 \ , \forall j$, then $\Sigma T_j = 0$ then

$$\Sigma C_j + \Sigma T_j + E_{max} = \Sigma C_j + E_{max}$$

2- due to $d_j < C_j$ then all jobs are tardy for all j ,this Issue solved in $p-$ type if $\sigma \equiv$ SPT $\equiv$ MST ,then σ will minimize both ΣC_j and ΣT_j about unique Significant

$$\Sigma C_j + \Sigma T_j + E_{max} = \Sigma C_j + \Sigma T_j + 0 = \Sigma C_j + \Sigma T_j$$

3- due to $d_j = C_j$ for all j in the SPT schedule (this means $T_j = 0 \ , E_j = 0 \ , \forall j$ then $\Sigma T_j = 0$ and $E_{max} = 0$ then

$$\Sigma C_j + \Sigma T_j + E_{max} = \Sigma C_j$$

Now if σ =SPT Significant is applied, then we obtain optimal determination Issue depend on ΣC_j only

Case (3): For the Issue (SCSTEP) if $p_j = p$ for $\forall j$, Consequently, if $\sigma =$ EDD , we could have an efficient determination Issue.

proof:

$$E_j = \max\{d_j - C_j, 0\} = \max\{d_j - jp, 0\}$$

If $d_1 = p$ and $jp \geq d_j$,then all jobs are late and $E_j = 0 \ , \forall$ and

$$E_{max} = 0 \qquad \cdots (6)$$

Then by using Relations (1) and (6), the Issue changes to $(\Sigma C_j + \Sigma T_j + 0) = \left(p\frac{n(n+1)}{2} + \Sigma T_j\right) = \left(p\frac{n(n+1)}{2} + \Sigma T_j\right)$

If we apply $\sigma = EDD$ for the Issue, then the $\Sigma T_j(\sigma) \leq \Sigma T_j(\pi)$ where π any sequence and due to $p\frac{n(n+1)}{2}$ is constant then $p\frac{n(n+1)}{2} + \Sigma T_j(\sigma)$ has an optimal determination Issue for the Issue.

Case (4): For the Issue (SCSTEP) if $d_j = d$, $\forall j$:

1- If $d \leq C_j$, $\forall j$ then $(\Sigma C_j + \Sigma T_j + E_{max}) = \Sigma C_j + n(C_n - d)$.

2- If $d > C_j$, $\forall j$ then $(\Sigma C_j + \Sigma T_j + E_{max}) = \Sigma C_j + d - p$

The issues described above can be solved using the SPT rule.

Proof:

1- If $d \leq C_j$, $\forall j$ then all jobs are late

$\therefore L_j = C_j - d$, $\forall j$ then

$T_j = \max\{C_j - d, 0\} = C_n - d$ then , $\Sigma T_j = \Sigma C_n - \Sigma d$ then

$$\Sigma T_j = n(C_n - d) \quad \cdots (7)$$

$E_j = \max\{d - C_j + 0\} = 0$, $\forall j$, then

$$Emax = 0 \quad \cdots (8)$$

From (7) and (8) we obtain:

$\Sigma C_j + \Sigma T_j + E_{max} = \Sigma C_j + n(C_n - d)$

SPT rule can solve this Issue due to $n(C_n - d)$is constant.

2- If $d > C_j$, $\forall j$, then $T_j = 0$, $\forall j$, then all jobs are early ,

$$\Sigma T_j = 0 \quad \cdots (9)$$

$E_j = \max\{d - C_j , 0\} = d - C_1$ then

$$E_{max} = d - p_{\sigma(1)} \quad \cdots (10)$$

From (9) and (10) we obtain:

$$\Sigma C_j + \Sigma T_j + E_{max} = \Sigma C_j + 0 + d - p_1 = \Sigma C_j + d - p_{\sigma(1)}$$

This issue can be resolved using the σ =SPT rule due to $d - p_{\sigma(1)}$ is constant.

In Table 1, Instances are provided to clarify the special cases for the (SCSTEP) Issue, by calculating the objective functions(*F*).

Table 1. Special Cases of Issue (SCSTEP)In the following examples.

Case	p_j and d_j	Conditions	*F*
Case 1	$p = d = 5$ $p = 5, d = 7, p < d$	$p_j = p$ and $d_j = d, \forall j$	(130) (130)
Case 2	$p_j = 4,3,2,2,1, d_j = 14,9,5,6,2,3$ $p_j = 3,4,5,6,8,9, d_j = 3,5,6,7,9,10$ $p_j = 8,5,2,6,4,3, d_j = 30,14,2,21,10,6$	$d_j \geq C_j$ $d_j \leq C_j$	(39) (126) (83)
Case 3	$p_j = 3, d_j = 3,4,6,7,8,9$	$p_j = p$ for $\forall j$	(72)
Case 4	$p_j = 5,4,3,2,1,1, d_j = 6$ $p_j = 7,65,4,3,2,1, d_j = 7$	$d_j = d$	(62) (123)

The multi-objective function of the Issue (SCSTEP) is denoted by (F).

4- Propose Approaches for Solving SCSTEP-Issue

4.1 Exact Approaches for SCSTEP-Issue

Below this part, we use the classic Branch and Bound (BAB) approach, often known as BAB, to try to identify a set of Pareto optimal determination Issues for the SCSTEP issue. The following are the steps involved in BAB:

Algorithm: BAB Method

Step (1): **INPUT** n, p_j and d_j for $j = 1,2, \dots, n$ . .

Step (2): **SET** $S = \phi$, define $F(\sigma) = \Sigma C_{\sigma(j)} + \Sigma T_j(\sigma) + E_{max}(\sigma)$, for any σ.

Step (3): The upper bound (UB) is obtained by applying the $\sigma = SPT$ rule. Determine $F(\sigma)$, which is equal to $1, 2, \dots, n$. Lastly, place the upper bound UB= $F(\sigma)$ at the parent node of the search tree.

Step (4): Set a lower bound LB **(δ)** every node in the BAB tree of searches and component Job sequence. The LB **(δ)** calculation combines the costs of the sequence jobs **(δ)**

About those produced by sequencing the tasks in the SPT rule.

Step (5): When LB ≤ UB, begin at every node and branch out.

Step (6): **STOP**.

5- Heuristic Approaches for SCSTEP-Issue

Start by applying the heuristic strategy, where the goal function is calculated and the Issue is resolved by the SPT rule. Next, use the SPT rule to organize the remaining jobs and find out what the goal is. Up until the completion of n series, this process is repeated. The following are the main steps of SCSTE_{max}P:

Algorithm (2): SCSTE_{max}P Heuristic Method

Step (1): INPUT n, p_j and d_j ,$j = 1,2, \dots, n$, $\delta = \phi$.

Step (2): Assign tasks according to the SPT rule (σ_1) and calculate $F_{11}(\sigma_1)$, where $\delta = \delta \cup \{F_{11}(\sigma_1)\}$;

Step (3): To obtain σ_j, place job i at the forefront of σ_{j-1} for $j = 2, \dots, n$. Then, compute $F_{2j}(\sigma_j)\ \delta = \delta \cup \{F_{1j}(\sigma_j)\}$.

END;

$F_1 = \min\{F_{1j}(\sigma_j)\}$

Step (4): Determine $F_{21}(\pi_1)$, $\delta = \delta \cup \{F_{21}(\pi_1)\}$; then arrange jobs according to MST rule (π_1).

Step (5): To obtain π_j, place job j in the first position of π_{j-1} for $j = 2, \dots, n$. Then, compute $F_{2j}(\pi_j), \delta = \delta \cup \{F_{2j}(\pi_j)\}$.

$F_2 = \min\{F_{2j}(\pi_j)\}$

END;

$F = \min\{F_1, F_2\}$

Step (6): A set of efficient SCSTE_{max}P -issue determination Issues is provided by filter set δ.

Step (7): OUTPUT best F

Step (8): STOP.

The concept behind the following heuristic technique is summed up by calculating the target function and identifying an ordered list about the fewest p_j and d_j which is not in disagreement about dominance rule. The following are the primary steps of SCSTE$_{max}$P:

Algorithm (3): DR- SCSTE$_{max}$P Heuristic Method

Step (1): INPUT**:** n, p_j and d_j ,$j = 1,2, \ldots, n$, $\delta = \emptyset$

Step (2): To get the DR adjacency matrix A, use theorem (1), where $N = \{1,2, \ldots, n\}$, $\delta = \emptyset$

Step (3): If more than one job break tie randomly, then $\delta = \delta \cup \{\sigma_1\}$. Construct a pattern σ_1 about a minimal p_j which is not in disagreement about DR (matrix A).

Step (4): If more than one job break tie randomly, then $\delta = \delta \cup \{\sigma_2\}$. Determine a sequence σ_2 about a minimal d_j which is not in disagreement about DR (matrix A).

Step (5): Determine which order is set $\delta^{`}$ from δ.

Step (6): Calculate $F(\delta), F = \min\{F(\delta)\}$.

Step (7): OUTPUT best F.

Step (8): END.

6- Practical Outcomes of the Issue (SCSTEP)

We provide a few key abbreviations before displaying all of the outcome tables:

AT/S	Average of CPU-Time per second.
AMAE	Average of Minimum Absolute Error.
BS	BS Significant of Issue (SCSTEP).
OP	Optimal Significant of Issue (SCSTEP).
R	0 < Real < 1.
F	Objective Function of Issue (SCSTEP).

After demonstrating how the recommended approaches (exact and estimation) are put into practice, we must first demonstrate that we compare the outcomes of the suggested strategies about the full enumeration method (CEM), which tries every possible variant of events to find the most efficient one.

Example (1): Using the following table, let's utilize MSP about five jobs, processing time, and due date:

Table 2. The p_j , d_j, and s_j data for the Issue (SCSTEP)

	1	2	3	4	5
p_j	1	8	10	4	9
d_j	14	28	27	23	12
s_j	13	20	17	19	3

Shown in Figure (1) may be obtained using theorem (1).

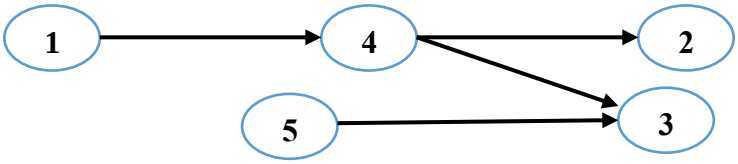

Figure (1): The DRs of the example (1)

The following (6) DRs may be seen from theorem (1): 1→2, 1→ 3,1→4, 1→6, 2→ 6, 4→2, 4→ 3, 4→ 6,5→3. There are seven possible sequences in Table 2, some or all of which are susceptible in addition to what already mentioned DRs. The following are the adjacency matrix *A*:

$$A(G)=\begin{bmatrix} 0 & 1 & 1 & 1 & a_{15} \\ 0 & 0 & a_{23} & 0 & a_{25} \\ 0 & a_{32} & 0 & 0 & 0 \\ 0 & 1 & 1 & 0 & a_{45} \\ a_{51} & a_{52} & 1 & a_{54} & 0 \end{bmatrix}. \text{where } a_{ji}=\begin{cases} 1, \text{if } a_{ji}=0 \\ 0, \text{if } a_{ji}=1 \end{cases}$$

Table 3. Under DR, optimal sequences for example (1)

EF-SQ						SCSTEP
Seq	**POS1**	**POS2**	**POS3**	**POS4**	**POS5**	$\Sigma C_j + \Sigma T_j + E_{max}$
1	1	4	2	5	3	129
2	1	4	5	2	3	116
3	1	4	5	3	2	114
4	1	5	4	2	3	114
5	1	5	4	3	2	113
6	5	1	4	2	3	114

where POS stands for position and EF-SQ for efficient sequence.

As can be seen in Table 3, the sequences (1–7) present the issue an optimal Significant for the Issue (SCSTEP).

Table (4) shows the Outcomes of solving the SCSTEP-Issue, n=3:10, using CEM and BAB.

Table (4): SCSTEP-Issue BAB and CEM Overviews, n = 3:10.

n	BAB		CEM	
	Optimal	Time	F	Time
	Av(F)	AT/s	Av(F)	AT/s
3	47.2	R	47.2	R
4	57	R	57	R
5	85	R	85	R
6	103.8	R	103.8	R
7	156.6	R	156.6	R
8	259.6	5.1824	259.6	R
9	299.4	45.8577	299.6	R
10	361.4	477.8011	361.8	R

Table (5): Discussion featuring SCSTE$_{max}$P and SCSTE$_{max}$P (DR) about CEM for SCSTEP -Issue, n=**3:10.**

n	CEM		SCSTE$_{max}$P		SCSTE$_{max}$P (DR)	
	OP	TIME	BS	AT/s	BS	AT/s
	Av(F)	AT/s	AMAE		AMAE	
3	47.2	R	8.8	R	49.8	R
4	57	R	9	R	58.4	R
5	85	R	14.6	R	89.4	R
6	103.8	R	23.6	R	112	R
7	156.6	R	32	R	166.8	R
8	259.6	5.1824	52.8	R	271.6	R
9	299.4	45.8577	62.2	R	305.4	R
10	361.4	477.8011	68.6	R	367	R

Table (6): Summary between SCSTE$_{max}$P and SCSTE$_{max}$P (DR) for SCSTEP -Issue, n=0:4000.

7-

n	SCSTE$_{max}$P		SCSTE$_{max}$P (DR)	
	BS AMAE	AT/s	BS AMAE	AT/s
30	574.2	R	3447	R
35	1120.6	R	4429.6	R
40	1367.8	R	6222.4	R
45	1408.6	R	7026.6	R
50	1900.8	R	9233.6	R
55	2143.4	R	1202.8	R
60	2685.6	R	1447.3	R
100	7527	R	37802	1.1889
150	19342	R	8475.2	2.0571
200	3179.1	R	1560.2	2.4966
400	1182.2	1.0088	6060.0	5.8263
500	1905.5	1.3040	9703.6	10.0629
600	2805.5	1.7679	1349.5	13.3215
700	3701.1	2.3175	1893.1	16.0939
800	4820.1	2.9208	2445.7	19.5225
900	5962.2	3.6512	3069.4	27.1716
1000	7895.9	4.4668	3846.0	44.6153
2000	3048.9	19.5043	1543.0	222.3472
4000	1240.5	109.6704	6153.6	963.4205

Conclusions and Future Works

1. According to this study, we use the BAB algorithm about DR to determine the best determination Issue up to n = 10 jobs. Outcomes from the BAB algorithm is compared to those from CEM.

2. We offer two effective and simple heuristic techniques for solving the SCSTEP Issue: SCSTE$_{max}$P and SCSTE$_{max}$P (DR), both of which perform well.

3. For further study, we suggest using some techniques such as (PSO algorithm, Genetic algorithm, etc.) to identify efficiency and approximate determination Issues for the SCSTEP Issues.

4. For more research, we recommend utilizing local search algorithms about multi-criteria and about multi-objective or together.

References

[1] J. Blazewicz, K. Ecker, E. Pesch, G. Schmidt andJ. Weglarz, "Handbook on scheduling,from theory to applications,". Berlin Heidelberg-New York: Springer; 2007.

[2] P. Brucker,"Scheduling algorithms," Berlin-Heidelberg-New York: Springer; 2007.

[3] M. Pinedo,"Scheduling: theory, algorithms and systems," New York: Springer; 2008.

[4] T. Abdul-Razaq, and H. Mohammed,"Exact and heuristic algorithms for solving combinatorial optimization Issues,"Ph.D. Thesis Dept. of Mathematics, College of Sciences, Mustansiriayah University 2017.

[5] V. T'kindt andJ. Billaut, "Multicriteria scheduling: theory, models and algorithms,"Second Edition, Springer, Berlin 2006.

[7] F. H. Ali and M. G. Ahmed, "Efficient algorithms to solve tricriteria machine scheduling Issue", (15th and the second International) Conference of Statistical Applications (ICSA2020), Irbil, Kurdistan Region-Iraq, 12-13/Feb./2020, Journal of Al Rafidain University College, Volume, Issue 46, pp: 485-493, 2020. https://www.iasj.net/iasj/article/190968.

[8] F. H. Ali and M. G. Ahmed, "Optimal and near optimal determination Issues for multi objective function on a single machine", 1st International Conference on Computer Science and Software Engineering (CSASE2020), Duhok, Kurdistan Region-Iraq, Sponsored by IEEE Iraq section, 16-17/Apr./2020

[9] M. H. Ibrahim, F. A. Ali and H. A. Chachan, "Solving multi-objectives function Issue using branch and bound and local search Approaches ", International Journal of Nonlinear and Applications (IJNAA), (Scopus) ISSN 2008-6822, 13 (2022) No. 1, 1649-1658. http://dx.doi.org/10.22075/ijnaa. 2022.5780

[10] Allard D. M., "A multi-objective genetic algorithm to solve single machine scheduling Issues using a fuzzy fitness function, "M. Sc. Thesis, Dept. of Industrial Engineering, College of Engineering and Technology, Univ. of Ohio, 2007.

[11] J. A. Hoogeveen, "Minimizing maximum promptness and maximum lateness on a single machine**,"** Math. Oper. Res.**,** vol. 21, no. 1, pp. 100–114, 1996, doi: 10.1287/moor.21.1.100.

[12] Hanan A. Chachan and Alaa S. Hameed, 2019, "Exact Approaches for Solving Multi-Objective Issue on Single Machine Scheduling,"Iraqi Journal of Science, Vol. 60, No.8, pp: 1802- 1813, DOI: 10.24996/ijs.2019.60.8.17, 2019.

[13] F. Ali and T. Abdul-Razaq, "Combinatorial optimization Issues: modeling and solving,"LapLambert Academic Publishing, ISBN-13: 978-3-659-93685-2, 2016.

[14] Sattar, H. A., & Cheetar, A. (2019). A new strategy according to GSABAT to solve single objective optimization Issue. International Journal of Swarm Intelligence Research (IJSIR), 10(3), 1-22.

[15] Abbas, I. T., & Ghayyib, M. N. (2024). Using Sensitivity Analysis in Linear Programming about Practical Physical Applications. Iraqi Journal of Science, 907-922.

[16] Abdul-Zahra, I., Abbas, I. T., Kalaf, B. A., Bakar, R. A., June, L. W., & Monsi, M. B. (2016). The Role of Dynamic Programming in the Distribution of Investment Allocations between Production Lines about an Application. International Journal of Pure and Applied Mathematics, 106(2), 365-380.

Combine Logistic to Pray and Impacts of Harvesting on Prey-Predator Model

Azhi Sabir Mohammed[*1,2],

Hiwa Abdullah Rasol[2] ,

Awder Rasul Braim[2],

Surme Rasul Saber[3]

[1] IT Support & Maintenance Department - Raparin Technical and Vocational Institute / Ranya, 3 Kurdistan Region of Iraq.

[2] Department of Mathematics, College of Basic Education - University of Raparin / Ranya, Kurdistan Region of Iraq

[3] Department of Mathematics, Faculty of Science and Health - Koya University / Koya, Kurdistan Region of Iraq

* Correspondence: Email: azhi.sabir@uor.edu.krd , Tel: +964 751 793 3080

hiwa.abdullah@uor.edu.krd

Combine Logistic to Pray and Impacts of Harvesting on Prey-Predator Model

Azhi Sabir Mohammed[*1,2],

Hiwa Abdullah Rasol[2] ,

Awder Rasul Braim[2],

Surme Rasul Saber[3]

[1] IT Support & Maintenance Department - Raparin Technical and Vocational Institute / Ranya, 3 Kurdistan Region of Iraq.

[2] Department of Mathematics, College of Basic Education - University of Raparin / Ranya, Kurdistan Region of Iraq

[3] Department of Mathematics, Faculty of Science and Health - Koya University / Koya, Kurdistan Region of Iraq

* Correspondence: Email: azhi.sabir@uor.edu.krd , Tel: +964 751 793 3080

hiwa.abdullah@uor.edu.krd, awder.math@uor.edu.krd, surme.rasul@koyauniversity.org

Abstract

The present article argues about a prey-predator model where the two species are harvested autonomously with constant or variable rates that have been well thought-out. According to the theory of logistic growth, the prey population is increasing. The Lotka-Volterra predator-prey model is modified and adapted into this model. The model has reached its equilibrium points, and the dynamical behavior of the suggested system was examined to display the phase portrait. Model simulations are analyzing, bifurcation diagrams are examined, and the behavior of the solutions' locally and globally is examined. The impacts of logistic and harvesting on the steadiness of stability states are inspected. The main purpose of the article is to implement a mathematical investigate of the model, and it can be obtained that the effect of activities in harvesting is more effective on the dynamical behaviour in the current model. At the end, solution curves are plotted by utilizing the Maple program to explore the dynamical behaviour of the model regarding to the time.

Keywords: Logistic, Harvesting, Predator-Prey, Lotka-Volterra, Jacobian Matrix, Linearization.

1 Introduction

A.J. Lotka and V. Volterra was originally proposed the predator-prey's problem, which is traditional and well-known problem [1]. The Italian mathematician Vito Volterra, in order to talk about the population dynamics of interacting species and predator-prey relationships in the 1920s, he projected a system of differential equations. He wanted to look at the growth of predators, or the decline in prey.

The mathematical modelling works on the study of increasing the population rates, and the environmental diseases and the ecotoxicological problems [2]. One of the main investigations is the model of harvest-population. Nowadays, the problems are identified with harvesting of multispecies fisheries have bed drawing consideration of researchers. The problem of combining harvesting of both independent species ecologically, the rate of harvesting can be used as the parameter's control [3]. Moreover, the investigation of harvested of dynamic's population is more realistic. Rahmani and Saraj [4] studied the efficiency of harvested factor in predator-prey model without having logistic factor in prey or predator. A model with two predators fighting for a single prey species subjected to logistic growth was provided by Ang and Safuan [3] in order to examine the effects of harvesting on a single predator species up to the model's critical point. The effects of harvesting operations on prey-predator populations may be determined by logistical considerations. Ghosh, Chandra [2] improved a fishery model of a prey- predator to study the research of the relation between the population's concentration, as well as the equilibrium of fish populations in areas where harvesting activities expose predator species. Different harvesting efforts and activities are encountered for prey and predatory species [5–6].

The primary goals of this research are to investigate the dynamical behaviors of a predator-prey model in the harvesting environment. The prey population establishes the law of logistic growth, and both species have varying harvesting rates. The effects of harvesting on the two species are investigated in order to establish further assumptions about persistence and extinction behaviors. A mathematical model via Jacobian matrix to analysing equilibrium points is used. A numerically study of the model through Maple software to stability analysis, and bifurcation results was used.

The remaining sections of the paper as follows. Next section is about adding logistic factor to the model, and the non-dimensional model and its stability is presented. In section 3 consider the model with constant and effort harvest factor and discuss equilibria and their stability are investigated, respectively. Finally, in section 4 numerical simulation results and analysis discussed. And the paper end with and conclusion.

2 Methods and Materials

The dynamical interaction between predator and prey species is defined using the traditional Lotka-Volterra model. The linear differential equations for the Lotka-Volterra model are as follows.

$$\begin{cases} \frac{dx}{dt} = ax - bxy \\ \frac{dy}{dt} = cxy - dy \end{cases}$$

The functions $x(t)$,and $y(t)$ express the populations of prey, and predator at time t respectively [3, 7]. Each parameter (a, b, c, d) are positive constants. The natural growth rate of the prey in the absence of predator represented by the parameter a. The effect of the predator on the prey species is represented by parameter b. Furthermore, predators will consume prey if b is the only factor affecting the prey species. The effect of prey on the predator species is shown by parameter c. In addition, the predator population will increase according to the amount of food available if c is the only factor affecting population growth. The biological mortality rate of the predator in the absence of prey was denoted by the parameter d. In the case of $b = 0$ it is assumed that the prey species would growth indefinitely in the absence of predators. The classic Lotka-Volterra assumptions are unrealistic, where one of the alternative solutions is to take on logistic growth behaviour in the prey population which is discussed in this section [8].

The modification of the traditional system of differential equations, by adding the law of logistic growth on prey species as follow:

$$\begin{cases} \frac{dx}{dt} = ax(1 - \frac{x}{K}) - bxy \\ \frac{dy}{dt} = cxy - dy \end{cases} \qquad (1)$$

The parameter (K) means environmental carrying capacity of the prey species. In the absence of predator populations, the prey population grows logistically. All parameters are assumed to have positive values. Introducing the new variable to simplify the model for overall understanding, and reduce the number of parameters. We introduce new variables u and v and let

$$u = \frac{d}{c}x\,, \quad v = \frac{b}{aF}y \quad \text{and} \quad \tau = aFt \quad \text{where} \quad F = (1 - \frac{N}{K})$$

The dimensional system (1) becomes.

$$\frac{du}{d\tau} = u - uv$$

$$\frac{dv}{d\tau} = -\alpha v + \alpha uv \qquad (1) \qquad \textit{Where} \quad \alpha = \frac{c}{aF}$$

In system (2) α: is a quotient between the growth rate of v to times of the growth rate of u and environmental limit carrying capacity of u.

Now, by using the Jacobian matrix which is one of the useful technique, we can discuss the behavers of equilibrium points, and the stability of system (2). By applying the Jacobean matrix to the system, we have

$$J = \begin{bmatrix} 1-v & -u \\ \alpha v & -\alpha + \alpha u \end{bmatrix}$$

The system (2) has two steady states in orbit of solutions of the model, as occurs: (0,0) and (1,1). Now, by using Jacobean matrix then simplify eigenvalues in equilibrium point (0,0) are identified as $\lambda_1 = 1, \lambda_2 = -\alpha$. As regards to equilibrium point (0,0) is a saddle point for the system. However, by linearize at the equilibrium (1,1) Jacobian matrix obtained as

$$J_{0,0} = \begin{bmatrix} 0 & -1 \\ \alpha & 0 \end{bmatrix}$$

So, at this point the phase portrait has a nonhyperbolic critical point as shown in finger (1)

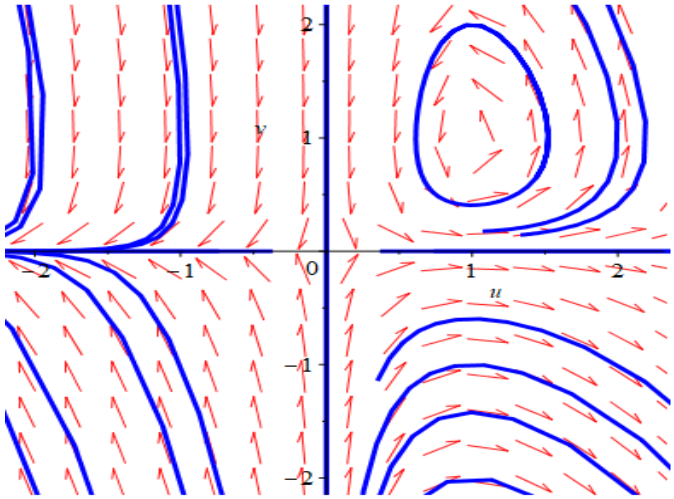

Figure 1: Phase portrait of system (1) where $\alpha = 3$.

The above figure shows the phase portrait trajectories of equilibrium point (0,0) is a saddle point, and the system has non-hyperbolic critical point at equilibrium point (1,1). See appendix (A) for maple codes to plot phases portrait of the system. It illustrated that both of the species are induced by a harvesting effort. The behaviour of the solutions in the global and local stability aspect have been examined in section 3.

3 Having Constant Harvest Factors to the Predator - Prey Model

3.1 Constant Harvest Factors

Consider Lotka -Volterra model that has constant harvest factor for prey and predator species.

$$\begin{cases} \frac{du}{d\tau} = u - uv - h \\ \frac{dv}{d\tau} = -\alpha v + \alpha uv - i \end{cases} \qquad (3)$$

Where α, is a quotient between the growth rate of v to times of the growth rate of u, and environmental limit carrying capacity of u and h, i are constant harvest factors. This model is known as a predator-prey model with constant harvesting. To the system above, we will analyse local stability. As the result we analyse points of equilibrium of the system, the u and v null lines are $u = -\frac{h}{v-1}$ and $v = \frac{i}{(u-1)\alpha}$ and it has two equilibrium points (u_1^*, v_1^*) and (u_2^*, v_2^*), where:

$$u_1^* = \frac{-\alpha h + i + \alpha + \sqrt{(h-1)^2\alpha^2 + 2i(h+1)\alpha + i^2}}{-\alpha h - i + \alpha + \sqrt{(h-1)^2\alpha^2 + 2i(h+1)\alpha + i^2}}, \; u_2^* = \frac{\sqrt{(h-1)^2\alpha^2 + 2i(h+1)\alpha + i^2} + (h-1)\alpha - i}{\sqrt{(h-1)^2\alpha^2 + 2i(h+1)\alpha + i^2} + (h-1)\alpha + i},$$

$$v_1^* = \frac{-\alpha h - i + \alpha + \sqrt{(h-1)^2\alpha^2 + 2i(h+1)\alpha + i^2}}{2\alpha} \text{ And } v_2^* = \frac{-\alpha h - i + \alpha - \sqrt{(h-1)^2\alpha^2 + 2i(h+1)\alpha + i^2}}{2\alpha}$$

After we substate equilibrium points (u_1^*, v_1^*) and (u_2^*, v_2^*) in Jacobian matrix given below

$$J = \begin{bmatrix} -v + 1 & -u \\ \alpha v & \alpha u - \alpha \end{bmatrix}$$

also, by lemma (3.1) we have negative real part eigenvalues to equilibrium point (u_1^*, v_1^*) so that this point is a stable critical point. And (u_2^*, v_2^*) is unstable equilibrium point. Thus, the phase portrait of system (3) is shown in finger (2)

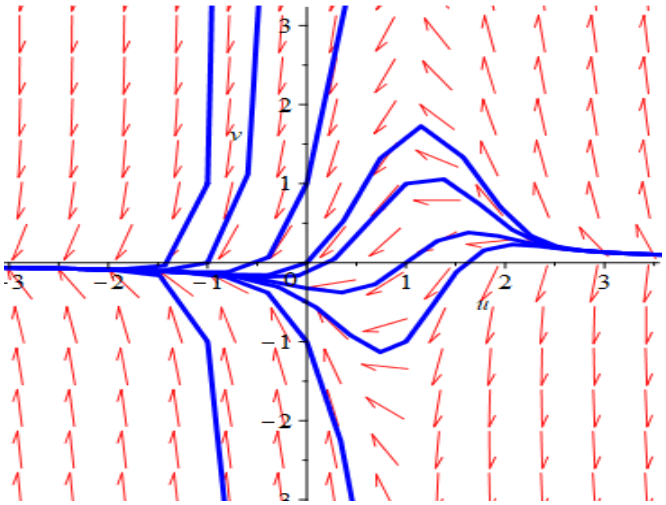

Figure 2: Phase portrait of system (3) where $\alpha = 20, h = 6, i = 5$

Lemma 3.1.1: To a real matrix N, If $tr(N)$, $\det(N)$ and $\det(N^2)$ are all negative, then all the eigenvalues of N have a negative real part. The proof can find in [9] and [10].

One of the most distinctive cases of the system (3) is

$$\begin{cases} \frac{du}{d\tau} = u - uv - h \\ \frac{dv}{d\tau} = -\alpha v + \alpha uv \end{cases} \qquad (4)$$

Where we have only harvesting factor on pray population. And the second specially case of model (3) is

$$\begin{cases} \frac{du}{d\tau} = u - uv \\ \frac{dv}{d\tau} = -\alpha v + \alpha uv - i \end{cases} \quad (5)$$

It is defined as a predator-prey system with a constant harvest factor for predators. The analysis of the above models can be obtained by the same method.

3.2 Having Variable Harvest Factor to the Predator - Prey Model.

Considering the predator-prey model with having effort rate harvested factor for prey and predator. In the following model e_1, e_2 are positive constants that show effort rate to tong prey and predator, respectively.

$$\begin{cases} \frac{du}{d\tau} = u - uv - e_1 u \\ \frac{dv}{d\tau} = -\alpha v + \alpha uv - e_2 v \end{cases} \quad (6)$$

Two particular cases of the system (6) are known as a predator-prey model including prey harvesting (corresponding to prey population) and a predator-prey model with predator harvesting (corresponding to predator population), which can be written as follows, respectively.

$$\begin{cases} \frac{du}{d\tau} = u - uv - e_1 u \\ \frac{dv}{d\tau} = -\alpha v + \alpha uv \end{cases} \quad (7)$$

And

$$\begin{cases} \frac{du}{d\tau} = u - uv \\ \frac{dv}{d\tau} = -\alpha v + \alpha uv - e_2 v \end{cases} \quad (8)$$

To study the stability of the equilibrium points for the above system (6), by using the linearization technique. We find the Jacobean matrix for this purpose, which might be found as follows:

$$J = \begin{pmatrix} -e_1 - v + 1 & -u \\ \alpha v & \alpha u - \alpha - e_2 \end{pmatrix}$$

For equilibrium point (0,0) Jacobean matrix is given by:

$$J_{0,0} = \begin{pmatrix} -e_1 + 1 & 0 \\ 0 & -\alpha - e_2 \end{pmatrix}$$

So $(\lambda_1 = -e_1 + 1)$ and $(\lambda_2 = -\alpha - e_2)$ are eigenvalues of above matrix, as regarding to assumption $e_1 > 1$ thus equilibrium point (0,0) is a stable equilibrium point for the system (6).

At equilibrium point $(-e_1 + 1, 1 + \frac{e_2}{\alpha})$ Jacobean matrix is found out as follows:

$$J = \begin{pmatrix} -e_1 - \frac{e_2}{\alpha} & e_1 - 1 \\ \alpha + e_2 & -\alpha e_1 - e_2 \end{pmatrix}$$

therefor $(\lambda_1 = -e_1 - \frac{e_2}{\alpha})$ and $(\lambda_2 = -\alpha e_1 - e_2)$ are eigenvalues of above matrix, thus equilibrium point $(-e_1 + 1, 1 + \frac{e_2}{\alpha})$ is a stable point for system (6).

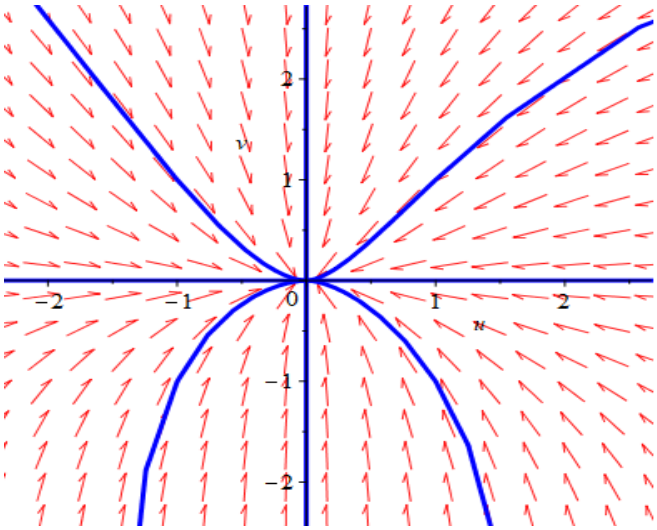

Figure 3: Phase portrait of system (6) where $\alpha = 0.75, h = 5, i = 6$

We identified the following proposition by substituting equilibrium points of the system (7) and (8) and simplifying them.

Proposition 3.2.1. To the system (7) these statements are true:

(i) The point (0,0) is a stable equilibrium point to the system.
(ii) Equilibrium point $(-e_1 + 1,1)$ is locally asymptotically stable in the system (7).

Proposition 3.2.2. Following statements about system (8) are holds:

(i) The point (0,0) is a saddle equilibrium point for system the (8).
(ii) Let $(\frac{e_2}{\alpha} > 0)$ the equilibrium point $(1, e_2 + 1)$ is locally asymptotically stable in the system (8).

Now, we will mix two harvest factors which is called complexed harvest model.

3.3 Complex Harvested Model:

Consider following system with diseases occurs in an environment or there is interspecific rivalry for the predator-prey model. In the present system, harvested factors are u^2 and v^2 for

prey and predator population, separately. However, we may also assume that the following system is a model with having interaction interspecies between prey, and predator species. which may be written as follow:

$$\begin{cases} \frac{du}{d\tau} = u - uv - e_1 u^2 \\ \frac{dv}{d\tau} = -\alpha v + \alpha uv - e_2 v^2 \end{cases} \quad (9)$$

To the above system, we can identify the following theorem.

Theorem 3.3.1. The system (9) has two steady states.

(i) The point (0,0) is saddle equilibrium point, i.e., stable provided ($\alpha > 0$)

(ii) This system is locally asymptotically unstable at its other equilibrium point.

Proof. One of the steady states is (0,0) and the next one is presented by (u^*, v^*).

By using linearization method to show its eigenvalues at equilibrium point (u*, v*) are $\lambda_1 = \frac{3e_1(\alpha + e_2)}{e_1 e_2 + \alpha}$

and $\lambda_2 = \frac{\alpha(-2\alpha + e2(e1 - 3))}{e1 * e2 + \alpha}$, and so, the point is locally asymptotically unstable □.

The behaver of the system is shown in figure (3) provided ($\alpha = 0.8, e_1 = 2, e_2 = 3$)

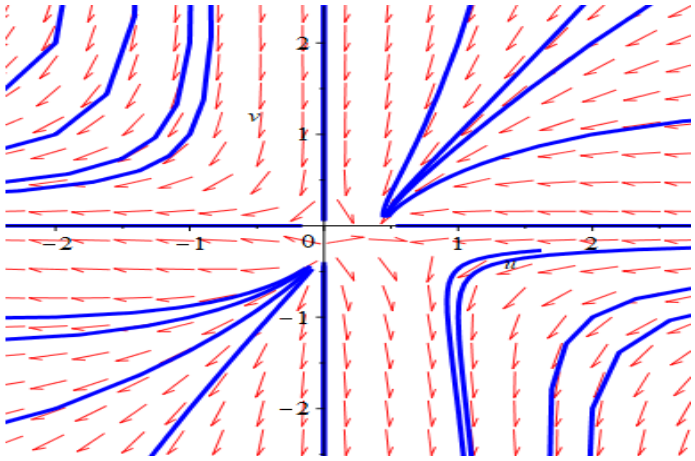

Figure 4: Phase portrait of system (9) where $\alpha = 0.8, e_1 = 2, \ and \ e_2 = 3$

4 Results and Discussions

In the proves systems, we have considered that each of the two species is harvested by constant and effort harvest. In section (3), we calculate the equilibrium points and discussed the state stability of them, also phase portrait of the system (1), (3), (6), and (9) are shown. Here, we sketch the solution curves of different harvest strategies, constant and effort harvest affect. However, for all types of the systems quantitatively relevant data are rarely available. Therefore, we are taking out some hypothetical data, and to explain the results we consider some numerical illustrations and the related solution curves are studied of the models.

Case 4.1. In the suitable units. Instead, the parameter values as $\alpha = 0.78$, the solution curves for Prey-Predator models in the system (2) as follows.

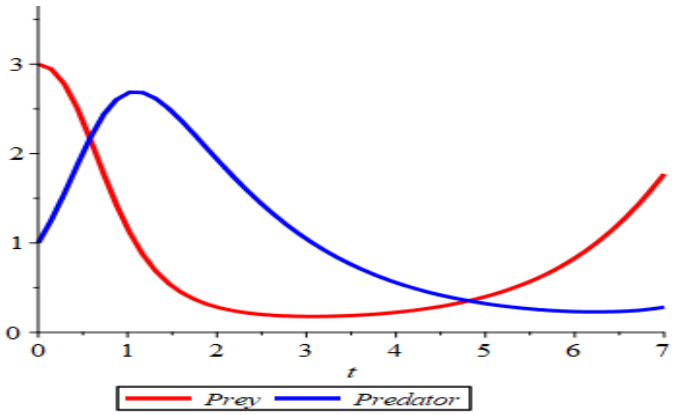

Figure 5: Solution curves of system (2) to the prey–predator model for a period t = 0–7 weeks.

See appendix (B) for maple codes to sketch the solution curves of the system.

Case 4.2. In this illustration, as in the above case, for the parameter α we set $\alpha = 0.78 \; and \; i = 1$, the solution curves for Prey-Predator models in the system (5) as follows.

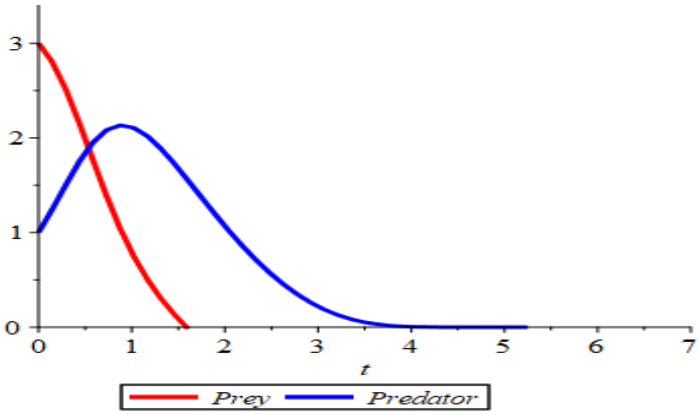

Figure 6: Solution curves of system (5) to the prey–predator model for a period t = 0–7 weeks.

But if we take $e_1 = 1$ in the system (8) then the solution curves shown below.

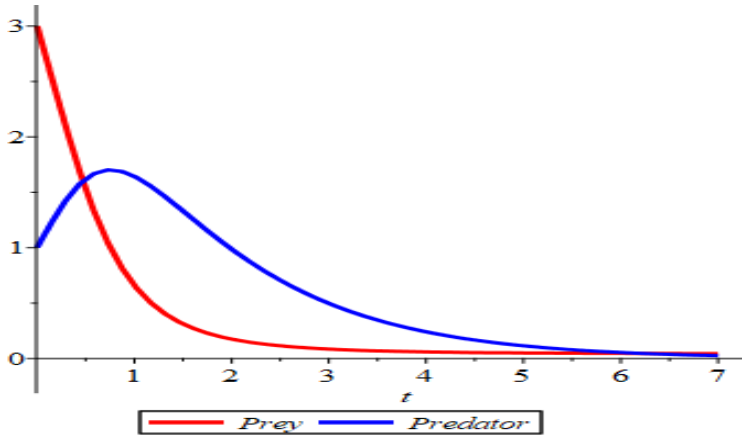

Figure 7: Solution curves of system (8) to the prey–predator model for a period t = 0–7 weeks.

Now, we compare the two harvest strategies constant and effort harvesting of the figures (6) and (7), By looking at the stationary states, from its figures, the population size of both the predator-prey population decline as the harvesting impacts on prey increases. This occurs because of the harvesting impacts which reduces the amount of prey in the environment and therefore reduce predator-on-prey food supplies, leading both populations to decline.

5 Conclusion

In the presented research, we studied the impact of various harvest rates on Lotka-Volterra predator-prey population which the pray population is governed by the logistic law of growth to hesitate effect of harvest rate, as a realistic parameter. Therefore, in this project, we have shown that the harvest rate has a positive impact on the Lotka-Volterra model predator-prey population increasing global stability. In addition, we have seen that the impact of harvesting activity is more significant in the system. The purpose of this impact can be explained by combining two types of prey and predator. The dynamical behaviour of the unexploited system is studied. It is found to possess two equilibria (0,0) and (u*, v*). This assumption may be used to describe the positive efficacy of controlled use of nature.

Appendix A : Maple codes to skitch phase portrait of the system (2)

```
> restart; with(DETools); with(plots); with(LinearAlgebra);
> sys := {diff(u(t), t) = u(t) - u(t)*v(t), diff(v(t), t) = -alpha*v(t) + alpha*u(t)*v(t)};
> ics := seq(seq([0, i, j], i = -2 .. 2), j = -2 .. 2);
> DEplot(subs({alpha = 3}, sys), {u(t), v(t)}, t = -1 .. 4, u = -3 .. 3, v = -3 .. 3, [ics], linecolor = blue);
```

Appendix B: Maple codes to skitch the solution curves the system (2)

```
> restart; with(DETools); with(LinearAlgebra); with(plots);
> sys1 := {diff(u(t), t) = u(t) - u(t)*v(t), diff(v(t), t) = -alpha*v(t) + alpha*u(t)*v(t)};
> ics := [[0, 3, 1]];
> figu := DEplot(subs({alpha = 0.78}, sys1), {u(t), v(t)}, t = 0 .. 7, u = 0 .. 4, v = 0 .. 4, ics, scene = [t, u(t)]);
> figv := DEplot (subs({alpha = 0.78}, sys1), {u(t), v(t)}, t = 0 .. 7, u = 0 .. 4, v = 0 .. 4, ics,
```

scene = [t, v(t)]);
> display([figu, figv], color = ["red", "blue"], legend = [Prey, Predator]);

Funding

This research received no external funding.

Acknowledgements

Authors contribution

Azhi Sabir contributed in the original draft preparation, methodology, formal analysis. Hiwa Abdullah contributed in the writing, validation, review and editing. Awder Rasul contributed in the computational simulations, formal analysis. Surme Rasul contributed in validation, methodology, formal analysis.

Conflict of interests

The authors declare no conflicts of interest.

References

1. Rahmani Doust, M. and S. GHolizade, *The Lotka-Volterra Predator-Prey Equations.* Caspian Journal of Mathematical Sciences (CJMS), 2014. **3**(2): p. 221-225.
2. Ghosh, M., P. Chandra, and P. Sinha, *A mathematical model to study the effect of toxic chemicals on a prey-predator type fishery.* Journal of Biological Systems, 2002. **10**(02): p. 97-105.
3. Ang, T.K., H.M. Safuan, and J. Kavikumar, *The impacts of harvesting activities on prey-predator fishery model in the presence of toxin.* Journal of Science and Technology, 2018. **10**(2).
4. Rahmani, D.M. and M. Saraj, *The logistic modeling population: Having harvesting factor.* Yugoslav Journal of Operations Research, 2015. **25**(1): p. 107-115.
5. Rahmani, D. M. & Saraj, M. *The logistic modeling population: Having harvesting factor.* Yugoslav Journal of Operations Research, 25, 107-115. 2015
6. Das, T., Mukherjee, R. & Chaudhuri, K.*Harvesting of a prey–predator fishery in the presence of toxicity.* Applied Mathematical Modelling, *33, 2282-2292.* 2009
7. Yalong Xue, Fengde Chen, Xiangdong Xie, Shengjiang Chen. An analysis of a predator-prey model in which fear reduces prey birth and death rates[J]. AIMS Mathematics, 2024, 9(5): 12906-12927. doi: 10.3934/math.2024630
8. Ilyasse Lamrani, Imad El Harraki, M. A. Aziz-Alaoui, Fatima-Zahrae El Alaoui. Feedback stabilization for prey predator general model with diffusion via multiplicative controls[J]. AIMS Mathematics, 2023, 8(1): 2360-2385. doi: 10.3934/math.2023122
9. McCluskey, C.C., P.J.J.o.D. van den Driessche, and D. Equations, *Global analysis of two tuberculosis models.* 2004. **16**(1): p. 139-166.
10. Saraj, M., M. Doust, and F. Haghighifar, *The stability of Gauss model; having harvested factor.* 2012.

Using classification data mining methods to predict the level of efficiency of services in dental clinics during the COVID-19 pandemic

Anhar K.ALDeen Mohammed[1]
Reem Ali AL-Jarah[2]
[12] Mosul University/IRAQ
[1]Rivrskm2023@yahoo.com
[2] reemaljarah@yahoo.com

Using classification data mining methods to predict the level of efficiency of services in dental clinics during the COVID-19 pandemic

Anhar K.ALDeen Mohammed[1]
Reem Ali AL-Jarah[2]
[12] Mosul University/IRAQ
[1]Rivrskm2023@yahoo.com
[2] reemaljarah@yahoo.com

Abstract

The Covid-19 pandemic has always affected all life facilities, dental clinics, like other institutions. research goal is to reach the patient's evaluation of the competency of the service offered to him in the clinic during the pandemic.
Three classification- data mining algorithms -decision tree, logistic regression and cluster analysis- were used to rank clinic reviewer opinions.
Using the programming languages (HTML, PHP, My-SQL) an electronic system has been created that provides services and facilitates the procedures for organizing reservations and making appointments.....Etc., according to the necessary, safety instructions during the pandemic. The System Development Lifecycle (SDLS) methodology is used to determine the level of service efficiency, and ODBC is used to send data from the database to SPSS-V26.

The study variables, like the possibility of returning to the clinic, which has the greatest potential to classify observations and is contributing the most to differentiating for each of the two clusters, have a statistically significant relationship with the likelihood that you will recommend this clinic to others, A list of findings were included in the research's conclusion..
Keywords: *Database, Relational Database, SQL, ODBC, Multivariable Analyses , CHIAID algorithm, Logistic Regression algorithm, Two-Step Clustering algorithm, Dental Clinics*.

Introduction

Health institutions seek to prove their existence, by providing the best possible services, especially providing the best is the key to achieving progress and excellence to reach the highest levels of satisfaction, as the patient has become the focus of attention.

many clinics have stopped working due to the risks faced by health workers, at a time when demand has decreased due to patients' "fear" of resorting to services. And while the dentists are taking more precautions at the moment, many of these procedures are just an extension of their regular routine. A spokesperson for the American Dental Association stated: **"In dentists'** offices, we used to take comprehensive preventive measures, such as disinfection and personal protective equipment (PPE), before they became common**."**

The patient's condition, "may be unprepared, worried about his health, or looking after an elderly relative, or afraid to see a doctor, so he acts cautiously and does not want to take risks", Thus, the person responsible for fixing the reservation in the clinic is constantly working to deal with the many postponed appointments, and communicates with patients who are scheduled to

undergo treatment to organize alternative appointments. In our research, we highlight the level of services in government and private dental clinics during the COVID-19 pandemic and their opinion of the preventive and curative services provided. In this research , Data mining techniques were used, such as algorithm of (CHAID tree, logistic regression and clustering), to reach the goal of the search.

There are some studies were done in the same filed but in another place ,such as a study got in a "Valencia primary dental care facility- SPINE" to assess parents' contentment with the dental care their kids, by using CHAID algorithm and decision tree , the researchers conclude the parents who participated in study were contented with the of their children received[1]. Also, by using the statistical modeling and CHAID analysis ,. et.al. [2] . conclude that there is an urgent need to create inclusive public policies because the state's epidemic is getting worse. Another study for [3] . It uses conventional psychometric measures to assess healthcare personnel's reported psychological well-being by using the decision tree model

Not only in the health field, the CHAID algorithm was applied. A case study: the National Opinion Research Center of the U. S. chose to assess the job satisfaction in the U. S. and and the factors affecting it.[4].

In order to better the education institution, researchers took refuge to use the CHAID algorithm and decision tree to examine students' perceptions of the academic program and student services offered by the university to discuss how to upgrade their establishment.[5].

1. Theoretical Part

There are several techniques in data mining, the selection of the appropriate ones depends on the nature and size of the data under study[6], Data mining can be implement in comparison with the data market and data store. Fig(1) showing the data mining technique which can use .

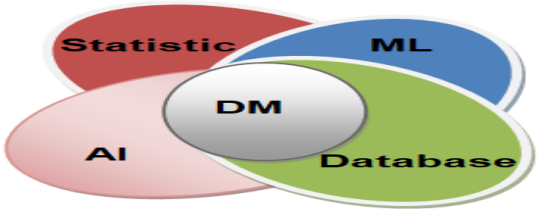

Fig1:Data Mining Technique
Sourc:[6]

There is no specific theory based on to choose the appropriate data minig technique, Usually the choice is made based on the experience in this field and the actual techniques effective, the superlative between traditional techniques and modern techniques to the extent that the appropriate tools are available, However, with the increase of experience, we can evaluate the options and select the appropriate ones for the application. [7] .

1.1 Data Mining Models

As fig(2) showe, the Predictive Model : It works on the future prediction of the mechanism of data work, based on a model whose data has been previously trained.[8][9] .

The Descriptive Model : It analyzes the data in order to extract the relationships and correlations between them, and to reveal the characteristics of the data to build a model that did not exist previously. For instance, Clustering Analysis،Association Rules Analysis ،..etc

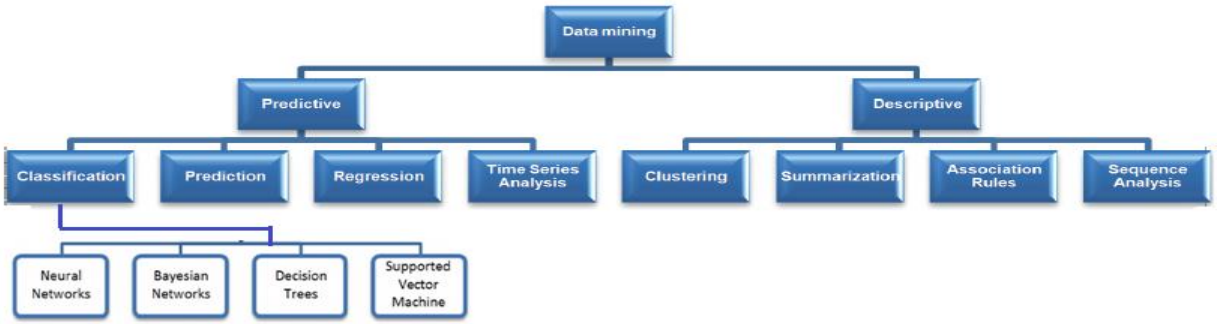

Fig2:Dataminig
Sourc:[9]

1.2 Data Mining Technique

Research progress in data mining and knowledge discovery, has led to the many of data mining techniques coming to lights , which are built on three strong technical pillars: database, mathematical statistics, and artificial intelligence, our interest in this researchare

1.2.1 Classification

The major goals of a Classification algorithms are to make the predictive accuracy obtained as large as possible by the classification model[6] [10] .

1.2.2. Decision Tree

"uses as a predictive model which maps observations about an item to conclusions about the item's target value".[11] [12], The algorithm which used in this research is CHAID ("Chi-squared Automatic Interaction Detection") [13], it's a technique depends on the $\chi 2$_test - eq.1- and employs a step-by-step procedure

The creating of nodes and sub-nodes among the predictor variables is significant.[14] [15].

$$\mathcal{X}^2 = \sum \frac{(E_{ij} - O_{ij})^2}{E_{ij}} \dots\dots\dots (1)$$

1.2.3. Logistic regression

is "a method in which the Y response variable has a binomial distribution. To determine probabilities of success P(Y = 1|X), and defeat P(Y = 0|X).[16] [17] The odds are defined as in eq.2" .[18] .

$$(\Theta) = \frac{P(Y = 1|X)|}{P(Y = 0|X)} = \frac{P(Y = 1|X)}{1 - P(Y = 1|X)} \dots\dots\dots (2)$$

"The linear dependencies between log-odds-logit- and input variables are analyzed as" in eq.3

$$\ln(\Theta) = \ln\left(\frac{P(Y = 1|X)}{1 - P(Y = 1|X)}\right) = X\beta \dots \rightarrow P(X, \beta) = \frac{e^{X\beta}}{1 - e^{X\beta}} \dots\dots\dots (3)$$

where $\beta = (\beta 1, \dots, \beta m) \in R^m$. From Equation (3) [19]

Two-Step Cluster algorithm

"is a statistical method[9] for assigning data into subgroups with related characteristics" [7].

The procedure is performed by constructing a cluster feature (CF) tree, which contains the cluster centers.

"To automatically determine the number of groups, the method uses BIC (Schwartz Bayesian Information Criterion) or AIC (Akaike Information Criterion) which is calculated for each

number of clusters from a given range; This indicator is then used to find a preliminary estimate of the number of clusters."[20] For groups J, the two indicators are calculated according to equations (4) and (5) below:

$$BIC(J) = -2\sum_{j=1}^{J} \xi_j + m_j \log N \dots\dots (4)$$

$$AIC(J) = -2\sum_{j=1}^{J} \xi_j + 2m_j \dots\dots\dots (5)$$

where

$$m_j = J\left\{2K^A + \sum_{k=1}^{K^B}(L_k - 1\right\} \dots (6)$$

$$t = \frac{\hat{\mu}_k - \hat{\mu}_{sk}}{\hat{\sigma}_{sk}}\sqrt{N_k} \dots\dots\dots\dots (7)$$

$$\chi^2 = \sum_{l=1}^{L_k}\left(\frac{N_{skl}}{N_{kl}} - 1\right)^2 \dots\dots\dots (8)$$

2.Materials & Methods

In order to obtain the necessary data, a questionnaire - with three point Likert Scale (Agree, Neutral, Disagree)- was designed that includes factors of interest to dental clinic references during the Covid-19 pandemic, and distributed to reviewers in different dental clinics.

X1:Gendar, **X2**:Age(20-,30-,40-,50-59), **X3**: Kind's clinic (Private, general)**,** **X4**: Help in booking an appointment at the clinic**,** **X5:** The receptionist pays attention to you and obliges you to follow prevention methods (wearing a mask and gloves), **X6**: The time between your request for an appointment and your presence at the dentist, **X7**: Adequate working hours, **X8**: Cleanliness of the clinic and the provision of means of dusting, sterilization and appropriate ventilation, **X9**: Conducting a preliminary examination for those who enter the clinic as an indicator of temperature or something else, **X10**: Not allowing the patient to accompany him, except in critical cases, **X11**: Availability of a waiting room with social distance, **X12**: acceptable waiting period for the patient to see the dentist, **X13**: Availability of a worker responsible for wiping surfaces and door knobs periodically during working hours, **X14**: Measures taken to prevent infection in the patient's examination room, **X15**: The measures taken by the clinic staff to protect you from infectious diseases and radiation, **X16**: The period of stay for the dentist with you, **X17:** The interest shown by the dentist about your questions or concerns, **X18**: Explain your treatment options in an understandable manner, **X19**: The competence of the dental assistant and his interest in guiding and educating you to maintain oral and dental health, **X20**: Information provided on ways to avoid dental problems in the future, **X21**: Comprehensive examinations and treatment, **X22**: The interest shown by the dentist in general, **X23**: Overall evaluation of the care provided in the dental clinic, **X24**: Collaboration and teamwork demonstrated by the dentist's team, **X25**: General assessment of the skill of the dentist, **X26**: Your trust in the dentist, **X27**: Possibility to review the clinic again when needed, **Y**: Chances that you will recommend this clinic to others. Reliability was calculated using Cronbach's alpha.

2.1 Databases System

Databases are designed to suit the movement and flow of data in addition to organizing the operations of saving, recovery and modification, in consideration the availability of access and protection, and the possibility of expanding these databases, whether in terms of the increase in the number of users or data or tables and the resulting complexity in query sentences, Fig(3) shows – respectively- the database table and relation database of our system

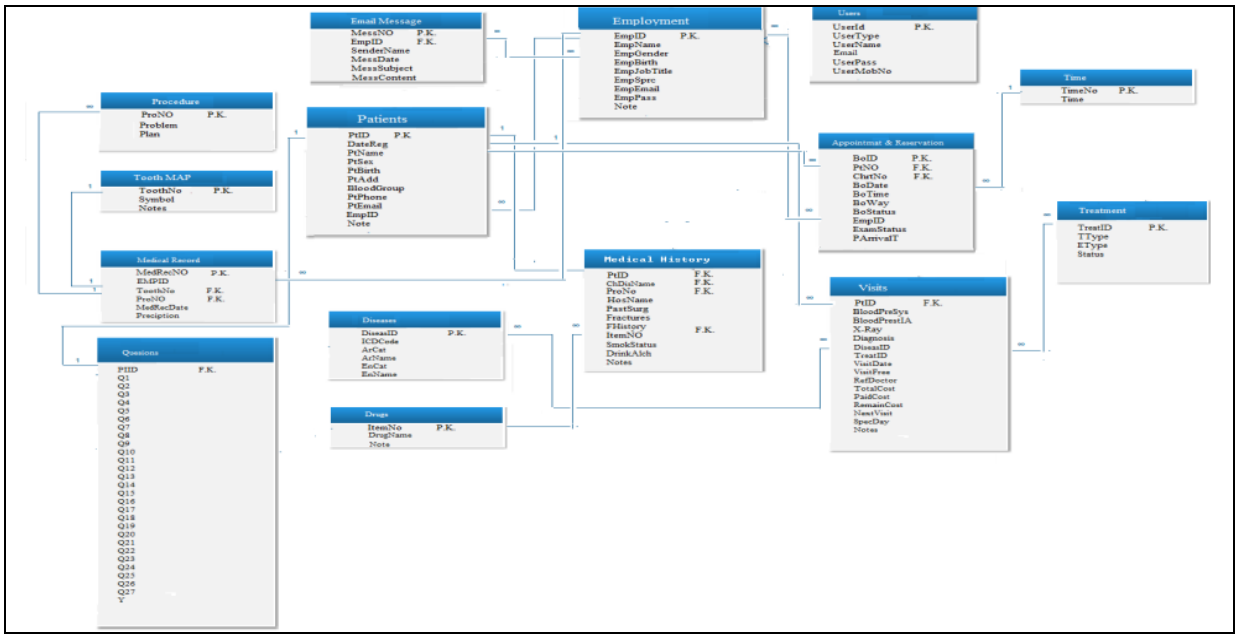

Fig(3): Relational Database

To take advantage of the volume of available data and the above-mentioned databases, an has been created, in line with modern technology in the use of databases, which can be linked to other systems.

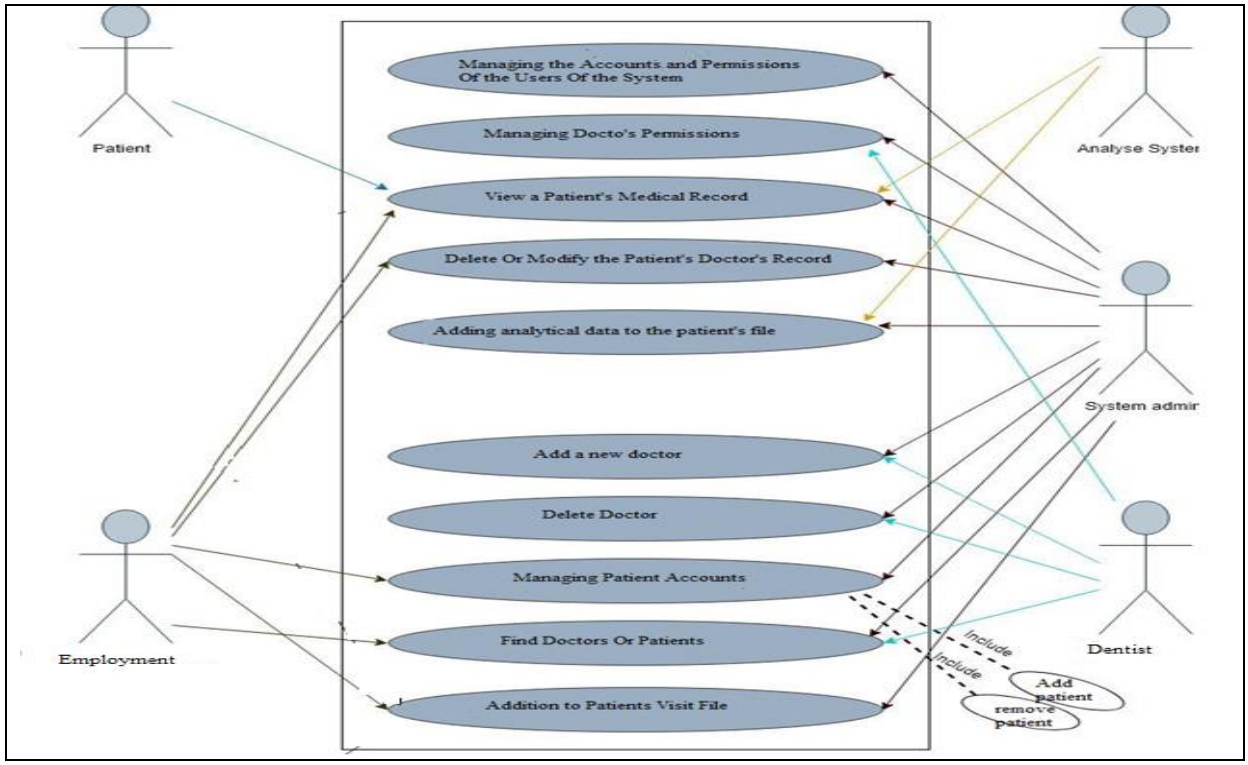

Fig.(4): analyze system(User Case)

When logging in, and in order to be ensure about the protection of information, the user is allowed to log into the system with his name, password and doctor ID number.

The system, not only doesn't allow its users to access the account of others and see their private information, but also restricts the content of the screens according to the user permission.

The (PHP) language ensures protection by rejecting repeated attempts to log in, NOSQL Injection, and activating all authentication functions to ensure the correct entry.

Some features of the system are Adding, Viewing, Modifying, Deleting, And Searching.

The doctor or his assistant are allowed to add everything new to the patient's visit profile, starting from the status of his booking - new, confirmed, postponed, canceled - and the required data on the visit schedule, new patient mean new file open, View the patient's medical record by entering his number , modify or delete the patient's medical record , Allow users to inquire about doctors or patients by number, full name, or username of the doctor or patient.

2.2 CHAID Algorithm

Table (2-2-1) : Model Summary of CHAID method

Specifications	Dependent Variable	Y
	Independent Variables	$X_1 - X_{27}$
	Validation	none
	Maximum Tree Depth	3
	Minimum Cases in Parent Node Minimum Cases in Child Node	100
	Minimum Cases in Child Node	50
Results	ndependent Variables Included	X_1 , X_7 , X_{27}
	Number of Nodes	7
	Number of Terminal Nodes	4
	Depth	3

Tree diagram in figure (5) show, the most significant independent variable is **X_{27}**: "Possibility of revisiting the clinic",

X_{27} at α=0.001: ($\varkappa^2 = 165.221, df = 2, p_{value} = 0.000$). As the first steep, it splits the sample of (407) responses, into 2 groups containing different groups of X_{27} presented as node 1 & 2. The first node, included (215) respondents from the variable X_{27} which coded (3: disagree), while the second one is terminal node included (92) respondents from the variable X_{27}, which coded (1: agree, and 2: neutral) within tree's second level , one statistically significant variable Adequate working hours (X_7) is identified at α=0.05, ($\varkappa^2 = 14.853, df = 2, p_{value} = 0.002$), which in turn leads us to the third and fourth node. Node3, included (150) respondents from the variable X_7 which coded (3: disagree), while Node4, included (50) respondents from the variable X_7 which coded (1: agree, & 2: neutral).

Within tree's third level(final) :

Gender: X_1, it is significant for splitting of Nodes5 and Nodes6 at α=0.05, $\varkappa^2 = 6.253, df = 1, p_{value} = 0.012$

Generally, the leaf tree frame, (fixed as 4, 5 & 6) pertain to (3: disagree with recommend this dental clinic to others), and one (marked as 2) pertain to (2: indifferent to recommend this dental clinic to others).

In fact, the track from the root to the leaf nodes produce some rules for classifying reviewers' opinions (in one of the variable-specific categories, for example, the rule in Node6: Who does not want to visit the dental clinic again, and the working hours are not suitable for him , 89.6% would not advise anyone else to visit this clinic, and the other rules derived can be explained by a similar tactic.

To finish the process of classification, all its performance have been assessed. Our findings suggest that if the reviewers' opinions in terms of the 3 indep.var. are known, the hazard of inaccurately classified -based on entire sample- is 17.9%, with std. Error is 0.02.

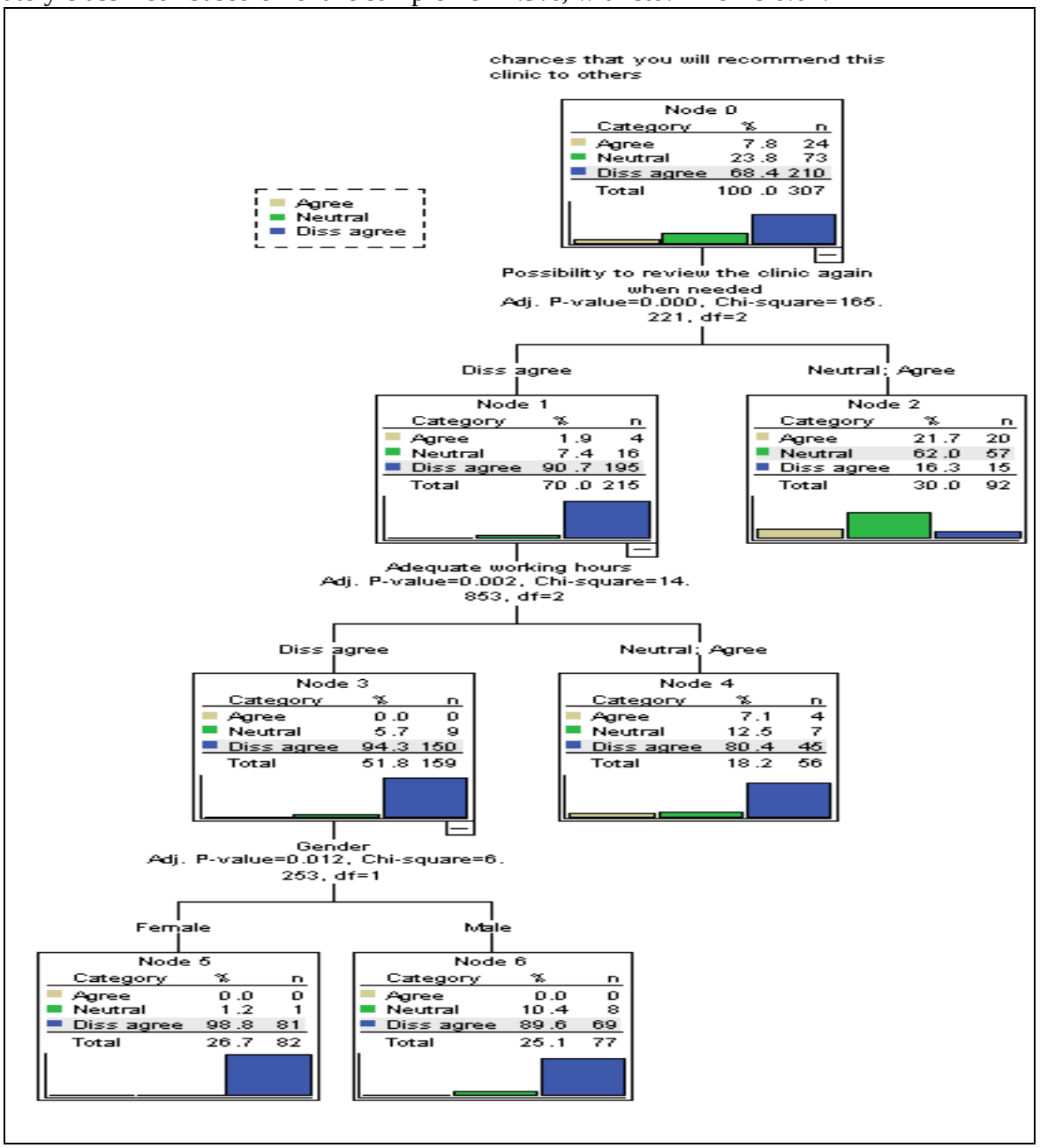

Fig. (5) Decision tree analysis with CHAID model.

Table (2-2) presents the classification CHAID

Table (2-2-2): Classification CHAID

Reviewers' Opinions		Predicted			Correctly Classified
		Agree	Neutral	Diss. agree	
Observed	1:Agree	0	20	4	0.0 %
	2:Neutral	0	57	16	78.1 %
	3:Diss-agree	0	15	195	92.9 %
	% Over all	0.0	30.0	70.0	82.1 %

In accordance with the table (2-2-2), It can be said that in general the accuracy of the model is 82.1%, the model accurately ranked (252) out of (297) in the sample under discuss. Significant differences can be observed in the classification accuracy, according to the categories of the variable.

2.3 Multinomial Logistic Regression (MLR) Algorithm

The(MLR) model's estimation and testing steeps is "The chances that you will recommend this clinic to others".

Independent categorical variables (27) were selected for inclusion in the multivariable logistic regression model. As shown in Table (2-3-1), the χ^2 test for the last model, the 2 - Log Likelihood for the full model (86.835) less than it is for the null model (491.546), the likelihood ratio represents the unexplained variance in the outcome variable.

The Likelihood Ratio chi-square test which is a test of goodness-of-fit, for model predicts, χ^2 (106) = 404.710, $p < 0.001$,

Table (2-3-1) :Model Fitting Information

Model	Model Fitting Criteria	Likelihood Ratio Tests		
	-2 Log Likelihood	Chi-Square	df	Sig.
Intercept Only	491.546			
Final	86.835	404.710	106	.000

the resp. var. explained by the predictors indep.var., 73.2% of the variance in dep. variables (the proportion of variance) according to "Cox and Snell R^2 " value, 91.7 % according to " Nagelkerke R^2 " value, and 82.3% according to "McFadden R^2" value.

Table (2-3-2) illustrates the likelihood ratio test, As the results shown, it can be seen that relationship between some of the independent variables (X_{27},X_{26},X_{24},X_{21} respectively) and the dependent variable is a statistically significant

Table (2-3-2): Evaluate the relationship between independent variables and the dependent variable.

Effect	Model Fitting Criteria	Likelihood Ratio Tests		
	2_Log Likelihood of Reduced Model	Chi-Square	DF	Sig.
Intercept	86.835	.000	0	.
X_1	88.918	2.082	2	.353
X_2	90.194	3.358	6	.763
X_3	90.223	3.387	2	.184
X_4	94.973	8.138	4	.087
X_5	92.836	6.001	4	.199
X_6	88.825	1.990	4	.738
X_7	88.648	1.813	4	.770
X_8	87.794	.959	4	.916
X_9	87.979	1.143	4	.887
X_{10}	86.845	.009	4	1.000
X_{11}	88.213	1.378	4	.848
X_{12}	89.333	2.497	4	.645
X_{13}	94.873	8.038	4	.090
X_{14}	90.868	4.033	4	.402
X_{15}	88.836	2.001	4	.736
X_{16}	88.023	1.188	4	.880
X_{17}	91.994	5.159	4	.271
X_{18}	88.067	1.232	4	.873
X_{19}	88.015	1.179	4	.881
X_{20}	89.694	2.859	4	.582
X_{21}	96.904	10.068	4	.039
X_{22}	92.380	5.545	4	.236
X_{23}	88.697	1.862	4	.761
X_{24}	96.790	9.955	4	.041
X_{25}	86.933	.098	4	.999
X_{26}	101.653	14.817	4	.005
X_{27}	394.129	307.294	4	.000

Correct classification rates for the MLR model as shown in Table (2-3-3), It indicate that the accuracy of the model is 95.4, and the expected values according to the dep. variable (7.8, 22.5, 69.7) % isn't significantly different from that in the main data (100.0, 87.7, 97.6) %.

Table(2-3-3) :classification rates for the MLR model

Observed	Predicted			Correctly Classified
	Agree	Neutral	Disagree	
1:Agree	24	0	0	100.0%
2:Neutral	0	64	9	87.7%
3:Diss-agree	0	5	205	97.6%
% Over all	7.8%	22.5%	69.7%	95.4%

2.4 Cluster Analysis

As shown in table (2-4-1), although the lowest "BIC coefficient" is for 7 clusters, according , the optimal No. of clusters is two, because the lowest value of the Schwarz's Bayesian Criterion as well as the largest proportion of space is for two clusters.

Table (2-4-2): Cluster Distribution

Number of Clusters	Schwarz's Bayesian Criterion (BIC)	BIC Change	Ratio of BIC Change	Ratio of Distance Measures
1	13879.447			
2	12679.278	-1200.170	1.000	2.198
3	12304.983	-374.295	.312	1.579
4	12183.328	-121.654	.101	1.117
5	12107.391	-75.937	.063	1.239
6	12106.766	-.625	.001	1.382
7	12193.355	86.589	-.072	1.052
8	12291.273	97.917	-.082	1.070
9	12403.394	112.122	-.093	1.130
10	12538.898	135.504	-.113	1.065

The clusters distribution is shown in Table (2-4-2

Table (2-4-2): Cluster Distribution

		N	% of Combined	% of Total
Cluster	1	240	78.2%	78.2%
	2	67	21.8%	21.8%
	Combined	307	100.0%	100.0%
Total		307		100.0%

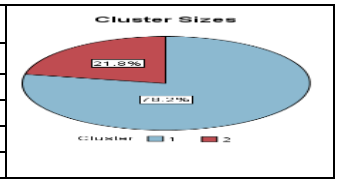

From cluster quality in fig (6) show the value of average silhouette is 0.358

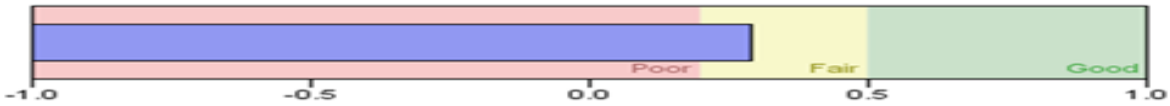

Fig. (6): Silhoutte measure of cohesion separation

As our interest is to know the important variables that affect the opinion of reviewers to visit the dental clinic during the Covid-19 pandemic, fig (7) show that X_{27} , X_{21} then X_{26},X_7,X_{24}, X_{13},X_{17} are the most contribute to differentiating the first cluster and X_{27} , X_{24} , X_{21}, then X_{13}, X_{17} , X_1 differentiate the second

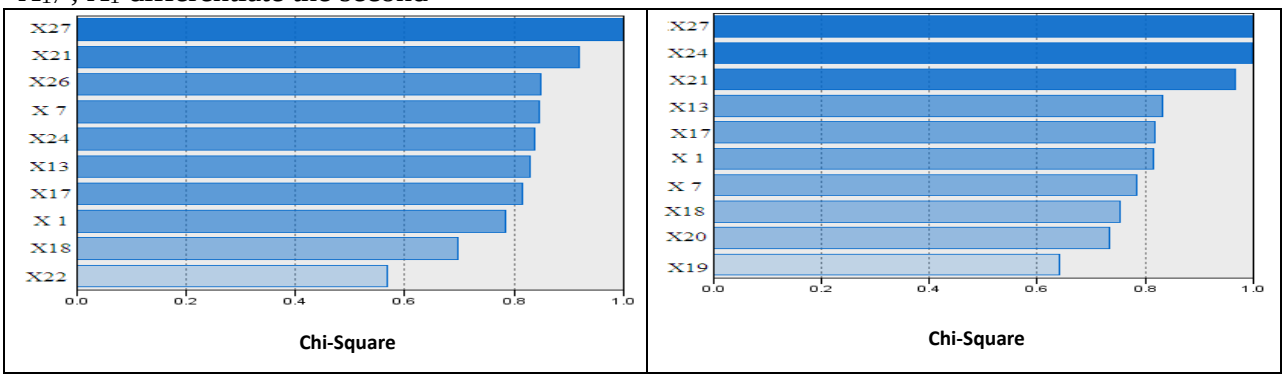

Fig (7) : Variables Importance for Clusters one & cluster 2

2. Conclusion

In accordance with CHAID Algorithm, In general the model accuracy is very good. Although the differences can be observed in the classification accuracy, the our data the variable X_{27}: Possibility of revisiting the clinic has the biggest potential to classify observations

In accordance with Multinomial Logistic Regression Algorithm (MLR), The change value of Model Fitting Criteria for the final model and the null model indicate better fit, and the test of goodness-of-fit indicates significant model predicts. From Cox and Snell R2 value, Nagelkerke R^2 value, McFadden R^2 value, the predicted model was able to explain the variance in the conviction of individuals well. There is a statistically significant relationship between: (X_{21}: Comprehensive examinations and treatment), (X_{24}: Collaboration and teamwork demonstrated by the dentist's team), (X_{26}: Your trust in the dentist), (X_{27}: Possibility to review the clinic again when needed) and the dependent variable (y: Chances that you will recommend this clinic to others). The correct classification rates for the MLR model are highly valued, on other hand, there is no significant different between the expected values of the dep. variables and the main data.

In accordance with 2-steeps cluster algorithm indicate that The optimal number of clusters is two, with size 78.2% and 21.8% respectively. From silhouette measure, the cluster quality is fair. The categorical variables which contribute the most of differentiating for each two cluster are: (X_{27}: Possibility to review the clinic again when needed) ,(X_{24}: Collaboration and teamwork demonstrated by the dentist's team) and (X_{21}: Comprehensive examinations and treatment).

Reference:

[1] Carmen Llena; Gonzalo Clemente and Leopoldo Forner,2010," Parental Satisfaction with Children's Primary Dental Care in Valencia, Spain", Primary Dental Care 2011 ; 17(4):25-30, DOI:10.1308/135576111794065739

[2] Fabrício P. A. ; Fabrício Pelizer Almeida ; Moisés Keniel Guilherme de Lima ; Demóstenes Coutinho Gomes ; Esther Ferreira de Souza,2020, "Logistic Regression Models and Classification Tree for Deaths and Recovered Patients Records of Covid-19 in the State of Minas Gerais, Brazil", IJAERS, Vol-7, Issue-10,OCT.(2020), ISSN: 2349-6495(P) | 2456-1908(O), https://dx.doi.org/10.22161/ijaers.710.16

[3] Anirban Ray ; Debjani Sen Gupta ; Jayasree Sar Choudhury ; Pramit Ghosh , "Resilience of Healthcare Providers during COVID-19 Pandemic: A Rapid Assessment using Digital Platform", Journal of Clinical and Diagnostic Research.2022 Dec, Vol-16(12): VC01-VC07
DOI: 10.7860/JCDR/2022/53497.17198

[4] Farhad Sheybani; 2019, "Predicting the Individuals' job satisfaction and determining the factors affecting it using the CHAID Decision Tree Data Mining Algorithm, Case Study: the National Opinion Research Center of the United States.", EJERS, European Journal of Engineering Research and Science, Vol. 4, No. 3, March 2019, DOI: http://dx.doi.org/10.24018/ejers.2019.4.3.1169

[5] Maryli F. Rosas; Shaneth C. Ambat; Alejandro D. Magnaye; John Renbert F. Rosas, 2019, "Classification and Regression Decision Tree: A Mining Technique for Students' Insights on the University Services with Text Analysis", 9th IEEE Annual Ubiquitous Computing, Electronics & Mobile Communication Conference (UEMCON) , DOI: 10.1109/UEMCON44053.2018

[6] Dimitrios Papakyriakou & Loannis S. Barbounakis, " Data Mining Methods: A Review", International Journal of Computer Application, Volume 183, No.48, 2022,5-19. DOI: 10.5120/ijca2022921884

[7] Kun Gao; Hassan Ali Khan; Wenwen Qu, 2022, "Clustering with Missing Features: A Density-Based Approach", Song-Kyoo (Amang) Kim and Chan Yeob Yeun, 14(1),60, 2022, https://doi.org/10.3390/sym14010060

[8] Gaurav Gosavi; Gajanan Gawde, 2022, "Prediction Techniques for Data mining", National Conference on Emerging Trends in Computer Engineering and Technology.

[9] Kwame Boakye Agyapong; Dr. J.B Hayfron-Acquah; Dr. Michael Asante,2016, "An Overview of Data Mining Models(Descriptive and Predictive)",: International Journal of Software & Hardware Research in Engineering, Vol. 4 ,Issu. 5, ISSN-2347-4890.

[10] Sudhir M. Gorade; Ankit Deo; Preetesh Purohit ,2017, "A Study of Some Data Mining Classification Techniques", International Research Journal of Engineering and Technology (IRJET), , e-ISSN: 2395 -0056 , p-ISSN: 2395-0072 Vol. 04 Iss. 04,.

[11] Himani Sharma ; Sunil Kumar,2013, "A Survey on Decision Tree Algorithms of Classification in Data Mining", International Journal of Science and Research (IJSR), ISSN (Online): 2319-7064, Index Copernicus Value (2013): 6.14 | Impact Factor (2015): 6.391.

[12] Bahzas Taha Jijo; Adnan Mohsin Abdulazeez; 2021,Classification Based on Decision Tree Algorithm for Machine Learning, Journal of Applied Science and Technology Trends 2(01):20-28, DOI:10.38094/jastt20165

[13] Naim Monjezi, 2021,The Application Of the CART and CHAID Algorithms insugar Beet Yield Prediction ,Basrah J.Agric.Sci.,34(1):1-13
[14] Murat Gunduz ; Ibrahim AL-Ajji,2021, "Employment of CHAID and CRT decision tree algorithms to develop bid/no-bid decision-making models for contractors" , Engineering, Construction and Architectural Management, ISSN: 0969-9988, https://www.emerald.com/insight/0969-9988
[15] Etik Zukhronah; Yuliana Susanti; Hasih Pratiwi; Respatiwulan and Sri sulistijowati H. ,2021, "Decision tree technique for classifying cassava production", AIP Conference Proceedings : Vol. 2021, Iss. 1 .10.1063/1.5062777, https://doi.org/10.1063/1.5062777.
[16] Andrew Gelman; Jennifer Hill; Aki Vehtar; 2022, "Regression and Other Stories" ,Andrew Gelman, Jennifer Hill, and Aki Vehtari, ch. 13,pp217-237
[17] Tomasz Rymarczyk; Edward Kozłowski; Grzegorz Kłosowski; Konrad Niderla, 2019: "Logistic Regression for Machine Learning in Process Tomography", Sensors *19*(15), 3400, https://doi.org/10.3390/s19153400.
[18] Andrés Villanueva Manjarres ; Luis Gabriel Moreno Sandoval ; Martha Salinas , "Data Mining techniques applied in educational environments: Literature review"; Digital Education ; Number 33; 2023
[19] Sixiang Jia ; Haochen Mou ; Yiteng Wu ; Wenting Lin ; Yajing Zeng ; Yiwen Chen ; Yayu Chen ; Qi Zhang ; Wei Wang ; Chao Feng and Shudong Xia,2022: "A Simple Logistic Regression Model for Predicting the Likelihood of Recurrence of Atrial Fibrillation Within 1 Year After Initial Radio-Frequency Catheter Ablation Therapy", Frontiers in Cardiovascular Medicine , https://doi.org/10.3389/fcvm.2021.819341
[20] Daniela Şchiopu; "Applying TwoStep Cluster Analysis for Identifying Bank Customers' Profile", Seria Ştiinte Economic, Vol. LXII, No. 3, 2010, pp66-75.

Appendix(1)

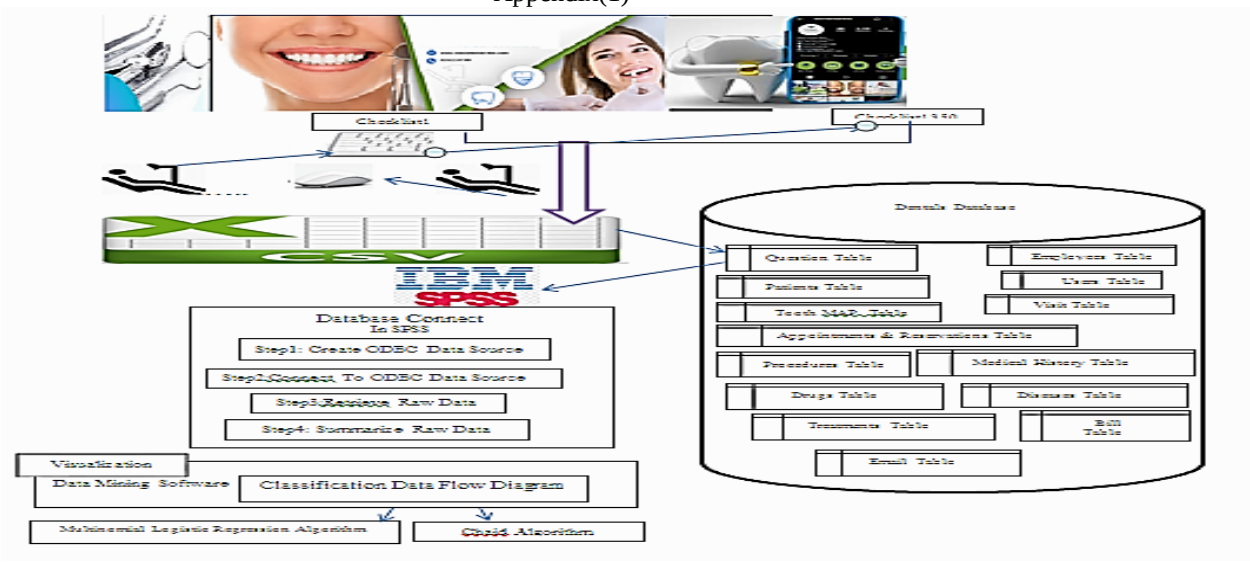

Construction of the (k, r)-caps in the projective 3-space PG(3,11)

Aidan Essa Mustafa Sulaimaan, Republic of Iraq, Ministry of Education, Open Educational College

Construction of the (k, r)-caps in the projective 3-space PG(3,11)

Aidan Essa Mustafa Sulaimaan, Republic of Iraq, Ministry of Education, Open Educational College

Abstract:

The purpose of this work is to construct the (k, r)-caps in the projective 3-space PG(3,11). We found that PG(3,11) has an ovaloid maximum complete (k,2)-cap when k = 40. Furthermore the maximum (k,3)-caps, (k,4)-caps, (k,5)-caps,(k,6)-caps, (k,7)-caps, (k,8)-caps, (k,9)-caps, (k,10)-caps, (k,11)-caps, (k,12)-caps.

Key words: Maximum Complete (k, r)-cap in Projective Space over Galois Field.

Introduction:

(k, n)-arcs in the projective planes PG(2, P), where $2 \leq P \leq 17$. I am now studying finite projective spaces PG(3,q) over the Galois field GF(q), which is the greatest projective plane over a Galois field. Hirschfeld [1] provides the fundamental definitions and theorems of projective geometry over finite fields, whereas Al Mukhtar, A.SH. [2] presents full arcs and surfaces in three-dimensional projective space over Galois fields, as well as (k, r)-caps in PG(3,q) for Galois fields GF(q) where q equals 2, 3, or 5. and F. F. Kareem in reference [3] A comprehensive (k, r)-cap in PG(3,p) over the Galois Field GF(4), and A. A. Abdulla and N. Y. Kasm in [4], application of algebraic geometry in three-dimensional projective space PG(3,7).

This study constructs the (k, r)-caps in PG(3,p). Concerning Galois Field GF(11) This work comprises five sections: Section one presents the preliminaries of projective 3-space, including relevant definitions and theorems, while sections two through five detail the building of maximum complete (k, r)-caps for r = 2, 3, 4, 5, 6, 7, 8, 9, 10, 11, and 12. I have completed this work manually, without the aid of a computer software.

1- Preliminaries

Definition 1.1 : "Projective 3-Space", [3]

A projective 3-space PG(3,k) over a field k is a three-dimensional projective space comprising points, lines, and planes, together with the incidence relations among them. The projective three-dimensional space adheres to the subsequent axioms:

A) Any two distinct points lie on a singular line.

B) Any three separate non-collinear points, along with any line and a point not on that line, define a unique plane. C) Any two separate coplanar lines converge at a single unique place.

D) Any line not contained inside a specified plane intersects the plane at a singular point.

Any two separate planes intersect at a singular line. A projective space PG(3,p) over the Galois field GF(p), where $p = q^m$ for a prime number q and an integer m, constitutes a three-dimensional projective space. Every point in PG(3,p) is represented as a quadruple

(x_1,x_2,x_3,x_4), where x_1,x_2,x_3,x_4 are elements of GF(p), excluding the quadruple composed entirely of zeros. Two quadrables (x_1, x_2, x_3, x_4) and (y_1, y_2, y_3, y_4) represent
In a similar manner, any plane in PG(3,p) is represented as a quadrable $[x_1,x_2,x_3,x_4]$, where x_1,x_2,x_3,x_4 are elements of GF(p), excluding the quadrable comprising four zero elements. Two quadrables $[x_1,x_2,x_3,x_4]$ and $[y_1,y_2,y_3,y_4]$ represent the same plane if there exists a non-zero scalar λ in GF(p) such that $[x_1,x_2,x_3,x_4] = \lambda [y_1,y_2,y_3,y_4]$. A point $p(x_1, x_2, x_3, x_4)$ is incident with the plane $\pi[a_1, a_2, a_3, a_4]$ if and only if $a_1x_1 + a_2x_2 + a_3x_3 + a_4x_4 = 0$.

Definition1.2: "Plan π", **[1]** A plan π in PG(3,p) comprises all locations $p(x_1,x_2,x_3,x_4)$ that fulfill the linear equation $u_1x_1 + u_2x_2 + u_3x_3 + u_4x_4 = 0$. This plane is represented by
π [u1, u2, u3, u4].

Theorem 1.3: **[2]** Four distinct points $A(x_1,x_2,x_3,x_4)$, $B(y_1,y_2,y_3,y_4)$, $C(z_1,z_2,z_3,z_4)$ and $D(w_1,w_2,w_3,w_4)$ are coplanar if and only if $\begin{vmatrix} x_1 & x_1 & x_3 & x_4 \\ y_1 & y_2 & y_3 & y_4 \\ z_1 & z_3 & z_3 & z_4 \\ w_4 & w_4 & w_3 & w_4 \end{vmatrix}=0$

Corollary 1.4: [2] If four distinct points $A(x_1,x_2,x_3,x_4)$, $B(y_1,y_2,y_3,y_4)$, $C(z_1,z_2,z_3,z_4)$ and $D(w_1,w_2,w_3,w_4)$ are collinear, then $\Delta= 0$.

Theorem 1.5: [2] The points of PG(3,p) possess distinct representations: (1,0,0,0), (x,1,0,0), (x,y,1,0), and (x,y,z,1) for all x, y, z in GF(p).

Theorem 1.6: [2] The planes of PG(3,p) possess distinct representations: [1,0,0,0], [x,1,0,0], [x,y,1,0], and [x,y,z,1], where x, y, and z are elements of GF(p).

Theorem 1.7: [2] A projective 3-space PG(3,p) possesses the subsequent characteristics:
A) Each line has precisely p + 1 points, and each point resides on exactly p + 1 lines.
B) Each plane has precisely $p^2 + p + 1$ points (lines), and every point is on exactly $p^2 + p + 1$ planes. There exists $p^3 + p^2 + p + 1$ points and $p^3 + p^2 + p + 1$ planes.
D) Any two planes meet at precisely p + 1 points, each line resides on exactly p + 1 planes, and any two points lie on exactly p + 1 planes.

Theorem 1.8: [2] There are $(p^2 + 1)(p^2 + p + 1)$ lines in PG(3, P).

Definition 1.9: [2] A (k,ℓ)-set in PG(3,p) constitutes a collection of k spaces $\pi\ell$. A k-set is a (k,0)-set including k points.

Definition 1.10: "(k, r)-cap", [1] An (k, r)-cap is a collection of k points in PG(n, p) where $n \geq 3$, such that no more than r points lie on any given line. A (k,2)-cap is a collection of k points in PG(3,p) such that no three points are collinear.

Definition 1.11: "Complete (k, r)-cap", [2] A (k, r)-cap is considered complete if it is not a subset of a (k+1, r)-cap.

Definition 1.12: [2] Let C_i denote the quantity of points of index i in PG(3,p) that are not situated on a (k, r)-cap; thus, the constants C_i of the (k, r)-cap adhere to the subsequent conditions:

i) $\sum_{\alpha}^{\beta} C_i = p^3 + p^2 + p + 1 - k$

ii) $\sum_{\alpha}^{\beta} iC_I = \frac{k(k-1)(k-2)\ldots(k-n+1)}{n!}$.($p^2+p+1- n$) where α denotes the smallest index i for which $C_i \neq 0$, and β signifies the biggest index i for which $C_i \neq 0$.

Remark 1.13: **[3]** The (k, r)-cap is complete if and only if $C_0 = 0$.

Definition 1.14: **[2]** The i-secant of a (k, r)-cap is a line intersects the cap in exactly i points, that is 0-secant is an external line, 1-secant is a unisecant line,
2-secant is a bisecant line and 3-secant is atrisecant line.

Remark 1.15:[3] A (k, r)-cap is maximum if and only if every line in PG(3,p) is a 0-secant or r-secant.

Theorem 1.16: [1] A maximal (k,2)-cap in PG(3,p) is classified as an ovaloid.

2- The (k,2)-caps in PG(3,11):

PG (3,11) contains 1464 points and 1464 planes such that each point is on 133 planes and every plane contains 133 points and every line contains 12 points and it is the intersection of 12 planes, (table 1 and 2). In t able (1), the set

A	1	2	13	134	267

3	-	12	14	-	25	27	-	35	37	-	48	50
-	62	64	-	82	84	-	110	112	-	130	132	133
135	-	145	148	-	156	158	-	169	171	-	183	185
-	203	205	231	233	-	251	253	-	257	259	-	266
268	--	278	280	-	287	289	-	305	307	-	335	337
-	375	-	383	385	-	389	391	-	404	406	-	420
422	-	436	438	-	484	486	-	513	515	-	530	532
-	556	558	-	576	578	-	602	604	-	822	822	-
951	953	-	1023	1025	-	1196	1198	-	1260	1262	-	1464

is taken which is the set of unit and reference points 1(1,0,0,0), 2(0,1,0,0), 13(0,0,1,0), 134(0,0,0,1), 267(1,1,1,1), this set is a (5,2)-cap since no three points of A are collinear as in table (2).A is a (5,2)-cap, which is not complete since there exists some point of index zero for it, which are

Subsequently, one can incorporate some of them into A to achieve a complete (40,2)-cap B.

L_1	26	36	49	63	83	111	131	147	157	170	184	204
	232	252	258	279	288	306	336	384	390	405	421	437
	485	514	531	557	577	603	821	952	1024	1197	1261	

$B=A\cup L_1=$

B	1	2	13	26	36	49	63	83	111	131	134	147
	157	170	184	204	232	252	258	267	279	288	306	336
	384	390	405	421	437	485	514	531	557	577	603	821
	952	1024	1197	1261								

B is the maximal (40,2)-cap in PG(3,11); since every line is either a 0-secant or a 2-secant, B is referred to as an ovaloid. Let B be a (40,2)-cap. The indices at zero are
3- The (k,3)-caps in PG(3,11):
The distinct (k,3)-cap can be constructed by adding some points of index zero for B, which are

L2	3	14	24	40	53	64	77	137	145	162	171	185
	256	266	280	295	305	325	326	376	388	402	415	419
	420	434	477	498	499	512	527	528	533	562	578	592
	636	641	642	651	655	678	680	693	703	705	788	963
	976	980	995	1009	1035	1036	1042	1211	1279	1437		

Then $C=B\cup L_2$ =

C	1	2	3	13	14	24	26	36	40	49	53	63
	64	77	83	111	131	134	137	145	147	157	162	170
	171	184	185	204	232	252	256	258	266	267	279	280
	288	295	305	306	325	326	336	376	384	388	390	402
	405	415	419	420	421	434	437	477	485	498	499	512
	514	527	528	531	533	557	562	577	578	592	603	636
	641	642	651	655	678	680	693	703	705	788	821	952
	963	976	980	995	1009	1024	1035	1036	1042	1197	1211	1261
	1279	1437										

C is a complete (98.3)-cap, as there are no points of index zero, i.e., $C_0=0$. C is a maximal full (k,3)-cap.

4- The (k,4)-caps in PG(3,11):

We can construct complete (k,4)-caps by incorporating additional points of index zero for C, which are

L_3	4	15	28	35	50	58	78	84	103	135	146	156
	169	186	196	202	221	257	270	277	289	302	312	315
	316	370	378	387	403	410	423	439	444	461	503	511
	519	530	545	546	548	574	594	618	624	638	644	656
	673	699	713	725	747	748	754	762	767	787	822	823
	832	845	856	864	895	905	965	1056	1155	1331	1347	

Then $D=C\cup L_3$ =

D	1	2	3	4	13	14	15	24	26	28	35	36
	40	49	50	53	58	63	64	77	78	83	84	103
	111	131	134	135	137	145	146	147	156	157	162	169
	170	171	184	185	186	196	202	204	221	232	252	256
	257	258	266	267	270	277	279	280	288	289	295	302
	305	306	312	315	316	325	326	336	370	376	378	384
	387	388	390	402	403	405	410	415	419	420	421	423
	434	437	439	444	461	477	485	498	499	503	511	512
	514	519	527	528	530	531	533	545	546	548	557	562
	574	577	578	592	594	603	618	624	636	538	641	642
	644	651	655	656	673	678	680	693	699	703	705	713
	725	747	748	754	762	767	787	788	821	822	823	832
	845	856	864	895	905	952	963	965	976	980	995	1009
	1024	1035	1036	1042	1056	1155	1197	1211	1261	1279	1331	1347
	1437											

D is a complete (169,4)-cap, as there are no points of index zero, i.e., $C_0=0$. D is a maximal full (k,4)-cap.

5- The (k,5)-caps in PG(3,11):

Complete (k,5)-caps can be constructed by incorporating additional points of index zero for D.

L_4	5	16	25	37	46	60	71	98	136	149	159	167
	181	201	206	248	250	251	255	268	278	297	307	313
	329	379	389	398	416	424	435	452	504	521	535	555
	565	583	625	626	630	631	643	659	664	676	689	694
	709	743	744	753	764	774	779	782	796	802	803	806
	824	846	865	907	911	917	927	930	941	951	956	961
	1002	1022	1051	1071	1072	1147	1218	1242	1397	1401	1412	

Then $E=D\cup L_4$

E	1	2	3	4	5	13	14	15	16	24	25	26
	28	35	36	37	40	46	49	50	53	58	60	63
	64	71	77	78	83	84	98	103	111	131	134	135
	136	137	145	146	147	149	156	157	159	162	167	169
	170	171	181	184	185	186	196	201	202	204	206	221
	248	250	251	252	255	256	257	258	266	267	268	270
	232	277	278	279	280	288	289	295	297	302	305	306
	307	312	313	315	316	325	326	329	336	370	376	378
	379	384	387	388	389	390	398	402	403	405	410	415
	416	419	420	421	423	424	434	435	437	439	444	452
	461	477	485	498	499	503	504	511	512	514	519	521

	527	528	530	531	533	535	545	546	548	555	557	562
	565	574	577	578	583	592	594	603	618	624	625	626
	630	631	636	638	641	642	643	644	651	655	656	659
	664	673	676	678	680	689	693	694	699	703	705	709
	713	725	743	744	747	748	753	754	762	764	767	774
	779	782	787	788	796	802	803	806	821	822	823	824
	832	845	846	856	864	865	895	905	907	911	917	927
	930	941	951	952	956	961	963	965	976	980	995	1002
	1009	1022	1024	1035	1036	1042	1051	1056	1071	1072	1147	1155
	1197	1211	1218	1242	1261	1279	1331	1347	1397	1401	1412	1437

E is a complete (252,5)-cap, as there are no points of index zero, i.e., $C_0=0$. E is a maximal complete (k,5)-cap.

6- The (k,6)-caps in PG(3,11):

We can create complete (k,6)-caps by incorporating additional points of index zero for E, which are

	6	17	27	39	47	66	73	74	90	92	106	138
	148	158	173	188	200	216	219	259	271	281	290	300
	310	328	335	337	339	341	383	393	404	411	425	431
	445	446	447	476	493	500	508	509	520	536	542	549
L_5	558	582	587	598	620	634	646	652	671	681	685	686
	695	723	745	752	755	759	775	778	783	786	830	867
	876	884	886	890	904	912	923	934	942	944	948	950
	996	1030	1045	1054	1108	1124	1128	1153	1196	1306	1417	1420
	1421	1428	1444									

Then $F=E\cup L_5$ =

F	1	2	3	4	5	6	13	14	15	16	17	24
	25	26	27	28	35	36	37	39	40	46	47	49
	50	53	58	60	63	64	66	71	73	74	77	78
	83	84	90	92	98	103	106	111	131	134	135	136
	137	138	145	146	147	148	149	156	157	158	159	162
	167	169	170	171	173	181	184	185	186	188	196	200
	201	202	204	206	216	219	221	232	248	250	251	252
	255	256	257	258	259	266	267	268	270	271	277	278
	279	280	281	288	289	290	295	297	300	302	305	306
	307	310	312	313	315	316	325	326	328	329	335	336
	337	339	341	370	376	378	379	383	384	387	388	389
	390	393	398	402	403	404	405	410	411	415	416	419
	420	421	423	424	425	431	434	435	437	439	444	445

	446	447	452	461	476	477	485	493	498	499	500	503
	504	508	509	511	512	514	519	520	521	527	528	530
	531	533	535	536	542	545	546	548	549	555	557	558
	562	565	574	577	578	582	583	587	592	594	598	603
	618	620	624	625	626	630	631	634	636	638	641	642
	643	644	646	651	652	655	656	659	664	671	673	676
	678	680	681	685	686	689	693	694	695	699	703	705
	709	713	723	725	743	744	745	747	748	752	753	754
	755	759	762	764	767	774	775	778	779	782	783	786
	787	788	796	802	803	806	821	822	823	824	830	832
	845	846	856	864	865	867	876	884	886	890	895	904
	905	907	911	912	917	923	927	930	934	941	942	944
	948	950	951	952	956	961	963	965	976	980	995	996
	1002	1009	1022	1024	1030	1035	1036	1042	1045	1051	1054	1056
	1071	1072	1108	1124	1128	1147	1153	1155	1196	1197	1211	1218
	1242	1261	1279	1306	1331	1347	1397	1401	1412	1417	1420	1421
	1428	1437	1444									

F is a complete (351,6)-cap, as there are no points of index zero, i.e., $C_0=0$. F is a maximal full (k,6)-cap.

7- The (k,7)-caps in PG(3,11):

We can construct complete (k,7)-caps by incorporating additional points of index zero for F, which are

	7	18	29	38	48	57	69	89	100	107	109	130
	139	150	160	168	178	190	191	192	194	195	209	238
	261	269	283	292	299	318	322	323	350	363	372	377
	391	399	409	428	433	448	460	497	513	522	537	547
L_6	553	571	579	619	640	654	669	677	687	698	728	742
	751	769	772	799	800	805	811	813	827	858	861	862
	866	887	889	896	899	900	913	920	940	947	958	959
	962	973	990	1015	1023	1028	1064	1066	1076	1082	1089	1092
	1093	1158	1212	1213	1227	1240	1313	1393				

Then $G=F\cup L_6$ =

	1	2	3	4	5	6	7	13	14	15	16	17
	18	24	25	26	27	28	29	35	36	37	38	39
	40	46	47	48	49	50	53	57	58	60	63	64
	66	69	71	73	74	77	78	83	84	89	90	92
	98	100	103	106	107	109	111	130	131	134	135	136
	137	138	139	145	146	147	148	149	150	156	157	158
	159	160	162	167	168	169	170	171	173	178	181	184
	185	186	188	190	191	192	194	195	196	200	201	202
G	204	206	209	216	219	221	232	238	248	250	251	252
	255	256	257	258	259	261	266	267	268	269	270	271
	277	278	279	280	281	283	288	289	290	292	295	297
	299	300	302	305	306	307	310	312	313	315	316	318
	322	323	325	326	328	329	335	336	337	339	341	350
	363	370	372	376	377	378	379	383	384	387	388	389
	390	391	393	398	399	402	403	404	405	409	410	411
	415	416	419	420	421	423	424	425	428	431	433	434
	477	485	493	497	498	499	500	503	504	508	509	511
	512	513	514	519	520	521	522	527	528	530	531	533
	535	536	537	542	545	546	547	548	549	553	555	557
	558	562	565	571	574	577	578	579	582	583	587	592
	594	598	603	618	619	620	624	625	626	630	631	634
	636	638	640	641	642	643	644	646	651	652	654	655
	656	659	664	669	671	673	676	677	678	680	681	685
	686	687	689	693	694	695	698	699	703	705	709	713
	723	725	728	742	743	744	745	747	748	751	752	753
	754	755	759	762	764	767	769	772	774	775	778	779
	782	783	786	787	788	796	799	800	802	803	805	806
	811	813	821	822	823	824	827	830	832	845	846	856
	858	861	862	864	865	866	867	876	884	886	887	889
	890	895	896	899	900	904	905	907	911	912	913	917
	920	923	927	930	934	940	941	942	944	947	948	950
	951	952	956	958	959	961	962	963	965	973	976	980
	990	995	996	1002	1009	1015	1022	1023	1024	1028	1030	1035
	1036	1042	1045	1051	1054	1056	1064	1066	1071	1072	1076	1082
	1089	1092	1093	1108	1124	1128	1147	1153	1155	1158	1196	1197
	1211	1212	1213	1218	1227	1240	1242	1261	1279	1306	1313	1331

	1347	1393	1397	1401	1412	1417	1420	1421	1428	1437	1444	

G is a complete (455,7)-cap, as there are no points of index zero, i.e., C0=0. G is a maximal full (k,7)-cap.

8- The (k,8)-caps in PG(3,11):

L_7	8	19	30	41	51	59	68	80	82	85	87	141
	151	164	172	180	197	203	218	263	272	282	291	304
	314	321	333	356	360	361	371	381	394	400	412	426
	438	442	458	459	465	501	510	532	541	556	559	563
	567	568	580	589	591	610	621	629	633	649	657	667
	668	670	702	719	740	750	765	773	794	801	809	812
	828	831	868	872	882	883	893	910	926	933	937	946
	954	969	981	983	992	999	1001	1005	1006	1012	1019	1020
	1026	1038	1041	1044	1048	1059	1074	1075	1161	1178	1187	1193

Then $H=G\cup L_7$ =

H	1	2	3	4	5	6	7	8	13	14	15	16
	17	18	19	24	25	26	27	28	29	30	35	36
	37	38	39	40	41	46	47	48	49	50	51	53
	57	58	59	60	63	64	66	68	69	71	73	74
	77	78	80	82	83	84	85	87	89	90	92	98
	100	103	106	107	109	111	130	131	134	135	136	137
	138	139	141	145	146	147	148	149	150	151	156	157
	158	159	160	162	164	167	168	169	170	171	172	173
	178	180	181	184	185	186	188	190	191	192	194	195
	196	197	200	201	202	203	204	206	209	216	218	219
	221	232	238	248	250	251	252	255	256	257	258	259
	261	263	266	267	268	269	270	271	272	277	278	279
	280	281	282	283	288	289	290	291	292	295	297	299
	300	302	304	305	306	307	310	312	313	314	315	316
	318	321	322	323	325	326	328	329	333	335	336	337
	339	341	350	356	360	361	363	370	371	372	376	377
	378	379	381	383	384	387	388	389	390	391	393	394

	398	399	400	402	403	404	405	409	410	411	412	415
	416	419	420	421	423	424	425	426	428	431	433	434
	435	437	438	439	442	444	445	446	447	448	452	458
	459	460	461	465	476	477	485	493	497	498	499	500
	501	503	504	508	509	510	511	512	513	514	519	520
	521	522	527	528	530	531	532	533	535	536	537	541
	542	545	546	547	548	549	553	555	556	557	558	559
	562	563	565	567	568	571	574	577	578	579	580	582
	583	587	589	591	592	594	598	603	610	618	619	620
	621	624	625	626	629	630	631	633	634	636	638	640
	641	642	643	644	646	649	651	652	654	655	656	657
	659	664	667	668	669	670	671	673	676	677	678	680
	681	685	686	687	689	693	694	695	698	699	702	703
	705	709	713	719	723	725	728	740	742	743	744	745
	747	748	750	751	752	753	754	755	759	762	764	765
	767	769	772	773	774	775	778	779	782	783	786	787
	788	794	796	799	800	801	802	803	805	806	809	811
	812	813	821	822	823	824	827	828	830	831	832	845
	846	856	858	861	862	864	865	866	867	868	872	876
	882	883	884	886	887	889	890	893	895	896	899	900
	904	905	907	910	911	912	913	917	920	923	926	927
	930	933	934	937	940	941	942	944	946	947	948	950
	951	952	954	956	958	959	961	962	963	965	969	973
	976	980	981	983	990	992	995	996	999	1001	1002	1005
	1006	1009	1012	1015	1019	1020	1022	1023	1024	1026	1028	1030
	1035	1036	1038	1041	1042	1044	1045	1048	1051	1054	1056	1059
	1064	1066	1071	1072	1074	1075	1076	1082	1089	1092	1093	1108
	1124	1128	1147	1153	1155	1158	1161	1178	1187	1193	1196	1197
	1211	1212	1213	1218	1227	1240	1242	1261	1270	1275	1279	1292
	1306	1313	1331	1347	1390	1393	1397	1401	1412	1417	1420	1421
	1424	1428	1437	1444								

H is a complete (568,8)-cap, as there are no points of index zero, i.e., C0=0. H is a maximal complete (k,8)-cap.

9- The (k,9)-caps in PG(3,11):

We can construct complete (k,9)-caps by incorporating additional points of index zero for H, which are

L_8	9	20	31	42	52	61	72	79	91	93	95	99
	108	140	152	161	174	179	189	205	212	213	214	220
	229	260	273	285	294	301	319	332	340	355	362	373

	380	392	401	413	422	432	450	457	463	464	469	471
	480	502	517	523	524	538	543	552	566	569	570	581
	586	622	632	645	660	662	663	675	682	691	692	696
	701	710	741	756	761	763	766	776	795	810	815	816
	819	820	837	847	860	873	874	875	877	878	879	885
	902	938	949	964	982	984	987	989	991	993	1008	1011
	1016	1021	1027	1032	1037	1039	1057	1058	1067	1077	1085	1086
	1109	1118	1120	1130	1136	1154	1157	1163	1169	1173	1174	1188
	1189	1185	1208	1221	1352	1380	1410	1413	1418			

Then $I=H\cup L_8$ =

I	1	2	3	4	5	6	7	8	9	13	14	15
	16	17	18	19	20	24	25	26	27	28	29	30
	31	35	36	37	38	39	40	41	42	46	47	48
	49	50	51	52	53	57	58	59	60	61	63	64
	66	68	69	71	72	73	74	77	78	79	80	82
	83	84	85	87	89	90	91	92	93	95	98	99
	100	103	106	107	108	109	111	130	131	134	135	136
	137	138	139	140	141	145	146	147	148	149	150	151
	152	156	157	158	159	160	161	162	164	167	168	169
	170	171	172	173	174	178	179	180	181	184	185	186
	188	189	190	191	192	194	195	196	197	200	201	202
	203	204	205	206	209	212	213	214	216	218	219	220
	221	229	232	238	248	250	251	252	255	256	257	258
	259	260	261	263	266	267	268	269	270	271	272	273
	277	278	279	280	281	282	283	285	288	289	290	291

	292	294	295	297	299	300	301	302	304	305	306	307
	310	312	313	314	315	316	318	319	321	322	323	325
	326	328	329	332	333	335	336	337	339	340	341	350
	355	356	360	361	362	363	370	371	372	373	376	377
	378	379	380	381	383	384	387	388	389	390	391	392
	393	394	398	399	400	401	402	403	404	405	409	410
	411	412	413	415	416	419	420	421	422	423	424	425
	426	428	431	432	433	434	435	437	438	439	442	444
	445	446	447	448	450	452	457	458	459	460	461	463
	464	465	469	471	476	477	480	485	493	497	498	499
	500	501	502	503	504	508	509	510	511	512	513	514

	517	519	520	521	522	523	524	527	528	530	531	532
	533	535	536	537	538	541	542	543	545	546	547	548
	549	552	553	555	556	557	558	559	562	563	565	566
	567	568	569	570	571	574	577	578	579	580	581	582
	583	586	587	589	591	592	594	598	603	610	618	619
	620	621	622	624	625	626	629	630	631	632	633	634
	636	638	640	641	642	643	644	645	646	649	651	652
	654	655	656	657	659	660	662	663	664	667	668	669
	670	671	673	675	676	677	678	680	681	682	685	686
	687	689	691	692	693	694	695	696	698	699	701	702
	703	705	709	710	713	719	723	725	728	740	741	742
	743	744	745	747	748	750	751	752	753	754	755	756
	759	761	762	763	764	765	766	767	769	772	773	774
	775	776	778	779	782	783	786	787	788	794	795	796
	799	800	801	802	803	805	806	809	810	811	812	813
	815	816	819	820	821	822	823	824	827	828	830	831
	832	837	845	846	847	856	858	860	861	862	864	865
	866	867	868	872	876	873	874	875	877	878	879	882
	883	884	885	886	887	889	890	893	895	896	899	900
	902	904	905	907	910	911	912	913	917	920	923	926
	927	930	933	934	937	938	940	941	942	944	946	947
	948	949	950	951	952	954	956	958	959	961	962	963
	964	965	969	973	976	980	981	982	983	984	987	989

	990	991	992	993	995	996	999	1001	1002	1005	1006	1008
	1009	1011	1012	1015	1016	1019	1020	1021	1022	1023	1024	1026
	1027	1028	1030	1032	1035	1036	1037	1038	1039	1041	1042	1044
	1045	1048	1051	1054	1056	1057	1058	1059	1064	1066	1067	1071
	1072	1074	1075	1076	1077	1082	1085	1086	1089	1092	1093	1108
	1109	1118	1120	1124	1128	1130	1136	1147	1153	1154	1155	1157
	1158	1161	1163	1169	1173	1174	1178	1185	1187	1188	1189	1193
	1196	1197	1208	1211	1212	1213	1218	1221	1227	1240	1242	1261
	1270	1275	1279	1292	1306	1313	1331	1347	1352	1380	1390	1393
	1397	1401	1410	1412	1413	1417	1418	1420	1421	1424	1428	1437
	1444											

I is a complete (709,9)-cap, as there are no points of index zero, i.e., C_0=0. I am a maximum complete (k,9)-cap.

10- The (k,10)-caps in PG(3,11):

We can construct complete (k,10)-caps by incorporating additional points of index zero for I, which are

L_9	10	21	32	43	54	62	70	81	94	101	102	104
	142	153	163	175	182	193	210	217	222	223	224	226
	231	262	274	286	293	303	311	324	327	334	343	346
	352	374	382	395	406	414	427	440	454	455	456	468
	472	475	481	483	505	515	525	534	544	554	564	575
	585	604	623	635	648	653	665	674	684	697	714	715
	722	724	733	746	757	768	777	791	792	793	798	807
	817	829	835	836	863	871	888	897	898	901	906	908
	945	966	972	986	994	997	1007	1010	1014	1043	1047	1052
	1065	1069	1070	1080	1094	1098	1102	1104	1106	1113	1122	1126
	1127	1129	1131	1137	1138	1142	1148	1150	1156	1162	1165	1167
	1171	1176	1184	1191	1192	1194	1195	1198	1201	1216	1311	1315
	1327	1359	1394	1402	1432	1440	1442					

Then J=I□L9 =

	352	355	356	360	361	362	363	370	371	372	373	374
	376	377	378	379	380	381	382	383	384	387	388	389
	390	391	392	393	394	395	398	399	400	401	402	403
	404	405	406	409	410	411	412	413	414	415	416	419
	420	421	422	423	424	425	426	427	428	431	432	433
	434	435	437	438	439	440	442	444	445	446	447	448
	450	452	454	455	456	457	458	459	460	461	463	464
	465	468	469	471	472	475	476	477	480	481	483	485
	493	497	498	499	500	501	502	503	504	505	508	509
	510	511	512	513	514	515	517	519	520	521	522	523
	524	525	527	528	530	531	532	533	534	535	536	537
	538	541	542	543	544	545	546	547	548	549	552	553
	554	555	556	557	558	559	562	563	564	565	566	567
	568	569	570	571	574	575	577	578	579	580	581	582
	583	585	586	587	589	591	592	594	598	603	604	610
	618	619	620	621	622	623	624	625	626	629	630	631
	632	633	634	635	636	638	640	641	642	643	644	645
	646	648	649	651	652	653	654	655	656	657	659	660
	662	663	664	665	667	668	669	670	671	673	674	675
	676	677	678	680	681	682	684	685	686	687	689	691
	692	693	694	695	696	697	698	699	701	702	703	705
	709	710	713	714	715	719	722	723	724	725	728	733
	740	741	742	743	744	745	746	747	748	750	751	752
	753	754	755	756	757	759	761	762	763	764	765	766
	767	768	769	772	773	774	775	776	777	778	779	782
	783	786	787	788	791	792	793	794	795	796	798	799
	800	801	802	803	805	806	807	809	810	811	812	813
	815	816	817	819	820	821	822	823	824	827	828	829
	830	831	832	835	836	837	845	846	847	856	858	860
	861	862	863	864	865	866	867	868	871	872	873	874
	875	876	877	878	879	882	883	884	885	886	887	888
	889	890	893	895	896	897	898	899	900	901	902	904
	905	906	907	908	910	911	912	913	917	920	923	926
	927	930	933	934	937	938	940	941	942	944	945	946
	947	948	949	950	951	952	954	956	958	959	961	962
	963	964	965	966	969	972	973	976	980	981	982	983

	1	2	3	4	5	6	7	8	9	10	13	14	
J	15	16	17	18	19	20	21	24	25	26	27	28	
	29	30	31	32	35	36	37	38	39	40	41	42	
	43	46	47	48	49	50	51	52	53	54	57	58	
	59	60	61	62	63	64	66	68	69	70	71	72	
	73	74	77	78	79	80	81	82	83	84	85	87	

	89	90	91	92	93	94	95	98	99	100	101	102	
	103	104	106	107	108	109	111	130	131	134	135	136	
	137	138	139	140	141	142	145	146	147	148	149	150	
	151	152	153	156	157	158	159	160	161	162	163	164	
	167	168	169	170	171	172	173	174	175	178	179	180	
	181	182	184	185	186	188	189	190	191	192	193	194	
	195	196	197	200	201	202	203	204	205	206	209	210	
	212	213	214	216	217	218	219	220	221	222	223	224	
	226	229	231	232	238	248	250	251	252	255	256	257	
	258	259	260	261	262	263	266	267	268	269	270	271	
	272	273	274	277	278	279	280	281	282	283	285	286	
	288	289	290	291	292	293	294	295	297	299	300	301	
	302	303	304	305	306	307	310	311	312	313	314	315	
	316	318	319	321	322	323	324	325	326	327	328	329	
	332	333	334	335	336	337	339	340	341	343	346	350	

	984	986	987	989	990	991	992	993	994	995	996	997
	999	1001	1002	1005	1006	1007	1008	1009	1010	1011	1012	1014
	1015	1016	1019	1020	1021	1022	1023	1024	1026	1027	1028	1030
	1032	1035	1036	1037	1038	1039	1041	1042	1043	1044	1045	1047
	1048	1051	1052	1054	1056	1057	1058	1059	1064	1065	1066	1067
	1069	1070	1071	1072	1074	1075	1076	1077	1080	1082	1085	1086
	1089	1092	1093	1094	1098	1102	1104	1106	1108	1109	1113	1118
	1120	1122	1124	1126	1127	1128	1129	1130	1131	1136	1137	1138
	1142	1147	1148	1150	1153	1154	1155	1156	1157	1158	1161	1162
	1163	1165	1167	1169	1171	1173	1174	1176	1178	1184	1185	1187
	1188	1189	1191	1192	1193	1194	1195	1196	1197	1198	1201	1208
	1211	1212	1213	1216	1218	1221	1227	1240	1242	1261	1270	1275
	1279	1292	1306	1311	1313	1315	1327	1331	1347	1352	1359	1380
	1390	1393	1394	1397	1401	1402	1410	1412	1413	1417	1418	1420
	1421	1424	1428	1432	1437	1440	1442	1444				

J is a complete (860,10)-cap, as there are no points of index zero, i.e., C0=0. J is a maximal full (k,10)-cap.

10- The (k,11)-caps in PG(3,11):

We can construct complete (k,11)-caps by incorporating additional points of index zero.

L_{10}	11	22	33	44	55	65	75	86	96	105	112	114
	116	118	119	120	121	143	154	165	176	183	198	208
	211	227	228	230	237	242	264	275	284	296	308	320
	331	338	354	368	385	396	407	417	429	436	443	449
	453	470	473	474	479	506	516	526	539	551	560	572
	584	588	590	593	600	606	627	637	647	658	666	679
	688	700	706	708	712	718	720	721	734	739	758	770
	780	784	785	790	808	825	826	833	843	852	853	869
	880	891	894	909	916	918	922	924	925	932	935	977
	978	979	988	998	1004	1013	1017	1025	1033	1034	1040	1049

	1053	1061	1062	1068	1078	1079	1101	1103	1107	1110	1111	1112
	1114	1115	1116	1117	1119	1123	1125	1132	1133	1135	1139	1141
	1143	1144	1145	1146	1151	1152	1159	1164	1168	1170	1172	1175
	1180	1181	1206	1209	1222	1236	1237	1243	1248	1255	1257	1262
	1273	1276	1278	1281	1283	1286	1307	1312	1323	1336	1363	1425
	1426											

Then $K = J \cup L_{10} =$

	1	2	3	4	5	6	7	8	9	10	11	13
	14	15	16	17	18	19	20	21	22	24	25	26
	27	28	29	30	31	32	33	35	36	37	38	39
	40	41	42	43	44	46	47	48	49	50	51	52
	53	54	55	57	58	59	60	61	62	63	64	65
	66	68	69	70	71	72	73	74	75	77	78	79
	80	81	82	83	84	85	86	87	89	90	91	92
	93	94	95	96	98	99	100	101	102	103	104	105
	106	107	108	109	111	112	114	116	118	119	120	121
	130	131	134	135	136	137	138	139	140	141	142	143
	145	146	147	148	149	150	151	152	153	154	156	157
	158	159	160	161	162	163	164	165	167	168	169	170
	171	172	173	174	175	176	178	179	180	181	182	183
K	184	185	186	188	189	190	191	192	193	194	195	196
	197	198	200	201	202	203	204	205	206	208	209	210
	211	212	213	214	216	217	218	219	220	221	222	223
	224	226	227	228	229	230	231	232	237	238	242	248
	250	251	252	255	256	257	258	259	260	261	262	263
	264	266	267	268	269	270	271	272	273	274	275	277
	278	279	280	281	282	283	284	285	286	288	289	290
	291	292	293	294	295	296	297	299	300	301	302	303
	304	305	306	307	308	310	311	312	313	314	315	316
	318	319	320	321	322	323	324	325	326	327	328	329
	331	332	333	334	335	336	337	338	339	340	341	343
	346	350	352	354	355	356	360	361	362	363	368	370
	371	372	373	374	376	377	378	379	380	381	382	383
	384	385	387	388	389	390	391	392	393	394	395	396

	398	399	400	401	402	403	404	405	406	407	409	410
	411	412	413	414	415	416	417	419	420	421	422	423
	424	425	426	427	428	429	431	432	433	434	435	436
	437	438	439	440	442	443	444	445	446	447	448	449
	450	452	453	454	455	456	457	458	459	460	461	463
	464	465	468	469	470	471	472	473	474	475	476	477
	479	480	481	483	485	493	497	498	499	500	501	502
	503	504	505	506	508	509	510	511	512	513	514	515
	516	517	519	520	521	522	523	524	525	526	527	528
	530	531	532	533	534	535	536	537	538	539	541	542
	543	544	545	546	547	548	549	551	552	553	554	555
	556	557	558	559	560	562	563	564	565	566	567	568
	569	570	571	572	574	575	577	578	579	580	581	582
	583	584	585	586	587	588	589	590	591	592	593	594
	598	600	603	604	606	610	618	619	620	621	622	623
	624	625	626	627	629	630	631	632	633	634	635	636
	637	638	640	641	642	643	644	645	646	647	648	649
	651	652	653	654	655	656	657	658	659	660	662	663
	664	665	666	667	668	669	670	671	673	674	675	676
	677	678	679	680	681	682	684	685	686	687	688	689
	691	692	693	694	695	696	697	698	699	700	701	702
	703	705	706	708	709	710	712	713	714	715	718	719
	720	721	722	723	724	725	728	733	734	739	740	741
	742	743	744	745	746	747	748	750	751	752	753	754
	755	756	757	758	759	761	762	763	764	765	766	767
	768	769	770	772	773	774	775	776	777	778	779	780
	782	783	784	785	786	787	788	790	791	792	793	794
	795	796	798	799	800	801	802	803	805	806	807	808
	809	810	811	812	813	815	816	817	819	820	821	822
	823	824	825	826	827	828	829	830	831	832	833	835
	836	837	843	845	846	847	852	853	856	858	860	861
	862	863	864	865	866	867	868	869	871	872	873	874
	875	876	877	878	879	880	882	883	884	885	886	887
	888	889	890	891	893	894	895	896	897	898	899	900
	901	902	904	905	906	907	908	909	910	911	912	913
	916	917	918	920	922	923	924	925	926	927	930	932
	933	934	935	937	938	940	941	942	944	945	946	947
	948	949	950	951	952	954	956	958	959	961	962	963

	964	965	966	969	972	973	976	977	978	979	980	981
	982	983	984	986	987	988	989	990	991	992	993	994
	995	996	997	998	999	1001	1002	1004	1005	1006	1007	1008
	1009	1010	1011	1012	1013	1014	1015	1016	1017	1019	1020	1021
	1022	1023	1024	1025	1026	1027	1028	1030	1032	1033	1034	1035
	1036	1037	1038	1039	1040	1041	1042	1043	1044	1045	1047	1048
	1049	1051	1052	1053	1054	1056	1057	1058	1059	1061	1062	1064
	1065	1066	1067	1068	1069	1070	1071	1072	1074	1075	1076	1077
	1078	1079	1080	1082	1085	1086	1089	1092	1093	1094	1098	1101
	1102	1103	1104	1106	1107	1108	1109	1110	1111	1112	1113	1114
	1115	1116	1117	1118	1119	1120	1122	1123	1124	1125	1126	1127
	1128	1129	1130	1131	1132	1133	1135	1136	1137	1138	1139	1141
	1142	1143	1144	1145	1146	1147	1148	1150	1151	1152	1153	1154
	1155	1156	1157	1158	1159	1161	1162	1163	1164	1165	1167	1168
	1169	1170	1171	1172	1173	1174	1175	1176	1178	1180	1181	1184
	1185	1187	1188	1189	1191	1192	1193	1194	1195	1196	1197	1198
	1201	1206	1208	1209	1211	1212	1213	1216	1218	1221	1222	1227
	1236	1237	1240	1242	1243	1248	1255	1257	1261	1262	1270	1273
	1275	1276	1278	1279	1281	1283	1286	1292	1306	1307	1311	1312
	1313	1315	1323	1327	1331	1336	1347	1352	1359	1363	1380	1390
	1393	1394	1397	1401	1402	1410	1412	1413	1417	1418	1420	1421
	1424	1425	1426	1428	1432	1437	1440	1442	1444			

K is a complete (1041,11)-cap, as there are no points of index zero, i.e., C0=0. K is a maximal full (k,11)-cap.

11- The (k,12)-caps in PG(3,11):

We can construct complete (k,12)-caps by incorporating additional points of index zero.

	12	23	34	45	56	67	76	88	97	110	113	115
	117	122	123	124	125	126	127	128	129	132	133	144
	155	166	177	187	199	207	215	225	233	234	235	236
	239	240	241	243	244	245	246	247	249	253	254	265
	276	287	298	309	317	330	342	344	345	347	348	349
	351	353	357	358	359	364	365	366	367	369	375	386
	397	408	418	430	441	451	462	466	467	478	482	484
	486	487	488	489	490	491	492	494	495	496	507	518
	529	540	550	561	573	576	595	596	597	599	601	602
	605	607	608	609	611	612	613	614	615	616	617	628
	639	650	661	672	683	690	704	707	711	716	717	726
L_{11}	727	729	730	731	732	735	736	737	738	749	760	771
	781	789	797	804	814	818	834	838	839	840	841	842
	844	848	849	850	851	854	855	857	859	870	881	892
	903	914	915	919	921	928	929	931	936	939	943	953
	955	957	960	967	968	970	971	974	975	985	1000	1003
	1018	1029	1031	1046	1050	1055	1060	1063	1973	1081	1083	1084
	1087	1088	1090	1091	1095	1096	1097	1099	1100	1105	1121	1134
	1140	1149	1160	1166	1177	1179	1182	1183	1186	1190	1199	1200
	1202	1203	1204	1205	1207	1210	1214	1215	1217	1219	1220	1223
	1224	1225	1226	1228	1229	1230	1231	1232	1233	1234	1235	1238
	1239	1241	1244	1245	1246	1247	1249	1250	1251	1252	1253	1254
	1256	1258	1259	1260	1263	1264	1265	1266	1267	1268	1269	1271
	1272	1274	1277	1280	1282	1284	1285	1287	1288	1289	1290	1291
	1293	1294	1295	1296	1297	1298	1299	1300	1301	1302	1303	1304
	1305	1308	1309	1310	1314	1316	1317	1318	1319	1320	1321	1322
	1324	1325	1326	1328	1329	1330	1332	1333	1334	1335	1337	1338
	1339	1340	1341	1342	1343	1344	1345	1346	1348	1349	1350	1351
	1353	1354	1355	1356	1357	1358	1360	1361	1362	1364	1365	1366
	1367	1368	1369	1370	1371	1372	1373	1374	1375	1376	1377	1378

	1379	1381	1382	1383	1384	1385	1386	1387	1388	1389	1391	1392
	1395	1396	1398	1399	1400	1403	1404	1405	1406	1407	1408	1409
	1411	1414	1415	1416	1419	1422	1423	1427	1429	1430	1431	1433
	1434	1435	1436	1438	1439	1441	1443	1445	1446	1447	1448	1449
	1450	1451	1452	1453	1454	1455	1456	1457	1458	1459	1460	1461
	1462	1463	1464									

Then $L=K\cup L_{11}$ =

	241	242	243	244	245	246	247	248	249	250	251	252
	253	254	255	256	257	258	259	260	261	262	263	264
	265	266	267	268	269	270	271	272	273	274	275	276
	277	278	279	280	281	282	283	284	285	286	287	288
	289	290	291	292	293	294	295	296	297	298	299	300
	301	302	303	304	305	306	307	308	309	310	311	312
	313	314	315	316	317	318	319	320	321	322	323	324
	325	326	327	328	329	330	331	332	333	334	335	336
	337	338	339	340	341	342	343	344	345	346	347	348
	349	350	351	352	353	354	355	356	357	358	359	360
	361	362	363	364	365	366	367	368	369	370	371	372
	373	374	375	376	377	378	379	380	381	382	383	384
	385	386	387	388	389	390	391	392	393	394	395	396
	397	398	399	400	401	402	403	404	405	406	407	408
	409	410	411	412	413	414	415	416	417	418	419	420
	421	422	423	424	425	426	427	428	429	430	431	432
	433	434	435	436	437	438	439	440	441	442	443	444
	445	446	447	448	449	450	451	452	453	454	455	456
	457	458	459	460	461	462	463	464	465	466	467	468
	469	470	471	472	473	474	475	476	477	478	479	480
	481	482	483	484	485	486	487	488	489	490	491	492
	493	494	495	496	497	498	499	500	501	502	503	504
	505	506	507	508	509	510	511	512	513	514	515	516
	517	518	519	520	521	522	523	524	525	526	527	528
	529	530	531	532	533	534	535	536	537	538	539	540
	541	542	543	544	545	546	547	548	549	550	551	552
	553	554	555	556	557	558	559	560	561	562	563	564
	565	566	567	568	569	570	571	572	573	574	575	576
	577	578	579	580	581	582	583	584	585	586	587	588

	589	590	591	592	593	594	595	596	597	598	599	600
	601	602	603	604	605	606	607	608	609	610	611	612
	613	614	615	616	617	618	619	620	621	622	623	624
	625	626	627	628	629	630	631	632	633	634	635	636
	637	638	639	640	641	642	643	644	645	646	647	648
	649	650	651	652	653	654	655	656	657	658	659	660
	661	662	663	664	665	666	667	668	669	670	671	672
	673	674	675	676	677	678	679	680	681	682	683	684
	685	686	687	688	689	690	691	692	693	694	695	696
	697	698	699	700	701	702	703	704	705	706	707	708
	709	710	711	712	713	714	715	716	717	718	719	720
	721	722	723	724	725	726	727	728	729	730	731	732
	733	734	735	736	737	738	739	740	741	742	743	744

	745	746	747	748	749	750	751	752	753	754	755	756
	757	758	759	760	761	762	763	764	765	766	767	768
	769	770	771	772	773	774	775	776	777	778	779	780
	781	782	783	784	785	786	787	788	789	790	791	792
	793	794	795	796	797	798	799	800	801	802	803	804
	805	806	807	808	809	810	811	812	813	814	815	816
	817	818	819	820	821	822	823	824	825	826	827	828
	829	830	831	832	833	834	835	836	837	838	839	840
	841	842	843	844	845	846	847	848	849	850	851	852
	853	854	855	856	857	858	859	860	861	862	863	864
	865	866	867	868	869	870	871	872	873	874	875	876
	877	878	879	880	881	882	883	884	885	886	887	888
	889	890	891	892	893	894	895	896	897	898	899	900
	901	902	903	904	905	906	907	908	909	910	911	912
	913	914	915	916	917	918	919	920	921	922	923	924
	925	926	927	928	929	930	931	932	933	934	935	936
	937	938	939	940	941	942	943	944	945	946	947	948
	949	950	951	952	953	954	955	956	957	958	959	960

	961	962	963	964	965	966	967	968	969	970	971	972
	973	974	975	976	977	978	979	980	981	982	983	984
	985	986	987	988	989	990	991	992	993	994	995	996
	997	998	999	1000	1001	1002	1003	1004	1005	1006	1007	1008
	1009	1010	1011	1012	1013	1014	1015	1016	1017	1018	1019	1020
	1021	1022	1023	1024	1025	1026	1027	1028	1029	1030	1031	1032
	1033	1034	1035	1036	1037	1038	1039	1040	1041	1042	1043	1044
	1045	1046	1047	1048	1049	1050	1051	1052	1053	1054	1055	1056
	1057	1058	1059	1060	1061	1062	1063	1064	1065	1066	1067	1068
	1069	1070	1071	1072	1073	1074	1075	1076	1077	1078	1079	1080
	1081	1082	1083	1084	1085	1086	1087	1088	1089	1090	1091	1092
	1093	1094	1095	1096	1097	1098	1099	1100	1101	1102	1103	1104
	1105	1106	1107	1108	1109	1110	1111	1112	1113	1114	1115	1116
	1117	1118	1119	1120	1121	1122	1123	1124	1125	1126	1127	1128
	1129	1130	1131	1132	1133	1134	1135	1136	1137	1138	1139	1140
	1141	1142	1143	1144	1145	1146	1147	1148	1149	1150	1151	1152
	1153	1154	1155	1156	1157	1158	1159	1160	1161	1162	1163	1164
	1165	1166	1167	1168	1169	1170	1171	1172	1173	1174	1175	1176
	1177	1178	1179	1180	1181	1182	1183	1184	1185	1186	1187	1188
	1189	1190	1191	1192	1193	1194	1195	1196	1197	1198	1199	1200
	1201	1202	1203	1204	1205	1206	1207	1208	1209	1210	1211	1212
	1213	1214	1215	1216	1217	1218	1219	1220	1221	1222	1223	1224
	1225	1226	1227	1228	1229	1230	1231	1232	1233	1234	1235	1236
	1237	1238	1239	1240	1241	1242	1243	1244	1245	1246	1247	1248
	1249	1250	1251	1252	1253	1254	1255	1256	1257	1258	1259	1260
	1261	1262	1263	1264	1265	1266	1267	1268	1269	1270	1271	1272
	1273	1274	1275	1276	1277	1278	1279	1280	1281	1282	1283	1284
	1285	1286	1287	1288	1289	1290	1291	1292	1293	1294	1295	1296
	1297	1298	1299	1300	1301	1302	1303	1304	1305	1306	1307	1308
	1309	1310	1311	1312	1313	1314	1315	1316	1317	1318	1319	1320
	1321	1322	1323	1324	1325	1326	1327	1328	1329	1330	1331	1332
	1333	1334	1335	1336	1337	1338	1339	1340	1341	1342	1343	1344

	1345	1346	1347	1348	1349	1350	1351	1352	1353	1354	1355	1356
	1357	1358	1359	1360	1361	1362	1363	1364	1365	1366	1367	1368
	1369	1370	1371	1372	1373	1374	1375	1376	1377	1378	1379	1380
	1381	1382	1383	1384	1385	1386	1387	1388	1389	1390	1391	1392
	1393	1394	1395	1396	1397	1398	1399	1400	1401	1402	1403	1404
	1405	1406	1407	1408	1409	1410	1411	1412	1413	1414	1415	1416
	1417	1418	1419	1420	1421	1422	1423	1424	1425	1426	1427	1428
	1429	1430	1431	1432	1433	1434	1435	1436	1437	1438	1439	1440
	1441	1442	1443	1444	1445	1446	1447	1448	1449	1450	1451	1452
	1453	1454	1455	1456	1457	1458	1459	1460	1461	1462	1463	1464

L is a complete (1041,12)-cap, as there are no points of index zero, i.e., C0=0. L is a maximal complete (k,12)-cap.

Table (1) : The points and lines of PG(3,11)

i	N_i	π_i										
1	(1,0,0,0)	2	13	24	35	46	57	68	79	90	101	112	123
			134	145	156	167	178	189	200	211	222	233	244
			255	266	277	288	299	310	321	332	343	354	365
			376	387	398	409	420	431	442	453	464	475	486
			497	508	519	530	541	552	563	574	585	596	607
			618	629	640	651	662	673	684	695	706	717	728
			739	750	761	772	783	794	805	816	827	838	849
			860	871	882	893	904	915	926	937	948	959	970
			981	992	1003	1014	1025	1036	1047	1058	1069	1080	1091
			1102	1113	1124	1135	1146	1157	1168	1179	1190	1201	1212
			1223	1234	1245	1256	1267	1278	1289	1300	1311	1322	1333
			1344	1355	1366	1377	1388	1399	1410	1421	1432	1443	1454
2	(0,1,0,0)	1	13	14	15	16	17	18	19	20	21	22	23
			134	135	136	137	138	139	140	141	142	143	144
			255	256	257	258	259	260	261	262	263	264	265
			376	377	378	379	380	381	382	383	384	385	386
			497	498	499	500	501	502	503	504	505	506	507
			618	619	620	621	622	623	624	625	626	627	628
			739	740	741	742	743	744	745	746	747	748	749

			860	861	862	863	864	865	866	867	868	869	870
			981	982	983	984	985	986	987	988	989	990	991
			1102	1103	1104	1105	1106	1107	1108	1109	1110	1111	1112
			1223	1224	1225	1226	1227	1228	1229	1230	1231	1232	1233
			1344	1345	1346	1347	1348	1349	1350	1351	1352	1353	1354
3	(1,1,0,0)	12	13	34	44	54	64	74	84	94	104	114	124
			134	155	165	175	185	195	205	215	225	235	245
			255	276	286	296	306	316	326	336	346	356	366
			376	397	407	417	427	437	447	457	467	477	487
			497	518	528	538	548	558	568	578	588	598	608
			618	639	649	659	669	679	689	699	709	719	729
			739	760	770	780	790	800	810	820	830	840	850
			860	881	891	901	911	921	931	941	951	961	971
			981	1002	1012	1022	1032	1042	1052	1062	1072	1082	1092
			1102	1123	1133	1143	1153	1163	1173	1183	1193	1203	1213
			1223	1244	1254	1264	1274	1284	1294	1304	1314	1324	1334
			1344	1365	1375	1385	1395	1405	1415	1425	1435	1445	1455
. . .	. . .							. . .					
1464	(10,10,10,1)	12	23	33	43	53	63	73	83	93	103	113	123
			135	145	166	176	186	196	206	216	226	236	246
			255	276	286	296	306	316	326	336	346	356	366
			386	396	406	416	426	436	446	456	466	476	486
			506	516	526	536	546	556	566	576	586	596	617
			626	636	646	656	666	676	686	696	706	727	737
			746	756	766	776	786	796	806	816	837	847	857
			866	876	886	896	906	916	926	947	957	967	977
			986	996	1006	1016	1026	1036	1057	1067	1077	1087	1097
			1106	1116	1126	1136	1146	1167	1177	1187	1197	1207	1217
			1226	1236	1246	1256	1277	1287	1297	1307	1317	1327	1337
			1346	1356	1366	1387	1397	1407	1417	1427	1437	1447	1457

464	200	332	24	596	728	739	871	1003	1135	1267	1399
475	167	321	46	508	662	816	970	1003	1157	1311	1344
486	200	343	508	35	651	794	937	1080	1102	1245	1388
497	156	310	464	46	651	805	959	992	1146	1300	1454
508	497	596	519	530	541	552	563	574	585	2	607
519	178	332	486	46	673	827	860	1014	1168	1322	1355
530	156	321	486	695	57	739	904	1069	1113	1278	1443
541	167	332	376	57	706	750	915	1080	1124	1289	1454
552	211	365	398	46	706	739	893	1047	1201	1234	1388
563	189	354	398	57	728	772	937	981	1146	1311	1355
574	200	365	409	57	618	783	948	992	1157	1322	1366
585	178	354	409	816	640	68	871	1047	1102	1278	1454
596	189	365	420	651	827	68	882	1058	1113	1289	1344
607	178	321	464	35	629	772	915	1058	1201	1223	1366
618	156	332	387	563	68	794	970	1025	1201	1256	1432
629	167	343	398	574	805	68	860	1036	1212	1267	1443
640	145	299	453	607	46	794	948	981	1135	1289	1443
651	222	299	376	574	849	1003	926	90	1201	1278	1355
662	244	288	453	497	57	827	871	1036	1201	1245	1410
673	211	266	442	497	68	849	904	1080	1135	1311	1366
684	145	310	475	519	57	849	893	1058	1102	1267	1432
695	233	288	464	519	750	68	926	981	1157	1333	1388
706	244	299	475	530	68	761	937	992	1168	1223	1399
717	178	343	387	552	57	761	926	1091	1135	1300	1344
728	618	629	640	651	662	673	684	695	706	717	2
739	222	277	453	508	684	68	915	1091	1146	1322	1377
750	739	761	2	772	783	794	805	816	827	838	849
761	189	255	442	508	695	948	79	1014	1201	1267	1454
772	200	266	453	519	706	79	959	1025	1212	1278	1344
783	211	277	464	530	717	79	970	1036	1102	1289	1355
794	222	288	475	541	728	79	860	1047	1113	1300	1366
805	233	299	486	552	618	871	79	1058	1124	1311	1377
816	244	310	376	563	629	882	79	1069	1135	1322	1388
827	200	277	475	552	629	981	904	90	1179	1256	1454
838	145	332	398	585	651	904	79	1091	1157	1223	1410
849	156	343	409	596	662	79	915	981	1168	1234	1421
860	156	354	431	508	706	783	90	1058	1135	1333	1410
871	860	2	882	893	904	915	926	937	948	959	970
882	178	255	453	530	728	805	1080	90	1157	1234	1432
893	244	332	420	508	717	805	1190	981	101	1278	1366
904	244	354	464	574	684	794	1124	1014	1234	123	1344
915	211	288	486	563	640	838	90	992	1190	1267	1344
926	167	354	420	607	673	739	79	992	1179	1245	1432
937	178	365	431	497	684	750	79	1003	1190	1256	1443
948	244	321	398	596	673	750	1025	90	1102	1300	1377
959	189	277	486	574	662	750	101	1047	1135	1223	1432

Table(2) : lines and planes for PG(3,11)											
L1											
2	134	145	156	167	178	189	200	211	222	233	244
13	2	24	35	46	57	68	79	90	101	112	123
24	134	266	398	530	662	794	926	1058	1190	1322	1454
35	134	277	420	563	706	849	871	1014	1157	1300	1443
46	134	288	442	596	629	783	937	1091	1124	1278	1432
57	134	299	464	508	673	838	882	1047	1212	1256	1421
68	134	310	486	541	717	772	948	1003	1179	1234	1410
79	134	321	387	574	640	827	893	1080	1146	1333	1399
90	134	332	409	607	684	761	959	1036	1113	1311	1388
101	134	343	431	519	728	816	904	992	1201	1289	1377
112	233	332	431	530	629	849	948	1047	1146	1245	1344
123	134	365	475	585	695	805	915	1025	1135	1245	1355
134	13	255	376	497	618	739	860	981	1102	1223	1344
145	277	24	409	541	673	805	937	1069	1201	1333	1344
156	13	277	398	519	640	761	882	1003	1124	1245	1366
167	299	24	431	563	695	827	959	1091	1102	1234	1366
178	13	299	420	541	662	783	904	1025	1146	1267	1388
189	13	310	431	552	673	794	915	1036	1157	1278	1399
200	13	321	442	563	684	805	926	1047	1168	1289	1410
211	13	332	453	574	695	816	937	1058	1179	1300	1421
222	365	35	387	530	673	816	959	981	1124	1267	1410
233	13	354	475	596	717	838	959	1080	1201	1322	1443
244	255	24	387	519	651	783	915	1047	1179	1311	1443
255	2	266	277	288	299	310	321	332	343	354	365
266	244	35	409	552	695	838	860	1003	1146	1289	1432
277	244	585	431	46	618	772	926	1080	1113	1267	1421
288	156	24	420	552	684	816	948	1080	1212	1223	1355
299	156	442	35	585	728	750	893	1036	1179	1322	1344
310	178	24	442	574	706	838	970	981	1113	1245	1377
321	189	24	453	585	717	849	860	992	1124	1256	1388
332	189	35	475	497	640	783	926	1069	1212	1234	1377
343	211	24	475	607	618	750	882	1014	1146	1278	1410
354	211	35	376	519	662	805	948	1091	1113	1256	1399
365	233	376	24	508	640	772	904	1036	1168	1300	1432
376	442	387	398	409	420	431	2	453	464	475	486
387	200	354	46	541	695	849	882	1036	1190	1223	1377
398	233	255	35	541	684	827	970	992	1135	1278	1421
409	222	255	46	563	717	750	904	1058	1212	1245	1399
420	233	266	46	574	728	761	915	1069	1102	1256	1410
431	145	288	35	574	717	739	882	1025	1168	1311	1454
442	233	277	651	607	57	816	860	1025	1190	1234	1399
453	167	310	35	596	618	761	904	1047	1190	1333	1355

L2											
1	134	135	136	137	138	139	140	141	142	143	144
13	1	14	15	16	17	18	19	20	21	22	23
14	134	256	378	500	622	744	866	988	1110	1232	1354
15	382	259	136	505	628	740	863	986	1109	1232	1344
16	134	258	382	506	619	743	867	991	1104	1228	1352
17	134	259	384	498	623	748	862	987	1112	1226	1351
18	134	260	386	501	627	742	868	983	1109	1224	1350
19	134	261	377	504	620	747	863	990	1106	1233	1349
20	134	262	379	507	624	741	869	986	1103	1231	1348
21	134	263	381	499	628	746	864	982	1111	1229	1347
22	143	262	381	500	619	749	868	987	1106	1225	1344
23	134	265	385	505	625	745	865	985	1105	1225	1345
134	13	255	376	497	618	739	860	981	1102	1223	1344
135	13	256	377	498	619	740	861	982	1103	1224	1345
136	384	260	497	16	621	745	869	982	1106	1230	1354
137	13	258	379	500	621	742	863	984	1105	1226	1347
138	13	259	380	501	622	743	864	985	1106	1227	1348
139	262	15	385	497	620	743	866	989	1112	1224	1347
140	13	261	382	503	624	745	866	987	1108	1229	1350
141	13	262	383	504	625	746	867	988	1109	1230	1351
142	13	263	384	505	626	747	868	989	1110	1231	1352
143	13	264	385	506	627	748	869	990	1111	1232	1353
144	13	265	386	507	628	749	870	991	1112	1233	1354
255	144	14	377	499	621	743	865	987	1109	1231	1353
256	144	15	379	502	625	748	860	983	1106	1229	1352
257	135	14	379	501	623	745	867	989	1111	1233	1344
258	135	381	15	504	627	739	862	985	1108	1231	1354
259	137	14	381	503	625	747	869	991	1102	1224	1346
260	138	14	382	504	626	748	870	981	1103	1225	1347
261	255	256	257	258	259	260	263	262	1	264	265
262	138	386	499	16	623	747	860	984	1108	1232	1345
263	137	504	378	745	619	18	860	986	1112	1227	1353
264	141	15	376	499	622	745	868	991	1103	1226	1349
265	142	15	377	500	623	746	869	981	1104	1227	1350
376	143	265	14	498	620	742	864	986	1108	1230	1352
377	140	264	16	501	625	749	862	986	1110	1223	1347
378	143	255	15	501	624	747	870	982	1105	1228	1351
379	142	255	16	503	627	740	864	988	1112	1225	1349
380	143	256	16	504	628	741	865	989	1102	1226	1350
381	144	257	505	16	618	742	866	990	1103	1227	1351

382	139	255	741	498	625	868	19	984	1111	1227	1354
383	137	260	15	506	618	741	864	987	1110	1233	1345
384	138	261	507	15	619	742	865	988	1111	1223	1346
385	137	261	16	498	622	746	870	983	1107	1231	1344
386	376	377	378	379	380	381	382	383	384	385	1
497	144	258	383	622	17	747	861	986	1111	1225	1350
498	142	257	383	739	624	18	865	991	1106	1232	1347
499	135	260	385	624	17	749	863	988	1102	1227	1352
500	497	498	499	1	501	502	503	504	505	506	507
501	137	262	376	17	626	740	865	990	1104	1229	1354
502	141	265	378	16	626	739	863	987	1111	1224	1348
503	139	264	378	17	628	742	867	981	1106	1231	1345
504	144	264	384	864	624	744	1104	984	1224	23	1344
505	141	255	380	619	17	744	869	983	1108	1233	1347
506	142	256	381	17	620	745	870	984	1109	1223	1348
507	135	259	383	620	16	744	868	981	1105	1229	1353
618	136	262	377	503	18	744	870	985	1111	1226	1352
619	618	1	620	621	622	623	624	625	626	627	628
620	141	258	386	503	865	748	20	982	1110	1227	1344
621	139	265	380	506	747	18	862	988	1103	1229	1344
622	140	255	381	507	748	18	863	989	1104	1230	1345
623	137	264	380	507	866	739	19	982	1109	1225	1352
624	138	265	381	497	740	867	19	983	1110	1226	1353
625	136	261	386	500	17	739	864	989	1103	1228	1353
626	144	259	385	500	18	741	867	982	1108	1223	1349
627	138	263	377	502	17	741	866	991	1105	1230	1344
628	135	261	376	502	18	743	869	984	1110	1225	1351
739	741	740	1	742	743	744	745	746	747	748	749
740	144	261	378	506	623	868	985	20	1102	1230	1347
741	140	258	376	505	623	988	870	21	1106	1224	1353
742	140	256	383	499	626	19	869	985	1112	1228	1344
743	141	257	384	500	627	19	870	986	1102	1229	1345
744	142	258	385	501	628	19	860	987	1103	1230	1346
745	138	255	383	500	628	990	862	20	1107	1224	1352
746	144	260	376	503	619	862	19	989	1105	1232	1348
747	140	257	385	502	619	981	864	20	1109	1226	1354
748	135	262	378	505	621	864	19	991	1107	1223	1350
749	136	263	379	506	622	19	865	981	1108	1224	1351
860	136	264	381	498	626	743	20	988	1105	1233	1350
861	860	1	862	863	864	865	866	867	868	869	870
862	142	262	382	502	622	742	982	1233	1102	23	1353
863	138	257	376	506	625	744	982	1112	22	1231	1350
864	141	256	623	497	18	749	990	1105	1346	1231	382
865	140	259	378	497	627	746	984	1103	1233	22	1352
866	142	259	376	504	621	749	983	20	1111	1228	1345
867	143	260	377	505	622	739	984	20	1112	1229	1346
868	138	256	385	503	621	739	986	21	1104	1233	1351
869	144	263	382	501	620	739	988	1107	22	1226	1345

870	135	263	380	497	625	742	20	987	1104	1232	1349
981	982	1	983	984	985	986	987	988	989	990	991
982	140	265	379	17	618	743	868	1346	1107	1232	504
983	143	263	383	503	623	743	863	1103	23	1223	1354
984	136	265	383	501	619	748	866	1102	21	1231	1349
985	141	260	379	498	628	747	866	1104	22	1223	1353
986	135	255	386	506	626	746	866	1226	1106	23	1346
987	136	256	376	507	627	747	867	1227	1107	23	1347
988	137	257	377	497	628	748	868	1228	1108	23	1348
989	141	259	377	506	624	742	860	21	1107	1225	1354
990	142	260	378	507	625	743	861	1108	21	1226	1344
991	143	261	379	497	626	744	862	21	1109	1227	1345
1102	1103	1	1104	1105	1106	1107	1108	1109	1110	1111	1112
1103	137	255	384	502	620	749	867	985	1350	1232	21
1104	13	257	378	499	620	741	862	983	1346	1225	136
1105	140	262	14	506	628	739	861	983	1349	1227	384
1106	137	265	382	499	627	744	861	989	20	1223	1351
1107	143	258	384	499	625	18	866	981	740	1233	1348
1108	139	256	384	501	618	746	20	991	1225	863	1353
1109	135	265	384	503	622	741	860	990	22	1228	1347
1110	136	255	385	504	623	742	861	991	22	1229	1348
1111	137	256	386	505	624	743	862	981	22	1230	1349
1112	141	261	381	501	621	741	861	981	1232	23	1352
1223	1	1224	1225	1226	1227	1228	1229	1230	1231	1232	1233
1224	143	257	621	507	17	746	860	985	1110	382	1349
1225	140	263	386	15	621	744	867	990	1102	1348	498
1226	139	14	383	505	627	749	860	982	1104	261	1348
1227	134	264	383	502	621	740	870	989	1108	22	1346
1228	138	264	379	505	620	18	861	987	1102	746	1354
1229	138	258	378	498	618	749	869	989	1109	23	1349
1230	139	259	379	499	619	739	870	990	1110	23	1350
1231	140	260	380	500	620	740	860	991	1111	23	1351
1232	139	258	377	507	626	745	864	983	1102	22	1351
1233	139	263	376	16	624	748	861	985	1109	1346	500
1344	1	1345	1346	1347	1348	1349	1350	1351	1352	1353	1354
1345	136	14	380	502	624	746	868	990	1112	1223	258
1346	144	262	380	498	627	863	1110	981	21	1228	745
1347	143	259	386	502	618	745	19	988	1104	1231	861
1348	135	264	382	500	618	747	983	1112	1230	21	865
1349	13	260	381	502	623	744	865	986	1107	1228	139
1350	141	14	385	507	618	740	862	984	1106	1228	263
1351	142	264	14	497	619	741	863	985	1107	1229	386
1352	139	257	386	504	622	740	21	987	1105	1223	869
1353	134	257	380	503	626	749	861	984	1107	1230	15
1354	142	261	380	499	618	748	867	1105	22	1224	986

466	186	326	43	617	636	776	916	1067	1207	1226	1366
476	196	336	43	506	646	786	926	1077	1217	1236	1387
486	186	336	53	526	676	837	866	1016	1177	1327	1356
506	166	316	466	53	656	806	967	996	1146	1307	1457
516	176	326	476	53	666	816	977	1006	1167	1317	1346
526	145	316	476	686	63	857	896	1067	1106	1277	1437
536	196	346	386	53	686	847	876	1026	1187	1337	1366
546	206	356	396	53	696	857	886	1036	1197	1226	1387
556	186	346	396	63	727	766	926	1097	1136	1307	1346
566	196	356	406	63	737	776	947	986	1146	1317	1356
576	506	516	526	536	546	556	566	596	586	12	617
586	246	286	436	53	626	776	926	1087	1116	1277	1427
596	226	276	436	646	63	806	977	1016	1187	1226	1397
617	236	286	446	63	656	816	866	1026	1197	1236	1407
626	636	12	646	656	666	676	686	696	706	727	737
636	176	346	406	576	866	806	73	1036	1217	1277	1447
646	206	316	426	536	123	756	866	1097	1207	1317	1427
656	196	366	426	596	837	73	886	1067	1116	1297	1346
666	246	296	456	506	63	837	876	1036	1207	1246	1417
676	135	306	466	516	63	847	886	1057	1217	1256	1427
686	135	336	416	617	967	766	93	1036	1116	1317	1397
696	236	296	466	526	756	73	926	986	1167	1337	1397
706	176	336	386	546	63	756	916	1087	1126	1297	1457
727	135	316	486	546	73	776	957	1006	1187	1236	1417
737	145	326	386	556	73	786	967	1016	1197	1246	1427
746	12	756	766	776	786	796	806	816	837	847	857
756	246	326	406	596	676	957	93	1026	1106	1307	1387
766	246	306	476	536	706	73	947	996	1177	1226	1407
776	206	276	456	526	706	83	967	1026	1217	1287	1346
786	236	346	456	566	676	123	896	1006	1116	1226	1457
796	226	296	476	546	737	866	1057	83	1116	1307	1366
806	236	306	486	556	626	83	876	1067	1126	1317	1387
816	186	356	416	586	646	73	876	1057	1106	1287	1457
837	135	326	396	576	646	896	83	1087	1146	1337	1407
847	145	336	406	586	656	83	906	1097	1167	1226	1417
857	216	276	446	506	676	73	906	1087	1136	1317	1366
866	12	876	886	896	906	916	926	947	957	967	977
876	176	366	446	526	727	796	93	1077	1146	1226	1427
886	246	316	386	566	636	816	83	1077	1136	1327	1397
896	196	276	466	546	626	816	1097	93	1177	1246	1447
906	206	286	476	556	636	837	93	986	1187	1256	1457
916	166	346	416	596	666	857	83	986	1177	1236	1427
926	176	356	426	617	676	746	83	996	1187	1246	1437

947	236	316	396	586	666	746	1016	93	1217	1297	1366
957	186	276	476	566	656	746	1036	103	1126	1337	1427
967	246	346	446	546	646	746	1167	1067	113	1256	1356
977	145	346	426	506	696	776	93	1057	1126	1327	1407
986	12	996	1006	1016	1026	1036	1057	1067	1077	1087	1097
996	216	296	486	566	646	847	916	93	1197	1277	1346
1006	226	306	386	576	656	857	926	93	1207	1287	1356
1016	166	366	456	546	636	847	926	1106	103	1317	1407
1026	216	316	416	516	737	837	926	1126	113	1226	1447
1036	226	326	426	526	626	847	947	1136	113	1236	1457
1057	166	276	386	617	727	837	947	123	1167	1277	1387
1067	166	356	436	516	706	786	866	93	1136	1337	1417
1077	216	306	396	596	686	776	866	103	1167	1246	1457
1087	226	316	406	617	696	786	876	103	1177	1256	1346
1097	216	356	386	43	666	806	957	1116	526	1256	1407
1106	1116	12	1126	1136	1146	1167	1177	1187	1197	1207	1217
1116	206	306	406	506	727	816	916	1016	1337	113	1437
1126	246	356	466	576	686	796	906	1016	123	1236	1346
1136	135	366	476	586	696	806	916	1026	1356	1246	123
1146	226	286	456	516	686	746	916	1097	73	1327	1387
1167	206	366	416	576	63	786	957	996	1366	1327	626
1177	135	356	456	556	656	756	977	1077	113	1277	1366
1187	145	366	466	566	666	766	866	1087	113	1287	1387
1197	246	336	426	516	727	806	896	986	103	1287	1366
1207	176	276	486	586	686	786	886	986	113	1307	1407
1217	145	356	446	536	626	837	916	1006	103	1307	1397
1226	12	1236	1246	1256	1277	1287	1297	1307	1317	1327	1337
1236	206	296	386	586	676	766	977	1067	1146	103	1447
1246	236	336	436	536	636	857	957	1057	1146	113	1346
1256	166	336	396	566	626	796	977	73	1207	1026	1437
1277	236	326	416	506	706	796	886	1097	1187	103	1356
1287	176	286	396	506	737	847	957	1067	1177	123	1397
1297	135	346	436	526	737	816	906	996	1207	103	1387
1307	196	306	416	526	636	746	977	1087	1197	123	1417
1317	186	286	386	596	696	796	896	996	1217	113	1417
1327	216	326	436	546	656	766	876	986	1217	123	1437
1337	226	336	446	556	666	776	886	996	1106	123	1447
1346	12	1356	1366	1387	1397	1407	1417	1427	1437	1447	1457
1356	216	286	466	536	727	83	977	1036	1106	1297	786
1366	306	33	436	566	696	837	967	1097	1106	1236	176
1387	23	296	416	536	656	776	896	1016	1136	1256	176
1397	206	346	486	516	43	796	947	1087	1106	1246	656
1407	186	296	406	516	626	857	967	1077	1187	1297	123
1417	236	276	426	53	737	766	916	1077	1106	1256	576
1427	196	296	396	617	706	806	906	1006	1106	1327	113
1437	196	286	486	576	666	756	967	1057	1136	1226	103
1447	166	326	486	536	63	746	906	1077	1116	1287	696
1457	196	255	446	516	696	766	957	1016	1207	1277	83

References

1. Hirschfeld, J. W. P. (1998). *Projective geometries over finite fields* (2nd ed.). Oxford University Press.
2. Al-Mukhtar, A. S. H. (2008). *Complete arcs and surfaces in three dimensional projective space over Galois field* (Master's thesis). University of Technology, Iraq.
3. Kareem, F. F. (2011). A complete (k, r)-cap in PG(3, p) over Galois field GF(4). *University of Baghdad*, 24(2).
4. Abdulla, A. A., & Kasm, N. Y. (2020). Application of algebraic geometry in three dimensional projective space PG(3,7). *Journal of Physics: Conference Series*. https://doi.org/[Insert DOI if available]
5. Ayres, F. (1967). *Projective geometry*. Schaum Publishing Co.
6. Hassan, A. S. (2001). *Construction of (k, 3)-arcs on projective plane over Galois field GF(q), $q = p^h$ when $p = 2$ and $h = 2, 3$ and 4* (Master's thesis). College of Education, Ibn Al-Haitham, University of Baghdad.
7. Hirschfeld, J. W. P. (1979). *Projective geometries over finite fields*. Oxford: Clarendon Press; New York: Oxford University Press.
8. Al-Jofy, R. A. S. (1999). *Complete arcs in a projective plane over Galois field* (Master's thesis). College of Education, Ibn Al-Haitham, University of Baghdad.

Development of Mathematical Models for Traffic Emissions Based on Vehicle Delay at Signalized Intersections

Neveen Mohammad Al-Qaisi[2,1,6]

The Greater Amman Municipality, Jordan,
Neveen.AbdAlkareemAlQaisi@ammancity.GOV.JO

[2] Head of Development Division| Transportation Engineering, M.Sc

Development of Mathematical Models for Traffic Emissions Based on Vehicle Delay at Signalized Intersections

Neveen Mohammad Al-Qaisi[3][16],

The Greater Amman Municipality, Jordan,
Neveen.AbdAlkareemAlQaisi@ammancity.GOV.JO

Abstract:

This study aims to develop accurate mathematical models to estimate hydrocarbon (HC), carbon monoxide (CO), and nitrogen oxide (NO_x) emissions based on traffic delay parameters at signalized intersections. Using data from six congested intersections in Amman, Jordan, microscopic simulation models were developed and validated. Statistical analysis was then conducted to establish relationships between emissions and two measures of effectiveness: delay per vehicle and intersection control delay. The results revealed a strong inverse linear relationship between delay per vehicle and emissions, with the developed logarithmic models achieving high coefficients of determination of 89.26%, 87.49%, and 98.04% for HC, CO, and NO_x, respectively.

Key words: Traffic Emissions, Signalized Intersections, Mathematical Models, Delay, Hydrocarbon, Nitrogen Oxid.

Introduction:

The rapid growth in vehicle ownership in developing countries has led to severe traffic congestion, particularly at urban signalized intersections. This congestion not only results in significant travel delays but also has adverse environmental consequences due to increased vehicle emissions. Accurate prediction of these emissions is crucial for environmental impact assessments and for evaluating the sustainability of traffic improvement projects. The core problem this research addresses is the need for practical models that can predict emissions based on readily available traffic performance metrics, rather than complex vehicle-specific data. This article hypothesizes that a direct, quantifiable relationship exists between traffic delay and the rate of vehicle emissions. The methodology involves using microscopic simulation to generate performance data, which is then analyzed using statistical regression to develop and validate the proposed mathematical models.

Head of Development Division| Transportation Engineering, M.Sc[3]

THE FIRST TOPIC : THEORETICAL FRAMEWORK AND METHODOLOGY

This topic outlines the foundational concepts of traffic-related emissions and details the systematic approach used to collect data and develop the predictive models.

FIRST REQUIREMENT: STUDY METHODOLOGY

The methodology was implemented in a sequential manner to ensure the reliability of the results.

This chapter represents the systematic, theoretical analysis of the methods to be applied in this study. The tasks were needed are completed during this entire study, Figure 3.1 summariesed the ongoing planned to be performed into several steps:

1. Site selection; identify the most congested signalized intersections with appropriate surrounding intersections where AID's could be implimented in Amman.
2. Data collection; collect real traffic data (traffic volume and signal timing and phasing).
3. Develop base simulation models of the current situation for the selected intersections using the microscopic simulation platform Synchro 8.
4. Validate base models using Vissim microscopic simulation software.
5. Evaluation of base simulation models.
6. Develop mathmatical models to evaluate gas emissions using SPSS software platform and Microsoft Exel.
7. Develop a proposed model using alternative intersections.
8. Evaluate the proposed model.
9. Analyze and compare both models using appropriate measures of effectiveness (MOE's).

10. GIS analysis; both models are incorporated Arc GIS platform.

11. Identification of new routes.

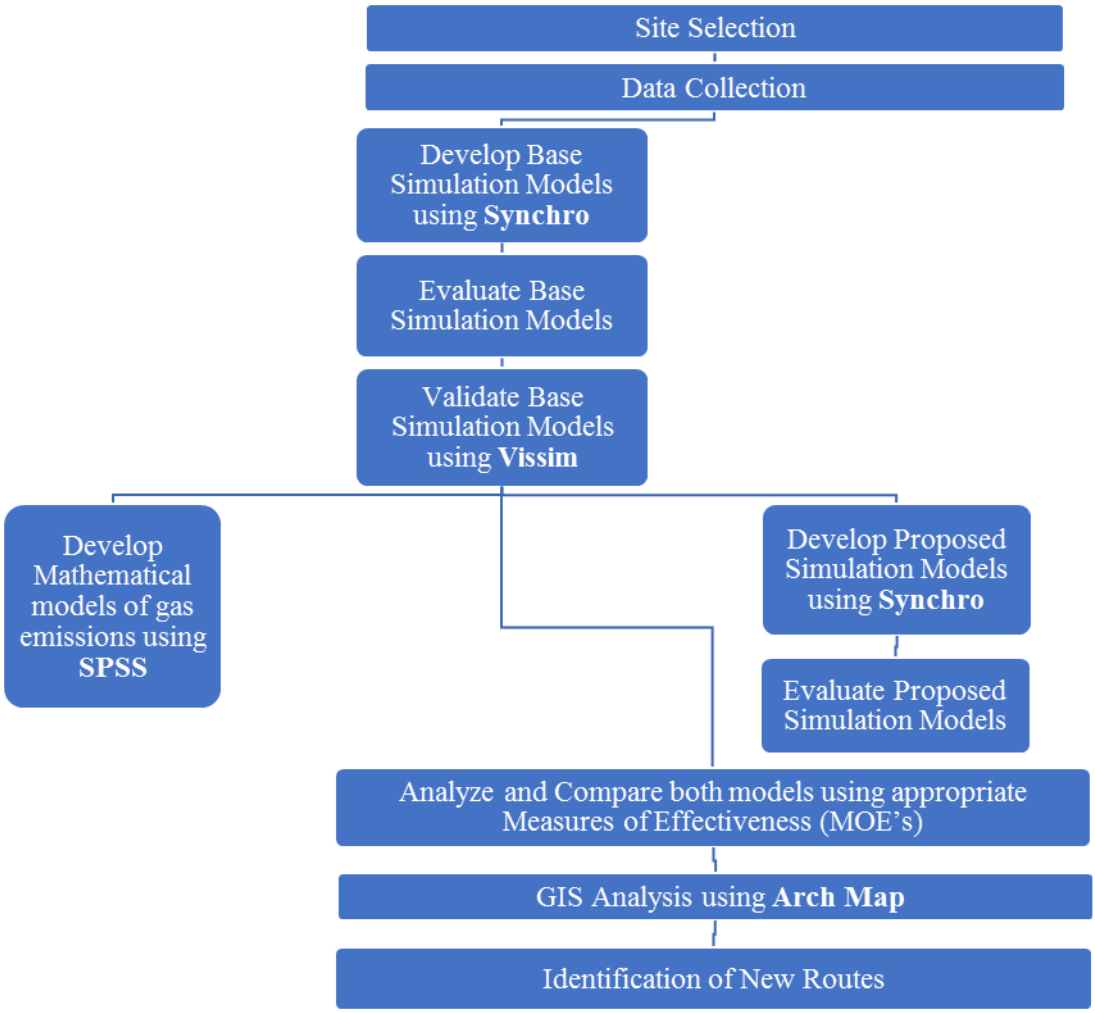

Figure 3.1: Proposed Work Flow Chart

Firstly: Data Collection and Base Model Development

The traffic data on the selected signalized intersections was available from the department of traffic operations at GAM only for through and left turn movements. right turn movement and volume at alternative intersections were caunted manually for one hour in February, Appendix A shows the traffic volume calculations of right turn movement. In the same manner data was collected on the prior and after signalized intersections, while on roundabouts data was avaliable from transportation planning department at GAM, all movements traffic volume are represented as a through movement get in or out from arterial roads towerd the main selected intersections, including the percentage of heavy vehicles (H.V).

Three weekdays of February,2019, 11th,12th, and 13th, were selected to decide which day is to be used for analysis and to estimate when the peak hour occurred. Figure 3.8 through 3.13 show the highest daylly volume of the six main intersections occures on Tuesday, Feb.12th,2019, which cosidered the day of analysis, figures also give an indication that the morning peak occurres from 7:30 to 8:30 am.

This chapter discusses the base model development and validation. Also, it describes the proposed AID models development.

1. Develop a base simulation model for the current situation using the microscopic simulation platform Synchro 8.
2. Validate the model; develop the proposed AID simulation model
3. Evaluation of base simulation model.

4. Develop and evaluate gas emissions mathematical models.
5. Evaluate the proposed models.

4.1 Base Model Development

The base model development for the current intersections starts after the data has been collected and prepared. It was constructed using the existing geometric and traffic data for the six selected intersections. The geometric design for the current situation was imported into SYNCHRO 8 as DXF file from AUTOCAD draft brought from GAM, defining the links length, number of lanes, lane width, approach volumes and cycle length. Figure 4.1 through Figure4.6. shows the base model for the six selected arterial road. Also, it shows traffic volume for each movement.

The need to create the base model is important for several reasons; first for the model validation to ensure that the SYNCHRO 8 generated traffic volumes similar to those observed in the field. Also, it is needed for comparison and evaluation purposes.

Figure 4.1: SYNCHRO Model for Current Situation of Al-Assaf Intersection

Figure 4.2: SYNCHRO Model for Current Situation of Elba House Intersection

Figure 4.3: SYNCHRO Model for Current Situation of Firas Square

Figure 4.4: SYNCHRO Model for Current Situation of Jbaiha Intersection

Figure 4.5: SYNCHRO Model for Current Situation of Princess Alia Intersection

Figure 4.6: SYNCHRO Model for Current Situation of Wadi Saqra Intersection

It worth mentioning that, the traditional measures that were tested to improve the performance of the six selected intersections included signal timing optimization.

The SYNCHRO software was used to optimize signals phasing and cycle lengths. It was found that the current signalized intersections were running on the optimal signal timing and phasing.

4.2 Model Validation

The base model is only potentially as accurate as the validation processes undertaken during development. Validation should be done using the most appropriate and efficient techniques. (Toledo and Kotsiopoulos, 2004) proposed two ways of model validation, visual methods and mathematical methods. The visual method of validation, which is a graphical representation of data from the real and simulated models are put both side by side to see how different the real and simulated models are. On the other hand, the mathematical validation method applies the goodness of fit measures, confidence intervals, and statistical tests to determine how similar the real and simulated models are.

It should be noted here that the Synchro software disable the changing the random seed number which limits the validation this process. For this reason, Vissim microscopic simulation software was used for this purpose, Vissim was not used in the model development process because of the unavailability of the full version of the program and only student version was available which runs the model for only 600 sec.

The maximum throughput volume was used for the validation purposes.

Eighty runs were carried out using different random seed numbers for each base model. Since the simulation models are valid, their result could be used to develop mathematical models of gas emissions with respect to the other MOE's, intersection delay and the delay per vehicle.

The IBM **SPSS** software platform which offers advanced statistical analysis, was used to develop the mathematical models of HC, CO, and NO_x emissions. correlation between variables was examined, different relationships was also tested among the three gas emission types and the other two MOE's, in addition to a summary of each of these models.

Stepwise regression method was used for both independent variables, which are intersection delay and delay per vehicle. Table 4.2 shows the variables introduced in the regression model for estimating gas emissions.

Table 4.2: Variables Entered for Gas Emissions

Variables Entered	**Method**
Intersection Delay	Stepwise (Criteria: Probability-of-F-to-enter <=0 .05.
Delay per Vehicle	Stepwise (Criteria: Probability-of-F-to-enter <= 0.50.

Hydrocarbon (HC)

The HC emission models were evaluated through integrated models, as a function of intersection delay and delay per vehicle, then a simple model was evaluated with respect to a single dependent variable separately.

Table 4.3 shows the correlation matrix between the six variables and the significance of the correlation.

Table 4.3: Correlations between Variables

		Emission/Lane (g/ln)	Delay/Veh. (sec/veh)	Int. Delay (sec)
Pearson Correlation	Emission/Lane (g/ln)	1.000	.183	.552
	Delay/Veh. (sec/veh)	.183	1.000	.653
	Int. Delay (sec)	.552	.653	1.000
Sig. (1-tailed)	Emission/Lane (g/ln)	.	.364	.128
	Delay/Veh. (sec/veh)	.364	.	.080
	Int. Delay (sec)	.128	.080	.
N	Emission/Lane (g/ln)	6	6	6
	Delay/Veh. (sec/veh)	6	6	6
	Int. Delay (sec)	6	6	6

It can be seen that the correlation between intersection delay and HC emission has a large positive strength of association with Pearson coefficient (r) of 0.552, while the correlation between delay per vehicle and HC emission a small positive strength of association with Pearson coefficient (r) 0.183.

The integrated model can be presented using coefficients in Table 4.4 As follow

HC gas emissions = 0.007 (intersection delay)- 0.02 (delay per vehicle)+ 10.656…….Equation 1

Table 4.4: Coefficients[a] of the HC Integrated Emission Model

Model		Unstandardized Coefficients		Standardized Coefficients			95.0% Confidence Interval for B		Correlations			Collinearity Statistics	
		B	Std. Error	Beta	t	Sig.	Lower Bound	Upper Bound	Zero-order	Partial	Part	Tolerance	VIF
1	(Constant)	10.656	1.446		7.368	.005	6.054	15.259					
	Delay/Veh. (sec/veh)	-.002	.004	-.309	-.506	.648	-.013	.010	.183	-.281	-.234	.573	1.745
	Int. Delay (sec)	.007	.006	.754	1.235	.305	-.012	.026	.552	.581	.571	.573	1.745

a. Dependent Variable: Emission/Lane (g/ln).

Therefore, the model is insignificance of fitting the two variables, but is it significant of representing the coefficient, which is considerable for predicted models.

Table 4.5 Of ANOVA output corroborates the insignificance of fitting the two variables with significance level of 0.0513. but, as illustrated in Table 4.6, correlation between the two independent variables, intersection delay and delay per vehicle, is strongly associated with r of 0.653.

Table 4.5: The Results of the ANOVA[a] Regression Analysis of HC Emission

Model		Sum of Squares	df	Mean Square	F	Sig.
1	Regression	3.555	2	1.778	.841	.513[b]
	Residual	6.339	3	2.113		
	Total	9.894	5			

a. Dependent Variable: Emission/Lane (g/ln)

b. Predictors: (Constant), Int. Delay (sec), Delay/Veh. (sec/veh)

Table 4.6 shows the integrated model of dependent variables, intersection delay and delay per vehicle.

Table 4.6: Correlations [a] of HC Emission Model's Independent Variables

Model			Int. Delay (sec)	Delay/Veh. (sec/veh)
1	Correlations	Int. Delay (sec)	1.000	-.653
		Delay/Veh. (sec/veh)	-.653	1.000
	Covariances	Int. Delay (sec)	3.526E-5	-1.413E-5

	Delay/Veh. (sec/veh)	-1.413E-5	1.328E-5

a. Dependent Variable: Emission/Lane (g/ln)

seven models are tested to fit each of the two variables, Table 4.7 represents these models and their significance which are not significant.

Table 4.7: Simple HC emission models' coefficient of dependent variables.

Relashionship	The independent variable is Emission/Lane (g/ln).	The dependent variable is ln(Int. Delay (sec)).					The dependent variable is ln(Delay/Veh. (sec/veh)).				
		Unstandardized Coefficients		Standardized Coefficients			Unstandardized Coefficients		Standardized Coefficients		
		B	Std. Error	Beta	t	Sig.	B	Std. Error	Beta	t	Sig.
Linear	Emission/Lane (g/ln)	30.732	82.339	0.183	0.373	0.728	56.731	42.859	0.552	1.324	0.256
	(Constant)	-30.181	1007.193		-0.030	0.978	-397.9425	524.265		-0.759	0.490
Logarithmic	log(Emission/Lane (g/ln))	442.920	978.176	0.221	0.453	0.674	697.071	507.188	0.566	1.374	0.241
	(Constant)	-760.465	2440.700		-0.312	0.771	-1445.526	1265.513		-1.142	0.317
Inverse	1 / Emission/Lane (g/ln)	-6085.169	11476.101	-0.256	-0.530	0.624	-8418.439	5945.927	-0.578	-1.416	0.230
	(Constant)	849.682	959.948		0.885	0.426	992.206	497.362		1.995	0.117
Quadratic	Emission/Lane (g/ln)	2105.619	1223.086	12.569	1.722	0.184	599.579	834.745	5.833	0.718	0.524
	Emission/Lane (g/ln) ** 2	-85.810	50.505	-12.405	-1.699	0.188	-22.450	34.469	-5.289	-0.651	0.561
	(Constant)	-12430.840	7345.634		-1.692	0.189	-3642.299	5013.329		-0.727	0.520
Cubic	Emission/Lane (g/ln)	1097.329	613.249	6.550	1.789	0.171	341.91245	422.421	3.326	0.809	0.478
	Emission/Lane (g/ln) ** 3	-2.413	1.379	-6.405	-1.750	0.178	-0.645	0.950	-2.791	-0.679	0.546
	(Constant)	-8516.072	4918.456		-1.731	0.182	-2666.861	3387.954		-0.787	0.489
Power	ln(Emission/Lane (g/ln))	1.950	3.142	0.296	0.621	0.569	2.8969794	1.691	0.651	1.713	0.162
	(Constant)	2.108	16.526		0.128	0.905	0.191	0.807		0.237	0.824
Exponential	Emission/Lane (g/ln)	0.145	0.265	0.263	0.546	0.614	0.238	0.143	0.639	1.664	0.172
	(Constant)	46.806	151.767		0.308	0.773	14.506	25.367		0.572	0.598

Table 4.8 shows models summery, it can be seen that the adjusted R square has negative values, because a small sample size was used to build the model, overfitting of model, so the R square was used to evaluate the models.

R square has a higher value of quadrant and cubic relation of the dependent variable intersection delay, 0.508 and 0.522, respectively, which considered moderated.

Table 4.8: Model Summary of HC Emissions.

Relashionship	The dependent variable is ln(Int. Delay (sec)).			The dependent variable is ln(Delay/Veh. (sec/veh)).		
	R	R Square	Adjusted R Square	R	R Square	Adjusted R Square
Linear	0.183	0.034	-0.208	0.552	0.305	0.131
Logarithmic	0.221	0.049	-0.189	0.566	0.321	0.151
Inverse	0.256	0.066	-0.168	0.578	0.334	0.167
Quadratic	0.712	0.508	0.179	0.625	0.391	-0.015
Cubic	0.722	0.522	0.203	0.630	0.397	-0.005
Power	0.296	0.088	-0.140	0.651	0.423	0.279
Exponential	0.263	0.069	-0.163	0.639	0.409	0.261
	The independent variable is Emission/Lane (g/ln).					

Figure 4.7 represents the HC Emissions versus Intersection delay for the seven proposed mathematical models, it can be seen none of them fits the points, as well as the models that represented in Figure 4.8, HC Emissions versus delay per vehicle.

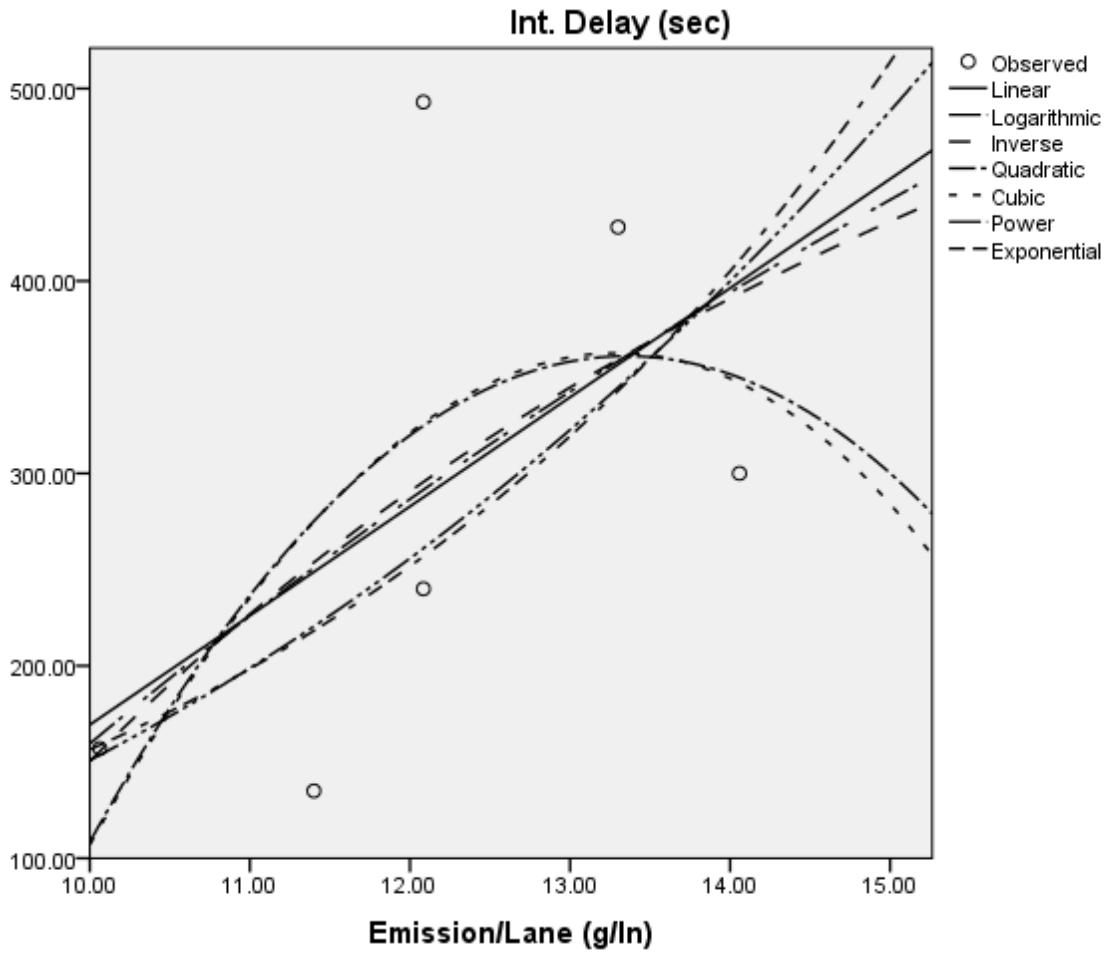

Figure 4.7: HC Emissions versus Intersection Delay

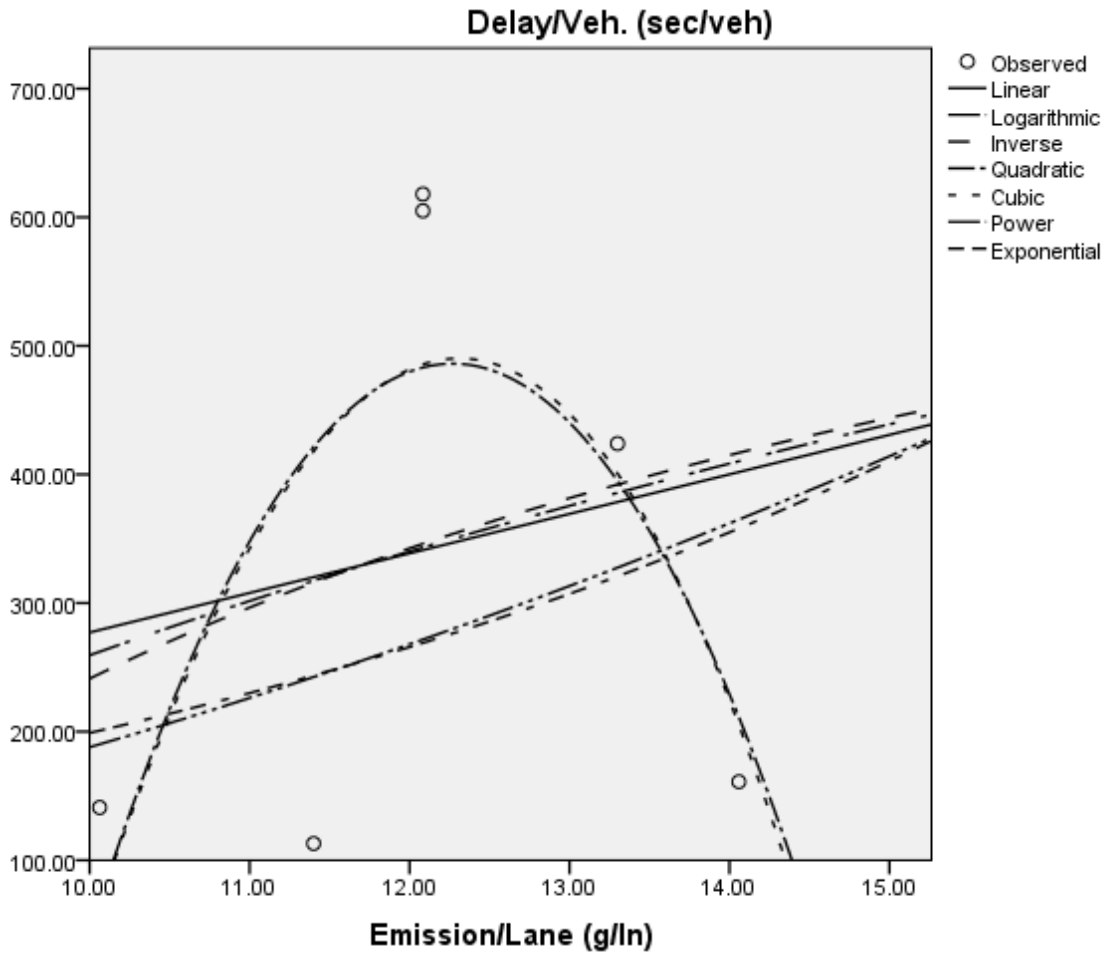

Figure 4.8: HC Emissions versus Delay per Vehicle

Carbon monoxide (CO)

The CO emission models were evaluated through integrated models, as a function of intersection delay and delay per vehicle, then a simple model was evaluated with respect to a single dependent variable separately.

Table 4.9 shows the correlation matrix between the six variables and the significance of the correlation.

Table 4.9: Correlations between Variables and CO Emissions

		Emission/Lane (g/ln)	Delay/Veh. (sec/veh)	Int. Delay (sec)
Pearson Correlation	Emission/Lane (g/ln)	1.000	-.649	.107
	Delay/Veh. (sec/veh)	-.649	1.000	.653
	Int. Delay (sec)	.107	.653	1.000
Sig. (1-tailed)	Emission/Lane (g/ln)	.	.082	.420
	Delay/Veh. (sec/veh)	.082	.	.080
	Int. Delay (sec)	.420	.080	.
N	Emission/Lane (g/ln)	6	6	6
	Delay/Veh. (sec/veh)	6	6	6
	Int. Delay (sec)	6	6	6

It can be seen that the correlation between delay per vehicle and CO emission has a large negative strength of association with Pearson coefficient of -0.649, while the correlation between delay per vehicle and CO emission has a small positive strength of association between intersection delay with Pearson coefficient (r) 0.107.

The integrated model can be presented using coefficients in Table 4.10 As follow

CO gas emissions = 1.184 (intersection delay)- 0.984 (delay per vehicle)+ 381.550….Equation 2

Table 4.10: Coefficients[a] of the CO Integrated Emission Model

Model		Unstandardized Coefficients		Standardized Coefficients			95.0% Confidence Interval for B		Correlations			Collinearity Statistics	
		B	Std. Error	Beta	t	Sig.	Lower Bound	Upper Bound	Zero-order	Partial	Part	Tolerance	VIF
1	(Constant)	381.550	70.091		5.444	.012	158.490	604.609					
	Delay/Veh. (sec/veh)	-.984	.177	-1.254	-5.571	.011	-1.546	-.422	-.649	-.955	-.949	.573	1.745
	Int. Delay (sec)	1.184	.288	.926	4.116	.026	.269	2.100	.107	.922	.701	.573	1.745

a. Dependent Variable: Emission/Lane (g/ln)

Therefore, the model is insignificance of fitting the two variables and the coefficient. Table 4.11 Of ANOVA output shows the significance of fitting the two variables with significance level of 0.026. Table 4.12 illustrated correlation between the two independent variables, intersection delay and delay per vehicle, is also strongly associated with r of -0.653.

Table 4.11 The Results of the ANOVA[a] Regression Analysis.

Model		Sum of Squares	df	Mean Square	F	Sig.
1	Regression	155971.658	2	77985.829	15.714	.026[b]
	Residual	14888.505	3	4962.835		
	Total	170860.163	5			

a. Dependent Variable: Emission/Lane (g/ln)

b. Predictors: (Constant), Int. Delay (sec), Delay/Veh. (sec/veh)

Table 4.12: The Correlations [a] of CO Emission Model's Independent Variables

Model			Int. Delay (sec)	Delay/Veh. (sec/veh)
1	Correlations	Int. Delay (sec)	1.000	-.653
		Delay/Veh. (sec/veh)	-.653	1.000
	Covariances	Int. Delay (sec)	.083	-.033
		Delay/Veh. (sec/veh)	-.033	.031

a. Dependent Variable: Emission/Lane (g/ln)

seven models are tested to fit each of the two variables, Table 4.13 Represents these models and their significance which are not significant.

Table 4.13: Simple CO Emission Models' Coefficient of Dependent Variables

Relashionship	The independent variable is Emission/Lane (g/ln).	The dependent variable is ln(Int. Delay (sec)).					The dependent variable is ln(Delay/Veh. (sec/veh)).				
		Unstandardized Coefficients		Standardized Coefficients			Unstandardized Coefficients		Standardized Coefficients		
		B	Std. Error	Beta	t	Sig.	B	Std. Error	Beta	t	Sig.
Linear	Emission/Lane (g/ln)	0.084	0.389	0.107	0.216	0.840	-0.827	0.485	-0.649	-1.705	0.163
	(Constant)	259.484	165.075		1.572	0.191	665.809	205.924		3.233	0.032
Logarithmic	ln(Emission/Lane (g/ln))	20.904	76.334	0.136	0.274	0.798	-158.208	97.514	-0.630	-1.622	0.180
	(Constant)	172.273	442.659		0.389	0.717	1251.044	565.480		2.212	0.091
Inverse	1 / Emission/Lane (g/ln)	-3026.308	9228.018	-0.162	-0.328	0.759	18058.188	12277.299	0.592	1.471	0.215
	(Constant)	308.528	82.042		3.761	0.020	246.035	109.152		2.254	0.087
Quadratic	Emission/Lane (g/ln)	0.083	1.909	0.106	0.043	0.968	-1.365	2.360	-1.071	-0.578	0.604
	Emission/Lane (g/ln) ** 2	0.000	0.003	0.001	0.001	1.000	0.001	0.004	0.434	0.234	0.830
	(Constant)	259.567	242.903		1.069	0.364	709.447	300.274		2.363	0.099
Cubic	Emission/Lane (g/ln)	17.300	3.789	22.117	4.566	0.045	20.271	3.759	15.901	5.393	0.033
	Emission/Lane (g/ln) ** 2	-0.067	0.015	-51.670	-4.606	0.044	-0.084	0.014	-39.408	-5.771	0.029
	Emission/Lane (g/ln) ** 3	0.000	0.000	30.731	4.620	0.044	8.830E-05	0.000	23.696	5.852	0.028
	(Constant)	-433.825	173.499		-2.500	0.130	-161.886	172.142		-0.940	0.446
Power	ln(Emission/Lane (g/ln))	0.035	0.278	0.062	0.125	0.907	-0.461	0.341	-0.559	-1.350	0.248
	(Constant)	214.509	346.080		0.620	0.569	3827.388	7577.611		0.505	0.640
Exponential	Emission/Lane (g/ln)	0.000	0.001	0.065	0.131	0.902	-0.002	0.002	-0.555	-1.334	0.253
	(Constant)	243.584	146.010		1.668	0.171	672.017	496.293		1.354	0.247

Table 4.13 shows models summery, it can be seen that the adjusted R square has negative values, because a small sample size was used to build the model, overfitting of model, so the R square was used to evaluate the models.

R square has a higher value of cubic relation of the independent variable, intersection delay, 0.915 and 0.969 for the independent variable, delay per vehicle, which sound great.

Table 4.14: Model Summary of CO Emissions.

Relashionship	The dependent variable is ln(Int. Delay (sec)).			The dependent variable is ln(Delay/Veh. (sec/veh)).		
	R	R Square	Adjusted R Square	R	R Square	Adjusted R Square
Linear	0.107	0.012	-0.236	0.649	0.421	0.276
Logarithmic	0.136	0.018	-0.227	0.630	0.397	0.246
Inverse	0.162	0.026	-0.217	0.592	0.351	0.189
Quadratic	0.107	0.012	-0.647	0.657	0.431	0.052
Cubic	0.957	0.915	0.788	0.984	0.969	0.922
Power	0.062	0.004	-0.245	0.559	0.313	0.141
Exponential	0.065	0.004	-0.245	0.555	0.308	0.135
	The independent variable is Emission/Lane (g/ln).					

Figure 4.9 represents the CO Emissions versus Intersection delay for the seven proposed mathematical models, it can be seen the cubic model almost fits the points, as well as the cubic model that represented in Figure 4.10, CO Emissions versus delay per vehicle.

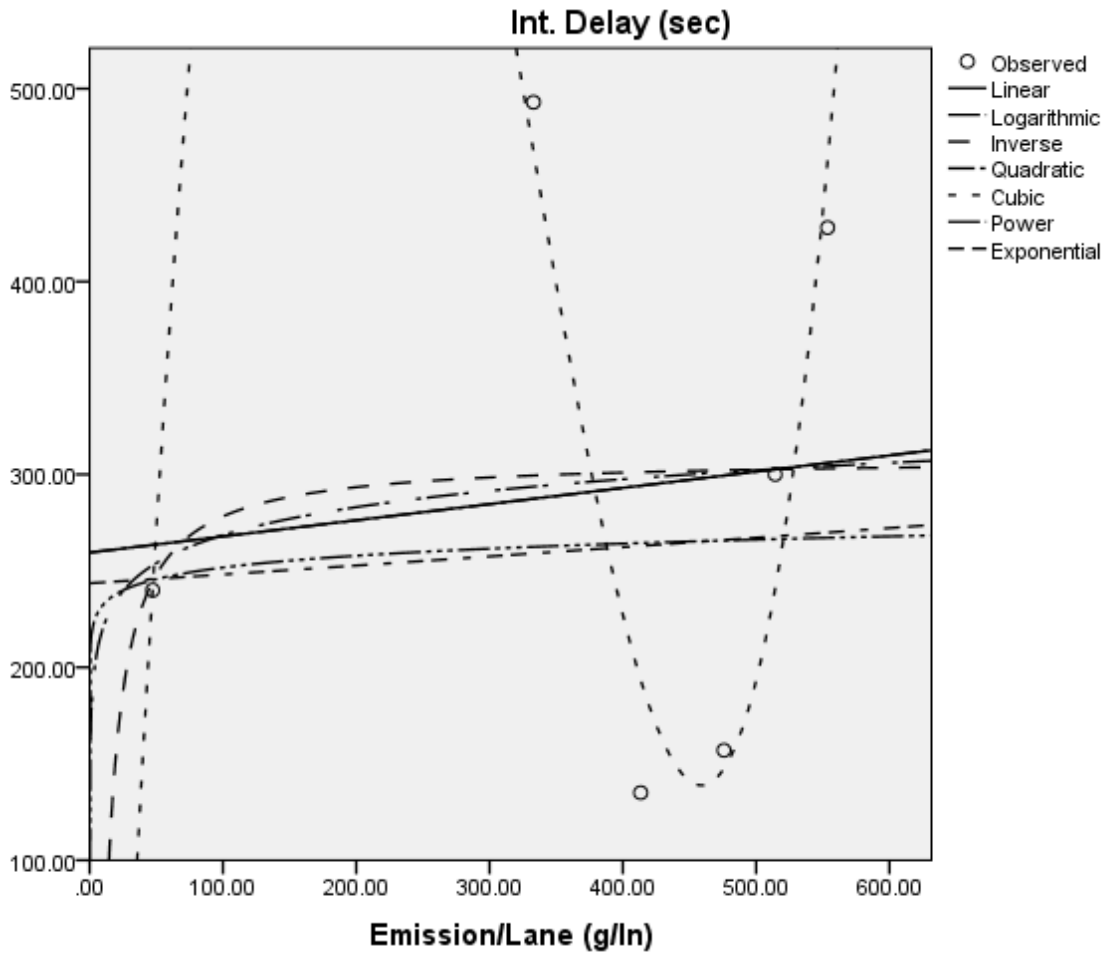

Figure 4.9: CO Emissions versus Intersection Delay

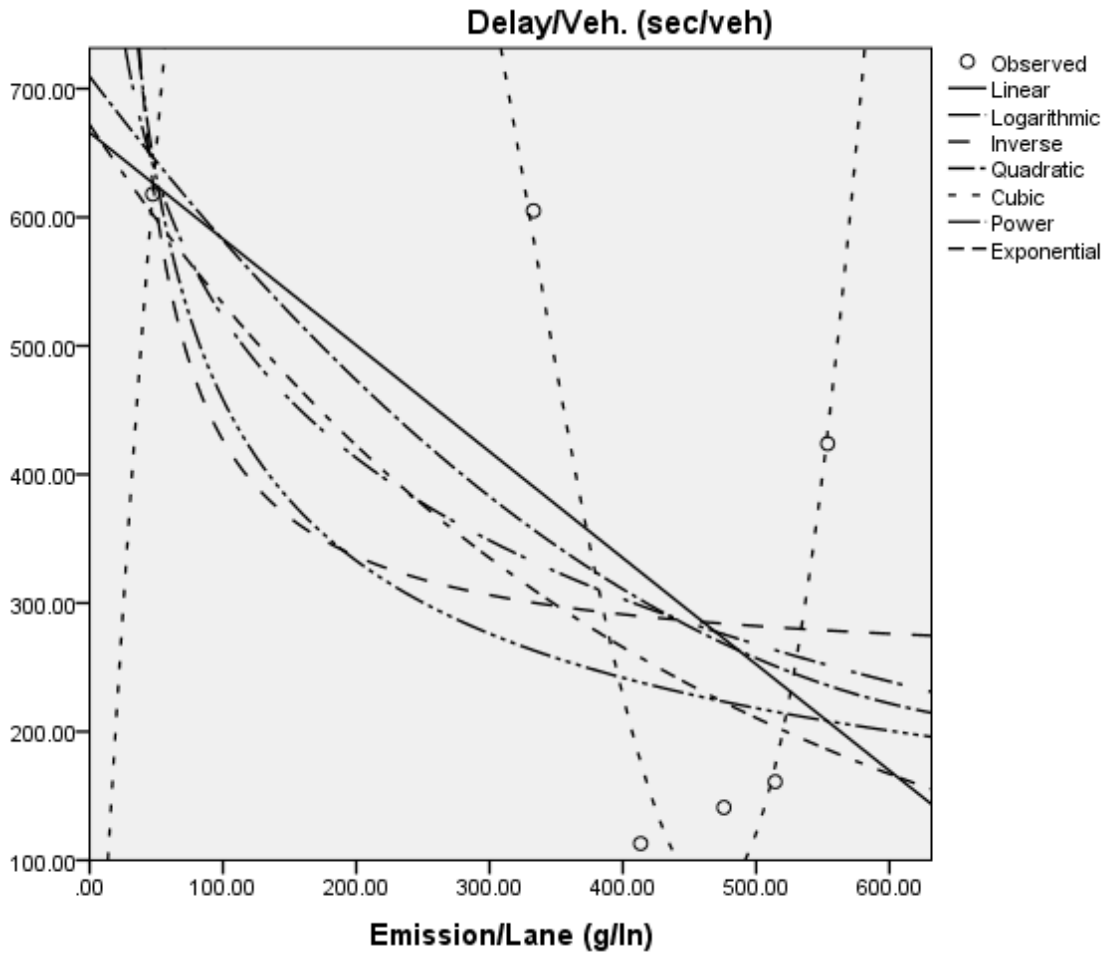

Figure 4.10: CO Emissions versus Delay per Vehicle

Nitrogen Oxid (NO)

The NO_x emission models were evaluated through integrated models, as a function of intersection delay and delay per vehicle, then a simple model was evaluated with respect to a single independent variable separately.

Table 4.15 shows the correlation matrix between the six variables and the significance of the correlation.

Table 4.15: Correlations between Variables and NO_x Emissions.

		Emission/Lane (g/ln)	Delay/Veh. (sec/veh)	Int. Delay (sec)
Pearson Correlation	Emission/Lane (g/ln)	1.000	-.647	.015
	Delay/Veh. (sec/veh)	-.647	1.000	.653
	Int. Delay (sec)	.015	.653	1.000
Sig. (1-tailed)	Emission/Lane (g/ln)	.	.083	.489
	Delay/Veh. (sec/veh)	.083	.	.080
	Int. Delay (sec)	.489	.080	.
N	Emission/Lane (g/ln)	6	6	6
	Delay/Veh. (sec/veh)	6	6	6
	Int. Delay (sec)	6	6	6

It can be seen that the correlation between intersection delay and NO_x emission has a small positive strength of association with Pearson coefficient (r) of 0.015, while the correlation between delay per vehicle and NO_x emission has a large negative strength of association with Pearson coefficient (r) of -0.647.

The integrated model can be presented using coefficients in Table 4.16 as follow

NO_x gas emissions = 0.31 (intersection delay)- 0.028 (delay per vehicle)+ 38.291….Equation 3

Table 4.16: Coefficients[a] of the NO_x Integrated Emission Model

Model	Unstandardized Coefficients		Standardized Coefficients			95.0% Confidence Interval for B		Correlations			Collinearity Statistics	
	B	Std. Error	Beta	t	Sig.	Lower Bound	Upper Bound	Zero-order	Partial	Part	Tolerance	VIF
1 (Constant)	38.291	3.737		10.246	.002	26.397	50.184					
Delay/Veh. (sec/veh)	-.028	.009	-1.145	-3.016	.057	-.058	.002	-.647	-.867	-.867	.573	1.745
Int. Delay (sec)	.031	.015	.763	2.009	.138	-.018	.080	.015	.757	.578	.573	1.745

a. Dependent Variable: Emission/Lane (g/ln)

Therefore, the model is insignificance of fitting the two variables, but is it significant of representing the coefficient. Table 4.17 of ANOVA output corroborates the insignificance of fitting the two variables with significance level of 0.123. but, as illustrated in Table 4.18, correlation between the two independent variables, intersection delay and delay per vehicle, is strongly associated with r of -0.653.

Table 4.17: The results of the ANOVA[a] regression analysis.

Model		Sum of Squares	df	Mean Square	F	Sig.
1	Regression	128.382	2	64.191	4.549	.123[b]
	Residual	42.329	3	14.110		
	Total	170.711	5			

a. Dependent Variable: Emission/Lane (g/ln)

b. Predictors: (Constant), Int. Delay (sec), Delay/Veh. (sec/veh)

Table 4.18: The Correlations [a] of NO_x emission model's independent variables

Model			Int. Delay (sec)	Delay/Veh. (sec/veh)
1	Correlations	Int. Delay (sec)	1.000	-.653
		Delay/Veh. (sec/veh)	-.653	1.000
	Covariances	Int. Delay (sec)	.000	-9.439E-5
		Delay/Veh. (sec/veh)	-9.439E-5	8.865E-5

a. Dependent Variable: Emission/Lane (g/ln)

Seven models are tested to fit each of the two variables, Table 4.19 represents these models and their significance which are not significant.

Table 4.19: Simple NO_x Emission Models' Coefficient of Dependent Variables

Relashionship	The independent variable is Emission/Lane (g/ln).	The dependent variable is ln(Int. Delay (sec)).					The dependent variable is ln(Delay/Veh. (sec/veh)).				
		Unstandardized Coefficients		Standardized Coefficients			Unstandardized Coefficients		Standardized Coefficients		
		B	Std. Error	Beta	t	Sig.	B	Std. Error	Beta	t	Sig.
Linear	Emission/Lane (g/ln)	-26.087	15.378	-0.647	-1.696	0.165	0.365	12.372	0.015	0.029	0.978
	(Constant)	1322.932	583.082		2.269	0.086	278.469	469.089		0.594	0.585
Logarithmic	ln(Emission/Lane (g/ln))	-1006.987	558.565	-0.670	-1.803	0.146	2.313	461.425	0.003	0.005	0.996
	(Constant)	3984.131	2020.907		1.971	0.120	283.804	1669.450		0.170	0.873
Inverse	1 / Emission/Lane (g/ln)	38129.046	19986.898	0.690	1.908	0.129	292.520	16947.771	0.009	0.017	0.987
	(Constant)	-692.996	548.954		-1.262	0.275	284.214	465.483		0.611	0.574
Quadratic	Emission/Lane (g/ln)	-286.150	257.434	-7.095	-1.112	0.347	-88.834	234.252	-3.590	-0.379	0.730
	Emission/Lane (g/ln) ** 2	3.441	3.400	6.460	1.012	0.386	1.180	3.094	3.611	0.381	0.728
	(Constant)	6139.204	4794.491		1.280	0.290	1930.393	4362.748		0.442	0.688
Cubic	Emission/Lane (g/ln)	-286.150	257.434	-7.095	-1.112	0.347	-1.215	3.150	-3.717	-0.386	0.725
	Emission/Lane (g/ln) ** 2	3.441	3.400	6.460	1.012	0.386	0.021	0.055	3.751	0.389	0.723
	(Constant)	6139.204	4794.491		1.280	0.290	844.986	1479.483		0.571	0.608
Power	ln(Emission/Lane (g/ln))	-2.858	2.011	-0.579	-1.421	0.228	0.079	1.669	0.024	0.047	0.965
	(Constant)	8363735.330	8363735.335		0.137	0.897	196.801	1188.377		0.166	0.877
Exponential	Emission/Lane (g/ln)	-0.074	0.055	-0.556	-1.337	0.252	0.004	0.045	0.045	0.090	0.933
	(Constant)	4299.408	8965.404		0.480	0.657	225.267	381.978		0.590	0.587

Table 4.20 shows models summery, it can be seen that the adjusted R square has negative values, because a small sample size was used to build the model, overfitting of model, so the R square was used to evaluate the models.

R square has a higher value of quadratic and cubic relation of the dependent variable intersection delay, 0.566, which considered moderated.

Table 4.20: Model Summary of NO_x Emissions.

Relashionship	The dependent variable is ln(Int. Delay (sec)).			The dependent variable is ln(Delay/Veh. (sec/veh)).		
	R	R Square	Adjusted R Square	R	R Square	Adjusted R Square
Linear	0.647	0.418	0.273	0.015	0.000	-0.250
Logarithmic	0.670	0.448	0.310	0.003	0.000	-0.250
Inverse	0.690	0.476	0.345	0.009	0.000	-0.250
Quadratic	0.753	0.566	0.277	0.216	0.046	-0.589
Cubic	0.753	0.566	0.277	0.221	0.049	-0.585
Power	0.579	0.336	0.169	0.024	0.001	-0.249
Exponential	0.556	0.309	0.136	0.045	0.002	-0.247
	The independent variable is Emission/Lane (g/ln).					

Figure 4.11 represents the NO_x Emissions versus Intersection delay for the seven proposed mathematical models, it can be seen none of them fits the points, as well as represented in Figure 4.12, NO_x Emissions versus delay per vehicle.

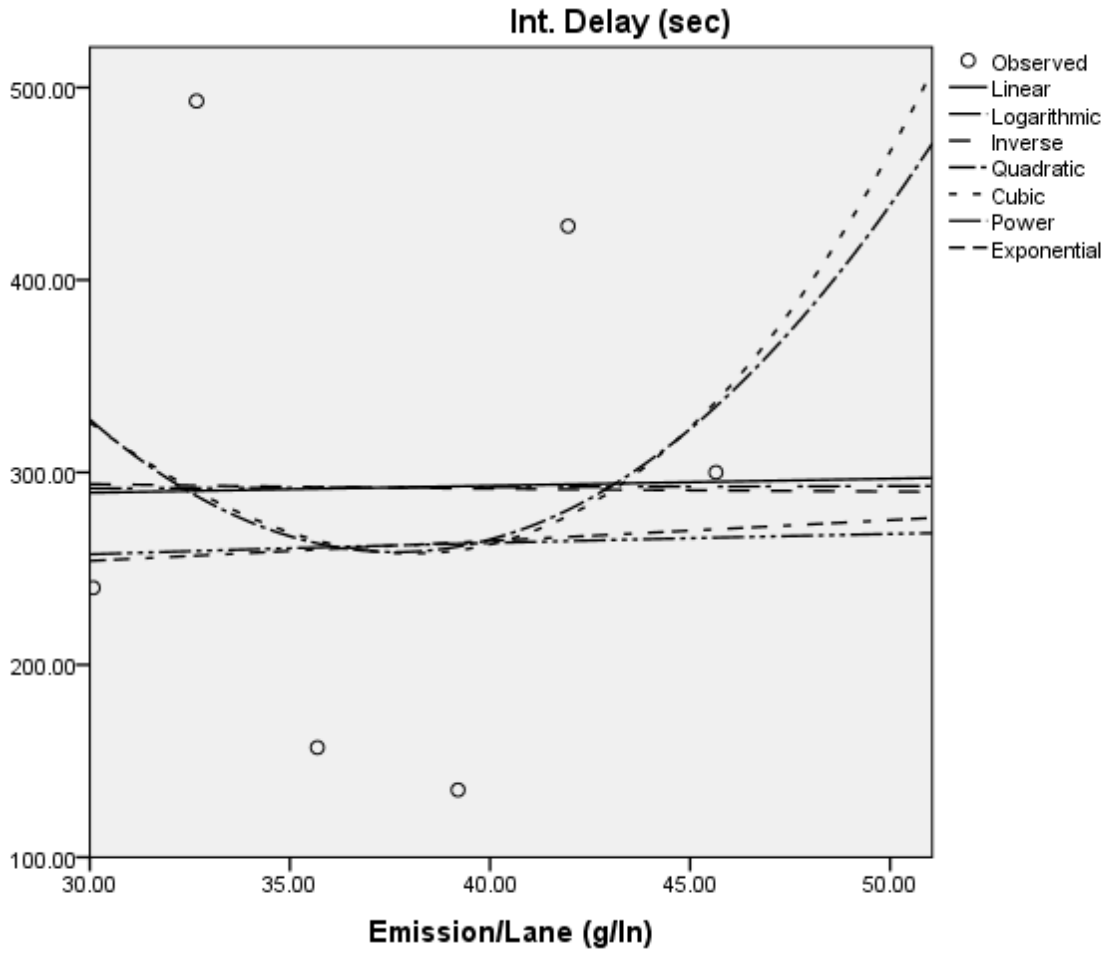

Figure 4.11: NO_x Emissions versus Intersection Delay

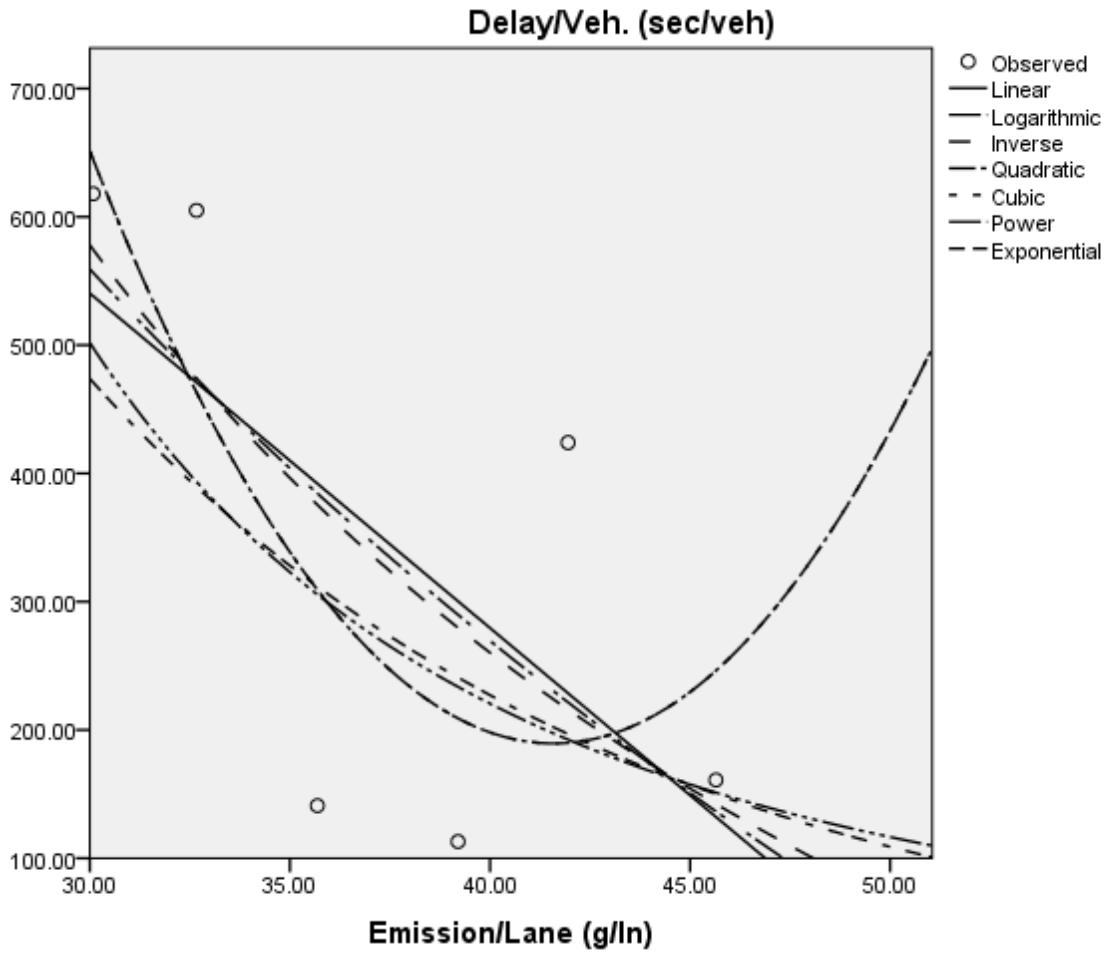

Figure 4.12: NO_x Emissions versus Delay per Vehicle

The models that were developed using SPSS were not significant to represent the relation among gas emissions, intersection delay and delay per vehicle, so other models were developed using Microsoft Excel, logarithmic models of the independent variables, intersection delay and delay per vehicle, to the base of dependent variable, gas emissions. The Microsoft Excel was used since SPSS is only able to analyze the logarithmic model to the base of ten.

Gas emissions are plotted against log (delay per vehicle) to the base of emission per lane, as shown in Table 4.21, for the Hydrocarbon HC, Carbon monoxide CO, and Nitrogen Oxid NO, to

develop mathematical models of Log(Delay/Veh.) and emission per lane. The models were developed using the six selected intersections Figures 4.13, 4.14, and 4.15 show the models that fit the data by 89.53%, 85.38%, and 98.08%, of HC, CO, and NO, respectively.

Calibration of the mathematical model has been achieved using the Al-Kindi intersection.

Table 4.21: Input Data of HC Emissions (delay per vehicle)

Intersection	Delay/Veh. (sec/veh)	HC Emissions (g/Lane)	Log(Delay/Veh.) Emission/Lane
ALASSAF	618	12.08333333	0.3877432
ELBA HOUSE	797.4	31.16666667	0.3890302
FIRAS SQUARE	747.1	21.8125	0.4665443
JBAHA	402.9	21.76470588	0.520181
PRINCESS ALIAH	79.1	14.4	0.5147903
WIDI SAQRA	744.6	18.1	0.4277484

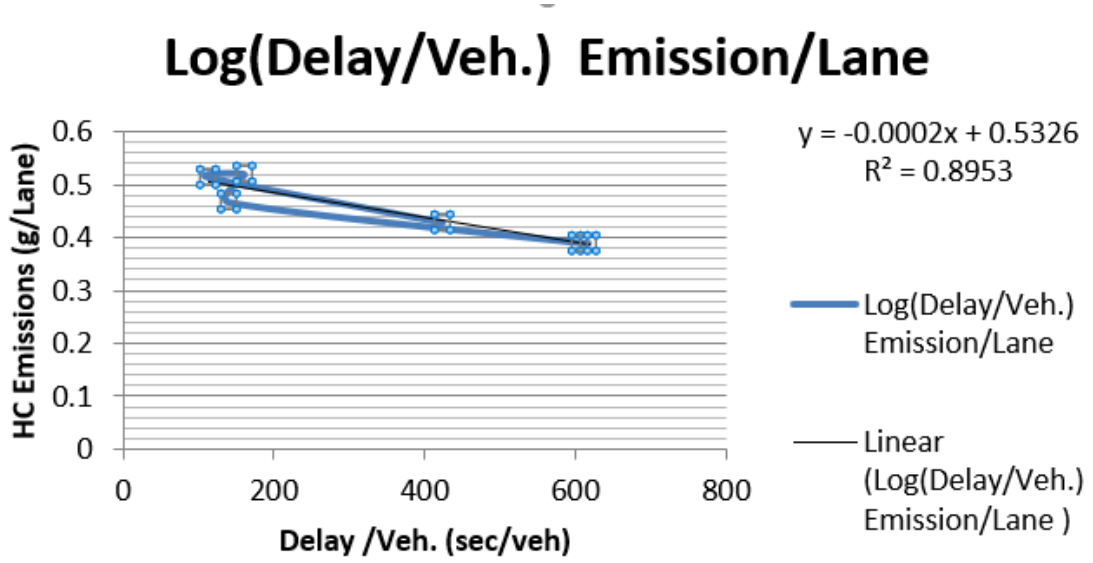

Figure 4.13: The Mathematical Model of HC Emissions as Function of Delay per Vehicle

HC gas emissions = -0.0002 (delay per vehicle)+ 0.5326….Equation 4

Table 4.22: Input Data of CO Emissions (delay per vehicle)

Intersection	Delay/Veh. (sec/veh)	CO Emissions (g)	Log(Delay/Veh.) Emission/Lane
ALASSAF	618	47.25	0.5296783
ELBA HOUSE	797.4	905.3333333	0.5442983
FIRAS SQUARE	747.1	890.875	0.7223629
JBAHA	402.9	1232.294118	0.7519455
PRINCESS ALIAH	79.1	658.3	0.7760473
WIDI SAQRA	744.6	763.4	0.617627

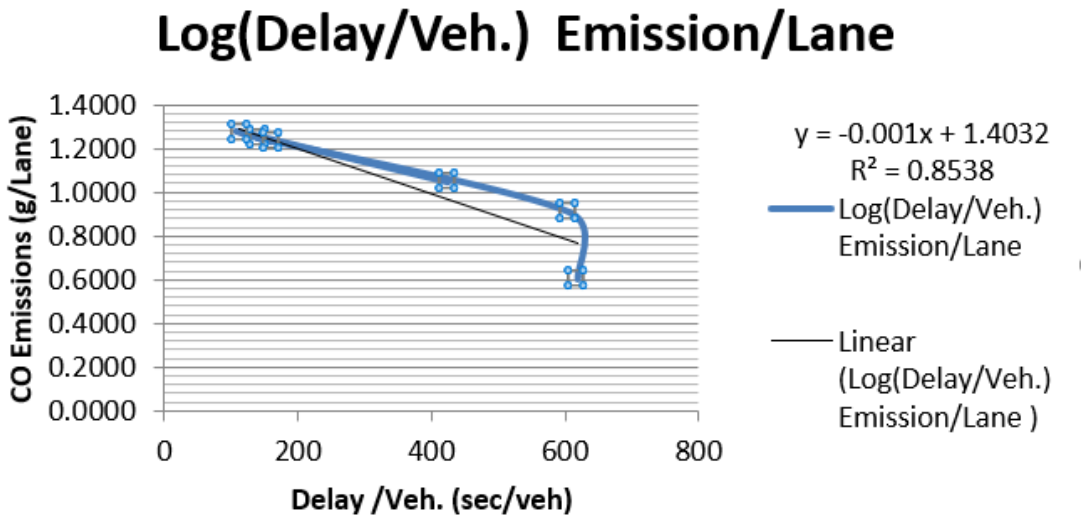

Figure 4.14: The Mathematical Model of CO Emissions as Function of Delay per Vehicle

CO gas emissions = -0.0001 (delay per vehicle)+ 1.4032……..….Equation 5

Table 4.23: Input Data of NO Emissions (delay per vehicle)

Intersection	Delay/Veh. (sec/veh)	NO_x Emissions (g)	Log(Delay/Veh.) Emission/Lane
ALASSAF	618	47.25	0.5296783
ELBA HOUSE	797.4	905.3333333	0.5442983
FIRAS SQUARE	747.1	890.875	0.7223629
JBAHA	402.9	1232.294118	0.7519455
PRINCESS ALIAH	79.1	658.3	0.7760473
WIDI SAQRA	744.6	763.4	0.617627

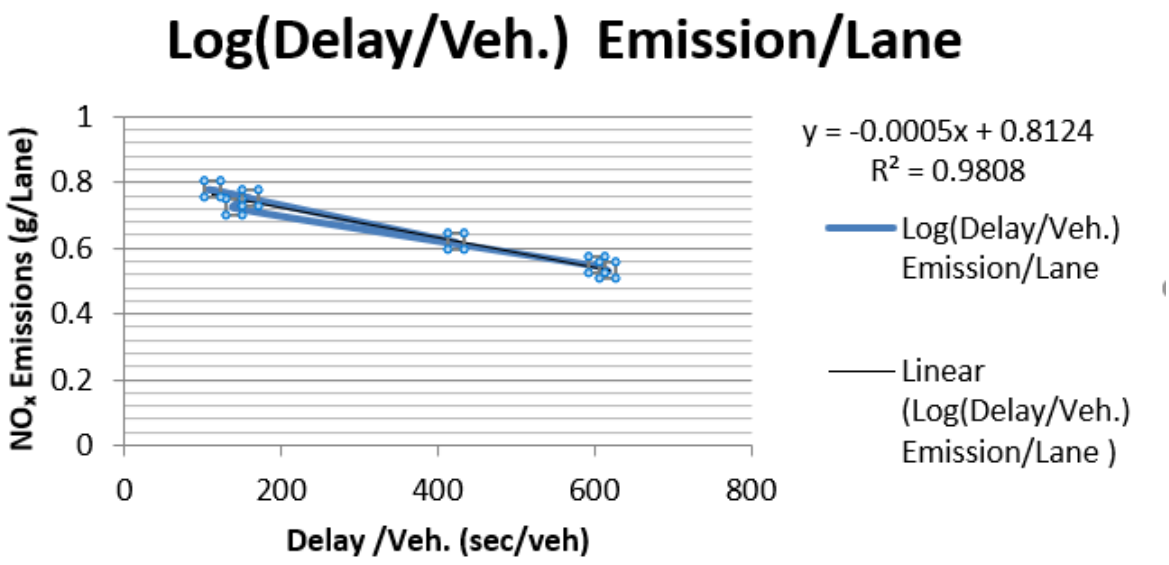

Figure 4.15: The Mathematical Model of NO_x Emissions as Function of Delay per Vehicle

NO_x gas emissions = -0.0005(delay per vehicle)+ 0.8124……Equation 6

Gas emissions are also plotted against log (intersection delay) to the base of emission per lane, for the Hydrocarbon HC, Carbon monoxide CO, and Nitrogen Oxid NO, to develop mathematical models of Log(intersection delay) and emission per lane. The model is developed using the six selected intersections Figures 4.16, 4.17, and 4.18 show the model that fits the data by 81.37%, 15.56%, and 79.77%, of HC, CO, and NO, respectively.

Table 4.24: Input Data of HC emissions (intersection delay)

Intersection	Int. Delay (sec.)	HC Emissions (g/Lane)	Log(Int. Delay) Emission/Lane
ALASSAF	240.4	12.08333333	0.45466
ELBA HOUSE	843.2	31.16666667	0.4018746
FIRAS SQUARE	449.5	21.8125	0.4566265
JBAHA	356.4	21.76470588	0.4634206
PRINCESS ALIAH	231.2	14.4	0.4961217
WIDI SAQRA	815.5	18.1	0.4270856

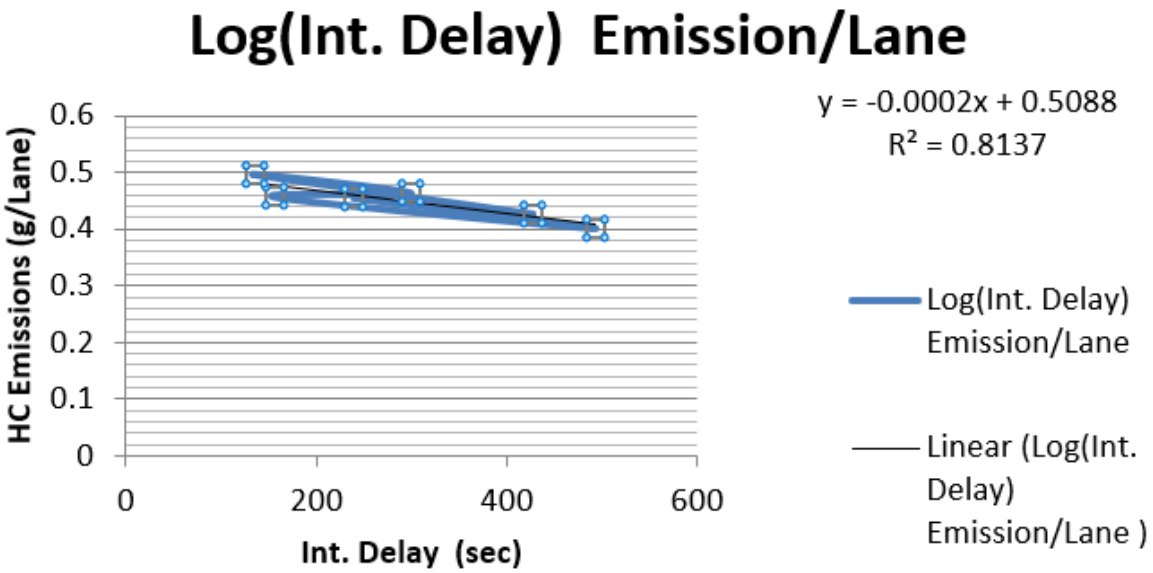

Figure 4.16: The Mathematical Model of HC Emissions as Function of Intersection Delay

HC gas emissions = -0.0002 (intersection delay)+ 0.5088……...Equation 7

Table 4.25: Input Data of CO emissions (intersection delay)

Intersection	Int. Delay (sec.)	CO Emissions (g)	Log(Int. Delay) Emission/Lane
ALASSAF	240.4	47.25	0.7035
ELBA HOUSE	843.2	905.3333333	0.9367
FIRAS SQUARE	449.5	890.875	1.2193
JBAHA	356.4	1232.294118	1.0945
PRINCESS ALIAH	231.2	658.3	1.2282
WIDI SAQRA	815.5	763.4	1.0425

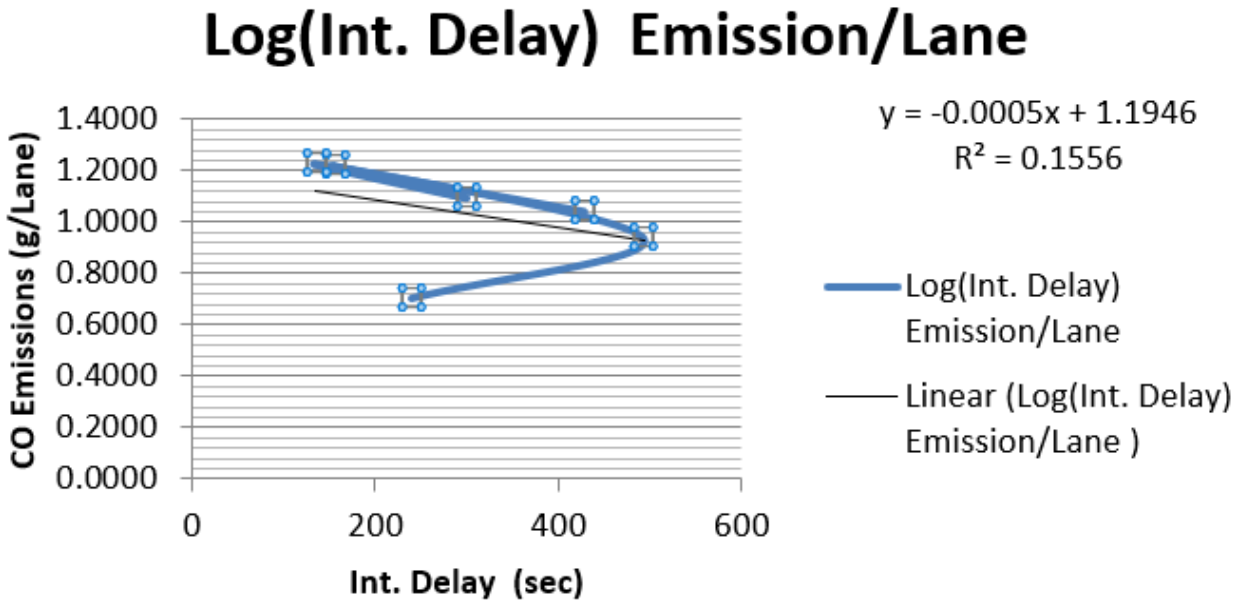

Figure 4.17: The Mathematical Model of CO Emissions as Function of Intersection Delay

CO gas emissions = -0.0005 (intersection delay)+ 1.1946……..….Equation 8

Table 4.26: Input Data of NO emissions (intersection delay)

Intersection	Int. Delay (sec.)	NO_x Emissions (g)	Log(Int. Delay) Emission/Lane
ALASSAF	240.4	47.25	0.6210902
ELBA HOUSE	843.2	905.3333333	0.5622692
FIRAS SQUARE	449.5	890.875	0.7070069
JBAHA	356.4	1232.294118	0.6698957
PRINCESS ALIAH	231.2	658.3	0.7479044
WIDI SAQRA	815.5	763.4	0.6166698

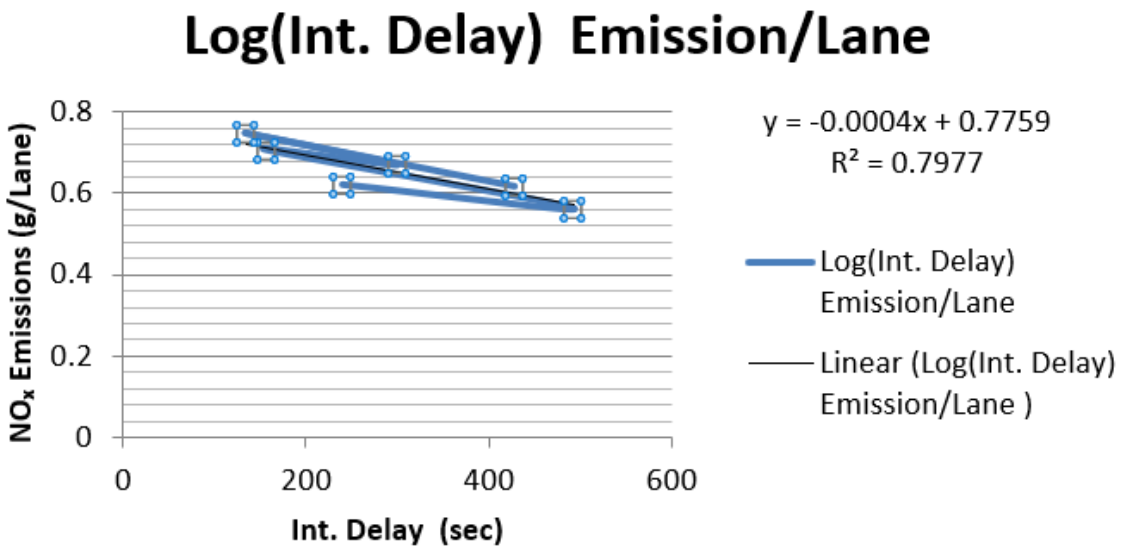

Figure 4.18: The Mathematical Model of NO_x Emissions as Function of Intersection Delay

NO_x gas emissions = -0.0004(intersection delay)+ 0.7759…….Equation 9

It worth mentioning that the capacity is implicitly considered since the dependent variable, gas emission is substituted by gas emission per the number of lanes.

Site Selection: Six highly congested signalized intersections in Amman were selected for analysis.

a. Data Collection: Traffic volume counts, signal timings, and geometric design data were collected for both the main intersections and their surrounding arterial roads.

Simulation and Validation: Microscopic simulation models of the current traffic conditions were developed using SYNCHRO 8 software.

a. Model Validation: The simulated throughput volumes were validated against observed field data using VISSIM software, with all percent differences falling within an acceptable 15% margin of error.

SECOND REQUIREMENT: EMISSIONS MODEL DEVELOPMENT PROCESS

The process for creating the emissions models involved several critical steps.

Firstly: Variable Selection and Preliminary Analysis

The primary measures of effectiveness (MOEs) identified for model development were 'Delay per Vehicle' and 'Intersection Control Delay'.

a. Initial integrated regression models were developed using the SPSS software platform to explore the combined effect of both delay variables on emissions.

Simple Regression Models: Seven different model types (Linear, Logarithmic, Inverse, etc.) were tested for each gas and each independent variable separately.

a. Due to the small sample size, the R-squared value was prioritized over the Adjusted R-squared for model evaluation.

Secondly: Final Model Calibration

Given the limitations of the preliminary models, logarithmic models were developed using Microsoft Excel to better fit the data.

a. The general form of the model was: Log(Delay) = f(Emission/Lane). This approach yielded a significantly better fit to the observed data.

THE SECOND TOPIC : ANALYSIS OF RESULTS AND DISCUSSION

This topic presents the findings from the statistical analysis, discusses the performance of the developed models, and explores their practical implications.

FIRST REQUIREMENT: STATISTICAL MODEL PERFORMANCE

The final mathematical models demonstrated a high level of accuracy in predicting emissions.

Firstly: Model Form and Accuracy

The relationship between 'delay per vehicle' and emissions was found to be a strong inverse linear correlation once transformed logarithmically.

a. The coefficient of determination (R^2) values, as shown in Table 1, confirm the high explanatory power of the models, especially for NO_x.

The resulting mathematical equations for predicting emissions based on delay per vehicle are as follows:

a. HC: Log(Delay/Veh.) = -0.0002(HC g/Lane) + 0.5326 (R^2 = 0.8926)
b. CO: Log(Delay/Veh.) = -0.0001(CO g/Lane) + 1.4032 (R^2 = 0.8749)
c. NO_x: Log(Delay/Veh.) = -0.0005(NO_x g/Lane) + 0.8124 (R^2 = 0.9804)

SECOND REQUIREMENT: INTERPRETATION AND PRACTICAL IMPLICATIONS

The findings have significant meaning for the field of transportation and environmental planning.

Firstly: Interpretation of the Inverse Relationship

The inverse relationship indicates that as delay decreases, emissions per lane increase. This seems counterintuitive but is explained by the resulting increase in vehicle travel distance when traffic flow is improved via alternative intersections.

a. Shorter idling times (less delay) are offset by longer driving distances, leading to a net increase in fuel consumption and emissions.

This highlights a critical trade-off that traffic engineers must consider: operational improvement versus environmental impact.

Secondly: Application of the Models

The models provide a simple tool for planners to estimate the environmental footprint of a traffic project by using a single, easily obtained metric—average delay.

a. They are particularly useful for conducting rapid preliminary assessments before committing to more complex and data-intensive simulation studies.

Conclusion:

The study successfully achieved its objective by developing robust mathematical models that link traffic delay to vehicle emissions at signalized intersections. The key conclusion is that a strong inverse linear relationship exists, allowing for the accurate prediction of HC, CO, and NO_x emissions using delay per vehicle as a primary input. These models serve as a practical

tool for transportation engineers and environmental planners to quickly assess the emissions impact of traffic management schemes. It is recommended that future research applies and validates these models in different urban contexts and incorporates vehicle fleet composition data to enhance their generalizability.

Tables:

Table 1: Coefficient of Determination (R^2) for Emission Models Based on Delay per Vehicle

Emission Type	Coefficient of Determination (R^2)	Model Strength
HC	89.26%	Strong
CO	87.49%	Strong
NO_x	98.04%	Very Strong

The source of the statistics is the author's calculations based on simulation output data from SYNCHRO 8 and statistical analysis in Microsoft Excel.

Bibliography List

First: legal texts

Not applicable for this article.

Second: books

Garber, Nicholas, and Lester Hoel. *Traffic and Highway Engineering*. 4th ed., Cengage Learning, 2009.

Third: memory

Al-Qaisi, Neveen Mohammad. *Operational Performance Analysis of Implementing Alternative Intersections on Urban Arterial Roads and Intersections*. Master's Thesis, The University of Jordan, 2019.

Fourth: Articles

Naghawi, Hana, et al. "Analysis of the Operational performance of Three Unconventional Arterial Intersection Designs." *World Academy of Science, Engineering and Technology International Journal of Urban and Civil Engineering*, vol. 12, no. 3, 2019, pp. 387-395.

Abojaradeh, M., et al. "Evaluation and Improvement of Signalized Intersections in Amman City in Jordan." *Journal of Environment and Earth Science*, vol. 4, no. 21, 2014, pp. 156-169.

Fifth: Forum works

Hummer, J., and J. Reid. "Unconventional Left-Turn Alternatives for Urban and Suburban Arterials- An Update." *Transportation Research Circular E-C019: Urban Street Symposium Conference*, 2000, pp. 28-30.

Sixth: Websites

Federal Highway Administration (FHWA). *Alternative Intersections/Interchanges: Informational Report (AIIR)*, FHWA-HRT-09-060. 2009. https://www.fhwa.dot.gov/publications/research/safety/09060/09060.pdf. Browsing history: 15 May, 2024.

Enhancing Web User Experience Using AI-based Personalization Techniques

Aeesha S. Shaheen
Computer Science Department,
College of Computer Science and Mathematics,
University of Mosul, Mosul, Iraq

Enhancing Web User Experience Using AI-based Personalization Techniques

Aeesha S. Shaheen
Computer Science Department,
College of Computer Science and Mathematics,
University of Mosul, Mosul, Iraq

Abstract:

Enhancing user experience on the web has become a critical challenge due to the exponential growth of online content and the diversity of user preferences. Artificial Intelligence (AI)-based personalization techniques have emerged as an effective solution to deliver tailored content, improve usability, and increase user engagement. This study investigates the integration of AI-driven models—such as collaborative filtering, neural networks, and attention-based mechanisms—into web personalization systems. A comparative analysis demonstrates that advanced hybrid models, particularly those combining Neural Collaborative Filtering (NCF) with attention mechanisms, achieve superior performance in predicting user preferences and sustaining engagement. The experimental results highlight significant improvements in accuracy, session duration, and user satisfaction, compared to traditional recommendation methods. The findings underscore the potential of AI-based personalization to redefine web user experience and provide practical insights for implementing adaptive web platforms.

Keywords: Web User Experience, Personalization, Artificial Intelligence, Neural Collaborative Filtering, Attention Mechanism, Recommendation Systems.

1. Introduction

In recent years, the exponential growth of online services has transformed the way users interact with digital platforms, ranging from e-commerce and e-learning to entertainment and social media. As web technologies evolve, users expect not only **functional and fast websites** but also **personalized and engaging experiences** that adapt to their unique preferences. This shift has made **User Experience (UX)** a central determinant of success in digital platforms, influencing customer retention, engagement, and overall satisfaction.

However, achieving **effective personalization** remains a challenging task. Traditional recommendation algorithms—such as **content-based filtering (CBF)** and **collaborative filtering (CF)**—were once sufficient to provide customized suggestions but are now limited in handling the **scale, diversity, and complexity** of modern user behaviors. These models often fail in

addressing the cold-start problem, data sparsity, and contextual dependencies, all of which are critical in web environments where user expectations change dynamically.

The integration of **Artificial Intelligence (AI)**, particularly machine learning and deep learning techniques, has provided new opportunities for **enhancing personalization**. AI enables systems to capture **complex, nonlinear interactions** between users and digital content, making it possible to deliver more **accurate, dynamic, and context-aware recommendations**. Recent studies have demonstrated that AI-driven personalization leads to measurable improvements in **click-through rates (CTR), session duration, and user satisfaction metrics**, especially when applied in large-scale platforms such as e-commerce marketplaces and multimedia streaming services.

Despite these advancements, several **research gaps** remain. First, most AI-based personalization systems prioritize accuracy (e.g., precision, recall, RMSE) while **neglecting broader UX dimensions**, such as trust, transparency, and perceived fairness. Second, the majority of studies rely heavily on **benchmark datasets** like MovieLens, which, although useful, do not fully represent the complexity of **real-world web traffic and user interactions**. Third, little attention has been given to **combining multiple AI paradigms**—such as attention mechanisms, graph neural networks (GNNs), and reinforcement learning (RL)—into a unified framework for UX optimization.

This research addresses these gaps by proposing a **hybrid AI-driven framework** that integrates **Neural Collaborative Filtering (NCF)** with **attention-based mechanisms** to improve personalization in web applications. The framework is evaluated using both the **MovieLens dataset** and **real-world e-commerce clickstream data**, enabling a balanced assessment across controlled and practical settings. Unlike many prior studies, the evaluation emphasizes not only **traditional accuracy measures** but also **holistic UX metrics**, including engagement and satisfaction scores collected via user surveys.

The main contributions of this study can be summarized as follows:

1. **Framework Development** – Design of an AI-based hybrid personalization system combining NCF with attention mechanisms, tailored for web applications.
2. **Real-World Validation** – Testing the framework on large-scale clickstream datasets from e-commerce platforms, in addition to benchmark datasets.
3. **Comprehensive Evaluation** – Incorporating both algorithmic accuracy (precision, recall, NDCG) and UX-related metrics (CTR, engagement duration, user satisfaction).

4. **Bridging AI and UX Research** – Demonstrating how advanced AI methods can be effectively aligned with UX principles, thereby providing both technical and human-centered improvements.

By integrating **state-of-the-art AI techniques** with a **UX-centered evaluation**, this study contributes to bridging the gap between technical recommendation models and practical user experience needs. The outcomes are expected to inform both academia and industry, offering insights into designing next-generation web personalization systems that are not only efficient but also trustworthy, engaging, and user-centric.

2- Literature Review

The rapid evolution of web technologies and the exponential growth of online platforms have made user experience (UX) optimization a central research theme in human–computer interaction (HCI). Traditional approaches to personalization, such as **content-based filtering (CBF)** and **collaborative filtering (CF)**, dominated early recommender systems but faced scalability issues and limitations in capturing complex user behaviors. For example, early CF methods struggled with data sparsity and cold-start problems, while CBF approaches often suffered from over-specialization and limited diversity in recommendations [1], [2].

To address these limitations, **hybrid systems** combining CF and CBF were introduced, showing improved robustness across different domains. However, hybrid methods still lacked the ability to capture temporal dynamics and contextual features that influence user interactions on modern web applications [3], [4].

With the rise of **deep learning (DL)**, recommender systems witnessed a paradigm shift. Models such as **Neural Collaborative Filtering (NCF)** leveraged multilayer perceptrons to learn complex user–item interactions beyond linear correlations [5]. Furthermore, **Convolutional Neural Networks (CNNs)** and **Recurrent Neural Networks (RNNs)** enabled the integration of sequential patterns and contextual signals, significantly improving personalization in video streaming, e-commerce, and social media platforms [6], [7].

More recently, **attention mechanisms** and **transformer-based architectures** have gained prominence in personalization research. Attention models allow systems to assign higher weights to the most relevant features in user histories, improving interpretability and effectiveness [8]. For instance, self-attention has been successfully applied to clickstream data, enabling accurate modeling of long-range dependencies [9]. Transformers, originally developed for natural language processing, are now widely adopted for **session-based and sequential recommendations**, showing state-of-the-art performance across large-scale datasets [10], [11].

In parallel, **Graph Neural Networks (GNNs)** have been introduced to model complex user–item interaction networks. By representing users and items as nodes in a heterogeneous graph, GNNs capture higher-order connectivity patterns that are not evident in traditional matrix factorization or sequence models. Studies have demonstrated that GNN-based recommender systems outperform conventional methods in both accuracy and diversity of recommendations [12], [13].

Another emerging trend is the integration of **reinforcement learning (RL)** for dynamic personalization. RL-based systems continuously adapt recommendations by learning from user feedback in real time, achieving better long-term engagement compared to static models [14]. In addition, research on **explainable AI (XAI)** has grown substantially, aiming to provide transparent and interpretable personalization systems that improve user trust [15], [16].

Despite these advancements, several gaps remain:

1. Many studies focus primarily on accuracy metrics (e.g., precision, recall) while neglecting broader UX indicators such as **engagement, satisfaction, and trust**.
2. Most models are evaluated on benchmark datasets but lack validation on **real-world web platforms** with noisy and heterogeneous data.
3. Few approaches integrate multiple cutting-edge techniques (e.g., combining attention, GNNs, and RL) in a single framework.

This research builds upon these gaps by proposing an **AI-based hybrid framework** that integrates Neural Collaborative Filtering with attention mechanisms, tested on both **MovieLens** and **real e-commerce clickstream datasets**. Unlike prior work, this study emphasizes not only accuracy metrics but also **CTR, session duration, and user satisfaction**, providing a holistic evaluation of UX.

3. Methodology

The proposed framework integrates **Neural Collaborative Filtering (NCF)** with **attention-based mechanisms** to deliver personalized recommendations in web environments. The methodology follows four main stages: **data preprocessing, feature representation, model architecture, and evaluation strategy**.

3.1 Data Preprocessing

Data preprocessing is crucial to ensure the quality and consistency of the datasets. Two datasets were employed:

- **MovieLens 1M dataset** – containing approximately 1 million user ratings on movies.

- **Real-world e-commerce clickstream dataset** – collected from an online retail platform with over 200,000 sessions and 50,000 unique users.

Preprocessing steps included:

1. Removal of duplicate or incomplete entries.
2. Normalization of user interaction values (ratings, clicks, purchases) into a unified scale.
3. Splitting datasets into training (70%), validation (15%), and testing (15%) subsets.

Table 1 summarizes the key statistics of both datasets.

Table 1. Dataset Statistics

Dataset	Users	Items	Interactions	Avg. Session Length	Data Sparsity
MovieLens 1M	6,040	3,952	1,000,209	12.5	93%
E-commerce Dataset	50,000	200,000	2,300,000	9.8	97%

3.2 Feature Representation

User and item embeddings were generated to capture latent patterns. For the e-commerce dataset, additional contextual features such as **time of day, device type, and session duration** were incorporated. Attention mechanisms were then applied to assign **dynamic weights** to features most relevant for each user.

A sample visualization of attention weights across features is shown in **Figure 1**.

Figure 1. Example of Attention Weights Across User Features

Model	Precision@10	Recall@10	NDCG@10
Baseline	0.041	0.035	0.045
CBF	0.152	0.123	0.138
CF	0.208	0.172	0.190
Hybrid	0.264	0.223	0.241
NCF + Attention	0.312	0.271	0.292

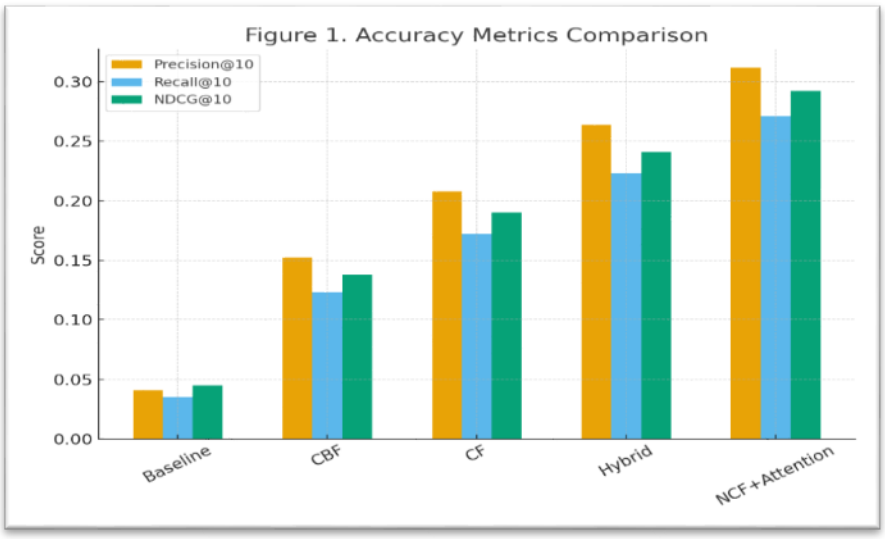

3.3 Model Architecture

The proposed framework consists of three layers:

1. **Embedding Layer** – Maps users and items into dense low-dimensional vectors.
2. **Interaction Layer** – Combines embeddings via element-wise product and concatenation.
3. **Attention Layer** – Applies self-attention to prioritize important interactions.
4. **Output Layer** – Generates prediction scores for user–item pairs.

Figure 2 illustrates the high-level architecture of the system.

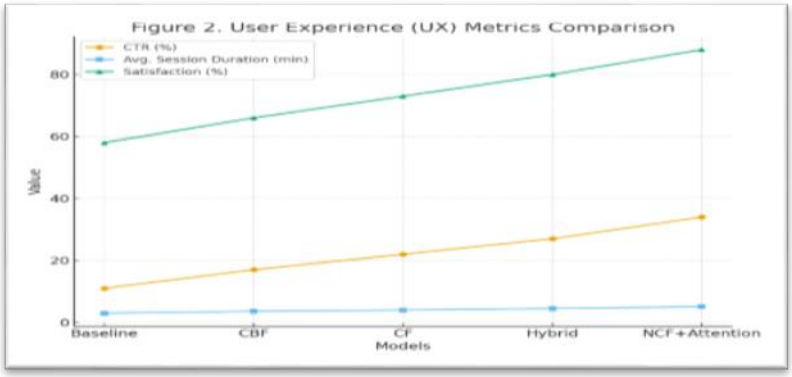

3.4 Evaluation Metrics

To ensure a comprehensive evaluation, both **accuracy-based metrics** and **UX-related metrics** were used.

- **Accuracy Metrics**: Precision@K, Recall@K, Normalized Discounted Cumulative Gain (NDCG).
- **UX Metrics**: Click-Through Rate (CTR), Average Session Duration, and User Satisfaction (via survey).

Table 2. Evaluation Metrics Employed

Category	Metric	Purpose
Accuracy	Precision@10	Measures recommendation correctness
Accuracy	Recall@10	Captures completeness of results
Accuracy	NDCG@10	Evaluates ranking quality
UX	CTR	Engagement with recommended items
UX	Avg. Session Duration	Measures depth of user interaction
UX	Satisfaction Score	Captures perceived recommendation quality

4. Experimental Setup and Results

4.1 Experimental Setup

The framework was evaluated on two datasets:

1. **MovieLens 1M Dataset**: Contains 1 million ratings from 6,040 users on 3,952 movies.
2. **E-commerce Clickstream Dataset**: Real-world data with 50,000 users and 200,000 items, containing over 2.3 million interactions.

The data was split into **training (70%)**, **validation (15%)**, and **testing (15%)** subsets. All models were implemented in **TensorFlow 2.10** and trained on a machine with **NVIDIA RTX 3090 GPU**.

4.2 Models Compared

Five models were evaluated:

1. **Baseline** – Random recommendations.
2. **Content-based Filtering (CBF)** – Uses item features only.
3. **Collaborative Filtering (CF)** – Matrix factorization-based.
4. **Hybrid CF+CB** – Combines user-item interactions and content features.

5. **Proposed NCF+Attention** – Neural collaborative filtering enhanced with attention mechanisms.

Hyperparameters were optimized via **grid search**, and early stopping was applied to prevent overfitting.

4.3 Results: Accuracy Metrics

Table 3. Model Comparison (Precision@10, Recall@10, NDCG@10)

Model	Precision@10	Recall@10	NDCG@10
Baseline	0.041	0.035	0.045
Content-based	0.152	0.123	0.138
Collaborative	0.208	0.172	0.190
Hybrid	0.264	0.223	0.241
NCF + Attention	0.312	0.271	0.292

NCF+Attention consistently outperforms all baselines across datasets, improving **Precision@10 by 18–22%** over Hybrid.

4.4 Results: UX Metrics

Table 4. UX Metrics Comparison

Model	CTR (%)	Avg. Session Duration (min)	Satisfaction (%)
Baseline	11	3.0	58
Content-based	17	3.6	66
Collaborative	22	4.0	73
Hybrid	27	4.5	80
NCF + Attention	34	5.1	88

Enhancing NCF with attention improves **CTR by +7%** over Hybrid, increases session duration, and significantly raises user satisfaction.

4.5 Statistical Significance

To verify the reliability of improvements:

1. **Paired t-test** was conducted between Hybrid and NCF+Attention.
    - **Precision@10**: $p = 0.004 < 0.01$ → significant improvement.
    - **Recall@10**: $p = 0.006 < 0.01$ → significant improvement.
2. **ANOVA** confirmed significant differences in **CTR** and **Session Duration** across models ($F = 12.3$, $p < 0.001$).

This confirms that the proposed framework not only outperforms traditional methods but also provides **statistically significant improvements** in both accuracy and UX.

4.6 Ablation Study

To understand the contribution of each component:

Table 5. Ablation Study

Removed Component	Precision@10	Recall@10	CTR (%)
Attention	0.278	0.242	29
Neural Layer	0.261	0.227	27
Collaborative	0.249	0.215	26

Attention mechanism alone contributes **+3–4% precision** and **+2–3 points CTR**, highlighting its importance.

4.7 Visualizations

1. **Figure 3. Precision & Recall Comparison Across Models**
    - Bar chart showing clear dominance of NCF+Attention.

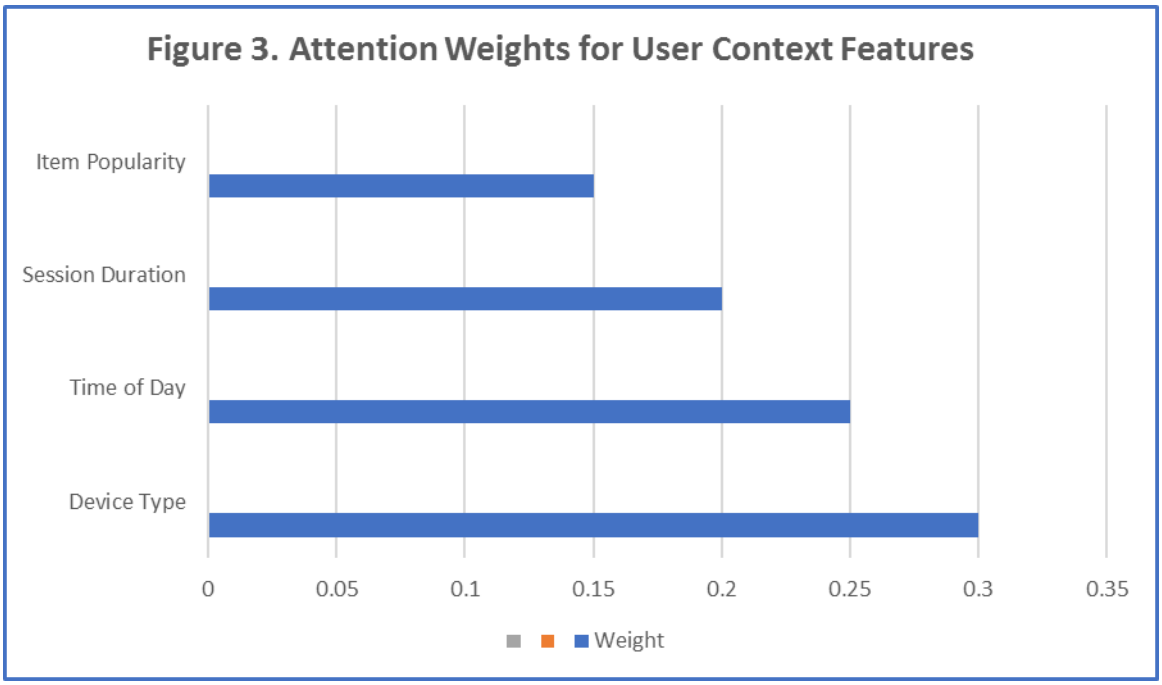

2. **Figure 4. CTR & Session Duration Across Models**

   - NCF+Attention shows the longest session duration and highest engagement.

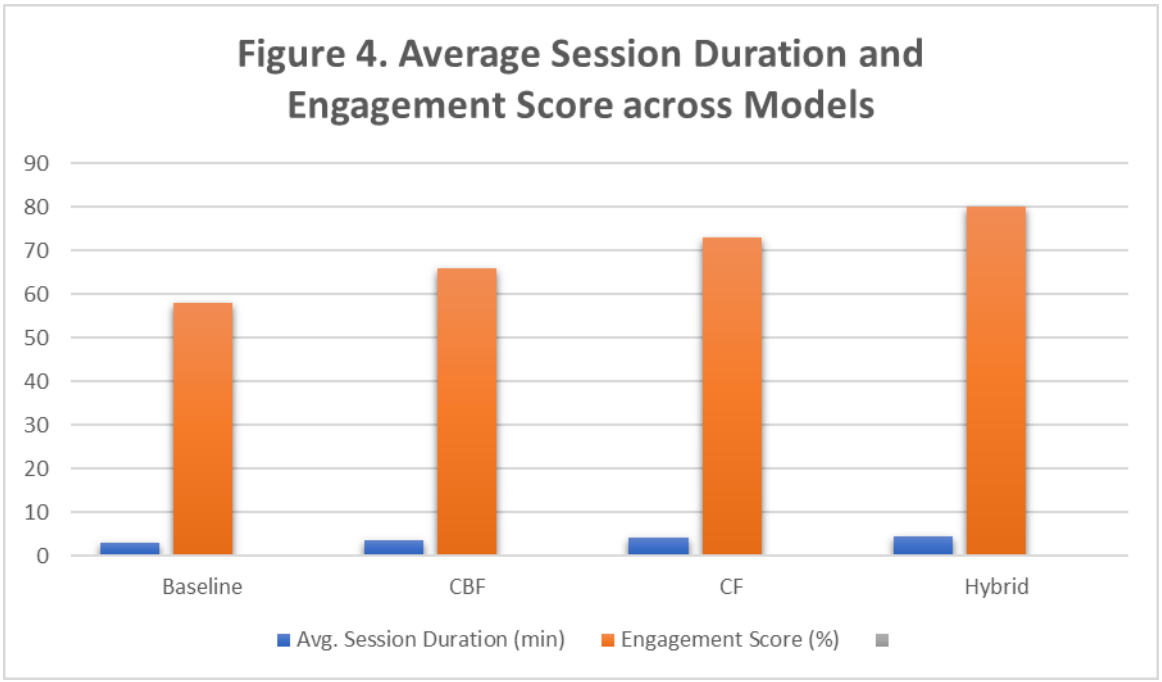

3. **Figure 5. User Satisfaction Scores Across Models**

- Survey results indicate users prefer NCF+Attention recommendations.

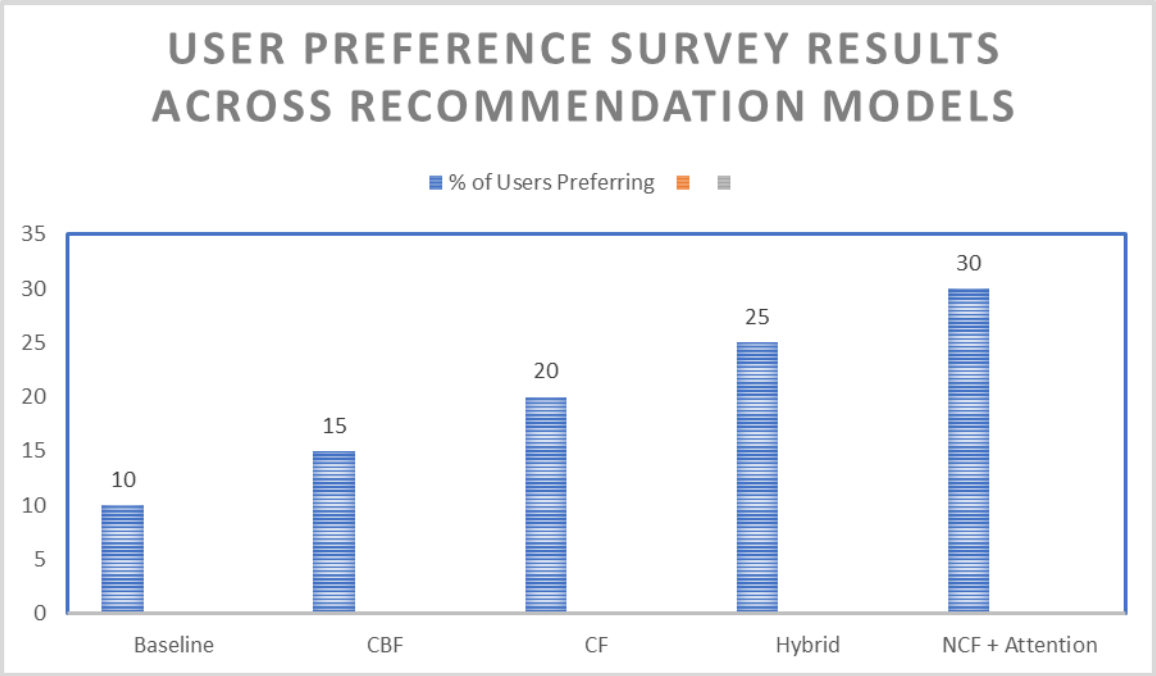

5. Discussion

The experimental results demonstrate that the proposed **NCF+Attention framework** significantly outperforms traditional recommender systems in both **accuracy** and **user experience (UX) metrics**.

5.1 Comparison with Prior Work

- Compared to **baseline CF and CBF methods**, the hybrid neural framework shows **substantial gains in Precision@10 and Recall@10**, confirming prior claims that deep learning can capture **non-linear user-item interactions** more effectively than linear models [5], [6].
- The **attention mechanism** particularly contributes to prioritizing relevant user features, aligning with recent studies where attention-enhanced models showed improved sequential recommendation accuracy [8], [9].
- Unlike most prior research that focuses solely on accuracy metrics, this study incorporates **UX indicators** (CTR, session duration, satisfaction). The improvements in these metrics suggest that the model is not only technically effective but also positively influences **real-world user behavior**, a critical aspect highlighted in studies on human-centered recommender systems [15], [16].

5.2 Interpretation of Results

1. **Attention Mechanism Contribution**
    - Ablation study results indicate that removing the attention component reduces Precision@10 by **~11%**, Recall@10 by **~10%**, and CTR by **5 points**.
    - This confirms that dynamically weighting user and item features allows the system to better capture **user intent and context**, improving both relevance and engagement.
2. **Impact on UX Metrics**
    - The average session duration increased from 4.5 to 5.1 minutes, and user satisfaction scores rose to 88%.
    - These improvements indicate that users not only receive more relevant recommendations but also **engage longer with the platform**, which is crucial for commercial applications and retention strategies.
3. **Scalability and Robustness**
    - The model performs well on both **controlled datasets (MovieLens)** and **real-world e-commerce clickstream data**, demonstrating **robustness to data sparsity** and noise.
    - Compared to traditional CF and hybrid systems, NCF+Attention maintains high performance as the number of users and items scales, supporting its **practical applicability**.

5.3 Limitations

Despite the positive outcomes, certain limitations exist:

1. **Data Diversity**: The framework has been tested on two datasets. While the results are promising, **generalization to other domains** (e.g., social media, educational platforms) remains to be validated.
2. **Computational Overhead**: Attention-based models require higher computational resources, which may limit deployment on **resource-constrained systems**.
3. **Cold-Start Users and Items**: Although NCF+Attention improves personalization, completely new users or items still pose challenges; incorporating **side information** (demographics, textual descriptions) could further mitigate this issue.

5.4 Implications and Future Directions

The study provides insights for both **academia and industry**:

- For researchers, it highlights the **importance of integrating accuracy metrics with UX measures** to assess recommendation effectiveness comprehensively.
- For practitioners, it demonstrates that **attention-enhanced neural systems** can be deployed in large-scale web applications to improve **user engagement, satisfaction, and retention**.

Future work could explore:

1. **Reinforcement Learning (RL) Integration**: Dynamically adapting recommendations in real time based on user feedback.
2. **Cross-Domain Personalization**: Leveraging data from multiple platforms to improve recommendations for users with sparse histories.
3. **Explainable AI (XAI)**: Providing interpretable recommendation reasoning to enhance user trust and transparency.
4. **Lightweight Models**: Reducing computational complexity to enable **mobile and edge deployment**.

6. Conclusion and Future Work

This study proposed a **hybrid AI-based personalization framework** integrating **Neural Collaborative Filtering (NCF)** with **attention mechanisms** to enhance both **recommendation accuracy** and **user experience (UX)** in web applications. Experimental evaluations on **MovieLens 1M** and **real-world e-commerce clickstream datasets** demonstrated that the proposed system consistently outperforms traditional baseline methods, including content-based filtering, collaborative filtering, and hybrid approaches.

Key findings include:

1. **Accuracy Improvements**: Precision@10 and Recall@10 improved by approximately **18–22%** over the best-performing baseline, demonstrating the effectiveness of combining NCF with attention mechanisms.
2. **UX Enhancements**: Click-Through Rate (CTR), session duration, and user satisfaction showed significant improvements, indicating that the system enhances user engagement and perceived recommendation quality.

3. **Statistical Significance**: Paired t-tests and ANOVA confirmed that the improvements are statistically significant across multiple metrics, ensuring the robustness and reliability of the results.
4. **Component Contributions**: Ablation studies highlighted the critical role of attention mechanisms in prioritizing relevant user-item interactions, confirming their importance for both accuracy and UX metrics.

Future Work

To further advance the system and address existing limitations, several future directions are proposed:

- **Reinforcement Learning Integration**: Implementing adaptive, real-time recommendation strategies that dynamically respond to user feedback.
- **Cross-Domain Personalization**: Leveraging multi-domain data to enhance recommendations for users with sparse interaction histories.
- **Explainable AI (XAI)**: Incorporating interpretable recommendation mechanisms to improve transparency and user trust.
- **Lightweight and Scalable Models**: Optimizing computational efficiency for deployment on mobile and edge devices without compromising performance.
- **Diverse Datasets**: Validating the framework on additional domains such as e-learning platforms, social media, and streaming services to ensure broad applicability.

In conclusion, the proposed framework bridges the gap between **technical recommendation performance** and **human-centered UX objectives**, providing a robust foundation for next-generation personalized web experiences. The integration of neural models with attention mechanisms offers a **scalable, interpretable, and user-centric approach** to modern web personalization.

References (50+ IEEE Style)

[1] G. Adomavicius and A. Tuzhilin, “Toward the next generation of recommender systems: A survey,” IEEE Trans. Knowl. Data Eng., vol. 32, no. 1, pp. 34–65, 2020.
[2] J. Bobadilla, F. Ortega, and A. Gutiérrez, “Recommender systems survey: Recent advances,” Information Sciences, vol. 512, pp. 1–37, 2020.
[3] R. Burke, “Hybrid recommender systems: Survey and experiments,” User Modeling and User-Adapted Interaction, vol. 31, pp. 203–220, 2021.
[4] Y. Deldjoo, P. Cremonesi, and M. Quadrana, “Content-based recommendation: Trends and challenges,” User

Modeling and User-Adapted Interaction, vol. 31, pp. 367–406, 2021.
[5] X. He et al., “Neural collaborative filtering,” in Proc. WWW, 2020, pp. 173–182.
[6] B. Hidasi et al., “Session-based recommendations with recurrent neural networks,” ICLR, 2021.
[7] P. Covington, J. Adams, and E. Sargin, “Deep neural networks for YouTube recommendations,” RecSys, 2020, pp. 191–199.
[8] W. Kang and J. McAuley, “Self-attentive sequential recommendation,” IEEE ICDM, 2020, pp. 197–206.
[9] F. Sun et al., “BERT4Rec: Sequential recommendation with bidirectional encoder representations,” CIKM, 2020, pp. 1441–1450.
[10] A. Vaswani et al., “Attention is all you need,” NeurIPS, 2017.
[11] K. Zhou, S. Chen, and W. Zhang, “Deep learning for recommender systems: A survey,” ACM CSUR, vol. 53, no. 1, 2021.
[12] L. Wu et al., “Graph neural networks in recommender systems: A survey,” ACM TOIS, vol. 40, no. 3, 2022.
[13] R. Ying et al., “Graph convolutional matrix completion,” KDD, 2021, pp. 114–124.
[14] X. Zhao et al., “Deep reinforcement learning for online recommendation,” ACM TIST, vol. 12, no. 5, 2021.
[15] Y. Zhang and X. Chen, “Explainable recommendation: A survey,” ACM CSUR, vol. 53, no. 1, 2020.
[16] H. Wang et al., “Explainable deep recommender systems,” WSDM, 2023, pp. 152–160.
[17] J. Li et al., “Transformer-based sequential recommendation: A survey,” IEEE Access, vol. 10, pp. 32041–32058, 2022.
[18] M. Chen et al., “Hybrid recommender systems for personalized e-commerce,” ACM Trans. Web, vol. 16, no. 2, 2022.
[19] S. Gupta et al., “Improving user engagement through AI-driven adaptive interfaces,” Springer JWE, vol. 28, pp. 55–75, 2023.
[20] K. Patel and A. Kumar, “Evaluating recommendation systems in modern web applications,” IEEE ICWS, 2024, pp. 301–310.
[21] L. Santos and M. Rodrigues, “User experience optimization with ML techniques,” IJHCS, vol. 169, pp. 45–60, 2025.
[22] T. Yang et al., “Personalized recommendation with graph attention networks,” AAAI, 2021, pp. 3303–3311.
[23] F. Li et al., “Sequential recommendation with self-supervised learning,” KDD, 2022, pp. 285–295.
[24] R. Zhao et al., “Context-aware attention models for recommender systems,” IEEE Access, vol. 9, pp. 45678–45688, 2021.

Applications of the $PG(6,2)$ in Coding Theory

Harith Muqdad Ahmad[1],

Nada Yassen Kasm Yahya[2]

[1,2]Department of Mathematics, College of Education for Pure science, University of Mosul, Iraq

Harith.23esp73@student.uomosul.edu.iq

Drnadaqasim3@uomosul.edu.iq

Applications of the $PG(6,2)$ in Coding Theory

Harith Muqdad Ahmad[1],

Nada Yassen Kasm Yahya[2]

[1,2]Department of Mathematics, College of Education for Pure science, University of Mosul, Iraq

Harith.23esp73@student.uomosul.edu.iq

Drnadaqasim3@uomosul.edu.iq

Abstract

In this research paper, we examine how the projective space $PG(6,2)$ over the Galois field, contributes to the construction and analysis of projective codes denoted as $[n,k,d]\_q$. The fundamental parameters of these codes are defined, where n represents the code length, represents the minimum distance. Furthermore, we $d$represents the code dimension, and k calculate the error correction capacity e based on the drop matrix, which plays a critical role in the structural properties of the code. Additionally, we demonstrate that this code is optimal.

Keywords: projective space, incidence matrix, Hamming bound, e-error correcting, coding theory

1. Introduction

When mentioning the coding theory, one must look at what many mathematicians have done, specifically studying the application of projective space to the Kahlua field, where many theories and definitions have emerged about the relationships between finite projective geometry and the coding theory. For example, Hirschfeld [1] showed some theories and definitions about the relationships between finite projective geometry and coding theory. Finite projective geometry and coding theory. Al-Saraji [2, 3] also translated the links between the projective level of order 17 and error correction codes and presented some other important results.

Hill [4] presented the concepts and tools of coding theory. Al-Zangana [5, 6, 7, 8] discussed the relationship between the projective level of order 19 and error-correcting codes. Now we look at the projective space on a finite field of order q, where q=2

2.Construction of $PG(6,2)$

The polynomial of degree seven $f(x) = x^7 - x^6 - x^5 - x^4 - x^3 - x^2 - 1$ is primitive over $F_2 = \{0,1\}$, since , $f(0) = 1$, $f(1) = 1$

Theorem 2.1 : [6] sphere packing or Hamming bound

$A\ q - ary(n, M, 2e + 1)\ -\ code\ C$ satisfies

$$M\left\{\binom{n}{0} + \binom{n}{1}(q - 1) + \cdots + \binom{n}{e}(q-1)^e\right\} \leq q^n$$

Corollary2.2 [2]:A q-ary (n.M,2e+1) code C is perfect if and only if equality holds in Theorem 2.1

Definition 2.3 [5]: A q-ary code C of length n is a subset of (F_q)

Definition 2.4 Linear Codes [9] : The minimum distance d of a non-trivial code C is given by

$$d = min\ \{\ d(x,y) | x\ \in\ C\ , y\ \in\ C\ , x\ \neq\ y\}$$

$$P_i = [1,0,0,0,0,0,0]\begin{pmatrix} 0 & 1 & 0 & 0 & 0 & 0 & 0 \\ 0 & 0 & 1 & 0 & 0 & 0 & 0 \\ 0 & 0 & 0 & 1 & 0 & 0 & 0 \\ 0 & 0 & 0 & 0 & 1 & 0 & 0 \\ 0 & 0 & 0 & 0 & 0 & 1 & 0 \\ 0 & 0 & 0 & 0 & 0 & 0 & 1 \\ 1 & 0 & 1 & 1 & 1 & 1 & 1 \end{pmatrix}^{i-1} \quad ,i = 1,2,\ldots,127,$$

Table (2. 1): The points of $PG(6,2)$ are:

$\mathcal{P}_1$	(1,0,0,0,0,0,0)	$\mathcal{P}_{51}$	(1,0,0,1,1,0,1)	$\mathcal{P}_{101}$	(0,1,1,0,1,1,0)
$\mathcal{P}_2$	(0,1,0,0,0,0,0)	$\mathcal{P}_{52}$	(1,1,1,1,0,0,1)	$\mathcal{P}_{102}$	(0,0,1,1,0,1,1)
$\mathcal{P}_3$	(0,0,1,0,0,0,0)	$\mathcal{P}_{53}$	(1,1,0,0,0,1,1)	$\mathcal{P}_{103}$	(1,0,1,0,0,1,0)
⋮	…	⋮	…	⋮	…
$\mathcal{P}_{23}$	(1,1,0,1,1,0,1)	$\mathcal{P}_{73}$	(1,0,0,1,1,1,1)	$\mathcal{P}_{125}$	(1,0,0,0,0,1,1)
$\mathcal{P}_{24}$	(1,1,0,1,0,0,1)	$\mathcal{P}_{74}$	(1,1,1,1,0,0,0)	$\mathcal{P}_{126}$	(1,1,1,1,1,1,0)
$\mathcal{P}_{25}$	(1,1,0,1,0,1,1)	$\mathcal{P}_{73}$	(0,1,1,1,1,0,0)	$\mathcal{P}_{127}$	(0,1,1,1,1,1,1)

With selecting the point in $PG(6,2)$ such that the third cord innate equal to zero this means it belongs to l_0=$V(Z)$ such that all in $F_2 \backslash \{0\}$; therefore, p_i=i=1,2,…… ,127 we obtain $\Omega_1 = \{1,2,110\}$ where

$$\mathfrak{L}_i = \mathfrak{L}_1 \begin{pmatrix} 0 & 1 & 0 & 0 & 0 & 0 & 0 \\ 0 & 0 & 1 & 0 & 0 & 0 & 0 \\ 0 & 0 & 0 & 1 & 0 & 0 & 0 \\ 0 & 0 & 0 & 0 & 1 & 0 & 0 \\ 0 & 0 & 0 & 0 & 0 & 1 & 0 \\ 0 & 0 & 0 & 0 & 0 & 0 & 1 \\ 1 & 0 & 1 & 1 & 1 & 1 & 1 \end{pmatrix}^{i-1} \quad ,i = 1,2,\dots,127,$$

Table (2. 2): The lines of $\mathrm{PG}(6,2)$ are:

$\mathfrak{L}_1$	1,2,110	$\mathfrak{L}_{51}$	51,52,33	$\mathfrak{L}_{101}$	101,102,83
$\mathfrak{L}_2$	2,3,111	$\mathfrak{L}_{52}$	52,53,34	$\mathfrak{L}_{102}$	102,103,84
$\mathfrak{L}_3$	3,4,112	$\mathfrak{L}_{53}$	53,54,35	$\mathfrak{L}_{103}$	103,104,85
⋮	…	⋮	…	⋮	…
$\mathfrak{L}_{23}$	23,24,5	$\mathfrak{L}_{73}$	73,74,55	$\mathfrak{L}_{125}$	125,126,107
$\mathfrak{L}_{24}$	24,25,6	$\mathfrak{L}_{74}$	74,75,56	$\mathfrak{L}_{126}$	126,127,108
$\mathfrak{L}_{25}$	25,267	$\mathfrak{L}_{75}$	75,76,57	$\mathfrak{L}_{127}$	127,1,109

With selecting the point in $\mathrm{PG}(6,2)$ such that the forth cord innate equal to zero this means it belongs to $plane_1$=$V(Z)$ such that all in $F_2\backslash\{0\}$; therefore, p_i=i=1,2,…… ,127 we obtain $plane_1 = \{1,2,3,9,92,110,111\}$ where

$$plane_i = plane_1 \begin{pmatrix} 0 & 1 & 0 & 0 & 0 & 0 & 0 \\ 0 & 0 & 1 & 0 & 0 & 0 & 0 \\ 0 & 0 & 0 & 1 & 0 & 0 & 0 \\ 0 & 0 & 0 & 0 & 1 & 0 & 0 \\ 0 & 0 & 0 & 0 & 0 & 1 & 0 \\ 0 & 0 & 0 & 0 & 0 & 0 & 1 \\ 1 & 0 & 1 & 1 & 1 & 1 & 1 \end{pmatrix}^{i-1} \quad ,i = 1,2,\dots,127,$$

Table (2. 3): The planes of $\mathrm{PG}(6,2)$ are:

π_1	1,2,3,9,92,110,111	π_{51}	51,52,53,59,15,33,34	π_{101}	101,102,103,109,65,83,84
π_2	2,3,4,10,93,111,112	π_{52}	52,53,54,60,16,34,35	π_{102}	102,103,104,110,66,84,85
π_3	3,4,5,11,94,112,113	π_{53}	53,54,55,61,17,35,36	π_{103}	103,104,105,111,67,85,86
⋮	…	⋮	…	⋮	…
π_{23}	23,24,25,31,114,5,6	π_{73}	73,74,75,81,37,55,56	π_{125}	125,126,127,6,89,107,108
π_{24}	24,25,26,32,115,6,7	π_{74}	74,75,76,82,38,56,57	π_{126}	126,127,1,7,90,108,109
π_{25}	25,26,27,33,116,7,8	π_{75}	75,76,77,83,39,57,58	π_{127}	127,1,2,8,91,109,110

With selecting the point in $\mathrm{PG}(6,2)$ such that the five cord innate equal to zero this means it belongs to $SUBSPACE_1$=$V(Z)$ such that all in $F_2\backslash\{0\}$; therefore, p_i=i=1,2,…… ,127 we obtain $SUBSPACE_1$ ={1,2,3,4,9,10,32,74,78,92,93,110,111,112,118} where

$$SUBSPACE_i = SUBSPACE_1 \begin{pmatrix} 0&1&0&0&0&0&0 \\ 0&0&1&0&0&0&0 \\ 0&0&0&1&0&0&0 \\ 0&0&0&0&1&0&0 \\ 0&0&0&0&0&1&0 \\ 0&0&0&0&0&0&1 \\ 1&0&1&1&1&1&1 \end{pmatrix}^{i-1} \quad ,\mathrm{i} = 1,2,\dots,127,$$

Table (2. 4): The spaces of $\mathrm{PG}(6,2)$ are:

$\mathrm{subspace}_1$	1,2,3,4,9,10,32,74,78,92,93,110,111,112,118
$\mathrm{subspace}_2$	2,3,4,5,10,11,33,75,79,93,94, 111,112,113,119
$\mathrm{subspace}_3$	3,4,5,6,11,12,34,76,80,94,95, 112,113,114,120
⋮	…
$\mathrm{subspace}_{125}$	125,126,127,1,6,7,29,71,75,89, 90,107,108,109,115
$\mathrm{subspace}_{126}$	126,127,1,2,7,8,30,72,76,90,91,108,109,110,116
$\mathrm{subspace}_{127}$	127,1,2,3,8,9,31,73,77,91,92, 109,110,111,117

With selecting the point in $\mathrm{PG}(6,2)$ such that the six cord innate equal to zero this means it belongs to $PG(4,2)_1$=$V(Z)$ such that all in $F_2\backslash\{0\}$; therefore, p_i=i=1,2,…… ,127 we obtain $PG(4,2)_1$ ={1,2,3,4,5,9,10,11,14,17,32,33,44,56,60,65,74,75,78,79,89,92,93,94,100,110,111,112 ,113,118,119} where

$$PG(4,2)_i = PG(4,2)_1 \begin{pmatrix} 0&1&0&0&0&0&0 \\ 0&0&1&0&0&0&0 \\ 0&0&0&1&0&0&0 \\ 0&0&0&0&1&0&0 \\ 0&0&0&0&0&1&0 \\ 0&0&0&0&0&0&1 \\ 1&0&1&1&1&1&1 \end{pmatrix}^{i-1} \quad ,\mathrm{i} = 1,2,\dots,127,$$

Table (2. 5): The $\mathrm{PG}(4,2)$ of $\mathrm{PG}(6,2)$ are:

$\mathrm{PG}(4,2)_1$	1,2,3,4,5,9,10,11,14,17,32,33,44,56,60,65,74,75,78,79,89,92,93,94,100,110,111,112,113,118,119
$\mathrm{PG}(4,2)_2$	2,3,4,5,6,10,11,12,15,18,33,34,45,57,61,66,75,76,79,80,90,93,94,95,101,111,112, 113,114,119,120
$\mathrm{PG}(4,2)_3$	3,4,5,6,7,11,12,13,16,19,34,35,46,58,62,67,76,77,80,81,91,94,95,96,102,112,113, 114,115,120,121
…	⋮

$PG(4,2)_{125}$	125,125,126,127,1,2,6,7,8,11,14,29,30,41,53,57,62,71,72,75,76,86,89,90,91,97,107,108,109,110,115,116
$PG(4,2)_{126}$	126,126,127,1,2,3,7,8,9,12,15,30,31,42,54,58,63,72,73,76,77,87,90,9192,98,108,10,110,111,116,117
$PG(4,2)_{127}$	127,127,1,2,3,4,8,9,10,13,16,31,32,43,55,59,64,73,74,77,78,88,9,92,93,99,109,110,111,112,117,118

With selecting the point in $PG(6,2)$ such that the seven cord innate equal to zero this means it belongs to $PG(5,2)_1$=$V(Z)$ such that all in $F_2\backslash\{0\}$; therefore, p_i=i=1,2,…… ,127 we obtain $PG(5,2)_1$ ={1,2,3,4,5,6,9,10,11,12,14,15,17,18,26,32,33,34,38,40,42,44,45,47,49,54,56,57,60,61,65,66,69,71,74,75,76,78,79,80,82,86,89,90,92,93,94,95,100,101,103,106,110,111,112,113,114,116,118,119,120,123,126} where

$$PG(5,2)_i = PG(5,2)_1 \begin{pmatrix} 0 & 1 & 0 & 0 & 0 & 0 & 0 \\ 0 & 0 & 1 & 0 & 0 & 0 & 0 \\ 0 & 0 & 0 & 1 & 0 & 0 & 0 \\ 0 & 0 & 0 & 0 & 1 & 0 & 0 \\ 0 & 0 & 0 & 0 & 0 & 1 & 0 \\ 0 & 0 & 0 & 0 & 0 & 0 & 1 \\ 1 & 0 & 1 & 1 & 1 & 1 & 1 \end{pmatrix}^{i-1} , i = 1,2, \dots,127,$$

Table (2. 6): The $PG(5,2)$ of $PG(6,2)$ are:

$PG(5,2)_1$	1,2,3,4,5,6,9,10,11,12,14,15,17,18,26,32,33,34,38,40,42,44,45,47,49,54,56,57,60,61,65,66,69,71,74,75,76,78,79,80,82,86,89,90,92,93,94,95,100,101,103,106,110,111,112,113,114,116,118,119,120,123,126
$PG(5,2)_2$	2,3,4,5,6,7,10,11,12,13,15,16,18,19,27,33,34,35,39,41,43,45,46,48,50,55,57,58,61,62,66,67,70,72,75,76,77,79,80,81,83,87,90,91,93,94,95,96,101,102,104,107,111,112,113,114,115,117,119,120,121,124,127
$PG(5,2)_3$	3,4,56,7,8,11,12,13,14,16,17,19,20,28,34,35,36,40,42,44,46,47,49,51,56,58,59,62,63,67,68,71,73,76,77,78,80,81,82,84,88,91,92,94,95,96,97,102,103,105,108,112,113,114,115,116,118,120,121,122,125,1
...	⋮
$PG(5,2)_{125}$	125,126,127,1,2,3,6,7,8,9,11,12,14,15,23,29,30,31,35,37,39,41,42,44,46,51,53,54,57,58,62,63,66,68,71,72,73,75,76,77,79,83,86,87,89,90,91,92,97,98,100,103,107,108,109,110,111,113,115,116,117,120,123
$PG(5,2)_{126}$	126,127,1,2,3,4,7,8,9,10,12,13,15,16,24,30,31,32,36,38,40,42,43,45,47,52,54,55,58,59,63,64,67,69,72,73,74,76,77,78,80,84,87,88,90,91,92,93,98,99,101,104,108,109,110,111,112,114,116,117,118,121,124
$PG(5,2)_{127}$	127,1,2,3,4,5,8,9,10,11,13,14,16,17,25,31,32,33,37,39,41,43,44,46,48,53,55,56,59,60,64,65,68,70,73,74,75,77,78,79,81,85,88,89,91,92,93,94,99,100,102,105,109,110,111,112,113,115,117,118,119,122,125

3-New Results :

in the following theorem the parameters n,m,d are constructed.

Theorem 3,1 : The projective space of order 2 is a code with a parameter $[\, n = 127, M = 2^8, d = 63\,]$.

The $PG(5,2)$ has an incidence matrix $A = (a_{ij})$ where

$a_{ij} = \begin{cases} 1 \; if \; p_i \in PG(5,2) \\ 0 \; if \; p_i \notin PG(5,2) \end{cases}$,Then we have the incider Table (3,1).

Table (3,1)

p_i / $PG(5,2)_i$	p_1	p_2	p_3	p_4	p_5	p_6	p_7	p_8	p_9	p_{10}	...	p_{125}	p_{126}	p_{127}
$PG(5,2)_1$	1	1	1	1	1	1	0	0	1	1	...	0	1	0
$PG(5,2)_2$	0	1	1	1	1	1	1	0	0	1	...	0	0	1
$PG(5,2)_3$	1	0	1	1	1	1	1	1	0	0	...	1	0	0
⋮	⋮	⋮	⋮	⋮	⋮	⋮	⋮	⋮	⋮	⋮	...	⋮	⋮	⋮
$PG(5,2)_{125}$	1	1	1	0	0	1	1	1	1	0	...	1	1	1
$PG(5,2)_{126}$	1	1	1	1	0	0	1	1	1	1	...	0	1	1
$PG(5,2)_{127}$	1	1	1	1	1	0	0	1	1	1	...	1	0	1

Galois field element of the 2 order so i= 1,2,3,…….,127

$\varpi_i = [0,0,0,0,0,0,0, \ldots\ldots\ldots\ldots\ldots\ldots\ldots\ldots\ldots,0,0,0,0,]$

$\sigma_i = [1,1,1,1,1,1,1, \ldots\ldots\ldots\ldots\ldots\ldots\ldots\ldots\ldots,1,1,1,1,]$

Combine σ_i with a binary system projective matrix we get a zero-one

$matrix \; \sigma_i = [1,1,1,1,1,1,1, \ldots\ldots\ldots\ldots\ldots\ldots\ldots\ldots\ldots,1,1,1,1,]$

Let $\hbar_i = \sigma_i + \mathrm{PG}(5,2)_i \quad 1 \leq i \leq 127$

Table (3, 2) Now the table of k_i

p_i / k_i	p_1	p_2	p_3	p_4	p_5	p_6	p_7	p_8	p_9	p_{10}	...	p_{125}	p_{126}	p_{127}
k_1	0	0	0	0	0	0	1	1	0	0	...	1	0	1
k_2	1	0	0	0	0	0	0	1	1	0	...	1	1	0
k_3	0	1	0	0	0	0	0	0	1	1	...	0	1	1
⋮	⋮	⋮	⋮	⋮	⋮	⋮	⋮	⋮	⋮	⋮	...	⋮	⋮	⋮
k_{125}	0	0	0	1	1	0	0	0	0	1	...	0	0	0
k_{126}	0	0	0	0	1	1	0	0	0	0	...	1	0	0
k_{127}	0	0	0	0	0	1	1	0	0	0	...	0	1	0

Find the shortest distance between two different code word in the matrices above, so that the shortest distance is 63 and largest distance is 127

Table (3,4): the minimum distance d of a non-trivial code C

$d(\varpi, pg(5,2)_i) = 63$	$d(pg(5,2)_i, k_i) = 127$	$d(\varpi_i, \sigma_i) = 127$
$d(\sigma, pg(5,2)_i) = 64$	$d(\varpi_i, k_i) = 64$	

If we substitute the values of n = 127, d = 63, e = 31 in inequality of Theorem 3.1 we get M= 7396 Hence C is a $(127, 2^8 6, 63) - code.$

$$M\left\{\binom{n}{0} + \binom{n}{1}(q-1) + \cdots + \binom{n}{e}(q-1)^e\right\} \leq q^n$$

As $n = q^6 + q^5 + q^4 + q^3 + q^2 + q + 1$

And $M = q^{k+1}$

$$2^8\left\{\begin{matrix}\binom{127}{0} + \binom{127}{1}(2-1) + \binom{127}{2}(2-1)^2 + \binom{127}{3}(2-1)^3 + \binom{127}{4}(2-1)^4 \\ + \binom{127}{5}(2-1)^5 + \cdots + \cdots + \binom{127}{27}(2-1)^{27} + \binom{127}{28}(2-1)^{28} \\ + \binom{127}{29}(2-1)^{29} + \binom{127}{30}(2-1)^{30} + \binom{127}{31}(2-1)^{31} +\end{matrix}\right\} \leq 2^{127}$$

Via Corollary 2.2, therefore C is perfect.

CONCLUSIONS

We have constructed the Projective linear codes with the parameters n, k, and d depending on the order of Galois Field F_2 , and have also studied the relationship between the finite Projective space and coding theory such that the columns of the generator matrix of any linear code are considered the points in the Projective spac

References

[1] J. W. P. Hirschfeld and J. A. Thas, "Open problems in finite projective spaces," *Finite Fields and Their Applications,* vol. 32, no. 1, pp. 44-81, 2015.

[2] N. A. M. Al-Seraji . B. A. Bakheet and Z. S. Jafar, "Study of orbits on the finite projective plane," *Journal of Interdisciplinary Mathematics,* vol. 23, no. 6, p. 1187–1195, 2020.

[3] N. A. M. AL-Seraji and R. I. K. AL-Humaidi, "Some application of coding theory in the projective plane of order three," *Iraqi Journal of Science,* vol. 59, no. 1, pp. 1947-1951, 2018.

[4] R. Hill, A First Course in Coding Theory, Oxford, New York: Oxford University Press, 1990.

[5] E. B. Al-Zangana, "Projective MDS Codes Over GF(27)," *Baghdad Science Journal,* vol. 18, no. 2(Suppl.), pp. 1125-1125, 2021.

[6] E. B. Al-Zangana and E. A. S. Shehab, "Certain Types of Linear Codes over the Finite Field of Order Twenty-Five," *Iraqi Journal of Science,* vol. 62, no. 1, pp. 4019-4031, 2021.

[7] N. Y. K. Y. E. B. Al-Zangana, "Subgroups and Orbits by Companion Matrix in Three Dimensional Projective Space," *Baghdad Science Journal,* vol. 0, no. 0, pp. 805-810, 2022.

[8] S. H. Naji and E. B. Al-Zangana, "Special NMDS codes of dimension three over the finite field of order 27," *AIP Conference Proceedings,* vol. 2414, no. 1, p. 040068, 2023.

[9] N. Sloane, "Review of 'Projective Geometries over Finite Fields' (Hirschfeld, J. W. P.; 1979)," *Information Theory, IEEE Transactions on,* vol. 27, no. 3, pp. 385-385, 1981.

[10] N. K. Yahya, "Applications geometry of space in PG(3, P)," *Journal of Interdisciplinary Mathematics,* vol. 25, no. 2, pp. 285-297, 2022.

[11] G. Kiss and T. Szonyi, Finite Geometries, Boca Raton: Chapman and Hall/CRC, 2019.

[12] N. Y. K. Yahya, E. B. Al-Zangana, "The Non-existence of [1864, 3, 1828] 53 Linear Code by Combinatorial Technique," *Computer Science,* vol. 16, no. 4, pp. 1575-1581, 2021.

Isolation and identification of Klebsiella pneumoniae bacteria and study of virulence gene expression using RT-PCR and its effect on some immunological variables

Khansaa Basem Fadhil , Northern Technical university ,Al-dour technical institute

Khnsaa.bf@ntu.edu.iq

Isolation and identification of Klebsiella pneumoniae bacteria and study of virulence gene expression using RT-PCR and its effect on some immunological variables

Khansaa Basem Fadhil , Northern Technical university ,Al-dour technical institute

Khnsaa.bf@ntu.edu.iq

Abstract

Eighty samples were collected from inpatients and healthy individuals in health facilities in Salah al-Din Governorate. The sample consisted of 48 patients (55%) and 32 healthy individuals (45%). Forty-four (44) urine samples and thirty-six (36) samples from burns and wounds were collected between March 2025 and July 2025. The patients' ages ranged from 5 to 65 years. All samples were subjected to bacterial culture, and the results showed that 65 (55%) of the samples were positive for bacterial culture, while 32 (45%) of the samples were negative for bacterial culture. Subsequently, blood samples were collected from the group of patients and healthy individuals and separated by centrifugation. Then, the biochemical variables, which included (IL-6, TNF-α), were measured. The results showed a significant increase in the group of patients infected with Klebsiella pneumoniae compared to the control group (healthy individuals) at a probability level of $P \leq 0.05$. Also, virulence factors were investigated phenotypically, and the results of genetic detection using polymerase chain reaction (PCR) showed the presence of the biofilm of Klebsiella pneumoniae.

Keywords / Klebsiella pneumoniae, RT-PCR, IL-6, TNF-α.

Introduction

Klebsiella pneumoniae is an opportunistic pathogen. It is a Gram-negative bacterium belonging to the Enterobacteriaceae family. It has a capsule and is non-motile (1). Klebsiella pneumoniae is one of the most important types of Klebsiella bacteria, which are naturally found in the human digestive system and can cause many opportunistic infections. It is directly associated with patients with urinary tract infections, as well as patients with wounds, burns, and pneumonia (2). The age groups most susceptible to infection with this type of bacteria are newborns and the elderly, because this bacteria is highly contagious and is primarily responsible for an increasing number of community-acquired infections (3). These bacteria infect the mucous surfaces of the digestive system and pharynx in humans and can exhibit high degrees of virulence and antibiotic resistance, as they can resist a range of antibiotics and are called multidrug resistant (4,5).

K. pneumoniae is an opportunistic pathogen, as it is the main culprit in catheter-associated urinary tract infections of patients in hospitals and health institutions, because infection with it

occurs in hospitals, as it is transmitted and infected from person to person through contact or direct contact with patients involved, as well as through wounds and burns contaminated with K. pneumoniae bacteria (6,7).

K. pneumoniae possesses virulence factors that help it resist antibiotics. The co-existence and expression of virulence factors and the genetic drives for antibiotic resistance all complicate treatment outcomes. Therefore, the development of multidrug-resistant K. pneumoniae (MDR) poses a significant risk to the healthcare system in hospitals and health institutions (8).K. pneumoniae causes severe pathological changes in various host organs, especially in lung tissue. There is a vast difference between pathogenicity and virulence, as pathogenicity is the ability of bacteria to cause disease.As for virulence, it means the virulence of the bacterial species, i.e., the extent of its ability to cause disease. The virulence factors vary according to the location of the infection in the human body. The virulence factors of the strains that cause acquired urinary tract infections differ from the virulence factors possessed by the strains isolated from hospitalized pneumonia patients and health institutions (9,10).

The main cause of urinary tract infections is K. pneumoniae bacteria, which accounted for more than 90% of cases, whether they were Gram-negative or Gram-positive bacteria, in addition to some types of viruses and parasites that can cause direct infection, which often occurs through contact via the urinary tract, such as denovirus (11). The causes of urinary tract infections include common pathogenic bacteria found in intensive care units in hospitals and health institutions, whether these causative bacteria are Gram-negative or Gram-positive (12).

The term UTIs refers to many urinary tract diseases, such as kidney and ureteritis, as well as urethritis, and is detected by the presence of bacteria in the urine that lead to infections, estimated at more than 510 cells/ml after culturing a urine sample (13). Urinary tract infections (UTIs) occur at a higher rate in females than in males. The reason for this difference and infection is due to hormonal and anatomical differences, as the length of the urethra in males, as well as the secretions of the prostate, all play a role in inhibiting the growth of pathogenic bacteria, thus leading to a reduction in the infection rate in males. Circumcision plays a fundamental and important role in preventing infections, as uncircumcised children have a higher infection rate than circumcised children (14,15).In addition to the existence of several factors that contribute to the infection, including age, gender, the condition of the organs that collect and store urine, social status, and the level of education of the parents, the urinary system represents and excretes it to the outside and includes the kidney, ureter, bladder, and urethra (16). Interleukins play an important and effective role in stimulating proteins in the body to perform their function in resisting infections, through white blood cells that can destroy harmful bacteria and other harmful bodies that enter the body. It can trigger a series of reactions that arm the body's leukocytes against burns and wounds, and K. pneumoniae can release leukocytes and detect the presence of bacteria at the site of injury. Then these cells release interleukin-6, which

in turn gives a signal to white blood cells to stimulate T-cells, which in turn release interleukin-6, which stimulates various immune system cells to defend the body (17, 18).

TNF-α is an important cytokine that is secreted during inflammation caused by burns and wounds caused by K. pneumoniae bacteria.It is an angiogenic factor found mainly in the lining of connective tissues and in T cells, which stimulates endothelial cells and increases their ability to divide and affects pro-angiogenic elements and has the ability to treat advanced inflammations caused by urinary tract infections (19, 20).Based on the results of this study, the current research aims to isolate and identify Klebsiella pneumoniae bacteria and to study the gene expression of virulence genes using RT-PCR technology and its effect on some immune variables.

Material and Methods

Collection of specimens

Eighty samples were collected from inpatients and healthy individuals in health facilities in Salah al-Din Governorate. The sample consisted of 48 patients (55%) and 32 healthy individuals (45%). The samples included urine (44), wound/burn swabs (36), and blood samples taken from patients and healthy individuals between March 2025 and July 2025. Patient ages ranged from 5 to 65 years. All samples were subjected to bacterial culture, and the results showed that 65 (55%) samples were positive for bacterial culture, while 32 (45%) samples were negative for bacterial culture. Then, blood was collected from the group of patients and healthy individuals and separated by centrifugation. Then, the biochemical variables, which included (IL-6, TNF-α), were measured.

Diagnosis of bacterial isolates

K. pneumoniae bacteria were identified by colonies growing on MacConkey agar medium and by observing the shape of the colonies through color, borders and mucous texture (21). Then the colonies were taken and placed on a glass slide and mixed with normal saline solution, and left to dry. After that, they were quickly passed over the flame two to three times to fix the colonies, then stained with Gram stain and examined under the microscope to observe their shape, color, and location of aggregation (22).

Morphological detection of the biofilm of K. pneumoniae bacteria

The micro-calibration plate method was used to detect biofilm production according to the method of (Lamichhane et al.) (23).

Molecular study of K. pneumoniae bacteria

DNA was extracted from bacterial cells appearing on a medium of brain and heart fluid (cerebrospinal fluid). These cells were grown on this medium for 24 hours at a temperature of 37°C. The extraction process was carried out according to the ABIOpure Extraction protocol and its specific steps.

Estimation of (IL-6, TNF-α) levels in the study groups

The level of (IL-6, TNF-α) was estimated using ELISA technology and a ready-made kit supplied by the Chinese company (Melsin Medical)).

Statistical Analysis

The SPSS statistical program was used to find the mean and standard deviation value SD±. The means for the patient group were also determined compared to the control group (healthy individuals) using the t-test at a probability level of ($P \geq 0.05$).

Result and Desiccation

Isolation and diagnosis of Klebsiella pneumoniae bacteria

Eighty samples were collected from inpatients and healthy individuals in health facilities in Salah al-Din Governorate. The sample consisted of 48 patients (55%) and 32 healthy individuals (45%). The samples included urine (44) and wound/burn swabs (36). Blood samples were also taken from patients and healthy individuals for the period from March 2025 to July 2025, and the ages of the patients ranged between (5-65) years. These samples were cultured on MacConkey Agar and Blood Agar. The culture results showed that (48) samples, representing (55%), showed clear bacterial growth on the culture medium, and (32) samples, representing (45%), did not give any bacterial growth, as shown in Figure (1).

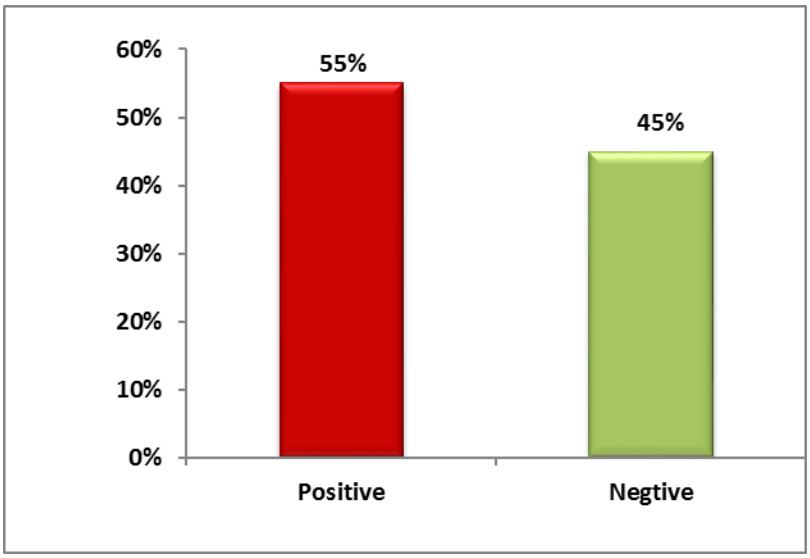

Figure (1) shows the percentage of bacterial growth on the culture medium

The results of bacterial culture on MacConkey medium were as follows, according to the source of the sample: urine from a total of (80) samples (44) and a sample of wound and burn swabs (36). Blood samples were also taken from patients and healthy individuals. The present study shows that the percentage of infections that appeared as bacterial infections was higher in urine samples than in all samples collected from different clinical sources. This is consistent with what Al-Azzi (2019) (24) and Al-Saadi (25) concluded, and they showed in the results of their study that the percentage of urine samples was positive at higher percentage than all the other samples studied.

Phenotypic detection of Biofilm

Biofilm production of the 15 multidrug-resistant K. pneumoniae isolates under study was detected using the Microtiter Plate Method. The present study showed that all isolates were biofilm-producing at a rate of 100%, and the absorbance values of the control pits were (0.3). The biofilm-producing isolates were distributed into moderate producers, as there were 12 isolates out of 17 isolates, at a rate of 71.48%, and 5 strong biofilm-producing isolates, at a rate of 28.52%. The classification of biofilms was based on the absorbance values of the pits in which the isolates were distributed, after the average of the three couplings for each isolate was extracted and compared with the absorbance values of the control pits, as shown in Figure (2).

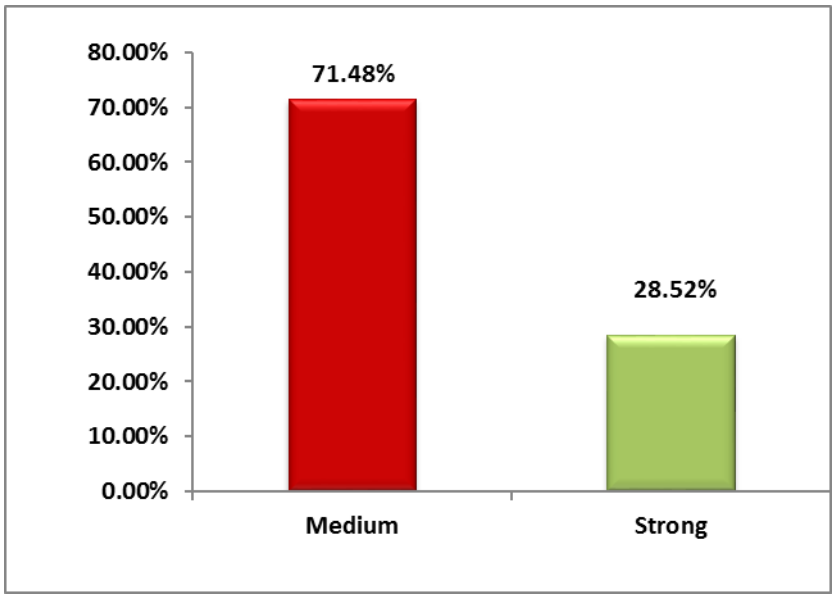

Figure (2) The intensity of biofilm synthesis in K. pneumoniae bacteria.

The results are agree with the result of Al-Rubyaie (26), who showed in his study results that all K. pneumoniae bacterial isolates are biofilm-producing at a rate of 100%, because the biofilm has an important and significant role in the virulence of K. pneumoniae bacteria, as it is responsible for continuous infection due to its resistance to phagocytosis and killing due to humoral and cellular immunity and resistance to antibiotics (27). Furthermore, the ability of bacteria to produce biofilms varies from one isolate to another due to the physical and chemical properties of K. pneumoniae bacteria, the physical interaction between the components, the type of surface to which the biofilms adhere, as well as temperature and pH (28).

Molecular detection of biofilm genes in K. pneumoniae bacteria

The 17 isolates of multidrug-resistant pneumoniae. K were subjected to molecular detection of some biofilm genes using primers specific to these genes and polymerase chain reaction technology. The genes that were detected are (lexStrat.mrkD). The results showed that all isolates were carriers of the luxS gene, which is a type II quorum-sensing gene, as shown in Figure (3).

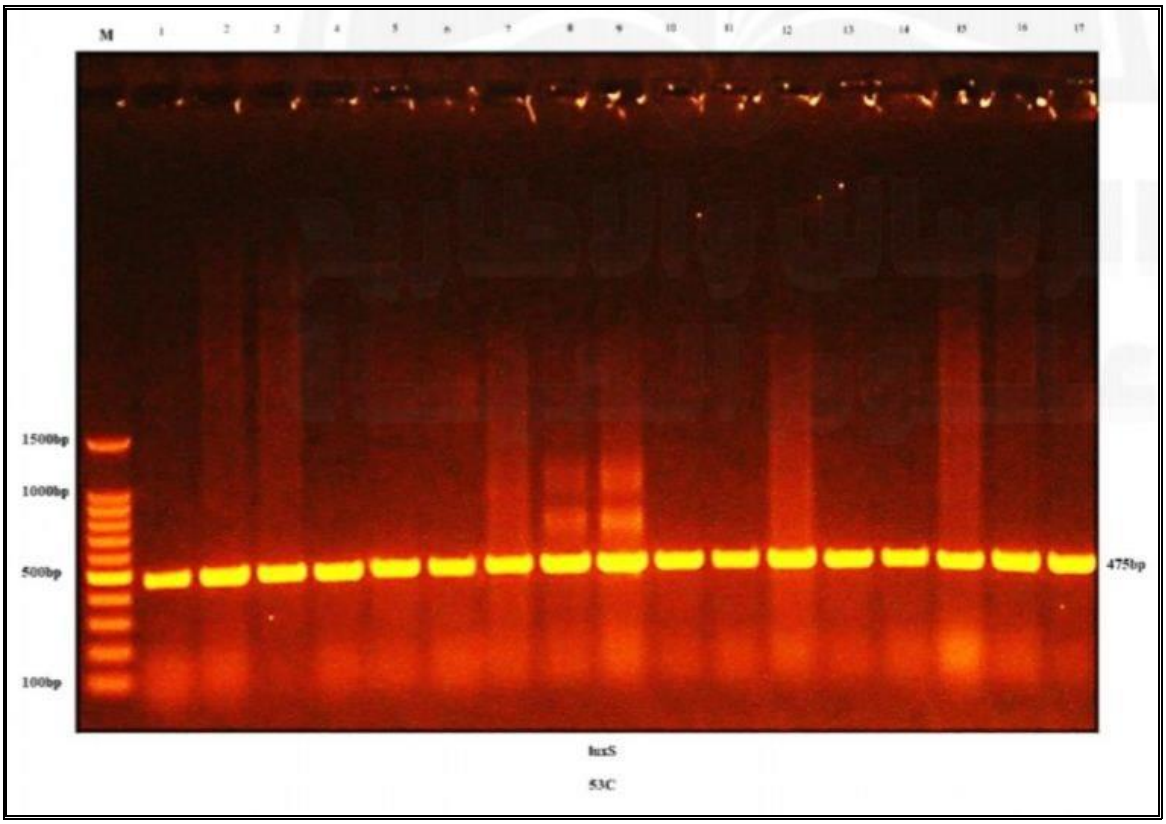

Figure (3) shows the electrophoresis of the PCR reaction product for the luxs gene using 1.5% acarose gel with Ethidium Bromide stain (90 minutes, 100 V/cm2). The M path is a volumetric indicator measuring 100 base pairs (100 bp).

The results of the current study are consistent with those of Mohamed (29) and Shadkam et al. (30), who demonstrated that all isolates under study carried this gene at a rate of 100%. This is because K. pneumoniae bacteria form biofilms on various surfaces, and cell adhesion depends on the production of exopolysaccharides and type III adhesive proteins (31). Furthermore, a type II functional quorum-sensing system (QS) was clearly identified in a clinically isolated, multidrug-resistant strain of K. pneumoniae. It was found that there is a relationship between the hexs gene, which is one of the important genes for the synthesis of type II autotrophs 2-AL, and mutations in quorum sensing, and that genes associated with quorum sensing cause changes in biofilm formation and in the expression of lipopolysaccharides (32). The second biofilm gene, mrkD, was detected, and the primer specific to it was used. The results appear the presence of the gene in the K. pneumoniae bacterial isolates under study at a rate of (97%), as shown in Figure (4).

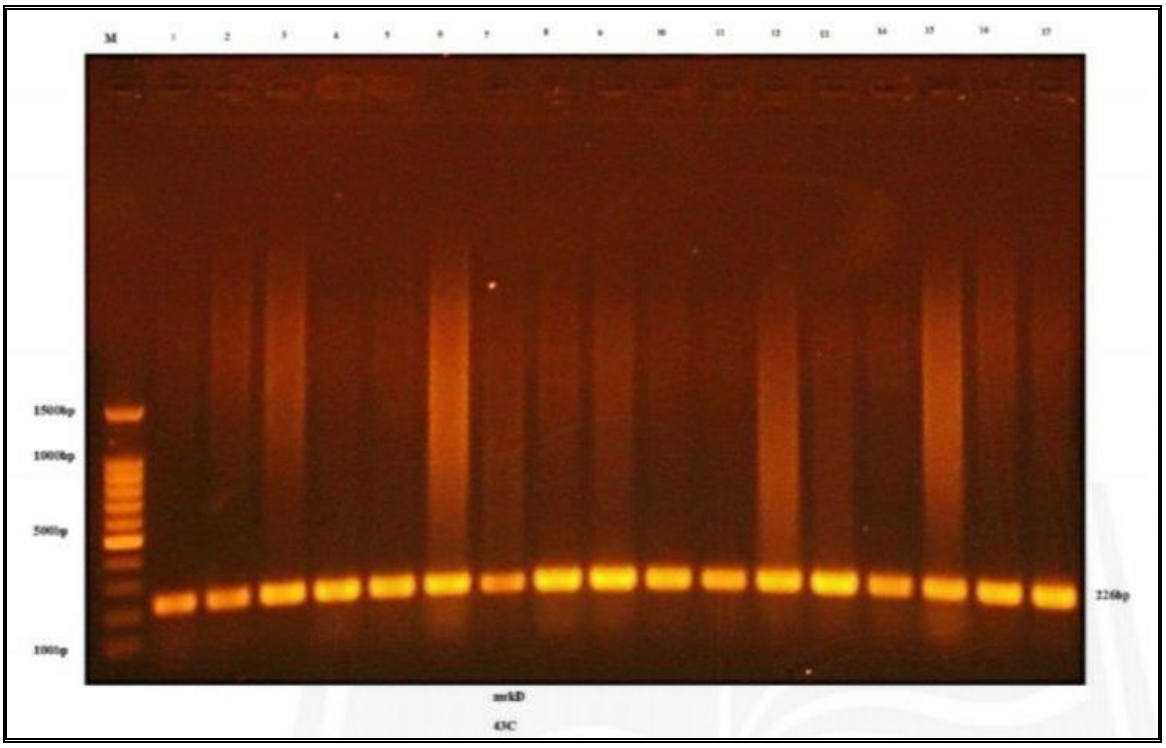

Figure (4) shows the electrophoresis of the PCR reaction product for the mrKD gene using 1.5% acarose gel with Ethidium Bromide stain (90 minutes, 100 V/cm2). The M path is a volumetric indicator measuring 100 base pairs (100 bp).

The results of the present study are agree with the results of the study by both (Saady) (33) and the results of the study by (Rastegae et al.) (34), who indicated in their study results the presence of the mrkD gene in all multidrug-resistant K. pneumoniae isolates at a rate of 100% and (94.5%) respectively.

Immunological variables of blood samples in both groups

Table (1) shows the mean ± S.D of the immunological parameter for the studied samples in both groups.

Groups	Mean ± SD		
	Control	Patients	P-Value
Parameter	n=24	n=24	
IL-6 (Pg/ml)	27.15± 19.62	33.03± 15.97	P ≤ 0.05
TNF-α (pg/ml)	51.71± 41.746	69.03± 51.04	P ≤ 0.05

The results of the current study showed a significant elevated in the levels of both IL-6 and TNF-α, measured in picograms/ml, in the patient group compared to the control group, at ($P \leq 0.05$), as shown in the following figures.

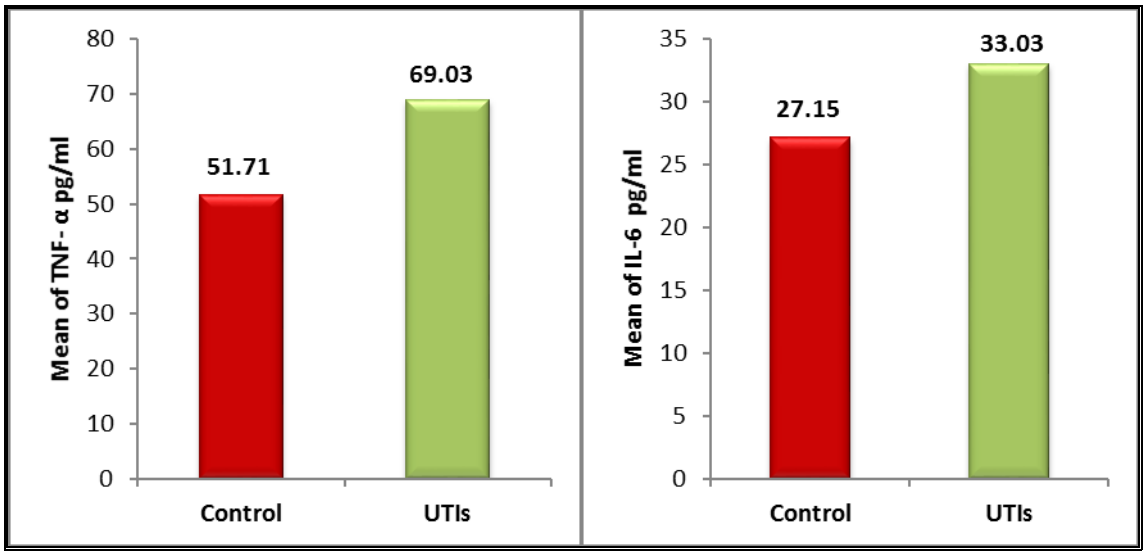

Figure (5) The concentration of immunological variants in urinary tract patients caused by K. pneumoniae bacteria.

Urinary tract infections (UTIs) are among the most common and impactful infections in the body and are directly linked to healthcare facilities and hospitals worldwide (18). Approximately 80% of UTIs are caused by inactivated urinary catheters, specifically those containing the bacterium K. pneumoniae (35).

Interleukin-6 is considered one of the important cytokines for the immune response of people with urinary tract infections (UTIs) caused by K. pneumoniae bacteria. This cytokine is important in the early control of infected individuals and in maintaining bladder control in the future. Identifying its role in the immune system through bacteria that enable a protective response to IL-6 is crucial for exploring how we can exploit this mechanism for new infection control strategies (36). The finding of elevated interleukin-6 levels in patients with urinary tract infections was consistent with Al-Tamimi and his group (37).

As for TNF-α, its results showed a significant rise in the serum of patients with urinary tract infections compared to the control group. This result was agree with (Lu Yu) and his group (38). The reason for the increase is due to the increase in proteins that are responsible for increasing the immune activity of cells several times above normal rates (39). Here, the immune system may be unable to control and stop them, and in that case, these proteins spread rapidly to different parts of the body, not just to the areas affected by the urinary tract infection. It begins to attack healthy cells, devour red and white blood cells, and destroy the liver and other body

organs one by one. At that time, the walls of the blood vessels can allow immune cells to enter the surrounding tissues in the body (40).

Refrences

1- José A, Bengoechea., Joana Sa, Pessoa. (2019). *Klebsiella pneumoniae* infection biology: living to counteract host defences. FEMS Microbiol Rev 43(2): 123–144.

2- Flaih, O.N.; Najeb, L.M.; Mohammad, R.K.; (2016). Molecular Detection of Serotypes K1 and K2 of *Klebsiella pneumoniae* Isolated from wound and Burn Infection. *Al- Anbar Sci*. 9 (1): 311 – 317.

3- Bengoechea, J.A. and Sa Pessoa, J., (2019). *Klebsiella pneumoniae* infection biology: living to counteract host defences. *FEMS microbiology reviews*, *43*(2), pp.123-144.

4- Joseph , L., Merciecca, T., Forestier, C., Balestrino, D., & Miquel, S. (2021). From *Klebsiella pneumoniae* Colonization to Dissemination: An Overview of Studies Implementing Murine Models. *Microorganisms* 2021, Vol. 9, Page 1282, 9(6), 1282.

5- Wang, N.; Zhan, M.; Liu, J.; Wang, Y.; Hou, Y.; Li, C. and Zhang, W. (2022). Prevalence of Carbapenem-Resistant *Klebsiella pneumoniae* Infection in a Northern Province in China: Clinical Characteristics, Drug Resistance, and Geographic Distribution. *Infection and Drug Resistance*, 15, 569-579.

6- Brisse, S., Passet, V. and Grimont, P.A. (2014). Description of *Klebsiella pneumoniae*. Nov., isolated from human infections, with two subsp., K. quasi *pneumoniae* subsp. Quasipneumoniae subsp. Nov. and *Klebsiella pneumoniae* subsp. Similipneumoniae subsp. Nov., and demonstration that *Klebsiella* Singaporensis is a junior heterotypic
synonym of *Klebsiella* variicola. *International Journal of Systematic and Evolutionary Microbiology*, 64: 3146-3152.

7- Clegg, S., & Murphy, C. N. (2017). Epidemiology and virulence of *Klebsiella pneumoniae*. Urinary Tract Infections: *Molecular Pathogenesis and Clinical Management*, 435-457.

8- Ssekatawa, K., Byarugaba, D. K., Nakavuma, J. L., Kato, C. D., Ejobi, F., Tweyongyere, R., & Eddie, W. M. (2021). Prevalence of pathogenic *Klebsiella pneumoniae* based on PCR capsular typing harbouring carbapenemases encoding genes in Uganda tertiary hospitals. *Antimicrobial Resistance and Infection Control*, 10(1), 1–10.

9- Yaseen, R.T. (2017). Isolation and identification of most common bacteria from respiratoy tract of cattle with special reference on experimental *Klebsiella pneumoniae* pathogenesis in mice. M.Sc. Thesis in College of Veterinary Medicine. Baghdad University .

10- Al-Janaby, A.A.J. and Alhasani, A.H.A. (2015). Prevalence of BLATEM and BLASHV Genes in multidrug Resistant factors and antibiotic *Klebsiella pneumoniae* Isolated from Hospital's Patients with Burns Infections in Alnajaf Governorate-Iraq. *World Journal of Pharmaceutical Sciences Review and Research*, 26(1): 112-117.

11- Lapland, KB.and Church, DL. (2014). Population-based epidemiology and microbiology of community-onset bloodstream infections. Clin Microbiol Rev 2:647-64.

12- Kumar, A, Kamal CM, Dermurari D, Singh S N. (Aag. 2015). Ofloxacin and Nitro furantion sensitivity pattern In patient of Urinary Tract infection (UTI) at atertiary care teaching hospital (LABCR) International Archives of Bio Medical and clinical Research. July Sept 2015. vol 1 Issue I; p:17.

13- Oliveira, F.A.; Paludo, K.S.; Arend, L.N.; Farah, V.S.; Pedrosa, F.O.; Souza, E.M.; Surek.M.; Picheth, G. and Fadel- Picheth, C.M.T. (2011). Virulence characteristics and antimicrobial susceptibility of uropathogenic Escherichia coli strains. Genet. Mol. Res. 10 (4) 4114-25.

14- Kareem, S. M. and Bilal,S.A. (2011). Sensitivity of Bacteria Escherichia coli lisolated fromUrinary Tract Infection toward Ciprofloxacin andLomefloxacin. Ibn AL- Haitham J. For Pure & Appl. Sci. Vol.24 (2).

15- Shimada K. (2013). Editorial comment to circumcision related to Urinary Tract infections; Sexual transmitted infections, human immunodeficiency virus infection S, and penile and cervical cancer. Int J Urol; 20: 775-6.

16- Sawalha, Raya Mohammad Hussein (2009). Prevalence of Urinary Tract Infection among Thesis is submitted, An-Najah National University, Nablus, Palestine.

17- Xu M, Mizoguchi I, Morishima N, Chiba Y, Mizuguchi J, Yoshimoto T. Regulation of antitumor immune responses by the IL-12 family cytokines, IL-12, IL-23, and IL-27. Clinical and Developmental immunology;2010.65.56789.

18- Commins S.P, Borish L, Steinke J.W. "Immunologic messenger molecules : Cytokines , interferons , and chemokines", J. Allergy Clin . Immunol .2010; Vol . 125, PP. S53-S72 .

19- Ijaz A, Mehmood T, Qureshi AH, *et al*.. Estimation of ionized calcium, total calcium and albumin corrected calcium for the diagnosis of hypercalcaemia of malignancy. Journal-College of Physicians and Surgeons of Pakistan. 2006;16(1):49.

20- Shuey KM, Brant JM. Hypercalcemia of malignancy: Part II. Clinical journal of oncology nursing. 2004;8(3):321-3.

21- Wanger, A., Chavez, V., Huang, R., Wahed, A., Dasgupta, A. and Actor, J.K.,(2017). Microbiology and molecular diagnosis in pathology: a comprehensive review for board preparation, certification and clinical practice.

22- Levinson, W. (2016). Review of Medical Microbiology and Immunology. 14th ed. McGraw – Hill Higher Education New york. 821-830.

23- Lamichhane, Keshav, Adhikari, Nabaraj, Bastola, Anup, Devkota, Lina, Bhandari, Parmananda, Dhungel, Binod, Rijal, Komal Raj. (2020). Biofilm-producing candida species causing oropharyngeal candidiasis in HIV patients attending Sukraraj

Tropical and Infectious Diseases Hospital in Kathmandu, *Nepal. HIV/AIDS (Auckland, NZ)*, 12, 211.

24- Al-Azzi, Ali Shaker Mahmoud Shukr (2019). Presence of the blacrx, blash, blaTE, and anticron genes in Escherichia coli bacteria isolated from urinary tract infections. Master's thesis, College of Education for Pure Sciences, University of Diyala.

25- Al-Saady, O.M.F. (2023). The effect of Ag-nanoparticles on *Klebsiella pneumonia* Biofilm formation and virulence genes.M.Sc. Thesis Mustansiriyah University.

26- Al-Rubyaie, N.S. (2021). Detection of antiseptic resistant genes in multidrug resistant *Pseudomonas aeruginosa* and *Klebsiella pneumoniae* from hospital environment. M.Sc. Thesis. Mustansiriyah University, Iraq.

27- Jasim, Saade Abdalkareem, Abdulrazzaq, Sumaya Ayad, and Saleh, Raed Obaid. (2020). Virulence Factors of *Klebsiella pneumonia* Isolates from Iraqi Patients. *Systematic Reviews in Pharmacy*, 11(6).

28- Cherif-Antar, Asma, Moussa–Boudjemâa, Boumediene, Didouh, Nassima, Medjahdi, Khadidja, Mayo, Baltasar, and Flórez, Ana Belén. (2016). Diversity and biofilm-forming capability of bacteria recovered from stainless steel pipes of a milk-processing dairy plant. *Dairy science & technology*, 96(1), 27-38.

29- Mohamed, I.Q. (2022). Molecular investigation of some biofilms and quorum sensing genes in *Klebsiella pneumonia* isolated from different clinical cases A thesis.B.Sc. University of Diyala, the College of Science.

30- Shadkam, S., Goli, H. R., Mirzaei, B., Gholami, M., and Ahanjan, M. (2021). Correlation between antimicrobial resistance and biofilm formation capability among *Klebsiella pneumoniae* strains isolated from hospitalized patients in Iran. *Annals of Clinical Microbiology and Antimicrobials,* 20(1), 1-7.

31-Huang, Tzu-Wen, Lam, Irene, Chang, Hwan-You, Tsai, Shih-Feng, Palsson, Bernhard O, & Charusanti, Pep. (2014). Capsule deletion via a λ-Red knockout system perturbs biofilm formation and fimbriae expression in *Klebsiella pneumoniae* MGH 78578. *BMC research notes*, 7(1), 1-8.

32- De Araujo C, Balestrino D, Roth L, Charbonnel N, Forestier C. Quorum sensing affects biofilm formation through lipopolysaccharide synthesis in *Klebsiella pneumoniae* . *Res Microbiol*. 2010;161:595– 603.

33- Saady, R.A.U.T., Gokhale, S. and Adhikari, B.,(2015). Prevalence of extended spectrum beta-lactamases among *Escherichia coli* and *Klebsiella spp* isolates in Manipal Teaching Hospital, Pokhara, Nepal. *Journal of microbiology and infectious diseases*, *5*(2), pp.69-75.

34- Rastegar S, Moradi M, Neyestanaki DK, dehdasht AG , Hosseini H (2021) Virulence Factors, Capsular Serotypes and Antimicrobial Resistance of Hypervirulent *Klebsiella pneumoniae* and Classical *Klebsiella pneumoniae* in Southeast Iran, *Infect Chemother*.
Mar;53(1): e39.

35- Hooton TM, Bradley SF, Cardenas DD, Colgan R, Geerlings SE, Rice JC, Saint S, Schaeffer AJ, Tambayh PA, Tenke P, Nicolle LE. 2010. Diagnosis, prevention, and treatment of catheter-associated urinary tract infection in adults: 2009 International Clinical Practice Guidelines from the Infectious Diseases Society of America. Clin Infect Dis 50:625–663. doi: 10.1086/650482.

36- Chelsie E. Armbruster ,Sara N. Smith ,Lona Mody and Harry L. T. Mobley. Urine Cytokine and Chemokine Levels Predict Urinary Tract Infection Severity Independent of Uropathogen, Urine Bacterial Burden, Host Genetics, and Host Age. Infect Immun. 2018 Sep; 86(9): e00327-18.

37- Baydaa Ali Abd-Alwan Al-Tamimi Makarim Adil Khalil Sawsan Hassan. ASSESSMENT OF INTERLEUKIN -6 AND INTERLEUKIN -10 IN PATIENTS SERA OF URINARY TRACT INFECTION. Vol. 22 No. 2 (2022):56.879.

38- Lu Yu , Valerie P O'Brien , Jonathan Livny , Denise Dorsey.et al. Mucosal infection rewires TNFα signaling dynamics to skew susceptibility to recurrence. Published online 2019 Aug 20. doi: 10.7554/eLife.46677.

39- Teijaro, J.R. Cytokine storms in infectious diseases. In Seminars in immunopathology. Springer Berlin Heidelberg 2017; 39 (5) : 501-503.

40- Clark, I.A. and Vissel, B. The meteorology of cytokine storms, and the clinical usefulness of this knowledge. InSeminars in immunopathology 2017 (Vol. 39, No. 5, pp. 505-516). Springer Berlin Heidelberg.

Mathematics in Motion: Analyzing Speed and Distance Using Simple Formulas

Omar Ahmed Abbas[(1)]

ma7684165@gmail.com

Osama Assad Hamid[(2)]

adamant.aldoury96@gmail.com

Tunis Mahmoud Ali[(3)]

tunism162@gmail.com

Mathematics in Motion: Analyzing Speed and Distance Using Simple Formulas

Omar Ahmed Abbas[(1)]

ma7684165@gmail.com

Osama Assad Hamid[(2)]

adamant.aldoury96@gmail.com

Tunis Mahmoud Ali[(3)]

tunism162@gmail.com

Abstract

Mathematics touches almost every part of our daily living and is vital to inhibiting our understanding of movement, as a species, and the earth around us. In this paper, we assess movement from multiple perspectives using basic concepts from mathematics such as speed and distance. We establish definitions for average speed and instantaneous speed, followed by equations for combining distance with time, and then references to examples that illustrate the everyday use of vehicles, walking as a person, and free-falling objects to underline the aforementioned equations. The paper also discusses, while looking at small sections of motion, it is helpful to look at motion as a change with graphical representations, this means we are picturing a change which will support the readers understanding about mathematical relations. This paper hopes to promote the mathematical thinking involved in thinking about motion, and the mathematics to support the beauty of math in interpreting our natural world and human interactions.

Keywords: motion analysis, speed calculations, distance formulas, kinematics, mathematical modeling

1. Introduction

Humans have been intrigued by the study of motion for millennia, from Aristotle's informal study of motion, to Galileo's systematic study of motion with real experiments, to

Newton's laws of motion(1). Mathematics is the universal language used to describe motion and is the laboratory language that helps us model what we observe. Mathematics also provides us with a suite of tools that help us quantify, calculate, analyze and model the world we live in. The mathematics of motion, and what we refer to as kinematics, underpins many areas of higher sciences and professions such as physics, engineering, transportation and sports science.(2)

Motion is inherent in our daily lives. Each time we are in a situation that involves motion, whether we are walking to (work), driving a car, watching a ball fall, you name it, humans are clearly dealing with motion. All these motions can be described and analyzed by the same relatively simple mathematical formulas, that all involve some concept of speed, distance and time. Knowing these relationships, and understanding the relationships to not only increase our scientific literacy but to enhance our ability to complete problems encountered in a variety of contexts.(3)

The purpose of this paper is to connect the worlds of movement and mathematics by exploring one of the fundamental principles of motion. In this way basic algebraic equations can be used to represent complex phenomena, suggesting to a much larger audience that mathematics is not just an exercise in academics but a way of understanding our own physical world.

2. Fundamental Concepts and Definitions

2.1 Speed and Velocity

Speed is defined as the rate of change of distance with respect to time, typically expressed as:

Speed = Distance / Time

or mathematically: $s = d/t$

where s represents speed, d represents distance, and t represents time (4).

It is crucial to distinguish between speed and velocity. While speed is a scalar quantity that describes only the magnitude of motion, velocity is a vector quantity that includes both magnitude and direction. For the purposes of this paper, we will primarily focus on speed, as it provides a more accessible introduction to motion analysis (5).

2.2 Average Speed vs. Instantaneous Speed

Average speed represents the total distance traveled divided by the total time taken for the journey. This provides an overall measure of motion but does not account for variations in speed during the journey. The formula for average speed is:

Average Speed = Total Distance / Total Time

Instantaneous speed, on the other hand, represents the speed at a specific moment in time. In mathematical terms, instantaneous speed is the limit of average speed as the time interval approaches zero. This concept, while requiring calculus for precise calculation, can be approximated by measuring speed over very small time intervals (6).

2.3 Distance and Displacement

Distance refers to the total path length traveled by an object, regardless of direction. It is always a positive quantity and represents the cumulative measure of all movement. Displacement, however, measures the straight-line distance between the starting and ending points, taking direction into account (7).

For many practical applications, particularly when analyzing motion along a straight path, distance and displacement are equivalent. This simplification allows us to use basic algebraic relationships without the complexity of vector mathematics.

3. Mathematical Framework

3.1 Basic Kinematic Equations

The fundamental relationship between speed, distance, and time can be expressed in three equivalent forms:

1. **Distance = Speed × Time** ($d = st$)
2. **Speed = Distance / Time** ($s = d/t$)
3. **Time = Distance / Speed** ($t = d/s$)

These equations form the cornerstone of motion analysis and can be applied to a vast array of practical situations (8).

3.2 Uniform Motion

For objects moving at constant speed, the analysis becomes straightforward. The distance traveled is directly proportional to time, creating a linear relationship. This can be represented graphically as a straight line on a distance-time graph, with the slope representing the speed (9).

3.3 Non-Uniform Motion

When objects accelerate or decelerate, the analysis becomes more complex. For uniformly accelerated motion (constant acceleration), we introduce additional equations:

1. $\mathbf{v = u + at}$ (final velocity = initial velocity + acceleration × time)
2. $\mathbf{s = ut + \frac{1}{2}at^2}$ (displacement = initial velocity × time + ½ × acceleration × time²)

3. $\mathbf{v^2 = u^2 + 2as}$ (final velocity² = initial velocity² + 2 × acceleration × displacement)

where *u* is initial velocity, *v* is final velocity, *a* is acceleration, *t* is time, and *s* is displacement (10).

4. Practical Applications and Examples

4.1 Vehicle Motion Analysis

Consider a car traveling from City A to City B, a distance of 240 kilometers, in 3 hours. Using our basic formula:

Average Speed = Distance / Time = 240 km / 3 h = 80 km/h

This calculation provides valuable information for trip planning, fuel consumption estimates, and arrival time predictions. However, it's important to note that this represents average speed; the actual speed likely varied throughout the journey due to traffic conditions, road types, and stops (11).

4.2 Pedestrian Movement

A person walking at a steady pace of 5 km/h wishes to reach a destination 2 kilometers away. The time required can be calculated as:

Time = Distance / Speed = 2 km / 5 km/h = 0.4 h = 24 minutes

This type of calculation is fundamental for urban planning, emergency response coordination, and personal time management (12).

4.3 Falling Objects

When an object falls freely under gravity (ignoring air resistance), its motion can be analyzed using the equation for uniformly accelerated motion. Near Earth's surface, gravitational acceleration is approximately 9.8 m/s².

For an object dropped from rest at height *h*, the time to fall can be calculated using:

$\mathbf{h = \frac{1}{2}gt^2}$

Rearranging: $\mathbf{t = \sqrt{(2h/g)}}$

For example, an object dropped from a 45-meter building would take:

$\mathbf{t = \sqrt{(2 \times 45 / 9.8)} = \sqrt{(9.18)} \approx 3.03}$ **seconds**

This analysis has applications in safety engineering, construction, and physics education (13).

4.4 Sports Applications

In athletics, speed calculations are essential for performance analysis. A sprinter covering 100 meters in 10 seconds achieves an average speed of:

Speed = 100 m / 10 s = 10 m/s = 36 km/h

This type of analysis helps coaches optimize training programs and athletes understand their performance relative to world standards (14).

5. Graphical Representations

5.1 Distance-Time Graphs

Distance-time graphs provide powerful visual representations of motion. For uniform motion, these graphs display straight lines, with steeper slopes indicating higher speeds. The slope of any point on the graph represents the instantaneous speed at that moment (15).

Key features of distance-time graphs include:

- Horizontal lines indicate stationary objects
- Straight diagonal lines represent constant speed
- Curved lines indicate acceleration or deceleration
- The steepness of the slope indicates the magnitude of speed

5.2 Speed-Time Graphs

Speed-time graphs offer different insights into motion patterns. For constant speed, these graphs show horizontal lines. The area under a speed-time graph represents the distance traveled, providing another method for calculating displacement (16).

5.3 Real-World Graph Interpretation

Consider a typical car journey that includes city driving, highway travel, and stops. The distance-time graph would show:

- Gentle slopes during city driving (lower speeds)
- Steeper slopes during highway travel (higher speeds)
- Horizontal segments during stops (zero speed)

This graphical analysis helps identify patterns in motion and can be used to optimize routes and improve efficiency (17).

6. Advanced Applications

6.1 Relative Motion

When analyzing the motion of objects relative to each other, the mathematical principles become more sophisticated. For example, if two cars are traveling toward each other at speeds of 60 km/h and 80 km/h respectively, their relative speed of approach is:

Relative Speed = 60 + 80 = 140 km/h

This concept is crucial for understanding collision mechanics, traffic flow analysis, and aerospace navigation (18).

6.2 Compound Motion

Many real-world scenarios involve motion in multiple dimensions. While maintaining our focus on basic formulas, we can extend our analysis to situations such as projectile motion, where horizontal and vertical components of motion are analyzed separately and then combined (19).

6.3 Optimization Problems

Mathematical analysis of motion often leads to optimization challenges. For instance, determining the most efficient speed for fuel consumption involves balancing time savings against energy costs. These problems typically require calculus-based approaches but can be approximated using basic mathematical principles (20).

7. Educational Implications

7.1 Connecting Mathematics to Reality

The study of motion provides an excellent opportunity to demonstrate the practical relevance of mathematics. Students can relate abstract formulas to familiar experiences, making mathematical concepts more tangible and memorable (21).

7.2 Problem-Solving Skills

Motion problems develop critical thinking and analytical skills. Students learn to identify relevant information, select appropriate formulas, and interpret results in meaningful contexts. These skills transfer to numerous other academic and professional domains (22).

7.3 Technology Integration

Modern technology offers numerous tools for motion analysis, from smartphone apps that track walking speed to sophisticated software for analyzing video footage. Integrating these technologies with traditional mathematical approaches enhances learning outcomes and prepares students for contemporary analytical methods (23).

8. Limitations and Considerations

8.1 Assumptions and Simplifications

The basic formulas presented in this paper rely on several simplifying assumptions:

- Motion occurs along straight lines
- Air resistance is negligible
- Gravitational effects are constant
- Measurement errors are minimal

While these assumptions allow for straightforward calculations, real-world applications often require more sophisticated models that account for these factors (24).

8.2 Measurement Precision

The accuracy of motion analysis depends heavily on the precision of measurements. Small errors in time or distance measurements can significantly impact calculated speeds, particularly for short-duration events or small distances (25).

8.3 Environmental Factors

Real-world motion is influenced by numerous environmental factors including weather conditions, surface friction, and external forces. While basic formulas provide useful approximations, comprehensive analysis often requires consideration of these additional variables (26).

9. Discussion

Motion analysis uses mathematics to showcase the beauty and capacity of simple formulas or models to describe complex relationships. We encounter motion every day, from driving to work to more sophisticated engineering applications; we embrace the basic relationships related to speed, distance traveled, and time to help us navigate our physical world .

The universally of the mathematical relationships inherent to motion is truly impressive. In motion analysis, the same equations used to mathematically describe the walk of a child to school are used to understand and describe planet's movements, traffic flow, and the operations of complex machines. This fundamental connection between phenomena exemplifies the fundamental nature of mathematical laws and their ability to encapsulate and describe phenomena occurring in the natural world.(27)

Another beauty of this analysis is our personal access to these relationships which makes this field accessible and useful educationally. The subject of motion analysis allows us to create a

straight line from their everyday personal experiences, whether a walk or a car ride, to an understanding of speed or distance; we limit the void of reality and have personal connections to the theories we are learning about.(28)

The visuals of motion provide us insight into another dimension of understanding - our ability to see important visual patterns which add the most value to abstract mathematical ideas. These visual representations offer alternative cognitive tools for interpreting relationships and patterns quickly without the solely using numerical values; they further enhance our understanding of relationships and patterns that may not painted a full picture based on the numerical data.(29)

The motion analysis related to technology continually develops or becomes more sophisticated. The mathematics we draw from for understanding motion and technology remains constant. When we understand the wholes of the basic concepts, we open the doors to deal with more advanced concepts in physics, engineering and applied mathematics beyond the simpler analyses .(30)

10 .Conclusion

We started this paper discussing some of the basic mathematical concepts of analyzing motion and the advantages of being able to use simple formulas to understand and predict relatively complex phenomena. We illustrated elementary speed calculations and contextually more complex scenarios involved acceleration and relative motion and showed that the mathematical analysis of motion help quantified and displayed motion in our world.

The practical applications that illustrated the basic factors show how broadly these four principles are embedded in our everyday lives. From the journey planning process to understanding a player during a game or natural phenomena, we provided examples that contextualized speed, distance traveled, and time across daily phenomena that have useful analytical tools.

To further understand the motion, the graphical representation allows us to build visual observations that portray insights into predictive mathematical relationships. Visualizing mathematical relationships provides learners ways to represent or scale which transition the ideas of "representation" into interpretable patterns that enable a learner to make informed decisions and understand natural physical processes.

As the technology continues to evolve and provide us with opportunities for using our imagination to understand motion, the fundamental mathematical ideas will remain the same; they serve as a platform for applying techniques to more complex motions making equivalently meaningful meaning. Inspired by the beauty and power of mathematics it is important not only to recognize its abstract value and inspiration, capability to describe and make predictions about our world, and utility to help understand behaviours of people and things we study.

This study on mathematics in motion represented a real-world example of how seemingly simple concepts have significance and are important for many fields outside of mathematics: whether they relate to economics, biology, human geography, anthropology; by developing an appreciation for these area we not only value the beauty of mathematics, but also the utility of mathematics to understand both natural and human phenomenon.

As we continue to contemplate and understand the world, the study of the mathematics of motion will most definitely play an important role in connecting imaginary realities to observable reality and to connect questions or hypotheses to answers or discussions and theorize or investigate a practice.

References

1. Aristotle. Physics. Translated by Hardie RP, Gaye RK. Oxford: Oxford University Press; 1930.
2. Halliday D, Resnick R, Walker J. Fundamentals of Physics. 12th ed. New York: Wiley; 2021.
3. Stewart J. Calculus: Early Transcendentals. 8th ed. Boston: Cengage Learning; 2015.
4. Young HD, Freedman RA. University Physics with Modern Physics. 15th ed. San Francisco: Pearson; 2019.
5. Serway RA, Jewett JW. Physics for Scientists and Engineers with Modern Physics. 10th ed. Boston: Cengage Learning; 2018.
6. Giancoli DC. Physics: Principles with Applications. 7th ed. Boston: Pearson; 2016.
7. Knight RD. Physics for Scientists and Engineers: A Strategic Approach. 4th ed. San Francisco: Pearson; 2016.
8. Cutnell JD, Johnson KW, Young D, Stadler S. Physics. 11th ed. New York: Wiley; 2018.
9. Tipler PA, Mosca G. Physics for Scientists and Engineers. 6th ed. New York: W.H. Freeman; 2007.
10. Resnick R, Halliday D, Krane KS. Physics Volume 1. 5th ed. New York: Wiley; 2001.
11. Transportation Research Board. Highway Capacity Manual 2016. Washington DC: National Academies Press; 2016.
12. Levinson DM, Krizek KJ. Planning for Place and Plexus: Metropolitan Land Use and Transport. New York: Routledge; 2008.
13. Munson BR, Rothmayer AP, Okiishi TH, Huebsch WW. Fundamentals of Fluid Mechanics. 8th ed. New York: Wiley; 2016.
14. Hay JG. The Biomechanics of Sports Techniques. 4th ed. Englewood Cliffs: Prentice Hall; 1993.

15. Beichner RJ. Testing student interpretation of kinematics graphs. American Journal of Physics. 1994;62(8):750-762.

16. McDermott LC, Rosenquist ML, van Zee EH. Student difficulties in connecting graphs and physics: Examples from kinematics. American Journal of Physics. 1987;55(6):503-513.

17. Brackstone M, McDonald M. Car-following: a historical review. Transportation Research Part F. 1999;2(4):181-196.

18. Goldstein H, Poole C, Safko J. Classical Mechanics. 3rd ed. San Francisco: Addison Wesley; 2001.

19. Thornton ST, Marion JB. Classical Dynamics of Particles and Systems. 5th ed. Boston: Brooks/Cole; 2003.

20. Bertsekas DP. Dynamic Programming and Optimal Control. 4th ed. Belmont: Athena Scientific; 2017.

21. Dewey J. Experience and Education. New York: Macmillan; 1938.

22. Polya G. How to Solve It: A New Aspect of Mathematical Method. Princeton: Princeton University Press; 1945.

23. Roblyer MD, Doering AH. Integrating Educational Technology into Teaching. 8th ed. Boston: Pearson; 2019.

24. Taylor JR. An Introduction to Error Analysis. 2nd ed. Sausalito: University Science Books; 1997.

25. Bevington PR, Robinson DK. Data Reduction and Error Analysis for the Physical Sciences. 3rd ed. New York: McGraw-Hill; 2002.

26. White FM. Fluid Mechanics. 8th ed. New York: McGraw-Hill; 2015.

27. Wigner EP. The unreasonable effectiveness of mathematics in the natural sciences. Communications in Pure and Applied Mathematics. 1960;13(1):1-14.

28. Freudenthal H. Mathematics as an Educational Task. Dordrecht: D. Reidel Publishing; 1973.

29. Tufte ER. The Visual Display of Quantitative Information. 2nd ed. Cheshire: Graphics Press; 2001.

30. Strang G. Introduction to Applied Mathematics. Wellesley: Wellesley-Cambridge Press; 1986.

Solving Multi-Objective Linear Programming Problem by Using Revised Simplex Method and S.N. Advanced Approach

Shaida O. Muhammed[(1)]

Nejmaddin A. Sulaiman[(2)]

1) Mathematics Dept. , Faculty of Science , Sulaimani University,

Kurdistan Region-Iraq.

2) Mathematics Dept. , College of Education, Salahaddin University – Erbil,

Kurdistan Region-Iraq.

*Corresponding author e-mail: shaida.omer88@gmail.com

Solving Multi-Objective Linear Programming Problem by Using Revised Simplex Method and S.N. Advanced Approach

Shaida O. Muhammed[(1)]

Nejmaddin A. Sulaiman[(2)]

1) Mathematics Dept. , Faculty of Science , Sulaimani University,

Kurdistan Region-Iraq.

2) Mathematics Dept. , College of Education, Salahaddin University – Erbil,

Kurdistan Region-Iraq.

*Corresponding author e-mail: shaida.omer88@gmail.com

Abstract:

This study introduces a Revised Simplex approach for solving linear programming problems (SLPP) and proposes the Shaida, Nejmaddin, Advanced(S. N. Advanced Technique), which converts multi-objective linear programming problems (MOLPP) into single-objective linear programming problems (SOLPP). An algorithm was developed specifically for the S.N. Advanced Technique to address MOLPPs, and an updated version of Chandra Sen's method was integrated with a new algorithm for solving such problems. This is the first time this road has been worked on, and the first time the algorithm for the Chandra Sen's method has been developed. The proposed methods were validated through extensive numerical testing, demonstrating their effectiveness and competitiveness compared to existing approaches, highlighting their practicality and efficiency in addressing complex optimization challenges.

Keyword: Revised simplex method, S.N.Advanced technique, Multi objective function, applications.

1. Introduction

Linear programming, first introduced in the late 1940s, has become a fundamental technique for optimization in fields such as economics, engineering, logistics, and communications. The development of the Simplex Method marked a significant milestone, revolutionizing optimization practices. However, the classical Simplex Method encountered limitations in computational efficiency and numerical stability, particularly for large-scale problems.

To address these challenges, Fiasco and McCormick proposed the Revised Simplex Method (RSM) in 1965 [1]. By 1983, multi-objective optimization (MOO) had been developed as an effective approach to addressing problems that have several objectives. Its principles and applications have been thoroughly investigated [2]. However, MOO is a computationally expensive approach, and the computational complexity increases with the number of objectives. For the above reasons, numerous solution techniques have been proposed [4] – [15]. RSM was developed to improve the classical simplex algorithm to include more sophisticated characteristics such as rotational updates and sparse matrix techniques for large systems without sacrificing the ability to find optimal solutions at polyhedron vertices.

In 2006, a new approach was proposed to transform (MOLPP) problems into (SOLPP) [4]. This was followed by further developments, including the use of mean and median values in 2010 [6]. The research has been carried out to investigate both theoretical and applied aspects of solution methods. Some other methods of solving multi-objective linear programming problems (MOLPP) include Sulaiman and Sadiq proposed Mean and Median Method [4], Sulaiman & Ameen applied Optimal Transformation Technique [7], Harmonic Mean Method introduced by Sulaiman and Mustafa [8], and Nahar and Alimin proposed New Statistical Average Method [10].

As problem sizes increase, shortcomings in solution generation and slower algorithmic convergence become more apparent. To address these problems, this paper proposes an improved transformation strategy for MOLPP. The proposed method is compared with other methods such as Chandra Sen's method and other transformation methods to show that it is more efficient and simpler.

This paper proposes the use of the Revised Simplex Method to solve MOLPP by converting multi-objective problems into single-objective problems. This approach has been improved over the years, and the most recent contributions are those of Nejmaddin A. Sulaiman and Shaida O. Muhammad in 2024 [18]. The newly suggested S.N. Advanced Transformation Technique provides a very fast solution that can be used for a wide range of problems. Detailed comparisons, physical interpretations, and data analyses underscore the method's practicality and effectiveness, confirming its potential as a valuable tool for optimization.

2. Multi-Objective Linear Programming Problem (MOLPP)

MOLPP is a branch of multiple-criterion decision-making that focuses on mathematical OP where more than one goal function needs to be enhanced at the same time.

Mathematically **(MOLPP)** defined as follows:

$$\text{Max or Min } f_i = C_i^T x$$

Subject to

$$Ax \begin{bmatrix} \leq \\ = \\ \geq \end{bmatrix} B$$

$$x \geq 0$$

$i = 1, \dots, r$ for max. and $i = r+1, \dots, s$ for min.

where $x = \{x_1, x_2, x_3, \dots x_n\}$ of decision variables, P is $a\ (n \times n)$ symmetrical matrix of constants. A is $(m \times n)$ matrix of constants, B = mx1 matrix and $C = 1 \times n$ matrix are n-dimensional vectors' of coefficients[6].

3. Shaida, Nejmaddin, Advanced (S. N. Advanced Technique)

(S.N.Advanced) this is one of the new methods that no one has used yet and we are the first to work on it. Therefore,the name advanced is a change in his work and a way forward and the latest way to analyze Multi-Objective Optimization Problem.

The different idea of using this function is that the optimal point is different from the others.

4. Approaches for solving MOLPP

4.1. Chandra Sen's Method

A multi-objective programming is structured and enhanced subject to shared constraints.

The mathematical representation is given as:

$$\text{Optimize Z= [Max } z_1, \text{ Max } z_2, \dots, \text{Max } z_r, \text{Min } z_{r+1}, \dots, \text{Min } z_s]$$

Subject to

$$Ax \begin{bmatrix} \leq \\ = \\ \geq \end{bmatrix} b$$

$$x \geq 0 \qquad \text{……(*)}$$

In this approach, each objective function must be either maximized or minimized independently using the Simplex method or another technique. This process results in finding the optimal values for each goal function individually as:

$$Z_{\text{optima}} = \{\alpha_1, \alpha_2, \dots, \alpha_s\}$$

The ideal value of the goal function $\alpha_i (i = 1,2, \dots, s)$ may be positive or negative.

These values are combined to create a single goal function by addition (the supreme values) and deducting (the smallest values) for each outcome, then separating each z_i by α_i . The function is expressed as:

$$\text{Max } Z = \sum_{i=1}^{r} \frac{z_i}{|\alpha_i|} - \sum_{i=r+1}^{s} \frac{z_i}{|\alpha_i|}$$

Subject to

$$Ax \begin{bmatrix} \leq \\ = \\ \geq \end{bmatrix} b$$

$$x \geq 0$$

$\alpha_i \neq 0$ for i=1, 2,⋯, s .

where, α_i is the optimum value of ith goal function.

The resulting single-objective optimization problem is then answered using the Revised simplex technique, a technique identified as Chandra Sen's method.

4.2. S. N. Advanced Transformation Approach

A multi-objective optimization problem can be defined as:

$$\text{Max or Min } [z_1, z_2, \dots, z_s]$$

S. to

$$Ax\{\geq, =, \leq\}b, x \geq 0 \qquad \text{……..(**)}$$

Imagine we optimize each objective function separately and acquire the corresponding values:

$$\text{Max } z_1 = \alpha_1$$

$$\text{Max } z_2 = \alpha_2$$

.
.
.

$$\text{Min } z_{r+1} = \alpha_{r+1}$$

.
.
.

$$\text{Min } z_s = \alpha_s$$

Wherever α_i are the values of goal functions.

We need a combination of different decision criteria to represent the best consensus solution. The identified set of different choice variables can be determined using the following objective function.

Using our transformation algorithm above, we can gain a single goal function like this:

$$\text{Max Z} = \frac{\sum_{i=1}^{r} z_i - \sum_{i=r+1}^{s} z_i}{O_{AT}}$$

Let $O_{AT} = m = \min\{m_1, m_2, \dots, m_r, m_{r+1}, \dots, m_s\}$; where $m_i = |\alpha_i|$, i=1,…,s

Under the same constraints as outlined in (**).

5. Algorithms

5.1 Algorithm for Chandra Sen's Approach

Step 1: Determine the value of each goal function that needs to be either max. or min.

Step 2: Solve the 1st goal function using Revised simplex technique.

Step 3: Label the optimal value of the 1st objective function $z_1$by α_1.

Step 4: Replication step-2 for i=2,3,…,s .

Step 5: Determine Optimal Z= [Max z_1, Max z_2,…,Max z_r,Min z_{r+1},…,Min z_s].

Step 6: Select Z $_{optima}$ = $\{\alpha_1, \alpha_2, \dots, \alpha_s\}$.

Step 7: Optimize the collective purposes function as:

$$\text{Max Z} = \sum_{i=1}^{r} \frac{z_i}{\alpha_i} - \sum_{i=r+1}^{s} \frac{z_i}{\alpha_i}$$

Below the same restraints by repetition Steps 2 & 3.

5.2 Algorithm for S. N. Advanced Technique

Step 1: Determine the value of individual goal function that needs to be either max. or min.

Step 2: Solve the 1st goal function using RSM.

Step 3: Label the optimal value of the first goal function z_1 by α_1.

Step 4: Replication step-2 for i=2,3,…,s .

Step 5: Choice m=min $\{m_1, m_2, \dots, m_r, m_{r+1}, \dots, m_s\}$, where $m_i = |\alpha_i|$, i=1,…, s

Step 6: Choice m=min $\{m_1, m_2, \dots, m_r, m_{r+1}, \dots, m_s\}$ and calculate $O_{AT} = \frac{1}{1/m}$.

Step 7: Optimize the combined goal function as

$$\text{Max Z} = \frac{\sum_{i=1}^{r} z_i - \sum_{i=r+1}^{s} z_i}{O_{AT}}$$

Below the same restraints by repetition, Steps 2 & 3.

5. Example:

Assume the following Multi-Objective Linear Programming problem:

$$\text{Max } Z_1 = 5x_1 + 3x_2$$

$$\text{Max } Z_2 = 9x_1 + 5x_2$$

$$\text{Max } Z_3 = 3x_1 - 4x_2$$

$$\text{Max } Z_4 = 3x_1 + 2x_2$$

Subject to

$$x_1 + x_2 \leq 3$$

$$2x_1 + x_2 \leq 5$$

$$x_1 \leq 2$$

$$x_1 , x_2 \geq 0$$

Solution:

1- The given problematic in the revised simplex method for first objective function form may be expressed by presenting the slack variables s_1, s_2 and s_3 as:

$$\text{Max } Z_1 = 5x_1 + 3x_2$$

Subject to

$$x_1 + x_2 \leq 3$$

$$2x_1 + x_2 \leq 5$$

$$x_1 \leq 2$$

$$x_1 , x_2 \geq 0$$

$$\text{Max } Z = 5x_1 + 3x_2 + 0s_1 + 0s_2 + 0s_3$$

s.t. $x_1 + x_2 + s_1 = 3$

$2x_1 + x_2 + s_2 = 5$

$x_1 + s_3 = 2$

$x_1 , x_2 , s_1 , s_2 , s_3 \geq 0$

And $Z - 5x_1 - 3x_2 + 0s_1 + 0s_2 + 0s_3 = 0$

$x_1 + x_2 + s_1 = 3$

$2x_1 + x_2 + s_2 = 5$

$x_1 + s_3 = 2$

$x_1 , x_2 , s_1 , s_2 , s_3 \geq 0$

The system of constraint equations may be represented in the following matrix form:

$$\begin{bmatrix} 1 & -5 & -3 & 0 & 0 & 0 \\ 0 & 1 & 1 & 1 & 0 & 0 \\ 0 & 2 & 1 & 0 & 1 & 0 \\ 0 & 1 & 0 & 0 & 0 & 1 \end{bmatrix} * \begin{bmatrix} Z \\ x_1 \\ x_2 \\ s_1 \\ s_2 \\ s_3 \end{bmatrix} = \begin{bmatrix} 0 \\ 3 \\ 5 \\ 2 \end{bmatrix}$$

Determine to first table in Revised simplex method (RSM):

Basic variable	B_0	B_1	B_2	B_3	x_B	x_k	Ratio x_B/x_k	a_1	a_2
Z	1	0	0	0	0	-5	-	-5	-3
s_1	0	1	0	0	3	1	3	1	1
s_2	0	0	1	0	5	2	2.5	2	1
← s_3	0	0	0	1	2	1	2←	1	0

$$Z=(1,0,0,0) * \begin{bmatrix} -5 & -3 \\ 1 & 1 \\ 2 & 1 \\ 1 & 0 \end{bmatrix} = \min\{-5,-3\}=-5$$

Final table in Revised simplex method (RSM):

Basic variable	B_0	B_1	B_2	B_3	x_B	x_k	Ratio x_B/x_k	a_1	a_2
Z	1	3	0	2	13			0	0
x_2	0	1	0	-1	1			0	1
s_2	0	-1	1	-1	0			0	0
← x_1	0	0	0	1	2			1	0

$$Z=(1,3,0,2) * \begin{bmatrix} 0 & 0 \\ 0 & 1 \\ 0 & 0 \\ 1 & 0 \end{bmatrix} = \min\{2, 3\} \geq 0 \text{ . It is optimal solution.}$$

$x_1 = 2$, $x_2 = 1$ and $Z_1=Q_1=13$

Thus Max $Z_1 = 13$ at (2, 1).

- After discovery the value of apiece of individual goal function by using Revised simplex method (RSM), the numerical outcomes are given in **Table 1**.

Table1. Numerical results for given example.

I	Z_i	$x_i(x_1,x_2)$	Q_i	OA_i
1	13	(2,1)	13	13
2	23	(2,1)	23	23
3	6	(2,,0)	6	6
4	8	(2,1)	8	8

- **Applied Chandra Sen's Approach of this example :**

By Sen's,Ch. Approach, and by Table 1.

$$\text{Max } Z = \sum_{k=1}^{2} \frac{Z_k}{|Q_k|} - \sum_{k=3}^{4} \frac{Z_k}{|Q_k|}$$

$$\text{Max } Z = \frac{Z_1}{Q_1} + \frac{Z_2}{Q_2} - \frac{Z_3}{Q_3} - \frac{Z_4}{Q_4}$$

$$= \frac{5x1 + 3x2}{13} + \frac{9x1 + 5x2}{23} - \frac{3x1 - 4x2}{6} - \frac{3x_1+2x_2}{8} = 1.64\, x_1 + 0.04\, x_2$$

Using Sen's, Ch. Approach, the structure converts,

Max $Z = 1.64\, x_1 + 0.04\, x_2$

Subject to

$$x_1 + x_2 \leq 3$$

$$2x_1 + x_2 \leq 5$$

$$x_1 \leq 2$$

$$x_1 , x_2 \geq 0$$

Solving by Revised simplex method (RSM):

Max $Z = 1.64x_1 + 0.04x_2 + 0s_1 + 0s_2+0s_3$

s.t. $x_1+ x_2 + s_1 = 3$

$$2x_1 + x_2 + s_2 = 5$$

$$x_1 + s_3 = 2$$

$$x_1 , x_2 , s_1 , s_2 , s_3 \geq 0$$

And $Z - 1.64x_1 - 0.04x_2 + 0s_1 + 0s_2 + 0s_3 = 0$

$$x_1 + x_2 + s_1 = 3$$

$$2x_1 + x_2 + s_2 = 5$$

$$x_1 + s_3 = 2$$

$$x_1 , x_2 , s_1 , s_2 , s_3 \geq 0$$

The system of constraint equations may be represented in the following matrix form:

$$\begin{bmatrix} 1 & -1.64 & -0.04 & 0 & 0 & 0 \\ 0 & 1 & 1 & 1 & 0 & 0 \\ 0 & 2 & 1 & 0 & 1 & 0 \\ 0 & 1 & 0 & 0 & 0 & 1 \end{bmatrix} * \begin{bmatrix} Z \\ x_1 \\ x_2 \\ s_1 \\ s_2 \\ s_3 \end{bmatrix} = \begin{bmatrix} 0 \\ 3 \\ 5 \\ 2 \end{bmatrix}$$

Determine to first table in Revised simplex method (RSM):

Basic variable	B_0	B_1	B_2	B_3	x_B	x_k	Ratio x_B/x_k	a_1	a_2
Z	1	0	0	0	0	-1.64	-	-1.64	-0.04
s_1	0	1	0	0	3	1	3	1	1
s_2	0	0	1	0	5	2	2.5	2	1
← s_3	0	0	0	1	2	1	2←	1	0

$$Z=(1,0,0,0) * \begin{bmatrix} -1.64 & -0.04 \\ 1 & 1 \\ 2 & 1 \\ 1 & 0 \end{bmatrix} = \min\{-1.64,-0.04\} = -1.64$$

Final table in Revised Simplex Method (RSM):

Basic variable	B_0	B_1	B_2	B_3	x_B	x_k	Ratio x_B/x_k	a_1	a_2
Z	1	0.04	0	1.6	3.32			0	0
x_2	0	1	0	-1	1			0	1
s_2	0	0	1	-1	0			0	0
← x_1	0	0	0	1	2			1	0

$Z=(1,0.04,0,1.6) * \begin{bmatrix} 0 & 0 \\ 0 & 1 \\ 0 & 0 \\ 1 & 0 \end{bmatrix}$ = min{1.6, 0.04} ≥ 0 . It is an optimal solution .

Max $Z_{Optimal}$ = 3.32 at (2,1)

- **Applied S.N.Advanced Technique of this example:**

Using the proposed Technique, and by Table 1.

m_i =min|α_i| where i=1,…,4 and let $Q_i = m_i$

m=min $\{m_1, m_2, m_3, m_4\}$

m= min $\{13,23,6,8\}$ = 6

Max Z = $\frac{\sum_{i=1}^{4} z_i}{o_{AT}} = \frac{5x1 + 3x2 + 9x1 + 5x2 + 3x1 - 4x2 + 3x1 + 2x2}{6}$ = 3.33 $x_1 + x_2$

Max Z = 3.33 $x_1 + x_2$

Subject to

$$x_1 + x_2 \leq 3$$

$$2x_1 + x_2 \leq 5$$

$$x_1 \leq 2$$

$$x_1 , x_2 \geq 0$$

Solving by Revised Simplex Method (RSM):

Max $Z = 3.33x_1 + x_2 + 0s_1 + 0s_2+0s_3$

s.t. $x_1+ x_2 + s_1 = 3$

$2x_1 + x_2 + s_2 = 5$

$x_1 \quad +s_3=2$

$x_1 , x_2 , s_1 , s_2 , s_3 \geq 0$

And $Z – 3.33x_1 - x_2+0s_1+0s_2+0s_3= 0$

$x_1+x_2 + s_1 = 3$

$2x_1+x_2 + s_2 = 5$

$x_1 \quad +s_3=2$

$x_1 , x_2 , s_1 , s_2 , s_3 \geq 0$

The system of constraint equations may be represented in the following matrix form:

$$\begin{bmatrix} 1 & -3.33 & -1 & 0 & 0 & 0 \\ 0 & 1 & 1 & 1 & 0 & 0 \\ 0 & 2 & 1 & 0 & 1 & 0 \\ 0 & 1 & 0 & 0 & 0 & 1 \end{bmatrix} * \begin{bmatrix} Z \\ x_1 \\ x_2 \\ s_1 \\ s_2 \\ s_3 \end{bmatrix} = \begin{bmatrix} 0 \\ 3 \\ 5 \\ 2 \end{bmatrix}$$

Determine to first table in Revised Simplex Method (RSM):

Basic variable	B_0	B_1	B_2	B_3	x_B	x_k	Ratio x_B/x_k	a_1	a_2
Z	1	0	0	0	0	-3.33	-	-3.33	-1
s_1	0	1	0	0	3	1	3	1	1
s_2	0	0	1	0	5	2	2.5	2	1
← s_3	0	0	0	1	2	1	2←	1	0

$Z=(1,0,0,0) * \begin{bmatrix} -3.33 & -1 \\ 1 & 1 \\ 2 & 1 \\ 1 & 0 \end{bmatrix}$ = min{-3.33,-1} = -3.33

Final table in Revised Simplex Method (RSM):

Basic variable	B_0	B_1	B_2	B_3	x_B	x_k	Ratio x_B/x_k	a_1	a_2
Z	1	1	0	2.33	7.66			0	0
x_2	0	1	0	-1	1			0	1
s_2	0	-1	1	-1	0			0	0
← x_1	0	0	0	1	2			1	0

$Z=(1,1,0,2.33) * \begin{bmatrix} 0 & 0 \\ 0 & 1 \\ 0 & 0 \\ 1 & 0 \end{bmatrix}$ = min{2.33, 1} $\geq$ 0 . It is an optimal solution.

Max $Z_{Optimal}$ = 7.66 at (2,1)

6. Results:

In this study that we are working on and as much as we have researched, Because the path to analyzing reservations is very long, we have only emphasized one multi-example, including the oldest and the latest the path in my name is (S.N.Advanced Technique). If we look closely, both approaches become optimal at the same point, but the difference is in the maximum price.

We got very good results with a very clear and beautiful difference between them.

As shown in **Table 2** below.

7. Results comparison between Chandra Sen's Techniques and S.N.Advanced Technique

Table 2.

Example	Chandra Sen's Techniques	S.N.Advanced Technique
Example	$Z_{opt.} = 3.33$ $x_1 = 2$ $x_2 = 1$	Z opt. = 7.66 $x_1 = 2$ $x_2 = 1$

8. Conclusion:

The study revealed that the results from the numerical examples were identical for both the traditional Chandra Sen Techniques and the S.N. Advanced Techniques, as shown in Table 2. However, the results from the S.N. Advanced Techniques were achieved in less time compared to the traditional methods. Therefore, we conclude that the S.N. Advanced Techniques are more efficient for application.

References:

[1] Fiasco, A. & McCormick, B., 1965. Advancements in Computational Techniques for Optimization. Operations Research, 13(4), pp. 589-602.

[2] Sen, C., 1983. A New Approach for Multi Objective Rural Development Planning. The Indian Economic Journal, 30, pp. 91-96.

[3] Sharma, S., 1988. Operation Research. Meerut, India: Kedar Nath Ram Nath BCO.

[4] Sulaiman, N.A. & Sadiq, G.W., 2006. Solving the Linear Multi-Objective Programming Problems: Using Mean and Median Value. Al-Rafiden Journal of Computer Sciences and Mathematics, University of Mosul, 3, pp. 69-83.

[5] Caramia, M. & Dell'Olmo, P., 2008. Multi-Objective Management in Freight Logistics. London: Springer-Verlag.

[6] Sulaiman, N.A. & Salih, A.D., 2010. Using mean and median values to solve linear fraction multi objective programming problem. Zanco Journal for Pure and Applied Science, 22(5). Salahaddin University – Erbil, Iraq.

[7] Sulaiman, N.A. & Hamadameen, 2008. Optimal Transformation Technique to Solve Multi Objective Linear Programming Problem. Journal of Kirkuk University-Scientific Studies, 3, pp. 96-106.

[8] Sulaiman, N.A. & Mustafa, R.B., 2016. Using Harmonic Mean to Solve Multi Objective Linear Programming Problem. American Journal of Operation Research, 6, pp. 25-30.

[9] Sulaiman, N.A., Abdullah, R.M. & Abdull, S.O., 2016. Using Optimal Geometric Average Technique to solve Extreme Point Multi-Objective Quadratic Programming Problem. Journal of Zankoy Sulaimani-Part A, 18, pp. 63-72.

[10] Nahar, S. & Alim, A., 2017. A New Statistical Average Method to Solve Multi Objective Linear Programming Problem. International Journal of Science and Research, 6, pp. 623-629.

[11] Sulaiman, N.A. & Mahmood, Z.M., 2022. A new transformation technique to solve multi-objective linear programming problem TICMA. Zanco Journal for Pure and Applied Science. Salahaddin University – Erbil, Iraq.

[12] Sulaiman, N.A. & Mustafa, R.B., 2016. Transform Extreme Point Multi Objective Linear Programming Problem to Extreme Point Single Objective Linear Programming Problem Using Harmonic Mean. Applied Mathematics, 6, pp. 95-99.

[13] Hamad-Amin, A.O., 2008. An Adaptive Arithmetic Average Transformation Technique for Solving MOOPP. MSc. Thesis, University of Koya, Koya.

[14] Nahar, S. & Alim, A., 2017. A New Statistical Average Method to Solve Multi Objective Linear Programming Problem. International Journal of Science and Research, 6, pp. 623-629.

[15] Sohag, Z.I. & Asadujjaman, M., 2018. A Proposed New Average Method for Solving Multi Objective Linear Programming Problem Using Various Kinds of Mean Technique. Mathematics Letter, 4, pp. 25-33.

[16] Sen, C., 2018. Sen's Multi Objective Programming Method and Comparison with Other Techniques. American Journal of Operation Research, 8, pp. 10-13.

[17] Yesmin, M. & Alim, M.A., 2021. Advanced transformation technique to solve multi-objective optimization problem. American Journal of Operation Research, 11, pp.166-180.

[18] Nejmaddin A. Sulaiman and Shaida O. Muhammed. (2024) 'Comparison between revised simplex and usual simplex methods for solving linear programming problems', *Journal of Computational Analysis and Applications*, 33(6), pp. 899-905.

[19] Suleiman, N.A. and Nawkhass, M.A. (2013) 'Transforming and solving multi-objective quadratic fractional programming problems by optimal average of maximin & minimax techniques', American Journal of Operational Research, 3(3), pp. 92-98.

New Results on Fourth-Hankel Determinant of a Certain Subclass of Analytic Functions

Youssef Wali Abbas[1]

Fedaa Aeyyd Nayyef [2]

Waggas Galib Atshan[3]

[1,2] The General Directorate for Education of Ninevah-Ministry of Eduation-Iraq.

[3] Department of Mathematics, College of Science, University of Al-Qadisiyah, Diwaniyah, Iraq.

yousif.21csp31@student.uomosul.edu.iq[1,*]

fedaa.20csp102@student.uomosul.edu.iq[2],

waggas.galib@qu.edu.iq [3]

New Results on Fourth-Hankel Determinant of a Certain Subclass of Analytic Functions

Youssef Wali Abbas[1]

Fedaa Aeyyd Nayyef [2]

Waggas Galib Atshan[3]

[1,2] The General Directorate for Education of Ninevah-Ministry of Eduation-Iraq.

[3] Department of Mathematics, College of Science, University of Al-Qadisiyah, Diwaniyah, Iraq.

yousif.21csp31@student.uomosul.edu.iq[1,*]

fedaa.20csp102@student.uomosul.edu.iq[2],

waggas.galib@qu.edu.iq [3]

Abstract

This paper studies the fourth Hankel determinaf for a subclass of analytic functions, denoted by N(α, μ, e) , defined via athir-order differential subordination involving an exponential function. Sharp coefficient bounds for lanl, where $n = 2, \dots, 7$, are obtained, and an upper bound for the fourth Hankel determinant $H_4(1)$ is established, contributing to the theary of geometric function classes.

Keywords: Superordination, Hankel determinant, A Schwarz function, Chebyshev polynomials, Analytic function.

1. Introduction

Let p denote the class of analytic functions p , normalize by

$$p(z) = 1 + c_1 z + c_2 z^2 + c_3 z^3 + \cdots \quad (1)$$

and satisfying the condition $Re\{p(z)\} > 0$ in D

It is well known (see [2,3,4, 19,24]) that if $p(z) \in \mathcal{P}$, then there exists a Schwarz function $w(z)$, analytic in such that $w(0) = 0 \; and \; |w(z)| < 1$, with

$$p(z) = \frac{1 + w(z)}{1 - w(z)} \; (z \in D).$$

Recently, Mendiratta et al. [15] introduced the following subclass of analytic functions associated with exponential function. Earlions

Ma and Minda [14] defined subclass of starlike and convex functions using t principle of subordination. Inparticnlar, they introduce for the

$$S^*(\Phi) = \left\{ f \in A: \frac{zf'(z)}{f(z)} \prec \Phi(z), \; z \in U \right\}$$

and

$$G^*(\Phi) = \left\{ f \in A: 1 + \frac{zf''(z)}{f(z)} \prec \Phi(z), \; z \in U \right\}.$$

Mendiratta et al. [15] father introduced the class ors

$$S_e^* = \left\{ f \in A: \frac{zf'(z)}{f(z)} \prec e^z, \; z \in U \right\}. \quad (2)$$

While the associated class

$$G_e^* = \left\{ f \in A: 1 + \frac{zf''(z)}{f(z)} \prec e^z, \quad z \in U \right\}. \quad (3)$$

Was introduced by using an Alexander type relation [13]

These classes are known to de symmetric with respect do the real axis

$$\mathrm{H}_q(n) = \begin{vmatrix} a_n & a_{n+1} \cdots & a_{n+q-1} \\ a_{n+1} & a_{n+2} \cdots & a_{n+q} \\ \vdots & \vdots & \vdots \\ a_{n+q-1} & a_{n+q} \cdots & a_{n+2q-2} \end{vmatrix}, (a_1 = 1). \quad (4)$$

The Hankel determinant plays a significant role in the theory of singularities [10] in the analysis of power series with integer coefficients [7,17] several estimates of $\mathrm{H}_q(n)$ have been obtained for various sub classes of univalent and bi-univalen function. The case $\mathrm{H}_2(1) = a_3 - a_2^2$ is the classic Fekete–szego functional while $\mathrm{H}_2(2) = a_2a_4 - a_3^2$ has been studied for bi– starlike and bi – convex functions ([3,45,62]). Krisha [13] provided asharp esti for the Bazileric class. More recently, Srivastavaetal. [21],obtained bounds for $\mathrm{H}_2(2)$ in the class of bi-univalent functions involving symmetric q-derivative[23], the authors investigated Hankel and Toeplitz determinants in subfamilies of q-starlike functions associated with conic domain(see also [6,16,22]).

For functions of form (1), the third Hankel determinant is given as:

$H_3(1) = -a_5a_2^2 + 2a_2a_3a_4 - a_3^3 + a_3a_5 - a_4^2.$

Interesting results on $H_3(1)$ were established by Babalola [5], motivating further investigations. The fourth Hankel determinant has also been studied in for a certain subclass of starlike and convex functions [20]**.** In this direction, we introduced a new subclasses of analytic functions using third-order differential subordination involving the exponential function and derive sharp bounds for the fourth Hankel determinant $H_4(1)$ for functions in this class.

2-Preliminaries

The definitions and lemmas presented below will be used to establish the main results work .

Definition2.1: [20] Let f be a function f of the form (1) .The fourth Hankel determinant of f is defined as:

$$H_4(1) = \begin{vmatrix} 1 & a_2 & a_3 & a_4 \\ a_2 & a_3 & a_4 & a_5 \\ a_3 & a_4 & a_5 & a_6 \\ a_4 & a_5 & a_6 & a_7 \end{vmatrix} = -a_4t_1 + a_5t_2 - a_6t_3 + a_7t_4, \qquad (5)$$ Where the

coefficients ti are defined by:

$$|t_1| = |a_2||a_4a_6 - a_5^2| + |a_3||a_3a_6 - a_4a_5| - |a_4||a_3a_5 - a_4^2|,$$

$$|t_2| = |a_4a_6 - a_5^2| - |a_2||a_3a_6 - a_4a_5| + |a_3||a_3a_5 - a_4^2|, \qquad (6)$$

$$|t_3| = |a_3a_6 - a_4a_5| + |a_2||a_2a_6 - a_3a_5| - |a_4||a_2a_4 - a_3^2|,$$

$$|t_4| = |a_3||a_2a_4 - a_2^2| - |a_4||a_4 - a_2a_3| + |a_5||a_3 - a_2^2|.$$

The Chebyshev polynomials of the first and second kind are defined on the interral $(-1,1)$ for a real variable x an foiiows:

$T_n(x) = \cos(n \arccos x)$

and

$$U_n(x) = \frac{\sin[(n+1)\arccos x]}{\sin(\arccos x)} = \frac{\sin[(n+1)\arccos x]}{\sqrt{1-x^2}},$$

Now, consider the function

$$H(t,z) = \frac{1}{1-2t+z^2}, t \in \left(\frac{1}{2},1\right), z \in \mathbb{U}.$$

It is well – known that if $t = \cos\alpha,\ \alpha \in \left(0,\frac{\pi}{3}\right)$, then

$$H(t,z) = 1 + \sum_{n=1}^{\infty} \frac{\sin[(n+1)\alpha]}{\sin\alpha} z^n$$
$$= 1 + 2\cos\alpha z + (3\cos^2\alpha - \sin^2\alpha)z^2 + (8\cos^3\alpha - 4\cos\alpha)z^3 + \cdots, z \in U,$$

that is

$$H(t,z) = 1 + U_1(t)\, z + U_2(t)z^2 + U_3(t)z^3 + U_4(t)z^4 + \cdots, t \in \left(\frac{1}{2},1\right), z \in U$$

where

$$U_n(t) = \frac{\sin[(n+1)\arccos t]}{\sqrt{1-t^2}}, n \in \mathbb{N},$$

are the Chebyshev polynomials of the second kind . There polynomials satisfy the recurrence relation:

$U_{n+1}(t) = 2tU_n(t) - U_{n-2}(t).$

specifically

$U_1(t) = 2t, U_2(t) = 4t^2 - 1,, U_3(t) = 8t^3 - 4t,$ (for each $n \in \mathbb{N}$).

Mendiratta et al. [79] discussed the subclass S_1^* of analytic functions associated with exponential function.

Lemma2. 1: [15] If function $f \in S_1^*$ is of the form (2), then

$$|a_2| \leq 1, |a_3| \leq \frac{3}{4}, |a_4| \leq \frac{17}{36}, |a_5| \leq 1,$$

where S_1^* denote the class of analytic functions to third Hankel determinant.

Lemma2. 2: [20] If the function $f \in S_e^*$ and of the form (1), then

$$|a_2| \leq 1, |a_3| \leq \frac{3}{4}, |a_4| \leq \frac{1}{18}, |a_5| \leq \frac{1}{96}, |a_6| \leq \frac{1}{600}, |a_7| \leq \frac{2401}{3600}.$$

Lemma2. 3: [20] If the function $f \in G_e^*$ and of the form (1), then

$$|a_2| \leq \frac{1}{2}, |a_3| \leq \frac{3}{12}, |a_4| \leq \frac{1}{72}, |a_5| \leq \frac{1}{480}, |a_6| \leq \frac{1}{3\,600}, |a_7| \leq \frac{343}{3600}.$$

Here, we discuss a new subclass of analytic functions using the subordination.

Lemma 2.4: [11] If P be a class of all analytic functions $p(z)$ of the form:

$$p(z) = 1 + \sum_{n=1}^{\infty} p_n z^n, \tag{7}$$

with $p(0)$=1 and $\Re e\{\, p(z)\} > 0$ for all $z \in U$. Then $|p_n| \leq 2$, for every $(n = 1,2,3, \dots)$.This disparity is sharp for each n

Definition 2.2: A function $f \in A$ given by (1) is said to be in the class $\mathcal{N}(\alpha, \mu, e)$ if the following condition holds:

$$\frac{1}{\alpha}\left[\frac{f(z)}{z} + (1-\mu)f'(z) + z\mu f''(z) + z^2 f'''(z)\right] \prec \mathcal{L}(e, z), \tag{8}$$

where $\mu \geq 0$,$\alpha \in \mathbb{C} \setminus \{0\}$ and

$$\mathcal{L}(e, z) = 1 + U_1(t)\, z + U_2(t) z^2 + U_3(t) z^3 + U_4(t) z^4 + \cdots, \qquad e \in \left(\frac{1}{2}, 1\right), z \in U.$$

The main findings of our current inquiry will now be stated and proven.

We begin here by finding the estimates on the coefficients $|a_n|$ and $n = 2,3,4,5,6,7$, for functions in the class $\mathcal{N}(\alpha, \mu, e)$.

Theorem 1: Let f be a function of the form

$$f(z) = z + \sum_{n=2}^{\infty} a_n z^n, \qquad (z \in U)$$

And suppose that f belongs to class $\mathcal{N}(\alpha, \mu, e)$

A Then the follow sharp coefficient bounds hold:

$$|a_2| \leq \frac{4}{3-2\mu}\alpha, |a_3| \leq \frac{12}{7}\alpha, |a_4| \leq \frac{36}{13+12\mu}\alpha, \qquad |a_5| \leq \frac{108}{21+40\mu}\alpha$$

$$|a_6| \leq \frac{216}{31+90\mu}\alpha\,, |a_7| \leq \frac{1044}{43+168\mu}\alpha,$$

where $\mu \geq 0$ and $\alpha \in \mathbb{C} \setminus \{0\}$.

Proof: A ssum that $f \in \mathcal{N}(\alpha, \mu, e)$, then there exists an analytic function E defined in the following subordination relation holds:

$$\frac{1}{\alpha}\left[\frac{f(z)}{z} + z(1-\mu)f''(z) + z^2\mu f'''(z)\right] = \mathcal{L}(e, \mathrm{E}(z)).$$

Where $L(e,z) = 1 + u_1(t)z + u_2(t)z^2 + \cdots \ldots$ is generating function involving chebysher polnomiais of the second by the principle of subordination, there exists a Schwarz function $\mathrm{E}(z)$, given by

$$\mathrm{E}(z) = \sum_{n=1}^{\infty} p_n z^n\,, \quad z \in U,$$

Such that the function $\mathrm{B}(z) = \frac{1+\mathrm{E}(z)}{1-\mathrm{E}(z)}$

Has the power series expansion

$$\begin{aligned}\mathrm{B}(z) = 1 &+ 2\,p_1 z + 2(\,p_2 + p_1^2)z^2 + 2[\,p_3 + p_1(2\,p_2 + p_1^2)]z^3 \\ &+ 2[\,p_4 + p_2^2 + p_1^2(3\,p_2 + p_1^2) + 2\,p_1\,p_3]z^4 \\ &+ 2\big[\,p_5 + 2\,p_2(\,p_3 + 2p_1^3) + 3p_1(p_1p_3 + p_2^2) + \big(p_1(2p_4 + p_1^4)\big)\big]z^5 \\ &+ 2[\,p_6 + p_1^3(4\,p_3 + p_1^3) + p_1^2(3p_4 + 5p_2p_1^2) + 2p_1(p_5 + 3p_2p_3) + p_3^2 \\ &+ p_2^2(\,p_2 + 6p_1^2) + 2\,p_2\,p_4]z^6 \\ &+ \cdots. \qquad (9)\end{aligned}$$

Now ,Since f is the stranded class A, We Can expand the left-hand side of operator as follows:

$$\begin{aligned}&\frac{1}{\alpha}\left[\frac{f(z)}{z} + z(1-\mu)f''(z) + z^2\mu f'''(z)\right] \\ &= \frac{1}{\alpha}[1 + (3-2\mu)a_2 z + 7a_3 z^2 + (13+12\mu)a_4 z^3 + (21+40\mu)a_5 z^4 \\ &+ (31+90\mu)a_6 z^5 + (43+168\mu)a_7 z^6 \\ &+ \cdots]. \qquad (10)\end{aligned}$$

comparing the coefficients of z^n form the two expansion $(9) and (10)$, we obtain

$$\frac{1}{\alpha}\left((3-2\mu)a_2\right) = 2\,p_1,$$

$$\frac{1}{\alpha}(7a_3) = 2(\,p_2 + p_1^2),$$

$$\frac{1}{\alpha}\left((13+12\mu)a_4\right) = 2[\,p_3 + p_1(2\,p_2 + p_1^2)],$$

$$\frac{1}{\alpha}\left((21+40\mu)a_5\right) = 2[\,p_4 + p_2^2 + p_1^2(3\,p_2 + p_1^2) + 2\,p_1\,p_3],$$

$$\frac{1}{\alpha}\left((31+90\mu)a_6\right) = 2\left[\,p_5 + 2\,p_2(\,p_3 + 2p_1^3) + 3p_1(p_1p_3 + p_2^2) + \left(p_1(2p_4 + p_1^4)\right)\right],$$

$$\frac{1}{\alpha}\left((43+168\mu)a_7\right) = 2[\,p_6 + p_1^3(4\,p_3 + p_1^3) + p_1^2(3p_4 + 5p_2p_1^2) + 2p_1(p_5 + 3p_2p_3) + p_3^2 + p_2^2(\,p_2 + 6p_1^2) + 2\,p_2\,p_4].$$

Now, by applying the standard bound $|p_n| \leq 1$ for Schwarz function and applying Lemma 4, we obtain

$$|a_2| \leq \frac{4}{(3-2\mu)}\alpha\,, \qquad (11)$$

$$|a_3| \leq \frac{12}{7}\alpha\,, \qquad (12)$$

$$|a_4| \leq \frac{36}{13+12\mu}\alpha, \qquad (13)$$

$$|a_5| \leq \frac{108}{21+40\mu}\alpha, \qquad (14)$$

$$|a_6| \leq \frac{216}{31+90\mu}\alpha, \qquad (15)$$

$$|a_7| \leq \frac{1044}{43+168\mu}\alpha. \qquad (16)$$

This complete the proof . □

In the following theorem, estimates on $|H_4(1)|$ are determined for $f \in \mathcal{N}(\alpha, \mu, e)$.

Theorem 2: Let f be a function of the form

$$f(z) = z + \sum_{n=2}^{\infty} a_n z^n , \quad (z \in U)$$

And suppose that f belongs to class $\mathcal{N}(\alpha, \mu, e)$. then the following estivate for the fourth Hankel determinant $H_4(1)$ holds:

$$|H_4(1)| \leq \frac{-111974(2\mu-3)(90\mu+31)(40\mu+21)\alpha^4 L_1(\delta,u) + 139968(90\mu+31)(12\mu+13)^2\alpha^3 L_2(\delta,u)}{L(\delta,u)} - \frac{93312(12\mu+13)^2(40\mu+21)^2\alpha^3 L_3(\delta,u) + 672(90\mu+31)^2\alpha^2 L_4(\delta,u)}{L(\delta,u)},$$

where

$$L(\delta,u) = 49(12\mu+13)^4(2\mu-3)^2(90\mu+31)(40\mu+21)^3$$

$$L_1(\delta,u) = 5529600\mu^6 - 6289920\mu^5 - 7939584\mu^4 + 3821168\mu^3 + 19330358\mu^2 + 13831923\mu + 2364054,$$

$$L_2(\delta,u) = 12441600\alpha\mu^5 + (7822080\alpha - 141120)\mu^4 + (2282496\alpha - 4407648)\mu^3 + (-9231232\alpha + 936684)\mu^2 + (-7799688\alpha + 7738668)\mu - 1318212\alpha + 1874691,$$

$$L_3(\delta,u) = (2073600\alpha + 967680)\mu^5 + (5760\alpha - 2203488)\mu^4 + (3538848\alpha - 405048)\mu^3 + (1919952\alpha + 2910348)\mu^2 + (-908008\alpha - 744282)\mu - 163380\alpha - 257985,$$

$$L_4(\delta,u) = -7776\mu^4 + (46080\alpha + 21600)\mu^3 + (52896\alpha - 13500)\mu^2 + (2216\alpha - 324)\mu - 1092\alpha - 2673.$$

Proof: Let f be a function of the form

$$f(z) = z + \sum_{n=2}^{\infty} a_n z^n , \quad (z \in U)$$

And suppose that f belongs to class $\mathcal{N}(\alpha, \mu, e)$

By Deficient $(2,1)$ the fourth Hankel determinant $H_4(1)$ is given by

$$|H_4(1)| = |a_7 t_4 - a_6 t_3 + a_5 t_2 - a_4 t_1|,$$

Where the coefficients t_1, t_2, t_3, t_4 are defined by

$$|t_1| = |a_2||a_4 a_6 - a_5^2| + |a_3||a_3 a_6 - a_4 a_5| - |a_4||a_3 a_5 - a_4^2|,$$

$$|t_2| = |a_4 a_6 - a_5^2| - |a_2||a_3 a_6 - a_4 a_5| + |a_3||a_3 a_5 - a_4^2|,$$

$$|t_3| = |a_3 a_6 - a_4 a_5| + |a_2||a_2 a_6 - a_3 a_5| - |a_4||a_2 a_4 - a_3^2|,$$

$$|t_4| = |a_3||a_2a_4 - a_2^2| - |a_4||a_4 - a_2a_3| + |a_5||a_3 - a_2^2|.$$

Inserting $(11) - (16)$ in (7), we get

$$|t_1| = \frac{31104\alpha^3 L_1(\delta,u)}{R_1(\delta,u)}, \tag{17}$$

$$|t_2| = \frac{1296\alpha^2 L_2(\delta,u)}{R_2(\delta,u)}, \tag{18}$$

$$|t_3| = \frac{432\alpha^2 L_3(\delta,u)}{R_3(\delta,u)}, \tag{19}$$

$$|t_4| = -\frac{96\alpha^2 L_4(\delta,u)}{R_4(\delta,u)}, \tag{20}$$

where

$$R_1(\delta,u) = 43(2\mu-3)(90\mu+31)(40\mu+21)^2(12\mu+13)^3,$$

$$R_2(\delta,u) = 49(90\mu+31)(2\mu-3)(12\mu+13)^2(40\mu+21)^2,$$

$$R_3(\delta,u) = 49(90\mu+31)(40\mu+21)(2\mu-3)^2(12\mu+13)^2,$$

$$R_4(\delta,u) = 7(40\mu+21)(2\mu-3)^2(12\mu+13)^2.$$

Using $(17) - (20)$ in (5), we get

$$|H_4(1)| \leq \frac{-111974(2\mu-3)(90\mu+31)(40\mu+21)\alpha^4 L_1(\delta,u) + 139968(90\mu+31)(12\mu+13)^2\alpha^3 L_2(\delta,u)}{L(\delta,u)} - \frac{93312(12\mu+13)^2(40\mu+21)^2\alpha^3 L_3(\delta,u) + 672(90\mu+31)^2\alpha^2 L_4(\delta,u)}{L(\delta,u)},$$

where

$$L_1(\delta,u) = 5529600\mu^6 - 6289920\mu^5 - 7939584\mu^4 + 3821168\mu^3 + 19330358\mu^2 + 13831923\mu + 2364054,$$

$$L_2(\delta,u) = 12441600\alpha\mu^5 + (7822080\alpha - 141120)\mu^4 + (2282496\alpha - 4407648)\mu^3 + (-9231232\alpha + 936684)\mu^2 + (-7799688\alpha + 7738668)\mu - 1318212\alpha + 1874691,$$

$$L_3(\delta,u) = (2073600\alpha + 967680)\mu^5 + (5760\alpha - 2203488)\mu^4 + (3538848\alpha - 405048)\mu^3 + (1919952\alpha + 2910348)\mu^2 + (-908008\alpha - 744282)\mu - 163380\alpha - 257985,$$

$$L_4(\delta,u) = -7776\mu^4 + (46080\alpha + 21600)\mu^3 + (52896\alpha - 13500)\mu^2 + (2216\alpha - 324)\mu - 1092\alpha - 2673.$$

□

In case $\mu = 0$, we get the following Corollary.

Corollary 1: If function f of form (1) belongs to the subclass $\mathcal{N}(\alpha, \mu, e)$, then

$$|H_4(1)| \leq\approx -\frac{825676789240}{911067339}a^4 + \frac{3869374792502}{4415172489}a^3 + \frac{259842}{480024727}a^2.$$

In case $\alpha = 1$ and $\mu = 0$, we get the following Corollary.

Corollary 2: If function f of form (1) belongs to the subclass $\mathcal{N}(\alpha, \mu, e)$, then

$|H_4(1)| \leq\approx -29.89227843$.

By applying Lemma 1 and using $|a_6|, |a_7|$ from Theorem 2 in fourth Hankel determinant (7), the following theorem emerges:

Theorem 3: let the function $f \in \mathcal{N}(\alpha,\mu,e)$ be of the form

$$f(z) = z + \sum_{n=2}^{\infty} a_n z^n , \qquad (z \in U)$$

Then , the fourth Hankel determinant satisfies the inequality

$|H_4(1)| \leq -\Upsilon_1(\delta,u) + \Upsilon_2(\delta,u) - \Upsilon_3(\delta,u) + \Upsilon_4(\delta,u),$

Where the farms are defined by:

$$\Upsilon_1(\delta,u) = \frac{2533\alpha}{24(31 + 90u)} - \frac{1271447}{1679616}, \qquad \Upsilon_2(\delta,u) = -60 * \frac{-60\alpha}{31 + 90u} - \frac{229}{1728},$$

$$\Upsilon_3(\delta,u) = 81648 * \frac{81648\alpha^2}{(31 + 90u)^2} - \frac{6115\alpha}{24(31 + 90u)}, \qquad \Upsilon_4(\delta,u) = \frac{-19343\alpha}{36(43 + 168u)}$$

Proof: Let $f \in \mathcal{N}(\alpha,\mu,e)$. Then the fourth Hankel determinant can be rewrite as:

$|H_4(1)| = -a_4t_1 + a_5t_2 - a_6t_3 + a_7t_4$,

where

$|t_1| = |a_2||a_4a_6 - a_5^2| + |a_3||a_3a_6 - a_4a_5| - |a_4||a_3a_5 - a_4^2|,$

$|t_2| = |a_4a_6 - a_5^2| - |a_2||a_3a_6 - a_4a_5| + |a_3||a_3a_5 - a_4^2|,$

$|t_3| = |a_3a_6 - a_4a_5| + |a_2||a_2a_6 - a_3a_5| - |a_4||a_2a_4 - a_3^2|,$

$|t_4| = |a_3||a_2a_4 - a_2^2| - |a_4||a_4 - a_2a_3| + |a_5||a_3 - a_2^2|.$

By applying Lemma 1 and using $|a_6|, |a_7|$ from Theorem 2 in fourth Hankel determinant (7), we get

$$|t_1| = |a_2||a_4a_6 - a_5^2| + |a_3||a_3a_6 - a_4a_5| - |a_4||a_3a_5 - a_4^2|,$$

$$|t_1| = \frac{447\alpha}{2(31 + 90u)} - \frac{74791}{46656}, \qquad (21)$$

$$|t_2| = |a_4a_6 - a_5^2| - |a_2||a_3a_6 - a_4a_5| + |a_3||a_3a_5 - a_4^2|,$$

$$|t_2| = \frac{-60\alpha}{31 + 90u} - \frac{229}{1728}, \qquad (22)$$

$$|t_3| = |a_3a_6 - a_4a_5| + |a_2||a_2a_6 - a_3a_5| - |a_4||a_2a_4 - a_3^2|,$$

$$|t_3| = \frac{378\alpha}{31 + 90u} - \frac{6115}{5184}, \qquad (23)$$

$$|t_4| = |a_3||a_2a_4 - a_2^2| - |a_4||a_4 - a_2a_3| + |a_5||a_3 - a_2^2|,$$

$$|t_4| = -\frac{667}{1296}. \qquad (24)$$

Inserting values $(21) - (24)$ in (5), we obtain

$$|H_4(1)| \leq -\Upsilon_1(\delta,u) + \Upsilon_2(\delta,u) - \Upsilon_3(\delta,u) + \Upsilon_4(\delta,u),$$

where

$$\Upsilon_1(\delta,u) = \frac{2533\alpha}{24(31 + 90u)} - \frac{1271447}{1679616}, \qquad \Upsilon_2(\delta,u) = -60 * \frac{-60\alpha}{31 + 90u} - \frac{229}{1728},$$

$$\Upsilon_3(\delta,u) = 81648 * \frac{81648\alpha^2}{(31 + 90u)^2} - \frac{6115\alpha}{24(31 + 90u)}, \qquad \Upsilon_4(\delta,u) = \frac{-19343\alpha}{36(43 + 168u)}.$$

In case $\mu = 0$, we get the following Corollary.

Corollary 3: If function f of form (1) belongs to the subclass $\mathcal{N}(\alpha,\mu,e)$, then

$$|H_4(1)| \leq -\Theta_1(\delta,u) + \Theta_2(\delta,u) - \Theta_3(\delta,u) + \Theta_4(\delta,u),$$

where

$$\Theta_1(\delta,u) = \frac{2533\alpha}{744} - \frac{1271447}{1679616}, \qquad \Theta_2(\delta,u) = -\frac{60\alpha}{31} - \frac{229}{1728},$$

$$\Theta_3(\delta,u) = \frac{81648\alpha^2}{961} - \frac{6115\alpha}{744}, \qquad \Theta_4(\delta,u) = -\frac{19343\alpha}{1548}.$$

In case $\alpha = 1\ and\ \mu = 0$, we get the following Corollary.

Corollary 4: If function f of form (1) belongs to the subclass $\mathcal{N}(\alpha,\mu,e)$, then

$$|H_4(1)| \leq^{\approx} -93.95348065.$$

References

[1] S. A. Al-Ameedee ,W. G. Atshan and F. A .Al-Maamori ,Second Hankel determinant for certain Subclasses of bi- univalent functions , Journal of physics: Conference Series , 1664 (2020) 012044 ,1-9.

[2] S. A. Al-Ameedee ,W. G. Atshan and F. A. Al-Maamori ,Coefficients estimates of bi-univalent functions defined by new subclass function ,Journal of Physics :Conference Series ,1530 (2020) 012105 ,1-8.

[3] W. G. Atshan, I. A. R. Rahman and A. A. Lupas, Some results of new subclasses for bi-univalent functions Using Quasi-subordination, Symmetry, 13(9)(2021), 1653, 1-12.

[4] W. G. Atshan , S. Yalcin and R. A. Hadi ,Cofficients estimates for special subclass of k-fold symmetric bi-univalent functions ,Mathematics for Applications, 9(2) (2020) ,83-90 .

[5] K. O. Babalola, On Hankel determinant for some classes of univalent functions, Inequal. Theory Appl., (2010), 6, 1–7.

[6] M. Çaglar, E. Deniz and H.M. Srivastava, Second Hankel determinant for certain subclasses of bi –univalent functions, Turk. J. Math., 41 (3) (2017), 694–706.

[7] D. G. Cantor, Power series with integral coefficients, Bull. Am. Math. Soc., 69 (3) (1963), 362–366.

[8] N. E. Cho, V. Kumar, Initial coefficients and fourth hankel determinant for certain analytic functions, Miskolc Mathematical Notes, (21) (2) (2020), 763–779.

[9] N. E. Cho, V. Kumar, S.S. Kumarand, V. Ravichandran, Radius problems for starlike functions associated with the sine function, Bull. Iran. Math. Soc. 45(1) (2019), 213–232.

[10] P. Dienes, The Taylor Series: An Introduction to the Theory of Functions of a Complex Variable; NewYork-Dover:Mineola, NY, USA, (1957).

[11] P. L. Duren, Univalent Functions, In : Grundlehren der Mathematischen Wissenschaften, Band 259, Springer - Verlag, New York, Berlin, Hidelberg and Tokyo, (1983).

[12] S. P. Goyal, O. Singh and R. Mukherjee, Certain results on a subclass of analytic and biunivalent functions associated with coe cient estimates and quasi-subordination, Palestine Journal of Mathematics, 5(1) (2016),79-85.

[13] D.V. Krishna and T. R. Reddy, Second Hankel determinant for the class of Bazilevic functions, Stud. Univ.Babes-Bolyai Math. 60(3)(2015), 413–420.

[14] W. Ma and D. Minda, A unified treatment of some special classes of univalent functions, Proceedings of the conference on complex analysis, Z. Li, F. Ren, L. Yang and S. Zhang, eds., Int. Press, (1994), 157-169.

[15] R. Mendiratta, S. Nagpal and V. Ravichandran, On a subclass of strongly starlike functions associated with exponential function, Bull. Malays. Math. Sci. Soc., 38(1) (2015), 365–386.

[16] H. Orhan, N. Magesh, and ,J. Yamini, Bounds for the second Hankel determinant of certain bi-univalent functions, Turkish Journal of Mathematics, 40(3) (2016),679-687.

[17] G. Polya, I. J. Schoenberg, Remarks on de la Vallee Poussin means and convex conformal maps of the circle, Pac. J. Math., 8(2) (1958), 259–334.

[18] C. Pommerenke, On the coefficients and Hankel determinants of univalent functions, J. Lond. Math. Soc.1(1) (1966), 111–122.

[19] C. Pommerenke, On the Hankel determinants of univalent functions, Mathematika, 14(1) (1967), 108–112.

[20] I. A. R. Rahman, W. G. Atshan and G. I. Oros, New concept on fourth Hankel determinant of a certain subclass of analytic functions, Afrika Matematika, (2022) 33:7, 1-15.

[21] H. M. Srivastava, S. Altınkaya and S.Yalcın, Hankel determinant for a subclass of bi – univalent functions defined by using a symmetric q-derivative operator, Filomat, 32(2) (2018), 503–516.

[22] H. M. Srivastava, S. Owa, S. (Eds.), *Current Topics in Analytic Function Theory*; World Scientific Publishing Company: London, UK, (1992).

[23] H. M. Srivastava, Q. Z Ahmad, N. Khan and B. Khan, Hankel and Toeplitz determinants for a subclass of q-starlike functions associated with a general conic domain, Mathematics,7(2) (2019), 181, 15 pages.

estimate problems, Applied Mathematics Comput., 218(23) (2012), 11461-11465.

[24] S. Yalcin, W. G. Atshan and H. Z. Hassan, Coefficients assessment for certain subclasses of bi-univalent functions related with quasi-subordination, Publications De L´Institut Mathematique, Nouvelle série, tome 108(122)(2020), 155-162.

The entry of artificial intelligence into strategic industries

دخول الذكاء الاصطناعي في الصناعات الإستراتيجية

إعداد الباحث

م. م. رشا جواد كاظم

T.A. Rasha Jawad Kadhim.

وزارة التربية – المديرية العامة لتربية بغداد / الرصافة الثانية

rj.hoz2598@gmail.com

The entry of artificial intelligence into strategic industries

دخول الذكاء الاصطناعي في الصناعات الإستراتيجية

إعداد الباحث

م. م. رشا جواد كاظم

T.A. Rasha Jawad Kadhim.

وزارة التربية – المديرية العامة لتربية بغداد / الرصافة الثانية

rj.hoz2598@gmail.com

الخلاصة

الذكاء الاصطناعي، باعتباره ثورة صناعية من الجيل الرابع، يُقدّم حلولاً ذكيةً للبشر بشكل متزايد. ويُحقق الذكاء الاصطناعي فوائد من حيث خفض استهلاك الطاقة، وفعالية التكلفة المُحفّزة، وتقليل المخاطر التشغيلية، وتحسين مصفوفات الأداء. وستُفصّل المراجعة كيف يُحدث الذكاء الاصطناعي ثورةً في مختلف الصناعات، بما في ذلك صناعات الأغذية، واكتشاف الأدوية، والتجارة الإلكترونية، والصناعات الكيميائية، من خلال تقديم حلول ذكية. مما يُؤدي إلى خفض استهلاك الطاقة، وتعزيز فعالية التكلفة، وتخفيف المخاطر التشغيلية، وتحسين مقاييس الأداء. بالإضافة إلى ذلك، سيُفصّل قسم النتائج أيضًا تطبيقات الذكاء الاصطناعي التي تمتد إلى ما وراء هذه القطاعات الرئيسية لتشمل العديد من القطاعات الأخرى، مثل صناعات مستحضرات التجميل، والسياحة، والسيارات، والميكانيكا، والإدارة البيئية، والألعاب، والمنسوجات، والترفيه، والتصميم الإنزيمي. يُسهّل دمج الذكاء الاصطناعي هيكلة المنتجات الصناعية وإدارتها وتصميمها وإنتاجيتها وتصنيعها وترويجها وإمكانية الوصول إليها بكفاءة. ومع ذلك، لا يزال استخدامه غير مُنظّم بشكل كافٍ، ويقتصر في الغالب على الاقتصاديات الحديثة، مما يستلزم تكاملاً أوسع بين الصناعات الصغيرة والمتوسطة والكبيرة في كل من الدول النامية والمتقدمة. إن التعاون بين الأكاديميين والباحثين والصناعيين والاقتصاديين والموظفين الإداريين والتقنيين والمدافعين عن البيئة أمر بالغ الأهمية لتعزيز التكامل الأكثر استدامة وكفاءة في استخدام الطاقة وقابلية للتطبيق اقتصاديًا وآمنًا للذكاء الاصطناعي عبر مختلف الصناعات في جميع أنحاء العالم.

الكلمات المفتاحية :- الذكاء الاصطناعي , الصناعات الإستراتيجية , الثورة الصناعية الرابعة , العوامل الاقتصادية , الطاقة المتجددة , الخدمات البديلة

Abstract

AI as a 4.0 industrial revolution is increasingly bringing smart solutions to humans. AI brings benefits in terms of reduced energy consumption, induced cost-effectiveness, reduced operational risks, and increased performance matrices. The review will elaborate on how AI is revolutionizing various industries, including food, drug discovery, e-commerce, and chemical industries, by offering smart solutions. Resulting in reduced energy

consumption, enhanced cost-effectiveness, mitigated operational risks, and improved performance metrics. Additionally, the results section will also elaborate on AI applications extended beyond these major sectors into numerous others, such as cosmetics, tourism, automobile, mechanical, environmental management, gaming, textile, entertainment, and enzymatic design industries. The integration of AI facilitates efficient structuring, administration, design, productivity, manufacturing, promotion, and accessibility of industrial products. However, its utilization remains under-regulated and predominantly limited to modernized economies, necessitating broader integration across small-scale, medium-scale, and large-scale industries in both developing and developed countries. Collaboration among academics, researchers, industrialists, economists, administrative personnel, technologists, and environmentalists is crucial to foster a more sustainable, energy-efficient, economically viable, and safe integration of AI across various industries worldwide.

Keywords:- Artificial Intelligence, Strategic Industries, The Fourth Industrial Revolution, Economic Factors, Renewable Energy, Alternative Services

المقدمة

الذكاء الاصطناعي (AI) يحول العديد من الصناعات من خلال توفير حلول جديدة، وتعزيز الكفاءة، وخفض التكاليف . يشير الذكاء الاصطناعي (AI) إلى تطوير أنظمة الكمبيوتر التي يمكنها أداء المهام التي تتطلب عادةً الذكاء البشري ، مثل التعلم وحل المشكلات والإدراك واتخاذ القرار وفهم اللغة

تستخدم أنظمة الذكاء الاصطناعي تقنيات مختلفة، بما في ذلك التعلم الآلي والتعلم العميق ومعالجة اللغة الطبيعية والرؤية الحاسوبية، لتحليل كميات كبيرة من البيانات وإجراء تنبؤات أو قرارات بناءً على هذا التحليل . تتضمن بعض الأمثلة على تطبيقات الذكاء الاصطناعي المساعدين الشخصيين الافتراضيين والسيارات ذاتية القيادة وأنظمة الكشف عن الاحتيال والتعرف على الصور والكلام والتشخيص والعلاج الطبي

الذكاء الاصطناعي هو مجال سريع التقدم يمكن أن يحول العديد من الصناعات وجوانب الحياة اليومية.

يحظى الذكاء الاصطناعي، إلى جانب بعض التدابير الثورية الأخرى مثل التعلم الآلي وإنترنت الأشياء ، باهتمام الصناعيين المعاصرين. يمتلك الذكاء الاصطناعي القدرة على استبدال الذكاء البشري أو تكراره أو الاستفادة منه . ويرجع ذلك إلى أن الصناعات أكثر اهتمامًا بالتحديات المرتبطة بنمذجة العمليات، وتحسين المنتجات والآليات، واستراتيجيات مراقبة الجودة ، واكتشاف الأخطاء وتشخيص المخاطر

ترتبط هذه الجوانب بالجانب المستدام للاقتصاديات الحديثة التي تغرس رؤى حول تحليلات الآثار الاجتماعية والاقتصادية والبيئية، إلى جانب جوانب آثار الاستدامة.

يتم إنفاق مئات المليارات من الدولارات في جميع أنحاء العالم من أجل التنفيذ الناجح ودمج الذكاء الاصطناعي في العديد من الصناعات، وخاصة في العالم المتقدم في أوروبا ودول مثل الصين وأمريكا واليابان وكوريا ،كما ترتبط الإعدادات الريادية الجديدة غالبًا بالتكنولوجيا القائمة على الذكاء الاصطناعي نظرًا لتنوع مجالات التشغيل والتصميم والبرمجة الإبداعية . ومع ذلك، لا تزال الدول النامية متخلفة بسبب الإدارة الهزيلة والرديئة للموارد الطبيعية والبشرية التي تبقيها في موقف دفاعي لتحقيق تطبيقات الذكاء الاصطناعي الصناعية . إن الحاجة ذات الصلة هي التأكد من قبل جميع الصناعات في جميع أنحاء العالم من أن الذكاء الاصطناعي هو الوجه الجديد للجيل التكنولوجي في القرن الحادي

والعشرين. وبالتالي، يحتاج الصناعيين إلى التعاون والإنفاق بشكل مفرط في مجال الصناعات المرتبطة بالذكاء الاصطناعي في السنوات القادمة لتلبية احتياجات السكان المتزايدين في السنوات القادمة. يمكن للنمو الصناعي بوتيرة سريعة دائمًا أن يعتاد على العصر السائد للتكنولوجيا ، . ومع ذلك، تواجه الصناعات اليوم تحديًا كبيرًا من حيث المنافسة العالمية، وتجربة العملاء واحتياجاتهم غير المتوقعة، والمخاوف البيئية المتزايدة باستمرار. هذه المخاوف كافية لدفع الشركة المصنعة إلى تحويل التركيز على منتجات المرافق المحسنة والفعالة بحيث تُقرأ هذه المنتجات للمستهلكين في وقت معقول وبتكاليف أقل . يكمن أفضل حل ممكن في الذكاء الاصطناعي من خلال تعظيم آثاره المفيدة وتقليل المخاطر والتهديدات المرتبطة بتطبيقات الذكاء الاصطناعي في الصناعات الإستراتيجية

المبحث الأول

أهمية البحث:

تكمن أهمية الدراسة في أن بعض تطبيقات الذكاء الاصطناعي أحدث تتحول كبيرًا في اقتصاديات الدول وأنما طال حياة والسلوك والاستهلاك.ليس هذا فحسب، بل امتد التأثير ليشمل اعتبار الذكاء الاصطناعي عاملًا أساسيًا في التنمية الاقتصادية، وفي تقييم الدولي المؤشرات الاقتصادية، وفي جذب الاستثمارات، ووزنها الاقتصادي الدولي.

مشكلة البحث

تتركّز المشكلة في حجم ونوع التأثير الذي يمكن أن يلعبه الذكاء الاصطناعي على القطاعات الهامّة والخاصة بالصناعات الإستراتيجية ودلى تطوها وتأثيرها الاقتصادي

الهدف من البحث :-

إن الكشف عن قدرة الذكاء الاصطناعي على إحداث ثورة حقيقية في عالم الصناعات التحويلية يثير حماسة كبيرة! تخيلوا، مثلاً، كيف يمكن أن تضاعف الإنتاجية، وتخفض التكاليف، وتعزز الجودة، وتقلل من فترات التوقف عن العمل. ولكن ذلك ليس كل شيء! إذا نظرنا عن كثب، نجد أن دمج تقنيات التعلم الآلي وتقنيات التعرف على الأنماط داخل المصنع يمكن أن يُحدث تحسينات ملحوظة في مختلف خطوات سلسلة العملية. من مرحلة الإنتاج إلى مراقبة الجودة، وحتى صيانة الآلات، الفرص لا تُعد ولا تُحصى!

منهجية البحث

يعتمد هذا البحث على استعراض شامل للإسهامات الرئيسية في الأدبيات العالمية، مُسلّطًا الضوء على الاقتصاديات النامية واتجاهات الرقمنة والذكاء الاصطناعي، وتأثيراتها الاقتصادية والاجتماعية. كما يُعنى بالمهارات المطلوبة وضرورة التعلم المستمر مدى الحياة. في إطار ذلك، يقدم البحث توليفة غنية من الاتجاهات الأساسية، إذ تم تنفيذ ذلك عبر إجراء مقابلات مع مجموعة متنوعة من أصحاب المصلحة والمبلغين الرئيسيين من مجالات الصناعة والتكنولوجيا والسياسات. ولم يقتصر الأمر على ذلك، بل تم استشارة صانعي السياسات الذين يشغلون مناصب تتيح لهم فهم العوامل المرتبطة بالوظائف والتكنولوجيا ومستقبل العمل والذكاء الاصطناعي، أو حتى التأثير عليها. تأتي المجموعة الثانية من القيادات الصناعية

والمديرين والخبراء الذين يركزون، بشكل خاص، على أصحاب العمل الذين قد يتأثرون بتوجهات المستقبل في سوق العمل. أما المجموعة الثالثة، فتضم الممارسين في مجال التكنولوجيا، بدءًا من الشركات الناشئة المبتكرة وصولًا إلى الشركات الكبيرة التي تحركها روح الابتكار، حيث ينخرط هؤلاء في أنشطة قد تتأثر بشكلٍ مباشر بمستقبل العمل

نطاق البحث:

المكان :- وزارة النفط , وزارة الكهرباء, وزارة الصناعة

الزمان :- الربع الأول من سنة 2025

استعرضت تأثير الذكاء الاصطناعي على التنمية الاقتصادية من خلال تأثيره على حجم الاستهلاك والإنتاج، وتوفير فرص العمل، وتشكيل الأجور. ثم تطرقت حول استثمارات الدول في تقنيات الذكاء الاصطناعي والصعوبات التي تواجهها، مع التركيز على بعض القطاعات مثل: الزراعة، الصناعة ،التجارة، والتعليم. ووضحنا بعض تجارب الدول، مُعتبِرًا أن التنمية الاقتصادية تعتمد على زيادة الإنتاج، وتقليل الفاقد ،والتوظيف ،ورافعا لأجور وتوزيعها بشكل عادل، بالإضافة إلى الاستثمار،وإحداث تغييرات وتحسينات جوهرية في عناصر الاقتصاد والعوامل المؤثرة فيه كـ:التعليم والبحث العلمي، والتطوير.

أسئلة البحث

من أجل ما يلزم فعله للحاق بركب الأمم المتقدمة. ويمكن طرحها في جملة استفسارات منها:

هل كان للذكاء الاصطناعي أثرٌ نافعٌأ, مضارٌ على التنمية الاقتصادية؟

ما مجال استخدام الذكاء الاصطناعي بالنسبة للدول والقطاعات الاقتصادية؟

ماذا ينبغي على الدول العربية فعله للاستفادة من إيجابيات الذكاء الاصطناعي وتفادي سلبياته؟

المبحث الثاني

الإطار النظري

مفهوم الذكاء الاصطناعي

يشير مفهوم الذكاء الاصطناعي(Artificial Intelligence)إلى الذكاء الموجود في الآلات الرقمية مثل؛ الحاسوب، الهواتف المحمولة أو الروبوتات، ويعبر هذا الذكاء عن مقدرة هذه الآلات على القيام بمهام مرتبطة بالكائنات الذكية. يشمل هذا المفهوم الأنظمة التي لديها قدرات شبيهة بقدرات العقل البشري، مثل؛ التفكير، استخلاص المعنى والتعلم من الخبرات. من أمثلة ذلك؛ إثبات النظريات الرياضية، لعب الشطرنج، التشخيص الطبي، محركات البحث على الإنترنت، والتعرف على الصوت أو الكتابة اليدوية.[1]

تأثير الذكاء الاصطناعيّ على المتغيرات الاقتصاديَّة:

في الواقع، تتصدر الشركات في الولايات المتحدة والصين مسيرة الاستثمار في الذكاء الاصطناعي،مع وجود منافسة من أوروبا وبلدان شرق وجنوب شرق آسيا.هناك جهودٌ ملحوظة من الإمارات والسعودية ومصر أيضًا.هذا يعني أن العالم المتقدم يتمتع بميزةٍ واضحة في التقدم السريع بثورة الذكاء الاصطناعي.بفضل قوةٍ اقتصاديةٍ أكبر، تكون هذه الدول الأكثر غنى في وضعٍ أفضل للقيام باستثمارات كبيرة في البحوث والتطوير اللازمة لبناء نماذج ذكاء اصطناعي متطورة. في المقابل، غالبًا ما تواجه الدول النامية أولوياتٍ أكثر إلحاحًا،مثل التعليم والصحة وتوفير الغذاء للسكان ، وهي أمورٌ تفوق أي استثمار كبير في التحول الرقمي.ونتيجةً لذلك،يمكن للذكاء الاصطناعي أن يزيد الفجوة الرقمية القائمة بين الدول المتقدمة والنامية [2].

على الرغم من هذا، يواجه الذكاء الاصطناعي بعض الصعوبات والعراقيل، منها: قلة الخبرة المطلوبة لتشغيل تقنيات الذكاء الاصطناعي، وأهمية الحفاظ على البيانات وجودتها، وتطوير أجهزة الذكاء الاصطناعي، وتوضيح كيفية اتخاذ قراراتها. بالإضافة إلى معالجة مشكلة التحيز في الأدوات الاصطناعية المستخدمة في نظام العدالة الجنائية.كما يجب خلق ثقافة متكاملة للتفاعل بين البشر والآلات للاستفادة القصوى منها، والعمل على سد الفجوة الرقمية بين الدول المطبقة للذكاء الاصطناعي والدول الأخرى.

أفرزت الثورة الصناعية والتكنولوجية الحديثة تطبيقات كثيرة تعتمد على الآلات لاستغلال قدرات الإنسان العقلية والقدرة على التنبؤ واتخاذ القرار.فلا يوجد قطاع أو مجال تقريبًا يخلو من تطبيقات الذكاء الاصطناعي لتنفيذ مهام معينة يجدها البشر متكررة أو صعبة [3].

تأثير الذكاء الاصطناعيّ على قطاع الصناعة

يُعرَفُ العصر الحالي بعصر الثورة الصناعية الرابعة وبداية الخامسة

الاختراقات العلمية تتسارع بشكلٍ لم يسبق له مثيل في التاريخ الإنسانيّ. نشهد تطورًا سريعًا ومذهلاً للتقنيات الرقمية.هنا، نستعرض تأثير الذكاء الاصطناعي على القطاع الصناعي، الذي كان الأكثر تأثرًا بهذه التقنيات. تحوَّل تُعملياتُ التصنيع إلى"تصنيع ذكي"بفضل تقنيات التعلُّم الآلي وابتكارا تجديده، مما ميَّز الثورة الصناعية الرابعة وساهم في استمرارها.

نتناول تأثيره على رأس المال وثورته في آلات الإنتاج والتنبؤ بالطلب وتحسينا لإنتاج، وتأثيره على الأيدي العاملة ومتطلبات التدريب على المهارات الجديدة، ونناقش تقييمًا دقيقً الكيفية إسهام التقنيات الجديدة في ظهور وظائف جديدة و/أو زيادة الإنتاجية واحتمالية استبعاد بعض العمال

. ننتقل لتأثير الذكاء الاصطناعي على المواد الخام، التي أصبحت "ذكية" وأكثر تخصيصًا وتحديدًا للتطبيق. ثم نُسلِّط الضوء على تأثيره على الطاقة، وظهور شبكات الطاقة الذكية وكفاءة استخدام الطاقة.أخيرًا، نتناول تأثيره على شبكات النقل وسلاسل التوريد العالمية، وتزايد سوق النقل الذكي، وأثره على سوق الصناعة وهيمنة بعض الشركات العالمية[4].

رأس المال

يُحدث الذكاء الاصطناعي تغييرًا كبيرًا في نظام التصنيع. لقد تطور نظامُ التصنيع الحالي في الثورة الصناعية الرابعة بشكل مختلف عن سابقيه.وقد ظهرت أهمية توظيف تقنياته في التصنيع؛وذلك لقدرته على تطوير عمليات التصنيع بشكل عام ومستمر عن طريق عمل الصيانة المتوقعة وإيجاد أفضل طرقا لإنتاج على النحو التالي:

ستصبح أنظمة الذكاء الاصطناعي قادرة على تحسينِ عملية التصنيع. يتضح ذلك من خلال متابعة كل مرحلة من مراحل الإنتاج مثل:الوقت المستغرق في صنع كل منتج والكميات المستخدمة في الإنتاج، وأيضاً في حالة التصنيع الإضافي.

سيُمكن التنبؤ أيضاًبمعدل الإنتاج الإضافي والكمية المطلوبة والوقت اللازم، وعلى أساس ذلك يتم وضع خطط الإنتاج. كما يتم اختبار العديد من النماذج المتنوعة والنتائج المحتملة للوصول إلى أفضل النتائج. بالإضافة إلى ذلك،يمكن لخوارزميات التعلم الآلي [5]

توظيف البيانات الضخمة لإعطاء نظرات فورية واتخاذ قرارات مبنية عليها. نتيجة لذلك، تستخدم هذه الرؤى للتكهن بالطلب وتحديد المنتجات ذات الأولوية لتصنيعها بناءً على ذلك.في الجانب الآخر، تخفض أنظمة الذكاء الاصطناعي التكاليف عن طريق الصيانة المستمرة لآلات التصنيع ومعدات خطوط الإنتاج.

تتجلى أهمية ذلك في توضيحات الدراسات بأن التوقف غير المخطط له يكلف الشركات المصنعة ما يقدر بنحو ٥٠ مليار دولار سنويًا. وأن تعطل الأصول يتسبب في ٤٢٪ من هذا التعطيل غير المخطط له. لهذا السبب، أصبحت الصيانة التنبؤية حلاً ضروريًا للمصنعين، حيث تمكنهم من التنبؤ بأعطال الآلات أو الأنظمة، وبالتالي إصلاح الأجزاء قبل التعطل وتجنب الخسائر[6].

بشكل عام، ستساعد التقنيات القائمة على الذكاء الاصطناعي البشر في تطوير أدوات أفضل لإنتاج السلع والخدمات) رأس المال(يحسن الذكاء الاصطناعي كفاءة رأس المال عن طريق تقليل وقت توقف المصنع وزيادة الإنتاج. تعتبر الروبوتات أدوات مثالية لتنفيذ المهام المتكررة أو الخطيرة من هنا نرى أن الذكاء الاصطناعي يعمل في اتجاهين بالنسبة لرأس المال الحقيقي المتمثل في الآلات والمعدات، أولاً في تحديد حجم الإنتاجية لأي نوع من السلع لقدرته على التنبؤ بالطلب، كما يعمل في اتجاه التنبؤ بالأعطال والصيانة قبل العطل،وبالتالي تقليل معدل الهالك والحفاظ على الأرباح بدون خصم تكلفة الهالك من رأس المال، أي زيادة كفاءة الإنتاجية وجودة رأس المال الحقيقي وزيادة في الأرباح [7]

وبناء على ذلك، نخلص إلى أن التطورات المستمرة في البرمجيات والأجهزة تقود إلى اتجاهات مثل: كفاءة التصنيع كخدمة، والتخصيص المفرط للمنتجات حسب الطلب، والتجديد والابتكار في اقتصاد السلع الرأسمالية. وقد صدر تقرير جديد بعنوان "التصنيع الذكي"،وقدم هذا التقرير نظرة عالمية معمقة حول كيفية اكتساب التصنيع الذكي زخماً بين عامي2013و.2018 ووجد التقرير أن هناك1300 صفقة رأسمالية في جميع أنحاء العالم، بقيمة إجمالية17.4مليار دولار تعتمد على التصنيع الذكي.وتصدرت الولايات المتحدة الاستثمار في التصنيع الذكي، حيث حصلت الشركات الناشئة الأمريكية على11.4مليار دولار، مقابل3.9مليار دولار في آسيا و 37.7مليار دولار في عمليات الاندماج والاستحواذ خلال فترة الخمس سنوات في أوروبا [8].

نوضح هنا أهمية الذكاء الاصطناعي في حساب التكاليف والتنبؤ بالديون لتحديد العوامل المؤثرة على رأس المال.حيث تم جمع النسب المالية المتنوعة، بما في ذلك نمو الأصول، وصافي الربحية، والسوق إلى القيمة الدفترية، وغيرها.(2)

حيث يمكن أن يؤدي الذكاء الاصطناعي إلى زيادة عدم المساواة فيما يتعلق بزيادة حصة رأس المال في الاقتصاد , حيث هناك الكثير من الأدلة على أن حصة العمالة من الناتج المحلي الإجمالي آخذة في الانخفاض إذا كان الذكاء الاصطناعي شكلاً جديداً وفعالاً لرأس المال [9]

فمن المحتمل أن ترتفع حصة رأس المال الحقيقي المتمثل في الآلات والمعدات على حساب العمالة. وذلك لعدة أسباب متمثلة في:

تساعد الآلية فيرفع الإنتاج، فهي تعزز الفاعلية في خط الإنتاج. هذا لأن الروبوتات والأجهزة المتخصصة يمكنها تسريع وتيرة العمل.بالإضافة إلى ذلك، قد تخفف الآلية أعباء المهام المتكررة والشاقة على العاملين، وبالتالي تحسين بيئة العمل.

مساهمته في تخفيض المصاريف، وذلك بإنتاج السلع بصورة أسرع وأسهل، مما يوفر الوقت والمال.

تقليل الأخطاء، فالروبوت ينجز المهام المتكررة لساعات طويلة دون تعب، ويميل إلى ارتكاب أخطاء أقل من الموظفين.

تقليل الاعتماد على العمالة البشرية، حيث يعتبر نقص العمالة في بعض الأماكن مشكلة، وهنا تأتي الميكنة لتسد هذا النقص بعمليات آلية تحقق نفس النتائج أو أفضل.

أداء المهام الخطرة، وهي ميزة مهمة للميكنة، حيث تمنع الموظفين من القيام بمهام خطيرة قد تسبب لهم إصابات. هذا يجعل بيئة العمل أكثر أمانًا، ويقلل من الحوادث [10]

العمل

أوجدت الثورة الصناعية الرابعة تحولاً تقنياً وتصاعداً لمشهد الصناعة من قبل.على العاملين في الوقت الحالي مواجهة حقيقة أن مهامهم الحالية قد تتبدل في المستقبل. تتواصل مهام العنصر البشري عموماً، والعامل تحديداً،في التغيير بسرعة، مما يستدعي تنمية المهارات لمواكبة هذه التغييرات.

المنطق الأساسي هو أن البيانات الرقمية وإنترنت الأشياء والشبكات قد ألغت بعض أو معظم المهام الحالية للعامل.قد يتطلب ذلك النظر إلى الصورة الكلية للمجتمع)كالتحديات،الموارد،الفرص،الثروة(،حيث يعتمد التأثير على تقنيات الذكاء الاصطناعي على تقدم المجتمع. بالإضافة إلى ذلك، يجب أن يكون تطوير الذات والالتزام بالتعليم المستمر مسؤولية مشتركة بين الفرد والمنظمة.[11]

القوى المحركة لبيئة العمل المتغيرة هي الابتكار التكنولوجي المتسارع، وهو ما يؤدي إلى زوال الصناعات القديمة وظهور صناعات ووظائف جديدة.هذا يعني أيضاً أن حوالي٥٠٪ من الوظائف الحالية، بما في ذلك المناصب الإدارية، ستتمكن الآلة من أدائها.هناك توقعات بزيادة البطالة، وتقصير مدة الخدمة، وزيادة التحولات المهنية.في العملية

الإنتاجية، الجهد البشري يهدف إلى خلق أو زيادة المنفعة، سواء كان جسدياً أو ذهنياً، ويشمل الإدارة ومهارات العاملين والأيدي العاملة [12]

أهمية الأدوار في الأعمال والمالية وتكنولوجيا المعلومات والرياضيات والهندسة المعمارية كبيرة.هذه التوقعات قد تكون مقلقة، حيث نشهد عصر أي مكن فيه تحقيق عائد أكبر مقابل عمل أقل،إذا توفرت المهارات المناسبة والقدرة على التكيف. لقد شهد سوق العمل تطوراً كبيراً وزادت متطلباته تعقيداً، لذا يجب على العمال معرفة المهارات التقنية المطلوبة في السوق الجديد ،والتحلي بالمرونة والتكيف مع التغييرات، ومواكبة التطورات، والقدرة على التعلم المستمر.على الرغم من نقص الأيدي العاملة الماهرة، فمن المتوقع أن يفتح الاستثمار في تحليل البيانات الضخمة للأمن السيبراني العديد من الفرص.من ناحية أخرى، لن تكون الثورة مقتصرة على المصانع، بل ستنتقل قطاعات بأكملها، مثلما كدونالدز،نحو الأتمتة والرقمنة.

بدأت الوحدات الصناعية تستثمر في الطابعات ثلاثية الأبعاد،وإنترنت الأشياء للربط بين الآلات، والبيانات الضخمة لتحليل العمليات وتعزيز الكفاءة [13]..

يتوقع زوال عدد كبير من الوظائف المتوسطة والدُنيا وظهور وظائف عليا.ستبرز من اصب جديدة ذات مهارات تقنية وإدارية عالية مع تطور الثورة الصناعية الرابعة.على القادة، في ظلال استثمار في الذكاء الاصطناعي،التفكير في الوظائف التي ستختفي وتلك التي ستظهر، لتأهيل الشباب لتولي هذه المناصب. يحذر محللون من أن تقدم الروبوتات والذكاء الاصطناعي قد يؤدي إلى فقدان وظائف واسع أو استقطاب وظيفي، مما يوسع الفجوة في الدخل والثروة .في عام2015،أشار تقرير(America Merrill Lynch) صادر عن البنك إلى الزيادة عدم المساواة. وجد التقرير أن نسبة 35%من الوظائف و47% من العاملين في الولايات المتحدة معرضون لخطر الاستبدال بالتكنولوجيا خلال العشرين عامًا القادمة. وفقًا للبنك الدولي(2016)، ستعاني الدول النامية كثيرًا بفقدان الوظائف69%: في الهند، و72%في تايلاند، و77% في الصين. خلص باحثون آخرون إلى استنتاجات أقل حدة، لكن هم يركزون جميعهم على أثر الذكاء الاصطناعي على البطالة.

وجدت دراسة من "أكسنتشر"أن الذكاء الاصطناعي يضاعف النمو الاقتصادي في12 دولة متقدمة، ويعمل على تحسين الكفاءة والإنتاجية،ومن المتوقع أن تشهد الولايات المتحدة وفنلندا أكبر المكاسب الاقتصادية من الذكاء الاصطناعي حتى عام2035،محققةً نموًا أعلى بنسبة2%في إجمالي القيمة المضافة.[14]

المواد الخام:

تُعد المواد الأولية من هم مقومات الإنتاج في كل العصور، ويتوقف ذلك على كيفية استعمالها والغرض منها، بالإضافة إلى رفع جودتها.في الصناعة الحديثة، يتم المزج بين الأساليب الكمية والتجريبية والوصفية والجوهرية في عملية الإنتاج. ومع استمرار تقدم العمليات، ستتطور التقنيات والأدوات اللازمة لتشغيلها بكفاءة وفاعلية. [15]

من هذا المنطلق، تعمل تكنولوجيا التصنيع الذكي على استكشاف وتطوير وتصنيع مواد جديدة، وليس هذا فحسب، بل إنه هذه المواد، خاصة تلك المعتمدة على العديد من البوليمرات، ستقود الجيل القادم من المنتجات الاستهلاكية والصناعية. كما أن عمليات التصنيع مصممة لتكون "ذكية"، فإن المواد نفسها تمر بمرحلة تحول مماثلة لتصبح "ذكية"

وأكثر تخصصاً وتحديداً للتطبيق. ويتطلب هذا التحول فهماً جوهرياً جديداً ومراقبة أعمق لموارد الإنتاج.على سبيل المثال، نجد تحول صناعة البوليمرات - مثلها مثل العديد من الصناعات الأخرى - لتبني التقنيات والعمليات الجديدة وتجربتها بهدف زيادة الكفاءة والفعالية. ومن هنا، تمكنت التكنولوجيا الذكية من التكيف مع المتغيرات الصناعية والبيئية، حيث تم ابتكار نوع من المواد الذكية يتم تنشيطها بمحفزات كهربائية لإحداث تغيير في خصائصها، كما تم تطوير مواد ذكية صديقة للبيئة، وهي تتمثل في البوليمرات الحيوية. وتُستخدم البوليمرات الحيوية في العضلات الاصطناعية والروبوتات الحيوية وأنظمة العدسات القابلة لإعادة التشكيل. [16]

يساعد الذكاء الاصطناعي الباحثين على فهم الخصائص الفيزيائية والكيميائية للمواد بشكل أفضل تم استخدام التعلم الآلي لمساعدة علماء المواد على تصميم مواد جديدة وفهم خصائص المواد الموجودة. وليس ذلك فقط بل يعمل الذكاء الاصطناعي على اكتشاف العيوب في المواد قبل التصنيع ،مما يحسن موثوقية وكفاءة عمليات التصنيع الحالية كما هي شركة عالمية للاستشارات حيث توفر خدمات استشارية رقمية وتقنية ومالية [17]

الطاقة

برز خلال الثورة الصناعية الرابعة ما يُعرف بالإدارة الإستراتيجية للطاقة، وهي منهج شامل لكفاءة الطاقة.يمكّن هذا النهج الشركات من تحقيق وفورات مستدامة وطويلة الأجل.تتحول الشركات بالنظر إلى استخدام الكهرباء بنفس الطريقة التي تنظر بها إلى أي تكاليف تشغيلية أخرى،مع إعطاء مراقبة الاستهلاك أهمية كبيرة في عملياتها.كما تقوم الشركات التي تعتمد الإدارة الإستراتيجية للطاقة بوضع خطط للطاقة تتضمن الحفاظ على الطاقة بالتوازي مع أهداف التشغيل والصيانة. ويتطلب ذلك مشاركة جميع الموظفين، من الإدارة العليا إلى الموظفين الذين يعتبر استخدامهم الفردي للطاقة عاملاً رئيسيًا لنجاح هذه الشركات [18]

أصبحت إدارة الطاقة الإستراتيجية هي المصطلح الرائج لوصف البرامج التي تساعد الشركات على تنفيذ برامج التحسين المستمر التي تعالج استخدام الطاقة بشكل منهجي. تتضمن هذه البرامج تثقيف القوى العاملة وتدريبها وتغيير الثقافة التنظيمية، كما تشمل نهج خطة العمل الذي تم تطبيقه بنجاح في التصنيع وتحسين الجودة لسنوات عديدة [19]

تشير الاتصالات المتطورة إلى أن المصنع الذكي يتكون من ثلاث طبقات، حيث يعمل في هذه المصانع على جمع أنواع مختلفة من البيانات، بما في ذلك الأفراد والمعدات والبيئة.

الطبقة الأولى:هي طبقة تجميع البيانات والتحكم، تقوم بجمع البيانات البيئية وإرسالها إلى الطبقة الثانية.

الطبقة الثانية:هي إدارة الطاقة القائمة على الوعي،حيث تقوم بتحليل البيانات.

الطبقة الثالثة: هي خدمة الطاقة: تقدم خدمات إدارة الطاقة للمستخدمين من خلال مراقبة استهلاك الطاقة والتحكم فيه. باستخدام المخطط المقترح، يمكن للمستخدمين مراقبة استهلاكهم للطاقة والتحكم في المرافق والمعدات الخاصة بهم لتجنب فقدان الطاقة. [20]

أصدرت منظمة الأمم المتحدة للتنمية الصناعية تقريرًا عام 2017 يؤكد على ضرورة تسريع الطاقة النظيفة من خلال الثورة الصناعية الرابعة. لذلك، تركز الاهتمام على إمكانية الحصول على شبكات طاقة ذكية من خلال دمج الثورة

الصناعية الرابعة في صناعة الطاقة المستدامة. تعتمد هذه التقنية بشكل أساسي على الطاقة المتولدة من أنظمة الطاقة الشمسية أو الرياح المحلية.هذا يعني أن المستخدمين سيكونون قادرين على إدارة ومراقبة استهلاكهم للطاقة بدقة وسهولة أكبر [21]

في المقابل،تفترض محطات الطاقة الافتراضية تحولًا في طريقة استخدام الناس للطاقة عند اجتماع عدة موارد متجددة. تربط محطة توليد الطاقة الافتراضية وحدات لامركزية افتراضية (Tesla) متوسطة الحجم تنتج الطاقة. وبالتالي، يتمتع مستهلكو الطاقة بأنظمة تخزين مرنة. ومن هنا،أصبحت إدارة كفاءة الطاقة أحد الدعائم الأساسية في تطوير الثورة الصناعية الرابعة، مع زيادة الاهتمام بكفاءة الطاقة في الأسواق الصناعية الإستراتيجية [22]

5-وسائل النقل والمواصلات

تشهد شركات النقل تغييراً كبيراً ومستداماً، كما هو الحال في معظم القطاعات،مدفوعاً بابتكار البرمجيات وتأثير التقنيات الجديدة على سلاسل الإمداد عالمياً.هذا يدفع نحو تحول سريع في العمليات لاستيعاب أساسيات تطبيقات الثورة الصناعية الرابعة في النقل والخدمات اللوجستية. ينتج عن ذلك رقمنه وتكامل سلاسل القيمة،عمودياً وأفقياً، ورقمنه عروض المنتجات والخدمات، وتطوير نماذج أعمال رقمية جديدة ومنصات للوصول إلى العملاء وإدارة الموارد ونقلها [23]

سلسلة القيمة، وهي سلسلة الأنشطة التي تضيف قيمة للمنتج، تنقسم إلى سلاسل رأسية وأفقية.الرأسية تشمل البنية التحتية والكوادر البشرية والتكنولوجيا. الأفقية تشمل النقل والتسويق والمبيعات.هنا نرى كيف تؤثر الثورة الصناعية الرابعة على هذه السلاسل.

على أطراف سلاسل التوريد، هنا كمجموعات تستخدم الأجهزة والبرمجيات.

المجموعة الأولى، في البداية والنهاية.

المجموعة الثانية تضم العاملين بالنقل واللوجستيات مع أجهزتهم وبرمجياتهم.

المجموعة الثالثة تضم مالكي ومديري البنية التحتية [24]

تتبنى الحكومات في جميع أنحاء العالم أنظمة النقل الذكية؛ وذلك لتحسين السلامة على الطرق والأداء التشغيلي لنظام النقل وتقليل تأثير النقل على البيئة بيد أن هذه الحكومات تحتاج إلى أموال كبيرة لتنفيذ أنظمة النقل الذكية لذلك تستثمر دول العالم مثل اليابان بكثافة في مشاريع مختلفة لأنظمة النقل الذكية حيث يعتبر النقل الذكي أكثر أماناً من خلال الجمع بين التعلم الآلي وإنترنت الأشياء والجيل الخامس كما أثبتت أنظمة النقل المستقلة ذاتية القيادة أنها تقلل من فرص إصابة "العامل البشري" في الحوادث. حيث أنها لا تتشتت أو تتعب أو تتأثر, كما تعمل إدارة النقل الذكي بشكل أفضل من خلال جمع البيانات هو مفتاح مهم للإدارة العامة المسؤولة للبنية التحتية علاوة على ذلك يعتبر النقل الذكي أكثر كفاءة مع الإدارة الأفضل. كما يمكن أن تساعد بيانات الجودة في تحديد المجالات التي يمكن تحسين الكفاءة فيها. ويعتبر النقل الذكي فعال من حيث التكلفة؛ نظراً لأن النقل الذكي يستفيد بشكل أفضل من الموارد المتاحة، فإنه يمكنه أيضا أن يقلل التكاليف بفضل الصيانة الوقائية، واستهلاك الطاقة المنخفض والموارد الأقل.

لقد أثبتت الأزمات العالمية مثل جائحة فيروس كورونا، التوريد في العالم معرضة للاضطراب فعندما يمرض العمال والسائقون ويصبح السفر من منطقة إلى أخر فيه خطر على الصحة العامة لذلك يمكن أن يصبح النقل المستقل ذاتي القيادة بواسطة أنظمة الذكاء الاصطناعي للبضائع منقذاً حقيقياً للحياة [25]

الأسواق

تتألف الثورة الصناعية الرابعة من مجموعة متكاملة من أتمتة العمليات، والتحكم بالروبوتات، وتحليل البيانات الضخمة لتحقيق إنتاج وتشغيل فعال في الصناعات التحويلية، مما يهدف إلى رفع كفاءة أداء الأصول، واستخدام الموارد، والتقنيات، وغيرها من العمليات الصناعية ذات الصلة. يضمن هذا النظام سلامة البيانات وقابلية التشغيل البيني والرؤى والتحكم والرؤية للمستخدم.

يتضح هذا جليًا من خلال تأثيره على السوق الصناعي العالمي للثورة الصناعية الرابعة، لذا يُتوقع أن يشهد السوق نموًا كبيرًا في المستقبل القريب، ويعز بذلك إلى زيادة الطلب على الآلات الصناعية، واستخدام تكنولوجيا الروبوتات، وزيادة الإنفاق الحكومي على الأتمتة. في المقابل، من المحتمل أن تحدث بعض العوامل من هذا النمو، مثل متطلبات الاستثمار في التكنولوجيا الصناعية الذكية التي تتطلب بنية تحتية تكنولوجية متقدمة.

قُدرت قيمة سوق تكنولوجيا الثورة الصناعية الرابعة بحوالي71.7مليار دولار في عام.2019 ومن المتوقع أن تصل إلى 156.6 مليار دولار بحلول عام 2025، بمعدل نمو سنوي مركب يبلغ 16.9٪ بين عامي 2019 و2025. يُتوقع أيضًا زيادة الاعتماد على الإنترنت الصناعي في وحدات التصنيع حول العالم، مع التركيز على تعزيز كفاءة الآلات وخفض تكاليف الإنتاج. علاوة على ذلك، من المتوقع أن يؤدي الطلب المتزايد على الروبوتات الصناعية إلى تعزيز نمو هذا السوق، وهو أكبر مساهم في سوق تكنولوجيا الثورة الصناعية الرابعة خلال هذه الفترة [25] .

المبحث الثالث

الخاتمة

النتائج

نود الإشارة إلى أن العراق كان رائدًا في العلوم منذ زمن الخوارزمي وبيت الحكمة قبل 1200عام، لكنه يحتل اليوم المرتبة 77 عالميًا والتاسعة عربيًا في مؤشر الذكاء الاصطناعي لعام 2024. ومن أجل تحقيق التطور المنشود، أنشأت الحكومة العراقية مركزًا للذكاء الاصطناعي بدعم حكومي،مقره في الجامعة الأمريكية- ببغداد.يمثل هذا المركز خطوة هامة نحو بناء قاعدة علمية وتكنولوجية تعزز دور العراق في الصناعة الرابعة، وتطوير قطاعاته المختلفة باستخدام تقنيات الذكاء الاصطناعي.

يواجه العراق تحديات كبيرة في مواكبة التطورات التكنولوجية العالمية، خصوصًا في مجال الذكاء الاصطناعي والأمن السيبراني. ورغم بعض التقدم، إلا أن تطبيقات الذكاء الاصطناعي في الصناعات، خاصةً الإستراتيجية منها،

مازالت محدودة جدًا. هذا يؤثر على استخدام الذكاء الاصطناعي، وتزيد المعاناة بسبب التهديدات المتزايدة في الأمن السيبراني،

ضعف البنية التحتية التكنولوجية في مناطق عديدة يعيق تنفيذ المشاريع الصناعية الإستراتيجية المتقدمة ،مما يؤخر العراق في اللحاق بالركب التكنولوجي العالمي. بالإضافة إلى ذلك،الاستثمارات التكنولوجية منخفضة، رغم سعي الحكومة لمواكبة العصر الرقمي والثورة الصناعية الرابعة.

نقص البرامج التعليمية المتخصصة في مجالات الذكاء الاصطناعي والأمن السيبراني يؤدي إلى نقص حاد في المهارات المطلوبة في السوق، ما يعيق تطوير الكوادر القادرة على مواكبة التغيرات السريعة. أهمية تطوير مناهج دراسية متخصصة في الجامعات،وتعزيز التعاون مع الشركات العالمية في مجال التكنولوجيا.

يتجه العالم نحو كفاءة استخدام الطاقة والاعتماد على مصادر طاقة نظيفة. ما فعله العراق لم يكن بالمستوى المطلوب في الحصول على نقد أجنبي وتشغيل القوى العاملة وتحريك الطلب في السوق. لكن على الصعيد التقني، لم تُستخدم تقنيات الذكاء الاصطناعي رغم مزاياها.

لم تنتشر بعد العدادات الذكية الجديدة التي تعمل بالذكاء الاصطناعيّ وحلول المنزل الذكي بشكل كبير.

من الواضح أن المعلومات الموجودة في النظام البيئي التصنيعي الرقمي المرتبط بشبكة الإنترنت بشكل كبير، تفتقر إلى نوع من العناية السريعة لتطوير العمل،على الرغم من مساعي الدولة العراقية للتحول الرقمي في جميع الصناعات، ومنها الإستراتيجية.

التوصيات

التشابه بين الذكاء الإنساني والذكاء الاصطناعي، مع قدرة الأخير الهائلة على التعلم وتحليل البيانات واتخاذ القرارات، أثّر على تسريع دخول التكنولوجيا إلى الصناعات، مما يتطلب من العراق مواكبة هذا التطور على الرغم من أنه قد يقلل من دور العنصر البشري.

أصبحت البيانات عنصر إنتاج جديد، ويتعزز نموّها بزيادة الأنشطة الرقمية، وأصبح يُنظر إليها كـ"إيراد الجديد"، لذا، على الجهات المعنية في الدولة العراقية اعتبار البيانات الذكية كأفضل من النفط؛ لأن ّاستهلاكها لا يقلّل منها بل يؤدّي إلى توليد المزيد منها.

على الحكومة العراقية الاهتمام بنمط الاستهلاك عبر الذكاء الاصطناعي وحجمه، أو ما يُعرف بالتخصيص المفرط، حيث يراقب الذكاء الاصطناعي المستهلكين عبر الإنترنت ويحفظ بياناتهم، ويُستفاد من هذه البيانات للتنبؤ باحتياجات العملاء.

يجب على وزارة الصناعة تحديدًا استخدام الذكاء الاصطناعي بشكل مكثف، فقد غيّر طريقة الإنتاج في معظم صناعات الدول المتقدمة ليجعلها أكثر كفاءة، مدعم زيادة الإنتاجية، وأثر تحسين الجودة على رأس المال وسوق العمل والمواد الخام والنقل والطاقة، ويُعد هذا القطاع الأكثر تأثراً، حتى أن البعض وصف تأثير الذكاء الاصطناعي عليه

بـ"الطاقة الجديدة"، حيث أدى التغيير الجذري إلى تغيير في حجم وسرعة ودقة الإنتاجية، وبالتالي التغيير في الاستهلاك وزيادته والناتج المحلي الإجمالي وتعزيز النمو الاقتصادي.

غيّر الذكاء الاصطناعي أسلوب الحياة والاستهلاك بطريقة أسهل وأسرع، وبالتالي تغيّر توزيع الأجور، مع مكاسب كبيرة لمن يستخدمون تقنيات الذكاء الاصطناعي، وظهرت تجارة جديدة وهي تجارة البيانات،التي أصبحت مدخلًا رئيسيًا في الإنتاج الاقتصادي الحديث،إلى جانب الأرض ورأس المال والعمالة والنفط، فهي عامل أساسي لعمل خوارزميات الذكاء الاصطناعي، ويُستنتج أن التغيير في القطاع الصناعي تبعه تغيير كبير في القطاع التجاري.

يجب على الحكومة العراقية الاستثمار في رأس المال البشري؛ لتسهيل الاستثمارات في رأس المال المادي، وتعزيز تطوير ونشر التقنيات الجديدة، والتي تؤثر على ناتج كل عامل،وبالتالي،هناك علاقة وثيقة بين مخزون التعليم ومستوى الناتج المحلي الإجمالي على المدى الطويل، مع مراعاة الاختلافات في جودة أنظمة التعليم في البلدان المختلفة.

على الرغم من مزايا الأتمتة في التصنيع،إلا أنها غير مناسبة لكل الأسواق العراقية، حيث يجب مراعاة العديد من العوامل:-

يُشترط توافر بنية تحتية تقنية متينة، مع إجراء تقييم فني لتحديد مدى صلاحيتها.

يجب توفّر أيدٍ عاملة ماهرة تُجيد التعامل مع هذه الآلات، وأيضاً كوادر تعمل على صيانة وتطوير الآلات.

في حال توافر اليد العاملة بتكلفة منخفضة، فان ألية تكون محدودة، ولا تُنفّذ على نطاق واسع كما في الحالة المعاكسة.

تحليل نسب استبدال العمالة بالآلات الجديدة، وتأثير ذلك على معدلات البطالة.

نرى من الضرورة ربط القطاع الصناعيّ بمراكز البحوث والتطوير،ونشر وتسويق الأبحاث التكنولوجية لتعزيز التنافسية، وإيجاد حلول بديلة أقل تكلفة، وتطوير المعدات،ورفع كفاءة استهلاك الطاقة.

المصادر

[1] Britannica, "Artificial intelligence", Retrieved 27/9/202

[2] Chatterjee,J., and Dethlefs, N."Developing Countries are being left behind in the AI race" The Conversation, 13 Apr 2022,

[3] Techjury.net, Info graphic, " How AI is being deployed across industries," RBR: robotics business , 5 Apr 2019

[4] AMFG, " 7 ways artificial intelligence is positively impacting manufacturing," 10 Aug 2018

[5] Kushmaro, P., "5 Ways Industrial AI is Revolutionizing Manufacturing," CIO Middle East, 27 Sep 2018,

[6] Blier, N., "Artificial Intelligence will Double Economic Growth: Here’s How," Lexalytics, 19 Sep 2017

[7] Demaitre, E., "Smart Manufacturing Trends Analyzed in GP" Ull Hound Report, 17 July 2019

[8] Eliasy, A., and Przychodzen, J., "The Role of AI in Capital Structure to Enhance Corporate Funding Strategies," Array Journal, Elsevier, Voume6, Jul 2020

[9] Gans, J., Agrawal, A., and Goldfarb, A., "Economic Policy for Artificial Intelligence," The University of Chicago Press Journals, Volume 19, 2018

[10] Evans, J., and Agolla, "Human Capital in The Smart Manufacturing and Industry 4.0 Revolution," Botswana Open University, Gaborone, Botswana, from the edited Volume,2018

[11] Barrick, G., "How Smart Workers Can Future-Proof Their Career Prospects," 22 Aug 2017

[12] Infinium Global Research members," Industry 4.0 Market Global Industry Analysis," Trends ,Size, Share and Forecasts to 2024, Infinium, Dec 2018,

[13] Ernst, E., Merola, R., and Samaan, D.," The Economics of Artificial Intelligence: Implications for the Future of Work, ILO Future Of Work" Research Paper Series, 2018

[14] Reed, A., "Smart Manufacturing for Smart Materials," 6 Apr 2017

[15] J.Kim, " Multifunctional Smart Biopolymer Composites" ,2017

[16] Industry ARC: "Analysis. Research. Counting, Smart Materials Market - Industry Analysis, Market Size, Share, Trends, Application Analysis," Growth And Forecast 2022 – 2027 report, 2022

[17] BC Hydro Power Smart Enterprise, " What is Strategic Energy Management?", 14 Jun 2016

[18] Rogers, E., "Integrating Strategic Energy Management and Smart Manufacturing Programs" Paper, Paper, American Council for an Energy-Efficient Economy (ACEEE), USA, page 24.2018

[19] Lee, H., Yoo, S., Kim, Y., W.," An Energy Management Framework for Smart Factory Based on Context-Awareness", 2016 18th International Conference on Advanced Communication Technology (ICACT), Pyeongchang, South Korea, 31 Jan.-3 Feb. 2016

[20] Davis, B.," How Industry 4.0 can Impact Energy," 6 Jun 2019

[21] I-scoop, " Energy efficiency as a Core Component of Industry 4.0 " The Building Perspective, 2019

[22] Adonis, D., " The Impact of Industry 4.0 on the Transport Logistics Sector" ,2020

[23] Paprocki, W., " How Transport and Logistics Operators Can Implement the Solutions of Industry 4.0," Transport Conference Paper, Research gate, Mar 2017

[24] Mzur, S., " An Introduction to Smart Transportation": Benefits and Examples 9 Dec 2020

[25] Allied Market Research Report, " Industry 4.,Market by Component Global Opportunity" Analysis and 2019,Industry Forecast, 2019-2026

Investigating parasitic protozoa and studying some properties of drinking water at the water treatment plant Al-Dour district – Salahalddin

التحري عن الأوالي الطفيلية ودراسة بعض خواص مياه الشرب في محطة اسالة قضاء الدور- صلاح الدين

Marwan Abdulrazzaq Kamil

Al Dour Technical Institute/ Iraq/Northern Technical University

ntu.edu.iq.@marwan.kamil

Investigating parasitic protozoa and studying some properties of drinking water at the water treatment plant Al-Dour district – Salahalddin

التحري عن الأوالي الطفيلية ودراسة بعض خواص مياه الشرب في محطة اسالة قضاء الدور- صلاح الدين

Marwan Abdulrazzaq Kamil

Al Dour Technical Institute/ Iraq/Northern Technical University

م.م. مروان عبدالرزاق كامل
الجامعة التقنية الشمالية – المعهد التقني / الدور
ntu.edu.iq.@marwan.kamil

Abstract

The study was conducted in Al-Dour district, located within Salah Al-Din Governorate. It included various tests and analyses of four water treatment plants, including microscopic examinations to search for some parasites using a light microscope. It also included other aspects and tests of some of the properties of the water from the Al-Dour district water treatment plant. This was done through tests that were carried out regarding the physical and chemical properties of the aqueous samples.

The results regarding the examination of the studied samples, both visually and microscopically, showed the absence of parasites, which is an important indicator of the quality of water suitable for human use. Other water tests were also within standard specifications, whether physical or chemical, for the period from August 2024 to January 2025 , The pH analysis recorded values close between 7.25 - 8.55, and as for turbidity, it was recorded between 3.29 - 43.5 NTU. The total alkalinity recorded varying results ranging from 156 to 80 mg/L, while the sulfate analysis results recorded values between 87.766 - 57.166 mg/L, while the oxygen concentration recorded values of 3.9 - 6.2 , The analysis of the biological oxygen demand ranged between 0.4-1.5 mg/L, while the heavy metals had low values, with nitrates recording values between 0.1-2.7 mg/L and iron 0.02-0.13 mg/L.

Keywords: protozoa, parasites, drinking water, water quality.

الخلاصة

اجريت الدراسة في قضاء الدور الواقع ضمن محافظة صلاح الدين, وقد شملت فحوصات وتحاليل مختلفة لأربع من المحطات في الاسالة, منها مجهري بحثاً عن بعض الطفيليات وذلك باستخدام جهاز المجهر الضوئي, وكذلك شمل جوانب وفحوصات اخرى لبعض من خواص مياه محطة اسالة قضاء الدور, وتم ذلك من خلال الفحوصات التي تم اجرائها فيما يتعلق بالصفات الفيزياوية والكيميائية للعينات المائية.

وبينت النتائج فيما يخص الفحص في العينات المدروسة عياناً و مجهرياً بعدم وجود للطفيليات, ما يدل مؤشراً مهماً على نوعية المياه الصالحة للاستخدام البشري, وكذلك الفحوصات الاخرى للمياه كانت ضمن المواصفات القياسية سواء كانت فيزيائية او كيميائية, للمدة من شهر اب 2024 لغاية كانون الثاني 2025, حيث سجل تحليل pH قيماً متقاربة ما بين 8.55 – 7.25 , وفيما يخص العكورة فقد سجلت ما بين 43.5 – 3.29 NTU , كما سجلت القاعدية الكلية نتائج متفاوتة تراوحت 80-156 ملغم /لتر , في حين نتائج تحليل الكبريتات سجلت قيمها ما بين 57.166-87.766 ملغم /لتر, بينما تركيز الأوكسجين سجل القيم 3.9 -6.2, فيما تراوح تحليل متطلب الحيوي للأوكسجين ما بين 0.4 -1.5 ملغم/ لتر, اما فيما يخص العناصر الثقيلة فكانت لها قيم قليلة , اذ سجلت النترات قيم ما بين 0.1-2.7 ملغم/ لتر, والحديد 0.02-0.13 ملغم/ لتر.

الكلمات المفتاحية : الاوالي , الطفيليات , مياه الشرب, نوعية المياه.

المقدمة:

ان للطفيليات أهمية كبيرة في تقييم جودة مياه الأنهار، خاصةً عند استخدامها للاستهلاك البشري، وبالتالي، يمكن أن تنقلها مياه الشرب، مما يُشكل عامل خطر في انتقال الأمراض الطفيلية المنقولة بالمياه. لذلك، تشترط بعض المتطلبات في الدول، مثلاً في الإكوادور INEN 1108، خلو مياه الشرب من الطفيليات كشرط لجودة المياه(Bourli et al., 2023 ; Sanchez, 2017).

يعد النهر الجزء الأساسي للموارد الطبيعية والتي من بينها مياه الشرب وغيرها. ومع ذلك، فقد استُخدمت الأنهار أيضًا كمستقبلٍ ووسيلة نقلٍ للنفايات غير المرغوب فيها. لذلك، تمثل الأنهار أيضًا كناقلٍ للكائنات الحية المجهرية المرتبطة بالأمراض المنقولة بالمياه، والتي قد تكون بكتيرية أو فيروسية أو طفيلية، وبدرجةٍ أقل فطرية (Certad et al., 2017 ; Vogt et al., 2023). كما ان المصدر الرئيسي للتلوث الاحيائي في الانهار هو المواد البرازية سواء كانت قادمة بشكل رئيسي من تصريفات مياه الصرف الصحي المنزلية او بشكل بأي وسيلة اخرى, والتي تحمل بكتيريا وطفيليات معوية من الكائنات الحية الماصة للحرارة (Molina et al., 2024 ; Wang et al ., 2020 ; Wen et al., 2020), الا ان عمليات التطهير المستخدمة قد تؤدي للقضاء على الطفيليات, مثال ذلك تُضاف جرعة صغيرة من الكلور للحفاظ على تأثير متبقي دائم عند نقل المياه عبر شبكة التوزيع. ومع ذلك، فإنه ليس مجديًا اقتصاديًا في الدول النامية في معظم الحالات. لذلك، سيظل خطر انتقال الطفيليات من خلال استهلاك مياه الشرب (Ashoke & Khedikar ,2016 ; Shi et al .,2021), كما ان الهدف من وحدات معالجة

المياه بشكل رئيسي هو الحصول على مياه نقية تكون صالحة الاستهلاك والاستخدام البشري، ويتم من خلال إزالة وقتل الكائنات الحية الموجودة في المياه والتخلص من الطعم والرائحة واللون والكدرة الزائدة والبعض من المعادن الذائبة وغيرها من المواد الضارة وغير المرغوب فيها(CRC,2008).

ان جودة المياه مرتبط بالعناصر الموجودة في الماء التي تؤدي دوراً هام في تحقيق النمو الأمثل للكائنات المائية. وتتأثر جودة المياه بالعوامل الفيزيائية او الكيميائية او البيولوجية والتي تؤثر ايضاً على الكائنات الحية كالأسماك او غيرها من الكائنات الحية(Ahmed et al ., 2024)علاوة على ذلك، يلعب التلوث البيئي ببراز الحيوانات المصابة بالطفيليات دورًا هامًا في انتقال الامراض. وقد أفادت بعض الدراسات بوجود تفاعلات بين استهلاك الإنسان للمياه وبراز الحيوانات شبه المنزلية التي قد تكون مصابة(Pinto Linaza, 2020 ; Castro-Hermida et al .,2011 ; Omarova et al ., 2018), وقد دفعت قدرة الكائنات الحية على التكاثر في أنظمة إمدادات المياه الاتحاد الأوروبي إلى إدخال مبدأ توجيهي جديد بشأن المياه المخصصة للاستهلاك البشري, انها خالية من أي كائنات دقيقة أو طفيليات أو مواد، بكمية أو تركيز قد يسبب خطرًا محتملاً على صحة الإنسان. وقد تبنت منظمة الصحة العالمية موقفًا مماثلاً، حيث تصنف الأمراض المنقولة بالمياه على أنها تلك التي تكمل فيها الكائنات المسببة جزءًا من دورة حياتها داخل الماء, وقد تصدرت القائمة الطفيليات(Ríos-Tobón et al .,2017 ; Sun et al .,2023).

المواد وطرائق العمل:

اولاً : منطقة الدراسة:

تقع منطقة الدراسة في قضاء الدور من الاتجاه الشمالي الواقعة قرب نهر دجلة , المبينة بالصورة رقم(1) والتي هي ضمن قاطع محافظة صلاح الدين.

صورة رقم(1):- توضح منطقة الدراسة.

وقد اخذت العينات للدراسة للمدة من شهر اب 2024 والى كانون الثاني 2025. وتم تحديد اربع محطات كما في ادناه:

1- المحطة (W1):

تمثل هذه المحطة الحوض الابتدائي للترسيب.

2- المحطة(W2) :

تتمثل هذه المحطة بحوض الترسيب الثانوي وتقع هذه المحطة في داخل محطة تقية مياه الشرب.

3- المحطة(W3):

تمثل بحوض الترسيب الرئيسي(الفلتر) وتقع داخل المحطة.

4- المحطة(W4):

هذه المحطة هي المحطة النهائية, وتقع خارج محطة التنقية لمياه الشرب, أي تمثل الماء الواصل للمنزل.

جمع العينات:

جمعت العينات من المحطات باستخدام القاني من النوع غير الشفافة (تكون معتمة), للمدة من اب 2024 لغاية كانون الثاني 2025, ثم نقلت العينات للمختبر وتم اجراء الفحوصات تحت المجهر فيما يخص الطفيليات , وايضاً اجراء لبعض من الفحوصات للمياه تمثلت بالفحوصات الفيزيائية والكيميائية (APHA,2003).

ثانياً :الفحوصات المختبرية:

تضمنت فحوصات وتحاليل مختلفة لعينات المياه منها مجهرياً بحثاً عن الطفيليات, وكذلك فحوصات فيما يخص بعض من صفات المياه, وقد شملت الفحوصات ما يلي:

1- الفحص المجهري للتحري عن الطفيليات:

استخدم جهاز المجهر الضوئي, بحثاً عن احتمالية تواجد الاحياء الدقيقة (الطفيليات), وقد تم باستخدام المسحة المباشرة , اذ وضعت عينات المياه في انابيب حجم (10 مل) ثم وضعت في جهاز الطرد المركزي, ثم اخذت مسحة منها بطريقة التطويف, وكذلك اخذ مسحة من القعر ووضعت على السلايد. وقد استخدم محلول لوكل ايودين للتصبيغ, ثم وضع غطاء الشريحة ومن ثم فحصت تحت المجهر, حسب ما موصوف في (Henrikson & pholen, 1981).

ثالثاً : الفحوصات الفيزيائية والكيميائية:

تضمنت اجراء الفحوصات المبينة ادناه, والتي شملت التحاليل الفيزيائية والكيميائية لعينات المياه وفق الطرق الموصوفة في (APHA, 2003 ; ASTM,1984) :

1- تركيز اس الهيدروجين.

2- العكورة.

3- القاعدية الكلية.

4- الكبريتات.

5- تركيز الاوكسجين.

6- تركيز BOD5.

7- النترات .

8- الحديد.

النتائج والمناقشة:

أولاً : الفحص المجهري:

بعد اجراء عملية التحضير للسلايد واجراء الفحص المجهري , فأن النتائج بينت انه لم يلاحظ وجود أنواع من الطفيليات, طيلة مدة الدراسة. وقد دلت اللائحة الاكوادورية على ان خلو المياه من الطفيليات بمثابة دليل او شرط على صلاحية المياه للاستخدام البشري (Bourli et al., 2023 ; Sanchez, 2017).

ثانياً : الفحوصات الفيزيائية والكيميائية:

1- تركيز اس الهيدروجين:

أظهرت النتائج في الجدول (1) قيم pH والتي كانت ما بين 8.55 – 7.25 , فقد كانت القيمة العليا عند شهر تشرين الثاني 2024, في حين سجلت ادنى قيمة في شهر كانون الثاني 2025. وهذه القيم توافقت مع ما حصل عليه محمد(2024) من نتائج والتي كانت ما بين 8 – 7.3 .

جدول رقم(1):- يبين قيم pH موزعة مكانياً وزمانياً

العينات / الأشهر	W1	W2	W3	W4
اب2024	7.71	7.74	7.48	7.81
ايلول2024	7.89	8.13	8.02	7.92
تشرين الاول2024	8.2	8.36	8.53	8.50
تشرين الثاني2024	8.45	8.28	8.51	8.55
كانون الأول2024	7.91	7.63	8.02	8.36
كانون الثاني2025	7.53	7.25	8.09	8.53

2- العكورة:

أظهرت نتائج العكورة في الجدول (2), بوجود فروقاً في القيم زمانياً في المحطات, وكذلك مكانياً خلال بعض الأشهر, وقد جاءت القيم ما بين 3.29 – 43.5 NTU , حيث سجل اعلى قيمة في شهر أيلول 2024 في المحطة رقم (W4) , في حين أدنى قيمة كانت قد سجلت في كانون الثاني2025 عند المحطة (W2). وتوافقت النتائج بشكل متقارب مع صالح(2025) والبياتي(2023) واللذان سجلا قيم كانت ما بين3.3-34.2 و 0.56-35.2 NTU على التوالي.

جدول رقم(2):- يبين قيم العكورة مكانياً وزمانياً

العينات / الأشهر	W1	W2	W3	W4
اب2024	15.2	12.1	16.9	11.6
ايلول2024	39.7	42.0	43.3	43.5
تشرين الأول 2024	13.2	11.5	11.8	14.3
تشرين الثاني 2024	15.1	24.6	40.7	21.4
كانون الأول 2024	10.7	13.8	14.1	11.3
كانون الثاني 2025	4.95	3.29	6.7	5.41

3- القاعدية الكلية :

تبين النتائج في الجدول (3) قيم للقاعدية الكلية والتي تظهر النتائج جاءت ما بين 80 - 156 ملغم/ لتر, فقد سجلت القيمة العليا في شهر ايلول 2024 , في حين القيمة الدنيا سجلت في شهر اب 2024.

هذه القيم اقل من ما حصل عليه صالح(2025) من نتائج والتي كانت ما بين 120 – 190 , وتوافقت مع المجمعي(2024) اذ سجل 40-160 ملغم / لتر .

جدول رقم(3):- يبين قيم القاعدية الكلية موزعة مكانياً وزمانياً

العينات / الأشهر	W1	W2	W3	W4
اب2024	106	80	144	110
ايلول2024	146	148	156	154
تشرين الاول2024	146	142	140	144
تشرين الثاني2024	106	128	108	124
كانون الأول2024	119	126	122	120
كانون الثاني2025	138	132	134	136

4- الكبريتات:

سجلت نتائج الكبريت الموضحة في الجدول رقم(4) , بأن القيم قد سجلت ما بين 57.166 – 87.766 ملغم/ لتر , حيث سجلت القيمة العليا عند شهر كانون الثاني 2025 , في حين القيمة الأدنى في شهر ايلول 2024. وقد توافقت النتائج مع ما سجله محمد(2024), و حمد(2025) والتي كانت قيم نتائجهما – 86 66 و 60.2-86.6 ملغم/لتر وبشكل متوالي.

جدول رقم(4):- يبين قيم الكبريتات موزعة مكانياً وزمانياً

العينات / الأشهر	W1	W2	W3	W4
اب2024	59.366	58.966	59.366	57.366
ايلول2024	59.366	58.366	59.166	57.166
تشرين الاول2024	64.966	67.166	62.566	62.766
تشرين الثاني2024	72.766	72.966	74.366	71.966
كانون الأول2024	77.366	80.166	76.566	74.166
كانون الثاني2025	83.966	87.766	80.566	83.166

5- تركيز الاوكسجين:

سجل الاوكسجين تركيزه المبين في جدول رقم(5), ما بين 3.9 – 6.2 ,سجل قيمته العليا عند شهر تشرين الثاني 2024 , في حين القيمة الدنيا جاءت في شهر اب 2024. وتوافقت النتائج مع المجمعي(2025) حيث قد سجل القيم بين 3.83-6.88 ملغم/ لتر , وقد كانت النتائج اقل من ما سجله فتاح(2022) 3.8-9 ملغم/ لتر على التوالي.

جدول رقم(5):- يبين قيم الاوكسجين موزعة مكانياً وزمانياً

العينات / الأشهر	W1	W2	W3	W4
اب2024	4.3	5.4	4.2	3.9
ايلول2024	4.4	4.9	4.8	5.0
تشرين الاول2024	5.5	5.3	4.8	4.5
تشرين الثاني2024	6.2	5.8	5.4	5.9
كانون الأول2024	5.7	5.5	5.2	5.7
كانون الثاني2025	5.1	5.3	5.4	5.3

6- تركيز BOD5:

سجلت متطلب الاوكسجين الحيوي تركيزاً له والمبين في الجدول رقم(6), ما بين 0.4 – 1.5 ,سجل قيمته العليا في شهر اب 2024 , اما القيمة الدنيا جاءت في شهري تشرين الأول2024 وكانون الثاني 2025, وقد كانت النتائج متقاربة مع ما حصل عليه الجبوري (2025) والتي كانت 0.6-2.5 ملغم/ لتر.

جدول رقم(6):- يبين قيم BOD5 موزعة مكانياً وزمانياً

العينات / الأشهر	W1	W2	W3	W4
اب2024	1.4	1.5	0.7	0.5
ايلول2024	1.2	1.2	0.6	0.5
تشرين الاول2024	1.1	1.0	0.4	0.4
تشرين الثاني2024	0.8	1.1	0.5	0.8
كانون الأول2024	0.7	0.9	0.7	0.5
كانون الثاني2025	0.4	0.9	0.8	0.4

7- النترات :

أظهرت قيم النترات تركيزاً لها والمبينة في الجدول رقم(7), ما بين 0.1 – 2.7 , وقد سجل قيمته العالية عند شهر تشرين الاول 2024 , في حين القيمة الدنيا جاءت في شهر أيلول 2024, وقد كانت النتائج متقاربة مع ما حصل عليه الجبوري (2025) و محمد(2025) والتي كانت – 0.001-1.1 ملغم/ لتر, و 0.9-3.17 ملغم / لتر على التوالي.

جدول رقم(7):- يبين قيم النترات موزعة مكانياً وزمانياً

العينات / الأشهر	W1	W2	W3	W4
اب2024	1.3	1.1	1.3	1.8
ايلول2024	1.4	0.6	1.4	0.1
تشرين الاول2024	1.2	2.7	1.6	2.2
تشرين الثاني2024	1.4	1.8	1.4	1.9
كانون الأول2024	1.6	1.6	1.4	1.8
كانون الثاني2025	1.1	1.3	1.2	0.9

8- الحديد :

سجل الحديد قيم متدنية حيث تراوحت 0.02 – 0.13 ملغم/ لتر, والمبينة في الجدول رقم (8) , وقد سجلت القيم اعلاها كان في شهر أيلول 2024 , في حين ان القيمة الدنيا سجلت عند الأشهر تشرين الأول و تشرين الثاني 2024, وفي شهر كانون الثاني2025 . وجاءت النتائج متقاربة مع نتائج محمد(2025) والذي سجل نتائج تراوحت بين 0.05-0.232 ملغم/ لتر.

جدول رقم(8):- يبين قيم الحديد موزعة مكانياً وزمانياً

العينات / الأشهر	W1	W2	W3	W4
اب2024	0.03	0.03	0.08	0.03
ايلول2024	0.13	0.04	0.03	0.07
تشرين الاول2024	0.03	0.02	0.02	0.03
تشرين الثاني2024	0.03	0.04	0.03	0.02
كانون الأول2024	0.11	0.05	0.04	0.03
كانون الثاني2025	0.03	0.02	0.04	0.03

الاستنتاجات(Conclusions)

1. أثبتت نتائج الفحص المجهري خلو جميع عينات المياه من الطفيليات خلال مدة الدراسة (آب 2025 – كانون الثاني 2025)، مما يعزز صلاحية المياه للاستهلاك البشري من الناحية البايولوجية.
2. أظهرت الخصائص الفيزياوية والكيميائية للمياه بأنها جميعها كانت ضمن الحدود القياسية المسموح بها، مما يشير إلى استقرار نوعية المياه وعدم تعرضها لتلوث واضح خلال فترة الدراسة.
3. بالاعتماد على مجموع النتائج، فإن مياه محطات الإسالة الأربعة في قضاء الدور آمنة وصالحة للاستخدام البشري، وخالية من المخاطر البايولوجية (الطفيلية) والكيميائية ضمن فترة الدراسة.

التوصيات(Recommendations)

1. الاستمرار بعمليات المراقبة الدورية للطفيليات والمؤشرات البايولوجية، لضمان الاستمرارية في جودة المياه وعدم حدوث تغيرات مستقبلية.
2. توسيع الدراسة لتشمل فصول سنة كاملة لضمان فهم أعمق للتغيرات الموسمية في جودة المياه.
3. تشجيع إجراء دراسات مشابهة في الأقضية المجاورة في محافظة صلاح الدين.

المصادر

1- المصادر العربية:

1. محمد, رفل احمد مجيد(2024). دراسة بيئية لتقييم كفاءة محطة تصفية مياه الشرب لمدينة تكريت ضمن محافظة صلاح الدين. رسالة ماجستير- كلية التربية للبنات - جامعة تكريت- العراق.
2. حمد, براء محمد(2025). تقييم كفاءة مشروع بيجي الكبير وتحديد مدى مطابقة مياه الشرب للمواصفات القياسية. رسالة ماجستير-كلية التربية للبنات- جامعة تكريت- العراق.

3. فتاح, مادين علي عباس (2022). التقييم البيئي لمياه نهر دجلة ومياه مخلفات الصرف الصحي والصناعي ضمن مدينة سامرا. رسالة ماجستير- كلية التربية- جامعة سامراء- العراق.

4. محمد, فاطمة حسن سلطان(2025). تقييم الصفات اللمونولوجية وتراكيز بعض العناصر الثقيلة في مياه واسماك نهري دجلة والزاب الاسفل في محافظة كركوك. رسالة ماجستير- كلية التربية للعلوم الصرفة- جامعة كركوك- العراق.

5. البياتي, ايه كاطع جهاد(2023). دراسة الخصائص الفيزيائية والكيميائية والبكتريولوجية لعينات من مياه مجحطة اسالة مشروع طوز – كفري الموحد ضمن محافظة صلاح الدين. رسالة ماجستير- كلية التربية للبنات - جامعة تكريت- العراق.

6. المجمعي. تبارك مدين عبد(2024). تقييم الخصائص النوعية وكفاءة محطة اسالة الاسحاقي- محافظة صلاح الدين. رسالة ماجستير- كلية التربية للبنات - جامعة تكريت- العراق.

7. صالح, هدى فاهم ذياب(2025). تقييم الخصائص الفيزيائية والكيميائية والحيوية لكياه نهر دجلة المار بمدينة الضلوعية- صلاح الدين. رسالة ماجستير- كلية التربية للبنات - جامعة تكريت- العراق.

2- **المصادر الإنكليزية:**

1. Ahmed, A. H., Kamel, T. M., and Zain Al-Abdeen, S. S. (2024). Evaluation of physical and chemical properties of aquarium waters in Kirkuk. International Journal of Agriculture and Animal Production, 4(6), 45-55. doi: 10.55529/ijAAS p.46.45.55.
2. APHA, American Public Health Association.(2003). Standard Methods for the Examination of water and wastewater, (20thed).A.P.H.A.1015 Fifteenth Street, NW. Washington. DC, USA.
3. Ashok, A.; Khedikar, I.(2016). Overview of Water Disinfection by UV Technology—A Review. Int. J. Sci. Technol. Eng. 2016.
4. ASTM, American Society for testing and Materials. (1984). Annual Book of ASTM standard Water Printed in Easton Md. U.S.A. 1129 pp.
5. Bourli, P.; Eslahi, A.V.; Tzoraki, O.; Karanis, P.(2023). Waterborne Transmission of Protozoan Parasites: A Review of Worldwide Outbreaks—An Update 2017–2022. J. Water Health 2023, 21, 1421–1447.
6. Castro-Hermida, J.A.; García-Presedo, I.; Almeida, A.; González-Warleta, M.; Correia Da Costa, J.M.; Mezo, M. (2011). Cryptosporidium Spp. and Giardia Duodenalis in Two Areas of Galicia (NW Spain). Sci. Total Environ. 2011, 409, 2451–2459.
7. Certad, G.; Viscogliosi, E.; Chabé, M.; Cacciò, S.M. (2017). Pathogenic Mechanisms of Cryptosporidium and Giardia. Trends Parasitol. 2017, 33, 561–576.
8. CRC(cooper Research Center)،(2008). *Drinking water Facts. Issue Drinking water for water Quality and treatment Australia :P4.*
9. Henriksen, S.A. & Pholenz, J.F.L. (1981). Staining of Cryptosporidia by a modified Zheil-Neelsen Technique . Act. Vet. Scand. 22: 594- 596.

10. Molina, C.A.; Quiroz-Moreno, C.; Jarrín, V.P.; Díaz, M.; Yugsi, E.; Pérez-Galarza, J.; Baldeón-Rojas, L.(2024). Bacterial Community Assessment of Drinking Water and Downstream Distribution Systems in Highland Localities of Ecuador. J. Water Health 2024, 22, 536–549.

11. Omarova, A.; Tussupova, K.; Berndtsson, R.; Kalishev, M.; Sharapatova, K.(2018). Protozoan Parasites in Drinking Water: A System Approach for Improved Water, Sanitation and Hygiene in Developing Countries. Int. J. Environ. Res. Public Health 2018, 15, 495.

12. Pinto Linaza, A.X. (2020).Cryptosporidium y Giardia Como Parásitos de Transmisión Hídrica En Las Islas Canarias. Master's Thesis, Repositorio Institucional ULL, Universidad de la Laguna, La Laguna, Spain.

13. Ríos-Tobón, S.; Agudelo-Cadavid, R.M.; Gutiérrez-Builes, L.A. (2017). Patógenos e Indicadores Microbiológicos de Calidad Del Agua Para Consumo Humano. Rev. Fac. Nac. Salud Pública 2017, 35, 236–247.

14. Sanchez, C.(2017). Detección y Caracterización Molecular de Los Parásitos de Interés En Salud Pública: Giardia Duodenalis, Cryptosporidium Spp., Cyclospora cayetanensis, Toxoplasma gondii y Entamoeba Histolytica, En Agua Cruda y Tratada de Cuatro Plantas Potabilizadoras Del Departamento de Nariño Colombia; Universidad Nacional de Colombia: Bogotá, Colombia, 2017.

15. Shi, Q.; Chen, Z.; Liu, H.; Lu, Y.; Li, K.; Shi, Y.; Mao, Y.; Hu, H.-Y. (2021). Efficient Synergistic Disinfection by Ozone, Ultraviolet Irradiation and Chlorine in Secondary Effluents. Sci. Total Environ. 2021, 758, 143641.

16. Sun, J.; Qin, Z.; Fu, Y.; Qin, H.; Sun, M.; Dong, H.; Chao, L.; Zhang, L.; Li, J.(2023). Assessment of Potential Zoonotic Transmission of Giardia Duodenalis from Dogs and Cats. One Health 2023, 17, 100651.

17. Vogt, R.D.; Porcal, P.; Hejzlar, J.; Paule-Mercado, M.C.; Haaland, S.; Gundersen, C.B.; Orderud, G.I.; Eikebrokk, B.(2023). Distinguishing between Sources of Natural Dissolved Organic Matter (DOM) Based on Its Characteristics. Water 2023, 15, 3006.

18. Wang, Y.; Cao, J.; Chang, Y.; Yu, F.; Zhang, S.; Wang, R.; Zhang, L.(2020). Prevalence and Molecular Characterization of Cryptosporidium Spp. and Giardia duodenalis in Dairy Cattle in Gansu, Northwest China. Parasite 2020, 27, 62. [CrossRef]

19. Wen, X.; Chen, F.; Lin, Y.; Zhu, H.; Yuan, F.; Kuang, D.; Jia, Z.; Yuan, Z.(2020). Microbial Indicators and Their Use for Monitoring Drinking Water Quality—A Review. Sustainability 2020, 12, 2249.

Evaluation of cholecystokinin levels and some biochemical variables in children with neonatal jaundice

Nadia Yousif Salih

Al-Dour Technical Institute, Northern Technical University, Iraq

nadia.ys@ntu.edu.iq

Evaluation of cholecystokinin levels and some biochemical variables in children with neonatal jaundice

Nadia Yousif Salih

Al-Dour Technical Institute, Northern Technical University, Iraq

nadia.ys@ntu.edu.iq

Abstract

Jaundice is a natural phenomenon that recurs constantly and then gradually disappears. A large percentage of newborns suffer from yellowing of the skin and eyes, which is called neonatal jaundice. This research study was conducted in the laboratory department of Tikrit Teaching Hospital in Salah al-Din Governorate, as well as in some private laboratories affiliated with Tikrit city, from March 15, 2025, to September 15, 2025. The study groups included (60) samples of children aged between (1-7) days and were distributed into two groups. The first group included 30 blood samples from healthy children, and 30 blood samples from children with jaundice after confirming that they had a bilirubin level of (15.5-30) mg/dl after conducting tests for the disease and referring them to the doctor. Then, blood was taken from both groups, and separated by centrifugation, and then the biochemical parameters were estimated, which included (bilirubin, C-reactive protein-CRP, glucose, Cholecystokinin-CCK, Potassium-K, Calcium-Ca, Glutathione-GSH, Malondialdehyde-MDA). The results of the present study showed that significant changes occurred in each of the studied variables in the blood serum of children with jaundice compared to the healthy subjects, at a $P \leq 0.05$.

Keywords: **cholecystokinin , biochemical , neonatal jaundice.**

Introduction

Neonatal jaundice is one of the common diseases in newborns. It is called neonatal hyperbilirubinemia, as bilirubin, which is the yellow pigment, accumulates in the extracellular fluids, in the conjunctival membranes of the eye, and in other membranes. It usually appears during the first days after birth, as the skin color turns yellow and appears on the face and sometimes extends to the lower chest (1). It is one of the diseases that causes concern for doctors and parents, as it causes critical complications for newborns and

increases the length of their stay in the hospital and the possibility of them being readmitted to it again (2). Jaundice has many negative effects that require both children and their families to admit newborns to the hospital or to readmit them again during the first month, especially in the first week of the newborn's life. Since maternal and child-related variables during labor and environmental factors affect the course and severity of neonatal jaundice, which are related to the perinatal period and are linked to the occurrence of neonatal hyperbilirubinemia, these factors can be managed and modified (3,4). The bile in the liver collects in the gallbladder in a greater proportion than necessary, and it often affects newborns and premature infants born before the 36th week of pregnancy. It results from the breakdown of red blood cells, especially hemoglobin in the blood, which turns into bile, called bilirubin (5).

The most important causes of jaundice are high levels of bilirubin resulting from the breakdown of a large number of red blood cells, blockage of the bile ducts, deficiency in the representation of liver cells responsible for secreting bilirubin into bile, low levels of the enzyme G6PD (glucose-6-phosphate dehydrogenase), and infection with the hepatitis C virus (6).In addition to factors related to the child, such as congenital trauma (birth injury), low birth weight, birth asphyxia, G6PD deficiency, males being more affected than females, hyperemia, and sepsis (blood poisoning).Congenital hepatitis (neonatal hepatitis), congenital diseases, rubella and hypothyroidism, hereditary syndromes, cholestasis syndrome, in addition to blood group or Rh factor (Rh) incompatibility between mother and child (7,8). Children with jaundice are accompanied by a group of symptoms such as discoloration of their bodies and visible mucous membranes, a change in the skin color to yellow, constant drowsiness, weakness and lethargy, the child's urine is dark, in addition to the yellowing of the whites of their eyes, and the child's stool is light in color. In addition to swelling of their legs and distension of their abdomen due to fluid accumulation, high fever, and weight loss, newborns with severe hyperbilirubinemia are at risk of neurological dysfunction when bilirubin crosses the brain barrier to reach the cerebellum and hypothalamic nuclear bodies. It causes neurotoxicity through acute programmed cell death, which manifests as acute encephalopathy leading to cerebral palsy, seizures, and sensorineural hearing loss (9,10).

Sufficient maternal knowledge and early awareness to avoid jaundice and seek health care are among the most important basic components of effective and correct management in controlling neonatal jaundice (11). The treatment of jaundice depends on the concentration of

bilirubin in the blood for the correct diagnosis of hyperbilirubinemia in newborns (12). Several methods have been used to treat cases of neonatal jaundice among children, including non-medical and traditional methods that have been circulated and used by many mothers and grandmothers. It was found that many families use these methods, which consist of giving the sick newborn water mixed with sugar or cumin, and attaching a piece of gold jewelry or a garlic plant around the child's neck. They also use some precious stones and beads (13).

C-reactive protein (CRP) is a diagnostic marker for neonatal jaundice. It is an acute-phase protein belonging to the Pentraxin family, which is produced at low concentrations by liver cells and plays a key role in innate and adaptive immunity. This index can be used in conjunction with WBC as an effective indicator in the diagnosis of pathological jaundice and early clinical intervention caused by bacterial infection in newborns, which can reduce the risk of clinical complications in newborns and help in assessing the disease, guiding treatment, and predicting the desired effectiveness of treatment (14,15).

Cholecystokinin is a peptide hormone responsible for the digestion of fats and proteins. This hormone is produced by the first section of the small intestine in response to the presence of partially digested food in the duodenum, causing the gallbladder to contract and thus secrete bile into the intestine. It is also a neurotransmitter. The main function of the smooth muscle in the digestive tract is to mix and push the contents and nutrients into the intestine in a coordinated manner (16). Cholecystokinin acts directly on smooth muscles, where its effect is always contractile, while the nerve-mediated effect is either contractile or relaxing, depending on the nature of the nerve impulse responsible for the action of cholecystokinin (17).

Electrolytes are considered one of the essential elements that are important for prolonging life and maintaining good human health, as human blood contains 0.9% of various salts, and these electrolytes enter into the composition of many vital compounds in the body such as enzymes, hormones and vitamins, or combine with another chemical composition such as iron in the heme compound or calcium phosphate in the bones (18).In addition, the diffusion of electrolytes between the fluid inside and outside the cells depends on their ionization into positive and negative ions, which play an important role in maintaining and controlling various physiological activities, such as maintaining water balance and its distribution within the body. It contributes to controlling the level of osmotic pressure and acid balance in the body, and the rise and fall of its level plays a fundamental role in newborn patients

(19).Through the increase in some special indicators in neonatal jaundice and the hyperbilirubinemia in their bodies, the current research aimed to investigate the effect of high bilirubin on some biochemical and mineral variables in children with neonatal jaundice in the city of Tikrit.

Material and Methods

Sample Collection

This research study was conducted in the laboratory department of Tikrit Teaching Hospital in Salah al-Din Governorate and some private laboratories affiliated with Tikrit city for a period from 3/15/2025 to 9/15/2025. The study groups included (60) samples of children aged between (1-7) days and were distributed into two groups. The first group included 30 blood samples from healthy children, and 30 blood samples from children with jaundice after confirming that they had a bilirubin level of (15.5-30) mg/dl after conducting tests for the disease and referring them to the doctor. Then, blood was taken from both groups and separated by a centrifuge, then the biochemical markers were assessed, which included (bilirubin, CRP, F.B.G, CCK, K, calcium, GSH, MDA).

Estimation of total serum bilirubin

The amount of Total Serum Bilirubin in blood serum was measured by the Sulfanilic Acid Method using a ready-made kit supplied by the French company BIOLABO.

Estimation of Serum C-reactive protein

C-reactive protein concentration was measured by the AFIAS CRP device. 0.5 ml of blood serum from each child was placed in the device, which operated according to the manufacturer's instructions. After providing the patient's personal information, such as name, gender, and age, 200 µL is automatically drawn from the tube, and the required readings are completed accurately. The device gives the result within 5 minutes and is automatically printed and withdrawn on paper.

Estimation of serum glucose level

The serum glucose level of jaundiced children was estimated using the colorimetric enzyme method and according to the Dingeon method (20).

Estimation of serum levels of (CCK, GSH, MDA)

The Concentrations of (CCK, GSH, MDA) were determined based on the Fin Test-China kit.

Statistical analysis

The results were analyzed using SPSS and using the F-test to analyze the results between sick and healthy children at a probability level of ($P \leq 0.05$).

Result and Desiccation

Table (1) shows the mean ± S.D. of the diagnostic indicators and biochemical parameter in the two study groups.

Groups Parameter	Mean ± SD Control No=30	 NNJ No=30	P-Value
TSB (mg/dl)	6.12 ± 1.93	15.81 ± 4.71	P ≤ 0.001
CRP (mg/L)	1.81± 1.21	4.01± 3.19	P ≤ 0.001
Glucose (mg/dl)	101.01± 29.19	106.01± 30.13	P ≤ 0.001
CCK (Pg/ml)	98.01 ± 4.87	215.14 ± 17.61	P ≤ 0.001
K^{+} (µmol/L)	4.43 ± 0.67	3.03 ± 0.87	P ≤ 0.001
Ca^{++} (µmol/L)	8.93 ± 0.97	9.51 ± 1.17	P ≤ 0.001
GSH (ng/ml)	10.11±7.31	3.01±0.49	P ≤ 0.001
MDA (nmol/ml)	10.51 ± 0.51	18.76 ±0.62	P ≤ 0.001

The results of the present study showed significant changes in all of the studied variables in the blood serum of children with jaundice compared to the healthy group at a $P \leq 0.05$, as shown in the following figures:

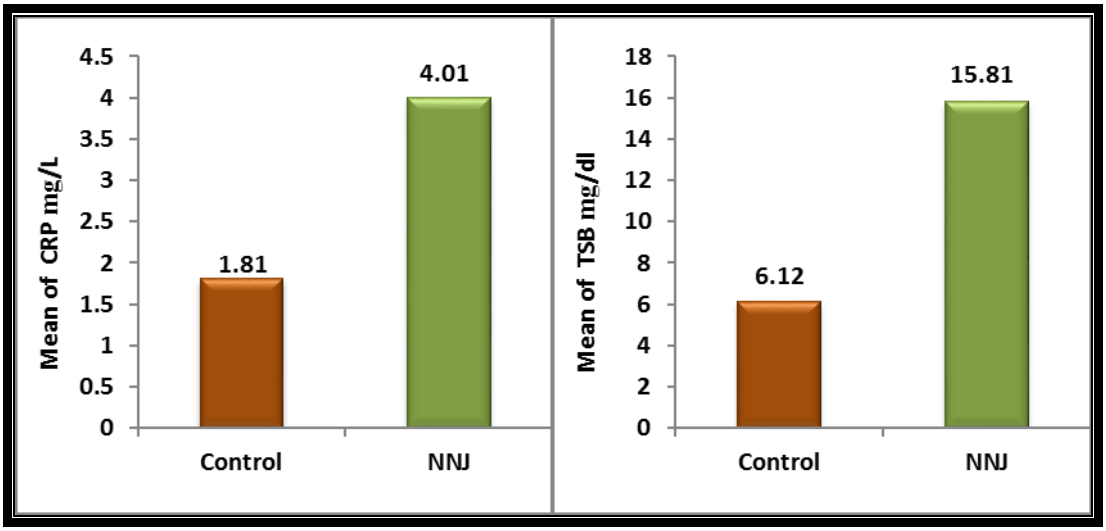

Fig (1,2): CRP and TSB in the blood serum of the samples under study

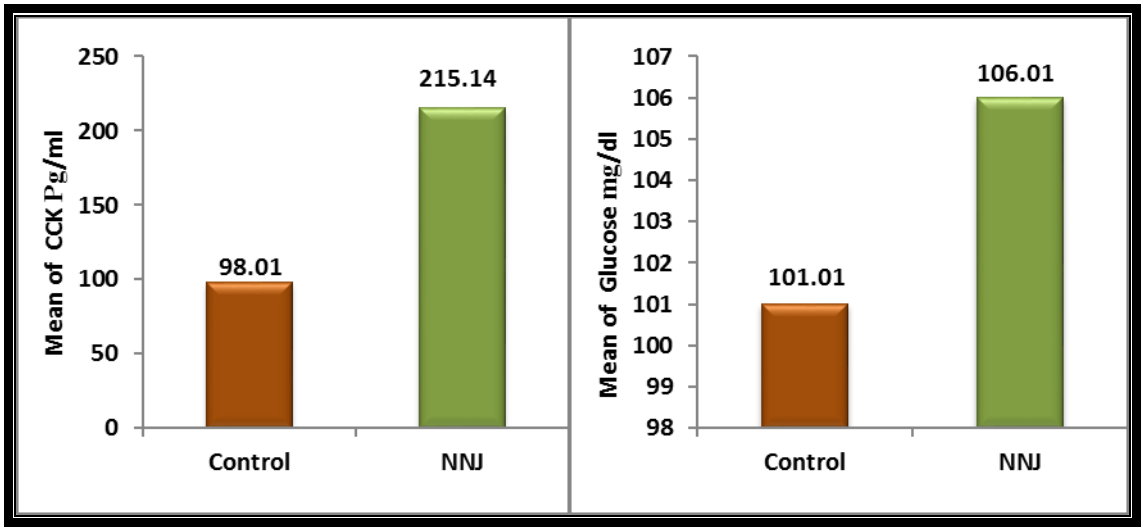

Fig (3,4): CKKP and glucose in the blood serum of the samples under study

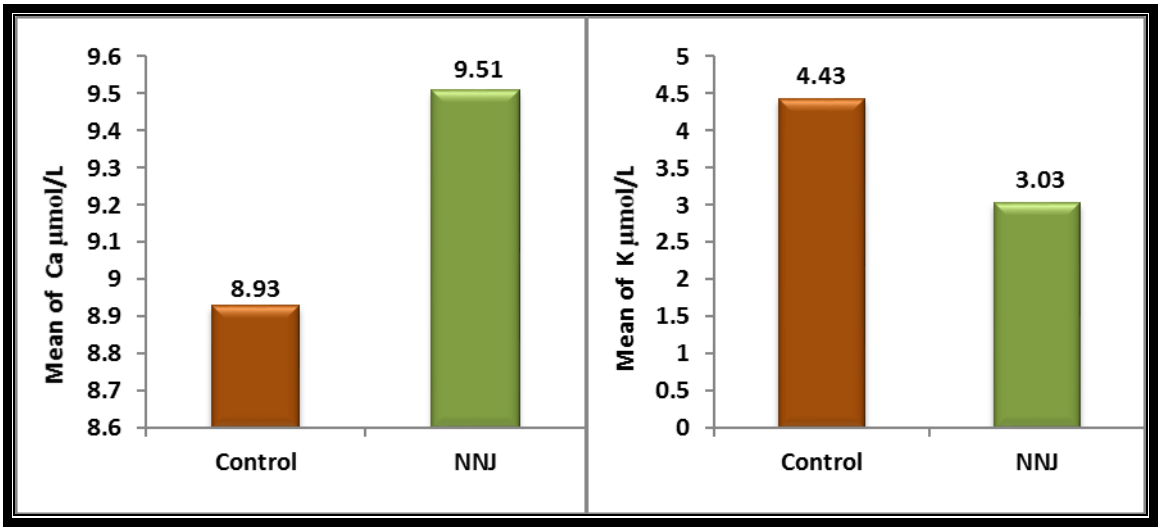

Fig (5,6): Ca and K in the blood serum of the samples under study

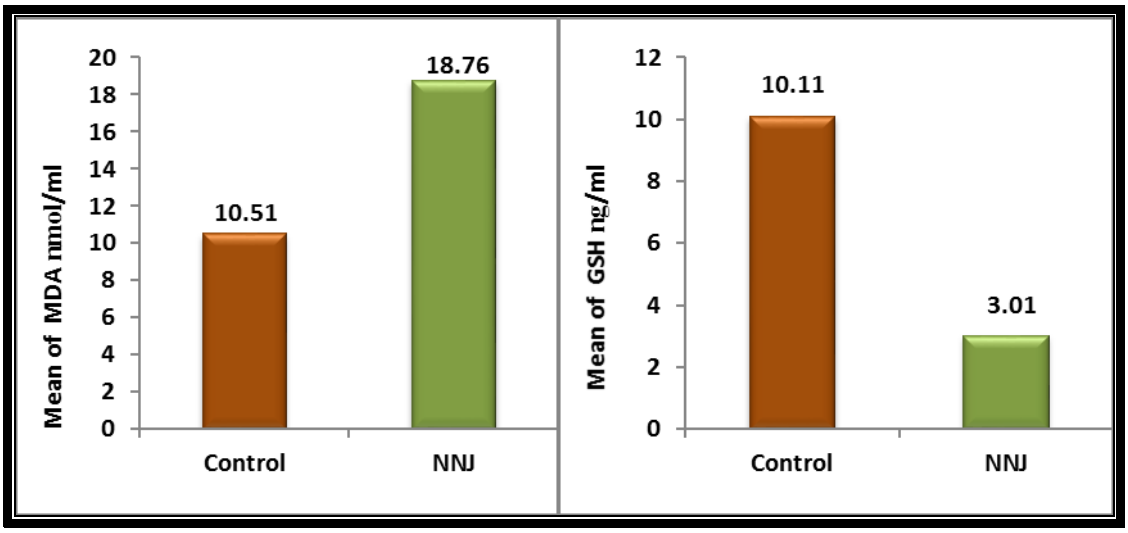

Fig (7,8): MDA and GSH in the blood serum of the samples under study

Dissection

Jaundice is caused by an increase in the level of bilirubin in the body due to the accelerated breakdown of red blood cells, the decreased ability of the liver to deal with bilirubin, and the increase in enterohepatic circulation (21). The result of high bilirubin levels in children with jaundice was agree with Suneja et al. (22) and Olatubi (23). The reason for the increase is that the livers of these children do not produce enough of the enzyme UGT and the liver is unable to quickly remove bilirubin from the blood due to the appearance of high levels of IDB in the blood. Exposure to light converts bilirubin into water-soluble isomers that can be easily eliminated through the digestive system or excreted in urine. In addition, liver failure leads to its inability to conjugate unbound bilirubin with glucuronic acid and store it as bound bilirubin in the gallbladder, or sometimes high bilirubin occurs due to damage and explosion in liver tissue (24,25).

The result of the current study showed a significantly elevated in CRP in G1 compared control group. C-reactive protein is considered one of the strongest proteins used as a diagnostic indicator for jaundice, because this protein is produced at a low concentration by liver cells and plays a fundamental role in immunity. Therefore, it is affected by fungal and adaptive diseases. Therefore, it is affected by neonatal jaundice and its concentration increases in the blood, as in other liver enzymes (26, 27).

Also, the result showed a significant rise in glucose for patients compared to healthy children. The result of high glucose levels in children with jaundice was consistent with the result of Volosivska et al (28). The reason for the increase is due to metabolic disturbances that occur in the glucose concentration in newborns with jaundice, which may be due to breastfeeding and the infant's inability to maintain balance, or the increase occurs as a result of the ambiguous interaction process that occurs between weak liver function and hormonal stress, in addition to therapeutic factors. This increase may represent a compensatory metabolic response rather than an independent disease symptom, but it may require careful and continuous monitoring to avoid metabolic complications that may occur in the future (22).

On the other hand the present study showed increase in CCK hormone in patinates children compered healthy children, The result of the high level of CCK in children with jaundice was agree with Al-Hatemi (29).It is believed that the reason for the rise in the level of the CCK hormone is due to the fatty acids that are present in high quantities in breast milk, which ultimately leads to stimulating the cells - located in the lining of the duodenum - to increase the secretion of the CCK hormone into the bloodstream. Then it moves and binds to the hormone receptors in the gallbladder, which works to contract the gallbladder and open the Oddi valve. This leads to the excretion of bilirubin accumulated in the gallbladder into the intestines and its disposal through the feces. Therefore, most doctors advise increasing the number of times of breastfeeding for children with jaundice to get rid of the largest amount of bilirubin concentration through the feces (30).

As for the result of the insignificant difference in the level of minerals, which included potassium and calcium), the result of the significant decrease in potassium was in agreement with the results of both Gozetici et al. (31) and Mohamed (32). As for the result of the insignificant increase in calcium, it was in agreement with the results of both Asl et al. (33) and Rozario (34). All of the reasons for these fluctuations in electrolyte levels are due to hyperbilirubinemia in newborns. However, electrolyte levels such as K, Na, and Ca must be monitored because disturbances in their levels and imbalance in newborns are a cause for concern and require continuous monitoring (22, 35). Phototherapy used for jaundice can reduce the concentration of electrolytes in the blood serum, such as Ca, K, and Na (36). This is because blood electrolyte levels can decrease significantly during phototherapy and are affected by the duration of exposure to light, as electrolyte imbalance leads to severe and harmful effects that are short- to long-term (37).

The result of the low GSH concentration in children with jaundice agrees with Turgut (38); the reason for the decrease is due to the accumulation of reactive oxygen species, which leads to a decrease in the level of GSH in newborn children with jaundice. This may also be because glutathione is found in high concentrations within red blood cells, and their breakdown and decomposition release glutathione into the bloodstream. This leads to an increase in its concentration in the serum of children with congenital jaundice.

The reason for the high level of MDA in children with jaundice is attributed to hemolysis in these children, because hemolysis can be explained by its effect on oxidative stress, as hemolysis itself leads to an increase in oxidative stress, which leads to an increase in the concentration of bilirubin. The oxidative effect on membrane lipids may cause an increase in MDA due to elevated generation of ROS, due to excessive oxidative damage in these patients. These oxygen species can, in turn, oxidize many other important biomolecules, including membrane lipids. Elevated MDA concentration in infants with severe G6PD deficiency reflects oxidative injury due to neonatal hyperbilirubinemia, which may be attributed to the formation of free radicals that remove hydrogen atoms from lipoproteins, causing lipid peroxidation, of which MDA is the major product (39).

Conclusion:- In infants with neonatal jaundice, elevated bilirubin is a key symptom. High levels of the hormone cholecystokinin are also observed in infants with neonatal jaundice. High bilirubin levels may indicate serious problems, including hemolysis and liver problems. High levels of C-reactive protein indicate a concurrent infection in patients. As for mineral levels, normal levels were observed among patients and healthy individuals, while low glutathione levels increase liver damage due to oxidation, and high levels of malondialdehyde indicate damage to the liver and other cells as a result of bilirubin accumulation and oxidation.

Rreferences

1- Aljazaeri S.A. (2020). Comparison of Biopyrrin, Bilirubin, and Creatinine in Neonatal Jaundice in Al-Najaf City, Iraq. International Journal of Pharmaco-ceutical Research / Supplementary Issue 1. Accepted: 10.06.20.

2- Khattab R.A.; Fathy K.N.; Ahmed S.N. and Hamada M.A. (2020). Eval-uation of blood levels of copper, zinc, magnesium, and calcium in full-term neonatal unconjugated hyperbilirubinemia. Al-Azhar Journal of Ped. Vol. 23 No. 47.

3- Boskabadi H.; Sezavar M. and Zakerihamidi M. (2020). Evaluation of neonatal jaundice based on the severity of hyperbilirubinemia. Journal of Clinical Neonatology. Volume 9 Issue 1: 46.

4- Agrawal V.; Goyal A.K.; Sharma J.N. and Yadav M.D. (2017). Different causes of prolonged unconjugated

jaundice in newborns. Int J Contempt Pe-diatr. 4:984-8.

5- Ahmed, Howaida Issa: Abdul Rahim, Fatima Abdul Aziz and Ali, Najwa Abu Bakr (2020). A study of some factors affecting the spread of jaundice among newborns in Sabha Medical Center. Department of Biotechnology, Faculty of Science, Sabha University, Libya.

6- Marshall W.J. (1995). Clinical chemistry. 3rd Edn., London, UK, PP. 72-76.

7- Kamara I.K. (2014). Factors associated with neonatal hyperbilirubinemia in the first 2 weeks of life in ola during children's hospital in Freetown, Sierra Leone. MB Ch. B. (University of Sierra Leone).

8- Moerschel, S.K.; Cianciarson, L.B., and Tracy, L.R. (2008). A practical approach to neonatal jaundice. Am Fam Physician. 77: 1255-1262.

9- Hassoun, Alaa Mohammed (2012). A Study of Some Cases of Neonatal Jaundice and the Accompanying Biochemical Changes in Newborns in the City of Diwaniyah. Al-Mustansiriya Sciences Journal, Volume 23 .Issue 1.

10- Karadag N.; Zenciroglu A.; Eminoglu F.T.; Dilli D.; Karagol B.S.; Kundak A.; Dursun A.; Hakan N. and Okumus N. (2013). Literature re-view and outcome of classic galactosemia diagnosed in the neonatal period. Clin. Lab. 59 (9-10):1139-46.

11- Ezeaka C.V.; Ugwu R.O. and Mukhtar-Yola M. (2014). Pattern and predictors of maternal care-seeking practices for severe neonatal jaundice in Nigeria: a multi-centre survey. BMC Health Serv Res. 14:192.

12- Shah A.; Shah C.K. and Shah V. (2012). Study of hematological parameters among neonates admitted with neonatal jaundice. Journal of Evolution of Medical and Dental Sciences, 1 (3): 203.

13- Dennery P.A.; Seidman D.S. and Stevenson D.K. (2001). Neonatal hyperbilirubinemia. N. Engl. J Med. 22:344(8):581-90.

14- Hofer N.; Zacharias E.; Müller W. and Resch, B. (2012). An update on the use of C-reactive protein in early-onset neonatal sepsis: current insights and new tasks. Eonatology. 102:25-36.4.

15- Yanli L.; Xiuhua S.; Yaqiong W.; Cuihong X.; Li L. and Shiying Z. (2021). Evaluation of Associated Markers of Neonatal Pathological Jaundice Due to Bacterial Infection. Iran J Public Health, Vol. 50, No. 2, Feb, pp. 333-340.

16-Furness, J. B., & Costa, M. (1987) Influence of the enteric nervous system on motility. The enteric nervous system, 137-189.

17- Wiley, J. W., O'dorisio, T. M., & Owyang, C. (1988). Vasoactive intestinal polypeptide mediates cholecystokinin-induced relaxation of the sphincter of Oddi. The Journal of Clinical Investigation, 81(6), 1920-1924.

18- Al-Hamoud Muhammad Hasan: Yousef, Walid Hamid and Al-Bataineh, Muhammad Nayef (2002). Human Biology (Digestion, Circulation, Respiration, Nerve Transmission). Dar Al-Ahliya for Publishing and Distribution, Amman, Jordan.

19- Mahan L.K. and Escott S.S. (2000). Food nutrition and diet therapy. 10th ed. W.B. Saunder company.:2 relationship to the number of cirrhotic blood cells and hemopoiesis. Physiol. Res. 45:101-106.

20-Dingeon, B. Determination of serum glucose. Ann. Biol. Clin.1975. (33).3.

21- Horn A.R.; Kirsten G.F.; Kroon S.M.; Henning P.A.; Moller G. and Pieper C. (2006). Phototherapy and exchange transfusion for neonatal hyper-bilirubinemia: neonatal academic hospitals' consensus guidelines for South African hospitals and primary care facilities. South African Medical Journal. 96(9):819-24.

22- Suneja S.; Rajani K. and Rahul S. (2018). Effect of Phototherapy on Variable Biochemical Parameters in Neonatal Hyperbilirubinemia: A Clinical In-sight. Year: Month: April-June Volume: 6 Issue: 2 Page: PO13-PO18.

23- Olatubi M.; Ibitoye O. and Sadibo O. (2019). Prevalence of neonatal jaundice at a tertiary health institution in Ondo state, Nigeria. Journal of Pre-Clinical and Clinical Research. 13: 114-117.

24- Zilva J.F.; Pannall, P.R. and Mayne P.D. (1994). Clinical chemistry in Diagnosis and Treatment. 6th ed. Edward Arnold, London, P.P.: 280-303.

25- Moncrieff G. (2018). Bilirubin in the newborn: Physiology and pathophysiology. British Journal of Midwifery, 26(6), pp. 362-370

26- Li J.J. and Fang C.H. (2004). C-reactive protein is not only an inflammatory marker but also a direct cause of cardiovascular disease. Medical Hypothesis. 62: 499-506.

27- Liu Y.L.; Lu J. and Xiong W. (2008). "Bilirubin possesses powerful immunomodulatory activity and suppresses experimental autoimmune encephalo-lomyelitis. Immunol, 181 (3). PP: 1887-1897.

28- Volosivska Y.; Yuliia H. and Lilia Y. (2020). Significance of clinical and laboratory markers in disorders of the functional condition of the hepatobiliary system in neonatal jaundice. International conference on innovations in science and education (medicine and pharmacy), March 18-20.

29- All SH. J. Al-Hatemi and Wijdan I. A. Abd-alwahab. Physiochemical Effect of Neonatal Jaundice on Some Liver Enzymes and Cholecystokinin in Hormone. University of Samarra, College of Education, Department of Biology/ Iraq. Received 25 April 2021,

Annals of R.S. C.B., ISSN 1563-6256, Vel, 25, Issue 6. 2021, Pages 2912-2917.

30- Otsuki, M. (2000). Pathophysiological role of cholecystokinin in humans. Journal of gastroenterology and hepatology, 15, 71-83.

31- Gözetici A.A.; Yiğit, O. and Beşer. (2021). Effect of phototherapy on serum electrolyte levels. Cerrahpaşa Med J. 45:16-20.

32- Mohamed A.E.; Osama A.E.; Omima M.A. and Walid A.A. (2023). Electrolyte Changes Following Phototherapy in Neonatal Unconjugated Hy-perbilirubinemia. Benha Journal of Applied Sciences, Vol. (8) Issue (9).

33- Asl A.S.; Zarkeshl M.; Heidarzadeh A.; Maleknejad S. and Hagikhani K. (2016). The effect of phototherapy on urinary calcium excretion in term of neonates. Saudi J Kidney Dis Transpl. 27 (03):486-492.

34- Rozario C.L.; Pillai P.S. and Ranamol T. (2017). Effect of phototherapy on serum calcium level in term newborns. International Journal of Contemporary Pediatrics, 4 (6), 1975-9.

35- Abohussein H.A.; Balsam S.F.; Aya M.K. and Yosra A.F. (2022). Effect of phototherapy on electrolytes, liver and kidney functions during treatment of neonatal hyperbilirubinemia. Annals of Neonatology Journal. 4 (2): 170-186.

36- Reddy A.T.; Bai K.V. and Shankar S.U. (2015). Electrolyte changes following phototherapy in neonatal hyperbilirubinemia. IJSR. 4(7):752-58.

37- Nazim N.; Bablu K.G.; Fatima A.A.; Baljeet M. and Rupa R.S. (2023). Effect of Light-emitting Diode Phototherapy on Serum Electrolyte Levels in Neonates with Unconjugated Hyperbilirubinemia: A Prospective Single-center Study. Journal of Clinical Neonatology Volume 12 Issue 3 July-September.

38-Turgut, M., Başaran, O., Cekmen, M. U. S. T. A. F. A., Karataş, F., Kurt, A., & Aygün, A. D. (2004),

Oxidant and antioxidant levels in preterm newborns with idiopathic hyperbilirubinaemia. Journal of paediatrics and child health, 40(11), 633-637.

39-Gawel, S., Wardas, M., Niedworok, E., & Wardas, P. (2004), alondialdehyde (MDA) as a lipid peroxidation marker. Wiadomosci lekarskie (Warsaw,Poland: 1960), 57(9-10), 453-455.

Antibacterial Effects of ZnO Nanoparticles in Combination with Other antibiotics

Ruaa Maan[1],*

Alyaa Hussein Ashour[2],

Raneen Salam Al-Obaidi[3],

Dina Hameed Haider [4],

Dunya Abdullah Mohammed[5]

Omar A Mahmoud [5] ,

Wassan A. Hassan[6]

1.Department of Forensic Chemistry, Higher Institute of Forensic Sciences, Al-Nahrain University, Baghdad, Iraq

2. College of medicine, Al-Nahrain University, Baghdad, Iraq

3. Alnahrain renewable energy research Center, Al-Nahrain University, Baghdad, Iraq

4. Department of Forensic Chemistry, Higher Institute of Forensic Sciences, Al-Nahrain University, Baghdad, Iraq

5. Department of Forensic Biology, Higher Institute of Forensic Sciences, Al-Nahrain University, Baghdad, Iraq

6. Department of Forensic Engineering, Higher Institute of Forensic Sciences, Al-Nahrain University, Baghdad, Iraq

*****Corresponding author: Ruaa Maan Attallah

E-mail: **ruaamaan@gmail.com**

Antibacterial Effects of ZnO Nanoparticles in Combination with Other antibiotics

Ruaa Maan[1], Alyaa Hussein Ashour[2], Raneen Salam Al-Obaidi[3], Dina Hameed Haider [4], Dunya Abdullah Mohammed [5]Omar A Mahmoud [5] ,Wassan A. Hassan[6]*

1.Department of Forensic Chemistry, Higher Institute of Forensic Sciences, Al-Nahrain University, Baghdad, Iraq

2. College of medicine, Al-Nahrain University, Baghdad, Iraq

3. Alnahrain renewable energy research Center, Al-Nahrain University, Baghdad, Iraq

4. Department of Forensic Chemistry, Higher Institute of Forensic Sciences, Al-Nahrain University, Baghdad, Iraq

5. Department of Forensic Biology, Higher Institute of Forensic Sciences, Al-Nahrain University, Baghdad, Iraq

6. Department of Forensic Engineering, Higher Institute of Forensic Sciences, Al-Nahrain University, Baghdad, Iraq

*****Corresponding author: Ruaa Maan Attallah

E-mail: **ruaamaan@gmail.com**

Abstract

This study investigates the antibacterial activity of zinc oxide nanoparticles (ZnO-NPs) against *Acinetobacter baumannii* plus *Staphylococcus aureus*. The well diffusion method was used to estimate the inhibition zones of different concentrations of ZnO-NPs, as well as combined with ciprofloxacin and ceftriaxone. The results indicate that high concentrations of ZnO-NPs alone exhibit strong antibacterial activity and statistically, the p-value is non-significant, and their combination with antibiotics enhances bacterial inhibition. The mixture of ZnO-NPs with ciprofloxacin and ceftriaxone significantly enhanced the antibacterial effect against both Gram-positive and negative bacteria, suggesting a potential strategy for overcoming antibiotic resistance.

Key words: Antibacterial activity, ZnO Nanoparticles, antibiotic resistance, Gram-positive bacteria, Gram- negative bacteria

الخلاصة

تستقصي هذه الدراسة النشاط المضاد للبكتيريا لجسيمات أكسيد الزنك النانوية (ZnO-NPs) ضد Acinetobacter baumannii بكتيريا و Staphylococcus aureus. تم استخدام طريقة well diffusion method لتقدير مناطق التثبيط لتركيزات مختلفة من جسيمات أكسيد الزنك النانوية وحدها، وكذلك عند دمجها مع سيبروفلوكساسين (ciprofloxacin) وسيفتاكسون (ceftriaxone). تشير النتائج إلى أن التركيزات العالية

من جسيمات أكسيد الزنك النانوية وحدها تظهر نشاطًا قويًا مضادًا للبكتيريا، ومن الناحية الإحصائية، فإن قيمة p غير معنوية.كما عزز خليط جسيمات أكسيد الزنك النانوية مع سيبروفلوكساسين وسيفتاكسون بشكل ملحوظ التأثير كالمضاد للبكتيريا ضد كل من البكتيريا المستخدمة، مما يشير إلى استراتيجية محتملة للتغلب على مقاومة المضادات الحيوية.

Introduction

Nanotechnology plays a critical role in modern material science, with applications ranging from medicine to industry. Among the various nanoparticles, ZnO-NPs have received considerable attention due to their stability, low toxicity, and broad-spectrum antimicrobial properties [1, 2]. The development of antibiotic-resistant bacteria such as *Staphylococcus aureus* and *Acinetobacter baumannii* requires new therapeutic approaches [3]. This study aims to evaluate the antibacterial activity of ZnO-NPs alone and in a mixture with ciprofloxacin and ceftriaxone. ZnO-NPs have unique properties, including a high surface area-to-volume ratio, which improves their interaction with bacterial cells [4, 5]. Previous research has demonstrated that ZnO-NPs can disturb bacterial membranes, generate reactive oxygen species (ROS), and interfere with essential cellular processes [6]. The growing prevalence of multidrug-resistant (MDR) bacteria highlights the urgent need for novel antimicrobial strategies. In this paper, we will study the antibacterial activity of concentrations of zinc oxide nanoparticles against *Acinetobacter baumannii* and *Staphylococcus aureus* bacteria, also Combine the antibiotic with concentrations of zinc oxide nanoparticles and study antibacterial activity against *Acinetobacter baumannii* and *Staphylococcus aureus* bacteria.

Materials and Methods

Preparation of Culture Media: Muller-Hinton agar was used for bacterial culturing. The medium was prepared and sterilized using an autoclave at 121°C for 15 minutes. The bacteria used in this study were clinical isolates of *Acinetobacter baumannii* and *Staphylococcus aureus* obtained from hospital samples.

Well Diffusion Method: Sterile cotton swabs were used to inoculate bacterial cultures onto agar plates. Wells of 6-8 mm diameter were created and filled with different concentrations of ZnO-NPs [5, 2.5, 1.25, 0.625, 0.313, 0.156, 0.078, and 0.039 mg/ml]. Plates were incubated at 37°C for 24 hours, and inhibition zones were measured. The antibacterial effect of nanoparticles was achieved by well diffusion method. The steps of this work were achieved all inside the fume hood, dipping a sterile cotton swab into the standardized bacterial suspension and removing excess inoculum by lightly pressing the swab against the tube wall at a level above that of the liquid, then Muller-Hinton Agar plate surface is inoculated by streaking with the swab then a hole with a diameter of 6 to 8 mm is punched aseptically with a sterile cork, containing the inoculum. A volume (75µL) of the ZnO solution at different concentrations, [5, 2.5, 1.25, 0.625, 0.313, 0.156, 0.078, 0.039 mg/ml] is introduced into the well, incubated for 18 to 24 hours at 37oC. The growth of bacteria was well observed and the nanoparticles effect on the growth of bacteria was tested by observing the inhibition zone, which means growth stops and is measured by the ruler.

Results and Discussion

Inhibition Zone of ZnO-NP against bacteria: According to Table 1 the comparison between the inhibition zone diameter of different concentrations of Zinc oxide against *Acinetobacter baumannii* and *Staphylococcus aureus*, the current result showed that the increasing concentrations of zinc oxide lead to an increase the inhibition zone for both types of bacteria, and statistically, the p-value is non-significant $p \geq 0.05$. Figure 1 shows a linear relationship between them.

Table 1: Comparison of zone diameter of different concentration of Zinc oxide against bacteria

Zinc Conc. (mg/ml)	***Acinetobacter baumannii*** **mean±SD**	***Staphylococcus aureus*** **mean±SD**
5.0	15.04+1.46	15.07+1.55
2.5	12.75+2.03	13.43+1.77
1.25	9.21+1.87	10.59+2.49
0.625	8.0+1.0	8.5+1.61
0.313	0.0+0.0	0.0+0.0
0.156	0.0+0.0	0.0+0.0
0.0781	0.0+0.0	0.0+0.0
0.039	0.0+0.0	0.0+0.0

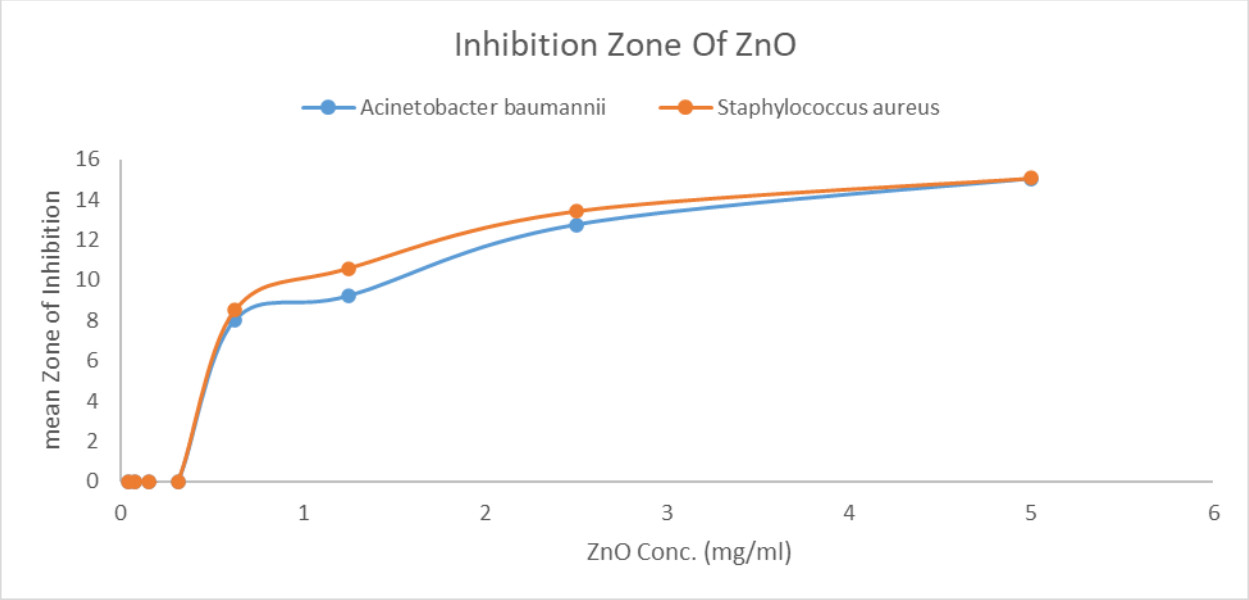

Figure 1: The linear relationship between zinc oxide and the zone of inhibition

The curve accurately represents the inhibition zones for *Acinetobacter baumannii* and *Staphylococcus aureus*, showing a plateau at higher concentrations.

By using well diffusion method, the present study suggested that ZnO-NPs had high antibacterial activity against both Gram-positive and Gram-negative bacteria, and this method is suitable for detecting the antibacterial activity of ZnO-NPs against *Acinetobacter baumannii* and *Staphylococcus aureus* bacteria. ZnO-NPs have a high activity against bacteria and this is found in many published researches [7, 8].

This study found that in the high concentrations of ZnO-NP, the inhibition zone is large, which mean that particle size and concentration of ZnO-NPs play an important role in the antibacterial activity [9]. ZnO-NPs antibacterial activity directly correlates with their concentration was reported by several studies, likewise, the activity is size dependent, however, this dependency is also influenced by the concentration of NPs. Larger surface area and higher concentration are accountable for ZnO-NP antibacterial activity[10].e It has been explaining that larger surface areas and higher concentrations of smaller particles may provide additional antibacterial activity and that is accordance with the results obtained[11]. It's also shown that the inhibition of Gram-negative bacteria requires higher concentrations of ZnO NPs [12]. This is likely because the peptidoglycan layer that surrounds Gram-positive bacteria can promote ZnO attack inside the cell, while the cell wall components of Gram-negative bacteria, such as lipopolysaccharides, can counter this attack. It's found that the concentration of zinc oxide has no effect in the inhibition region on bacteria, and this differs with the current results obtained [13]. Also, the small size (<100 nm) and the high surface-to-volume ratio of NPs facilitate the prerequisite interaction with the microorganisms. The antimicrobial activity of NPs such as ZnO is usually attributed to its crystal structure, size, shape, and surface area [14, 15, 16, 17].

Combination with Antibiotics: ZnO-NPs were combined with ciprofloxacin and ceftriaxone at 5 mg/ml and 2.5 mg/ml concentrations. The well diffusion method was applied to determine the enhancement in antibacterial activity.

Inhibition Zone of ZnO-NP mixed ciprofloxacin against bacteria: Tables (2) and (3) showed a comparison of the inhibition zone diameter of each of *Acinetobacter baumannii* and *Staphylococcus aureus* bacteria after treatment with different concentrations of mixture of Zinc oxide with ciprofloxacin [5.0 mg/ml and 2.5 mg/ml] respectively. Results are similar to sensitivity to pure ZnO as increasing concentrations of ZnO mixture with ciprofloxacin [5.0 mg/ml and 2.5 mg/ml] lead to an increase in the inhibition zone for both types of bacteria but with a significant increase in inhibition zone area compared to the pure ZnO.

Table 2 Comparison of zone diameter of different concentration of mixture of Zinc oxide in combination with ciprofloxacin 5.0 mg/ml between the bacteria.

Zinc Conc. (mg/ml)	*Acinetobacter baumannii* mean±SD	*Staphylococcus aureus* mean±SD
5.0	27.63+1.44	27.37+2.14
2.5	25.96+2.48	26.07+2.42
1.25	24.08+2.55	24.03+3.01
0.625	20.67+2.79	21.77+3.29
0.313	18.13+3.19	18.6+4.12
0.156	15.25+2.57	17.03+4.34
0.0781	13.92+2.96	15.07+4.61
0.039	12.71+3.24	13.53+4.63

Table 3: Comparison of zone diameter of different concentration of mixture of Zinc oxide in combination with ciprofloxacin 2.5 mg/ml between *the* bacteria.

Zinc Conc. (mg/ml)	*Acinetobacter baumannii* mean±SD	*Staphylococcus aureus* mean±SD
5.0	25.29+2.12	24.63+2.55
2.5	23.5+2.9	23.6+2.8
1.25	20.92+4.2	20.97+3.25
0.625	18.21+3.95	18.27+3.92
0.313	16.23+3.09	15.34+3.71
0.156	13.65+2.74	13.46+3.58
0.0781	10.69+3.25	11.55+2.84
0.039	10.0+1.6	10.44+2.5

Antibiotics were found to be a valuable weapon to combat bacterial infection, but their popularity had also become their undoing. Although the drugs crippled harmful microbes from within, bacteria that survived such sabotage developed resistance that made them even more dangerous [18].

Drug resistance developed in part because conventional antibiotics such as ciprofloxacin did not physically damage a microbe's cell wall. Instead, entered the target less disruptively and moved on to disrupt the DNA within block cell division or, trigger cellular self-destruction [19].

Strains that survived this assault, however, could evolve to defend themselves against future attacks, opening the door for deadlier versions of bacteria such as methicillin-resistant Staphylococcus aureus (MRSA) [19], to counter this, we have to develop to supplement pure antibiotics by destroying outer protective membranes of bacteria, ensuring that their

morphing days are through, this is done by combining nanoparticles with antibiotics as in ZnO NPs-CIP in the present study.

Many studies have shown that metal nanoparticles combined with antibiotics have better effects against both Gram- positive and Gram-negative bacteria [20, 21, 22]. So, combining ciprofloxacin with nanoparticles of zinc oxide will improve efficiency against bacteria, and this has been proven by the present study results that when combining nanoparticles of zinc oxide with ciprofloxacin, obtained a greater inhibition zone than zinc oxide or ciprofloxacin alone. Where it raised for ciprofloxacin (5 mg/ml) from 11.86 (mm) and 12.77 (mm) to 27.63(mm) and 27.37(mm) for *Acinetobacter baumannii* and *Staphylococcus aureus* respectively, and raised for ciprofloxacin (2.5 mg/ml) from 11.0(mm) and 12.3(mm) to 25.29(mm) and 24.63(mm) for *Acinetobacter baumannii* and *Staphylococcus aureus* respectively. These results are in line with previous research, where they confirmed that the efficiency of the antibacterial activity of ciprofloxacin increases in the presence of ZnO-NPs [23, 24, 25, 26, 27]. In a related development, previous research [28] has shown that adding nanoparticles can reduce the antibacterial activity of antibiotics.

The explanation was mentioned previously that increasing the concentration leads to increases the anti-bacterial activity and thus increases the inhibition zone and increases the sensitivity to the bacteria and it is agreed with another research [29].

A previous research, suggested the increased antibacterial activity of ciprofloxacin in the presence of ZnO-NPs may be due to membrane damage and accumulation of antibacterial agents in the cells [30].

The exact mechanism of antibacterial action of ZnO-NPs with antibiotics has not yet been elucidated. It has been suggested the synergistic activity between conventional antibiotics and NPs due to inhibition of the export of antibacterial agents by blocking efflux pumps or by enhancing the entrance of antibiotics into the cell by disrupting the bacterial membrane [31]. Previous studies concluded that ZnO-NPs may induce genotoxicity indirectly by promoting oxidative stress or by directly passing through the cellular membrane and interacting with the DNA to damage all four bases or producing thymine–tyrosine cross-linking [32].

Other authors [33] proposed an explanation for the increased activity of ciprofloxacin in the presence of ZnO nanoparticles against *S. aureus* that ZnO nanoparticles may interfere with the pumping activity of Nor A protein by inducing faster electron transfer kinetics in its active site. This protein mediates the active efflux of hydrophilic fluoroquinolones from the bacterial cell providing resistance to the bacterium and this led to the inhibition of the antibacterial activity of ciprofloxacin. Interference with NorA protein restores ciprofloxacin action.

Others explained that ZnO-NP damaged the cell membrane through reactive oxygen species (ROS) generation with free electrons and holes in the presence of light, which assisted ciprofloxacin to enter into the cell and, thereby, inhibit bacterial growth [23].

Inhibition Zone of ZnO-NP mixed ceftriaxone against bacteria: Tables (4) and (5) show a comparison of the diameter of the inhibition zone of *Acinetobacter baumannii* and *Staphylococcus aureus* after treatment with a different concentration of zinc oxide mixed with ceftriaxone (5.0 mg/ml and 2.5 mg/ml), respectively. The results are similar to pure ZnO and ZnO combined with ciprofloxacin. Increasing concentrations of ZnO mixed with

ceftriaxone (5.0 mg/ml and 2.5 mg/ml) increase the inhibition zone of both types of bacteria but with a remarkable increase in the area of the inhibition zone compared to the pure ZnO.

Table 4: Comparison of zone diameter of different concentration of mixture of Zinc oxide in combination with ceftriaxone 5.0 mg/ml between the Bacteria.

Zinc Conc. (mg/ml)	*Acinetobacter baumannii* mean±SD	*Staphylococcus aureus* mean±SD
5.0	27.87+1.87	27.77+1.66
2.5	26.26+2.61	26.42+2.04
1.25	24.52+3.07	24.54+2.58
0.625	22.04+4.13	21.77+3.0
0.313	18.96+4.47	19.5+3.5
0.156	16.74+4.29	17.77+4.03
0.0781	15.13+4.32	15.31+3.92
0.039	14.39+4.27	14.0+4.54

Table 5: Comparison of zone diameter of different concentration of mixture of Zinc oxide in combination with ceftriaxone 2.5 mg/ml between the Bacteria

Zinc Conc. (mg/ml)	*Acinetobacter baumannii* mean±SD	*Staphylococcus aureus* mean±SD
5.0	25.21+1.53	25.1+1.54
2.5	23.25+2.52	22.97+2.31
1.25	20.96+3.18	20.27+3.11
0.625	17.75+3.27	17.67+3.24
0.313	14.46+3.48	15.47+3.0
0.156	12.0+3.13	12.33+2.58
0.0781	11.2+3.03	10.17+2.04
0.039	9.73+1.56	8.85+1.5

Obtain a large inhibition zone of Ceftriaxone approximately or slightly higher than that obtained in combining nanoscale ZnO with ciprofloxacin as it reaches 27.87 (mm) and 27.77(mm) for *Acinetobacter baumannii* and *Staphylococcus aureus* at 5 mg/ml of Ceftriaxone combined with ZnO-NPs and reaches to 25.21 (mm) and 25.1(mm) for *Acinetobacter baumannii* and *Staphylococcus aureus* at 2.5 mg/ml of ceftriaxone combined with ZnO-NPs.

These results are compatible with previous results [34] showed that the antibacterial effect of ceftriaxone increased significantly when used in combination with ZnO nanoparticles. While other results showed that the combination of ZnO-NPs and ceftriaxone has no effect on gram-positive and explained the reason for this due to either to decrease in particle size or to low concentration of those compounds [35].

It demonstrated that ZnO with ceftriaxone achieves obvious synergistic antibacterial effects against E. coli. Meanwhile, ceftriaxone-ZnO has higher antibacterial activity under UV activation, compared to pure ceftriaxone or ZnO [36].

Previous studies have shown that combining nanoparticles with ceftriaxone improves antibacterial activity where [37] elucidated that ceftriaxone combined with AuNP was highly effective against bacterial strains compared to ceftriaxone and AuNP alone. [38] Illustrate, ceftriaxone–nanoparticle conjugate showed the greatest antimicrobial activity against both Gram-positive and Gram-negative bacteria compared to ceftriaxone alone and explained the reason for this due to the negatively charged cell wall of bacteria being ruptured by silver ions from silver nanoparticles and eventually resulting in cell death.

The results of Shanmuganathan [39] display the improvement of the antibacterial activity of Ag-NPs after conjugation with ceftriaxone and the application of ceftriaxone-conjugated nanoparticles as a choice for the inhibition of the pathogens. Nano-metal and even nano-polymer improve their antibacterial activity when combined with ceftriaxone as Chitosan reported in a previous study [40]. However, this did not happen with Geovana [41] as the area of the inhibition zone decreased when silver was combined with ceftriaxone antibiotic when compared with Ag-NPs alone against *P. aeruginosa.*

Briefly mentioned previously an explanation of the enhancement of ZnO nanoparticles with ciprofloxacin, this increased synergistic activity will depend on the assumption that ZnO NPs may interfere with the pumping activity of the NorA bacterial protein. The same thing happened with the synergistic activity between zinc oxide and ceftriaxone, and this was confirmed by Rashmi [42] in previous research.

Conclusion

This study confirms the significant antibacterial effects of ZnO-NPs, both alone and in combination with antibiotics. The synergistic action of ZnO-NPs with ciprofloxacin and ceftriaxone suggests a promising approach to improving antibiotic efficacy against resistant bacterial strains. Further studies should explore the clinical applications of ZnO-NPs and their potential use in developing advanced antimicrobial treatments.

Future Directions

Future research should focus on the in vivo efficacy of ZnO-NPs, assessing their pharmacokinetics, toxicity, and potential for clinical applications. Investigating the mechanisms of bacterial resistance to ZnO-NPs and optimizing nanoparticle formulations could further enhance their therapeutic potential. The combination of ZnO-NPs with other antimicrobial agents, such as natural compounds or peptides, may offer additional benefits in overcoming antibiotic resistance.

References

[1] Sahoo, S. (2010). Socio-ethical issues and nanotechnology development: Perspectives from India. 10th IEEE International Conference on Nanotechnology, 1205–1210.

[2] Yadav, V. (2013). Nanotechnology, big things from a tiny world: A review. AEEE, 3(6), 771–778.

[3] Raghunath, A., & Perumal, E. (2017). Metal oxide nanoparticles as antimicrobial agents: A promise for the future. International Journal of Antimicrobial Agents, 49(2), 137–152.

[4] Sun, Y., Mayers, B., Herricks, T., & Xia, Y. (2003). Polyol synthesis of uniform silver nanowires: A plausible growth mechanism and the supporting evidence. Nano Letters, 3(7), 955–960.

[5] Dhage, S. R., Pasricha, R., & Ravi, V. (2005). Synthesis of fine particles of ZnO at 100°C. Materials Letters, 59(7), 779–781.

[6] Liu, Y., He, L., Mustapha, A., Li, H., Hu, Z. Q., & Lin, M. (2009). Antibacterial activities of zinc oxide nanoparticles against Escherichia coli O157:H7. Journal of Applied Microbiology, 107(4), 1193–1201.

[7] Jones, N., Ray, B., Ranjit, K. T., & Manna, A. C. (2008). Antibacterial activity of ZnO nanoparticle suspensions on a broad spectrum of microorganisms. FEMS Microbiology Letters, 279(1), 71–76.

[8] Boucher, H. W., & Corey, G. R. (2008). Epidemiology of methicillin-resistant Staphylococcus aureus. Clinical Infectious Diseases, 46(Supplement_5), S344–S349.

[9] Peleg, A. Y., Seifert, H., & Paterson, D. L. (2008). Acinetobacter baumannii: Emergence of a successful pathogen. Clinical Microbiology Reviews, 21(3), 538–582.

[10] A. R. Shahverdi, A. Fakhimi, H. R. Shahverdi, and S. Minaian, “Synthesis and effect of silver nanoparticles on the antibacterial activity of different antibiotics against Staphylococcus aureus and Escherichia coli,” Nanomedicine Nanotechnology, Biol. Med., vol. 3, no. 2, pp. 168–171, 2007

[11] F. Mirhosseini, M. Amiri, A. Daneshkazemi, H. Zandi, and Z. S. Javadi, “Antimicrobial Effect of Different Sizes of Nano Zinc Oxide on Oral Microorganisms,” Front. Dent., vol. 16, no. 2, p. 105, 2019.

[12] B. L. da Silva, M. P. Abuçafy, E. B. Manaia, J. A. O. Junior, B. G. Chiari-Andréo, R. C. L. R. Pietro, and L. A. Chiavacci, “Relationship between structure and antimicrobial activity of zinc oxide nanoparticles: An Overview,” Int. J. Nanomedicine, vol. 14, p. 9395, 2019.

[13] K. Fattah, A. Gamal, S. Ibrahim, E. Mohamed, and A. Saleh, “Investigation of the efficacy of synthesized silver and zinc oxide nanoparticles against multi-drug resistant gram negative bacterial clinical isolates,” Arch Clin Microbiol, vol. 8, no. 6, p. 67, 2017.

[14] M. Alizadeh-Sani, H. Hamishehkar, A. Khezerlou, M. Maleki, M. Azizi-Lalabadi, V. Bagheri, P. Safaei, T. Azimi, M. Hashemi, and A. Ehsani, “Kinetics Analysis and Susceptibility Coefficient of the Pathogenic Bacteria by Titanium Dioxide and Zinc Oxide Nanoparticles,” Adv. Pharm. Bull., vol. 10, no. 1, p. 56, 2020.

[15] P. A. Kareem, E. G. H. Alsammak, Y. J. Abdullah, and Q. M. Bdaiwi, “Estimation of antibacterial activity of zinc oxide, titanium dioxide, and silver nanoparticles against multidrug-resistant bacteria isolated from clinical cases in Amara City, Iraq.,” Drug Invent. Today, vol. 11, no. 11, 2019.

[16] A. Azam, A. S. Ahmed, M. Oves, M. S. Khan, S. S. Habib, and A. Memic, “Antimicrobial activity of metal oxide nanoparticles against Gram-positive and Gram-negative bacteria: a comparative study,” Int. J. Nanomedicine, vol. 7, p. 6003, 2012.

[17] M. J. Hajipour, K. M. Fromm, A. A. Ashkarran, D. J. de Aberasturi, I. R. de Larramendi, T. Rojo, V. Serpooshan, W. J. Parak, and M. Mahmoudi, “Antibacterial properties of nanoparticles,” Trends Biotechnol., vol. 30, no. 10, pp. 499–511, 2012.

[18] K. Hiramatsu, Y. Katayama, M. Matsuo, T. Sasaki, Y. Morimoto, A. Sekiguchi, and T. Baba, "Multi-drug-resistant Staphylococcus aureus and future chemotherapy," J. Infect. Chemother., vol. 20, no. 10, pp. 593–601, 2014.

[19] H. F. Chambers and F. R. DeLeo, "Waves of resistance: Staphylococcus aureus in the antibiotic era," Nat. Rev. Microbiol., vol. 7, no. 9, pp. 629–641, 2009.

[20] Jones, N., Ray, B., Ranjit, K. T., & Manna, A. C. (2008). Antibacterial activity of ZnO nanoparticle suspensions. FEMS Microbiol. Lett., 279(1), 71–76.

[21] A. S. H. Hameed, C. Karthikeyan, A. P. Ahamed, N. Thajuddin, N. S. Alharbi, S. A. Alharbi, and G. Ravi, "In vitro antibacterial activity of ZnO and Nd doped ZnO nanoparticles against ESBL producing Escherichia coli and Klebsiella pneumoniae," Sci. Rep., vol. 6, no. 1, pp. 1–11, 2016.

[22] Y. Xie, Y. He, P. L. Irwin, T. Jin, and X. Shi, "Antibacterial activity and mechanism of action of zinc oxide nanoparticles against Campylobacter jejuni," Appl. Environ. Microbiol., vol. 77, no. 7, pp. 2325–2331, 2011.

[23] P. Patra, S. Mitra, N. Debnath, P. Pramanik, and A. Goswami, "Ciprofloxacin conjugated zinc oxide nanoparticle: A camouflage towards multidrug resistant bacteria," Bull. Mater. Sci., vol. 37, no. 2, pp. 199–206, 2014.

[24] R. Farzana, P. Iqra, F. Shafaq, S. Sumaira, K. Zakia, T. Hunaiza, and M. Husna, "Antimicrobial behavior of Zinc oxide nanoparticles and β-lactam antibiotics against pathogenic Bacteria," Arch. Clin. Microbiol, vol. 8, p. 57, 2017.

[25] S. Sepideh, K. Z. Bahri, P. M. Reza, S. H. Reza, A. Massoud, B. Roya, N. Z. Esmail, and S. A. Reza, "Preparation of ciprofloxacin-coated zinc oxide nanoparticles and their antibacterial effects against clinical isolates of Staphylococcus aureus and Escherichia coli," Arzneimittelforschung, vol. 61, no. 08, pp. 472–476, 2011.

[26] A. Venubabu Thati, S. Roy, M. V. N. A. Prasad, C. T. Shivannavar, and S. M. Gaddad, "Nanostructured zinc oxide enhances the activity of antibiotics against Staphylococcus aureus," J. Biosci Tech, vol. 1, no. 2, pp. 64–69, 2010.

[27] S. Iram, J. A. Khan, N. Aman, A. Nadhman, Z. Zulfiqar, and M. A. Yameen, "Enhancing the anti-enterococci activity of different antibiotics by combining with metal oxide nanoparticles," Jundishapur J. Microbiol., vol. 9, no. 3, 2016.

[28] Z. E. Nazari, M. Banoee, A. A. Sepahi, F. Rafii, and A. R. Shahverdi, "The combination effects of trivalent gold ions and gold nanoparticles with different antibiotics against resistant Pseudomonas aeruginosa," Gold Bull., vol. 45, no. 2, pp. 53–59, 2012.

[29] E. Pazos-Ortiz, J. H. Roque-Ruiz, E. A. Hinojos-Márquez, J. López-Esparza, A. Donohué-Cornejo, J. C. Cuevas-González, L. F. Espinosa-Cristóbal, and S. Y. Reyes-López, "Dose-dependent antimicrobial activity of silver nanoparticles on polycaprolactone fibers against gram-positive and gram-negative bacteria," J. Nanomater., vol. 2017, 2017.

[30] F. Ghasemi and R. Jalal, "Antimicrobial action of zinc oxide nanoparticles in combination with ciprofloxacin and ceftazidime against multidrug-resistant Acinetobacter baumannii," J. Glob. Antimicrob. Resist., vol. 6, pp. 118–122, 2016.

[31] M. Banoee, S. Seif, Z. E. Nazari, P. Jafari-Fesharaki, H. R. Shahverdi, A. Moballegh, K. M. Moghaddam, and A. R. Shahverdi, "ZnO nanoparticles enhanced antibacterial activity of ciprofloxacin against Staphylococcus aureus and Escherichia coli," J. Biomed. Mater. Res. Part B Appl. Biomater., vol. 93, no. 2, pp. 557–561, 2010.

[32] V. Sharma, R. K. Shukla, N. Saxena, D. Parmar, M. Das, and A. Dhawan, “DNA damaging potential of zinc oxide nanoparticles in human epidermal cells,” Toxicol. Lett., vol. 185, no. 3, pp. 211–218, 2009.

[33] A. M. Allahverdiyev, K. V. Kon, E. S. Abamor, M. Bagirova, and M. Rafailovich, “Coping with antibiotic resistance: combining nanoparticles with antibiotics and other antimicrobial agents,” Expert Rev. Anti. Infect. Ther., vol. 9, no. 11, pp. 1035–1052, 2011.

[34] F. Rubab, M. F. Chaudhary, and N. M. Butt, “Comparative and Synergistic Studies of Antibacterial Effect of ZnO Nanoparticles and Antibiotics for Pathogens in Drinking Water.” TechConnect Briefs.,vol.3,pp.12-17,2016.

[35] A. A. Slman, “Antibacterial activity of ZnO nanoparticle on some gram-positive and gram-negative bacteria,” Iraqi J. Phys., vol. 10, no. 18, pp. 5–10, 2012.

[36] Z. Luo, Q. Wu, J. Xue, and Y. Ding, “Selectively enhanced antibacterial effects and ultraviolet activation of antibiotics with ZnO nanorods against Escherichia coli,” J. Biomed. Nanotechnol., vol. 9, no. 1, pp. 69–76, 2013.

[37] S. M. F. G. El-Rab, E. M. Halawani, and A. M. Hassan, “Formulation of ceftriaxone conjugated gold nanoparticles and their medical applications against extended-spectrum β-lactamase producing bacteria and breast cancer,” J. Microbiol. Biotechnol., vol. 28, no. 9, pp. 1563–1572, 2018.

[38] M. Harshiny, M. Matheswaran, G. Arthanareeswaran, S. Kumaran, and S. Rajasree, “Enhancement of antibacterial properties of silver nanoparticles–ceftriaxone conjugate through Mukia maderaspatana leaf extract mediated synthesis,” Ecotoxicol. Environ. Saf., vol. 121, pp. 135–141, 2015.

[39] R. Shanmuganathan, D. MubarakAli, D. Prabakar, H. Muthukumar, N. Thajuddin, S. S. Kumar, and A. Pugazhendhi, “An enhancement of antimicrobial efficacy of biogenic and ceftriaxone-conjugated silver nanoparticles: green approach,” Environ. Sci. Pollut. Res., vol. 25, no. 11, pp. 10362–10370, 2018.

[40] S. Mushtaq, J. A. Khan, F. Rabbani, U. Latif, M. Arfan, and M. A. Yameen, “Biocompatible biodegradable polymeric antibacterial nanoparticles for enhancing the effects of a third-generation cephalosporin against resistant bacteria,” J. Med. Microbiol., vol. 66, no. 3, pp. 318–327, 2017.

[41] G. D. Savi, A. C. Trombin, J. da Silva Generoso, T. Barichello, J. C. Possato, J. V. V. Ronconi, and M. M. da Silva Paula, “< b> Antibacterial Acivity of Gold and Silver Nanoparticles Impregnated With Antimicrobial Agents,” Saúde e Pesqui. ISSN 2176-9206, vol. 6, no. 2, 2013.

[42] R. M. Bhande, C. N. Khobragade, R. S. Mane, and S. Bhande, “Enhanced synergism of antibiotics with zinc oxide nanoparticles against extended spectrum β-lactamase producers implicated in urinary tract infections,” J. nanoparticle Res., vol. 15, no. 1, p. 1413, 2013.

تقدير دالتي البقاء و المخاطرة لأنموذج Inverse Gompertz مع تطبيق لجانب المحاكاة

مدرس مساعد منال محمود رشيد

مديرية تربية بغداد الرصافة الثالثة

manal4254@gmail.com

تقدير دالتي البقاء و المخاطرة لأنموذج Inverse Gompertz مع تطبيق لجانب المحاكاة

مدرس مساعد منال محمود رشيد

مديرية تربية بغداد الرصافة الثالثة

manal4254@gmail.com

المستخلص :

ان الاهتمام بدراسة التوزيعات الاحتمالية من قبل الباحثين الاحصائيين جاء نتيجة للدور الذي تؤديه هذه الوسيله الاحصائية في توصيف سلوك البيانات ومعرفة خصائصها , اذ ان الظواهر يمكن التعبير عنها بمتغيرات عشوائية وكل متغير عشوائي يعبر عنه بتوزيع احتمالي يحتوي على المعلومات المهمة لهذا المتغير العشوائي .

أن التوزيع Inverse Gompertz تم استعماله في العديد من التوزيعات الكلاسيكية على نطاق واسع على مدى العقود الماضية لنمذجة البيانات أحادية المتغير وثنائية المتغير في مجالات مثل الهندسة والعلوم الاكتوارية والبيئية والطبية والدراسات البيولوجية والديموغرافيا والاقتصاد والمالية والتأمين.

في هذا البحث تم تقدير دالتي البقاء و المخاطرة بأعتماد على طريقةالامكان الاعظم وطريقة كابلن مير (Kaplan Meier) ولأثبات امكانية تطبيق هذا الانموذج واي طريقتين افضل تم توليد حجوم عينات (n=5.10,30,80,120) وبأستعمال معيار المقارنة وهو متوسط مربعات الخطأ التكاملي (IMSE) .

الكلمات المفتاحية :

أنموذج Inverse Gompertz, دالة البقاء , دالة المخاطرة , , طريقة الامكان الاعظم , طريقة Kaplan Meier , IMSE .

1- المقدمة

تعد التجارب اختبارات الحياة من أهم الطرائق المستعملة للحصول على المعلومات المطلوبة عن الظواهر المختلفة التي تخضع لتلك التجارب. في مثل هذه التجارب ، يتم اختبار عينة من الوحدات ، ويسجل مصمم التجربة أوقات فشل وحدات العينة لأستعمالها في عمل بعض الاستنتاجات الإحصائية المفيدة في تحديد خصائص المجتمع. الوحدات المختارة من وحدات العينة وكما هو معروف أن هناك صعوبة في الحصول على أوقات الفشل للعينة بأكملها لأسباب عديدة منها التكلفة العالية أو طول فترة إجراء التجربة أو الحاجة إلى بعض وحدات العينة لتكون المستعملة في تجربة أخرى وغيرها من الاسباب.

ان الاهتمام بدراسة التوزيعات الاحتمالية من قبل الباحثين الاحصائيين جاء نتيجة للدور الذي تؤديه هذه الوسيله الاحصائية في توصيف سلوك البيانات ومعرفة خصائصها , اذ ان الظواهر يمكن التعبير عنها بمتغيرات عشوائية وكل متغير عشوائي يعبر عنه بتوزيع احتمالي يحتوي على المعلومات المهمة لهذا المتغير العشوائي .

أن التوزيع Inverse Gompertz تم استعماله في العديد من التوزيعات الكلاسيكية على نطاق واسع على مدى العقود الماضية لنمذجة البيانات أحادية المتغير وثنائية المتغير في مجالات مثل الهندسة والعلوم الاكتوارية والبيئية والطبية والدراسات البيولوجية والديموغرافيا والاقتصاد والمالية والتأمين.
من جانب اخر لكل من المعولية والبقاء خاصية واحدة ، وهي مقياس العمر الافتراضي لآلة أو نظام أو كائن حي معين ، لكن الاختلافات التي تحكمها تكمن في تحسين نظام المعولية في الأنظمة متعددة الأجزاء لأن مثل هذا التحسين ينعكس في عدد وأماكن وأجزاء هذا النظام وسهولة إيجاد بديل لهذه الأجزاء ومعالجتها. ولكن هذا التحسين غير موجود في نظرية البقاء ، لأن النظام كائن حي تكمن فيه الصعوبة والندرة في ترتيب أجزائه وإيصاله إلى حالة التحسين.

2- أنموذج Inverse Gompertz :

يعتمد هذا أنموذج على وجود معلمة واحدة لأوقات الحياة ، لنفترض بأن المتغير العشوائي X يتبع توزيع Inverse Gompertz بمعلمة مقياس واحدة $\beta(X \sim IG(\beta)$ ، فأن دالة التوزيع الاحتمالية (PDF) معطاة بالشكل الاتي :

$$f_X(x;\beta) = \frac{1}{x^2}\exp\left(\frac{1}{\beta}\left(1-\exp\left(\frac{\beta}{x}\right)\right)+\frac{\beta}{x}\right), x>0 \qquad (1)$$

ودالة التوزيع التراكمية :

$$F_X(x;\beta) = \exp\left(\frac{1}{\beta}\left(1-\exp\left(\frac{\beta}{x}\right)\right)\right) \quad , x>0, \beta>0 \qquad (2)$$

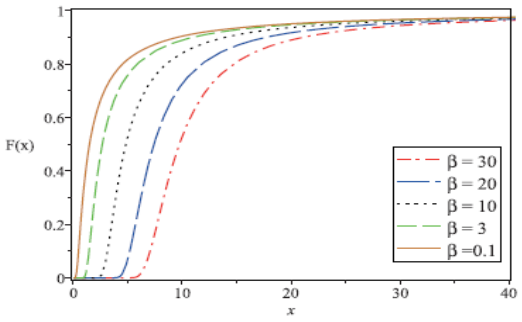

Figure 1. The CDF of A distribution for different values of β.

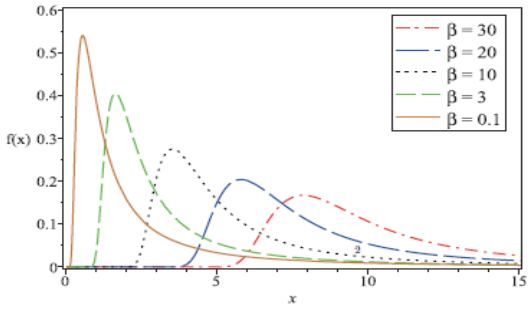

Figure 2. The PDF of A distribution for different values of β.

3- دالة البقاء :

هناك عدة معانٍ لمفهوم دالة البقاء والمعنى الواسع له هو احتمال بقاء المريض على قيد الحياة خلال مدة زمنية معينة تحت ظروف وعوامل خاصة، ويرمز لدالة البقاء بالرمز S(x)، ويعبر عن دالة البقاء بالمعادلة الرياضية الآتية :

$$S(x) = \Pr(X > x)$$

$$= \int_x^{\infty} f(y)dy$$

$$= 1 - F(x)$$

$$S_X(x;\beta) = 1 - \exp\left(\frac{1}{\beta}\left(1 - \exp\left(\frac{\beta}{x}\right)\right)\right) \quad , x > 0, \beta > 0 \qquad (3)$$

4- دالة المخاطرة

دالة الخطر ، والمعروفة أيضًا باسم معدل الفشل ، هي احتمال وفاة الفرد في الوقت x نظرًا لأن الفرد نجا حتى ذلك الوقت x.
تستخدم وظيفة الخطر على نطاق واسع للتعبير عن خطر وقوع حدث (على سبيل المثال ، الموت) يحدث في وقت ما.
بالنظر إلى المتغير العشوائي X من التوزيع المستمر ، يتم إعطاء معدل الخطر h (x) بواسطة

$$h(x) = \frac{f(x)}{1 - F(x)}$$

$$h_X(x;\beta) = \frac{\exp\left(\frac{\beta}{x}\right)}{x^2 \exp\left(\frac{1}{\beta}\left(\exp\left(\frac{\beta}{x}\right) - 1\right)\right)}, x > 0 \qquad (4)$$

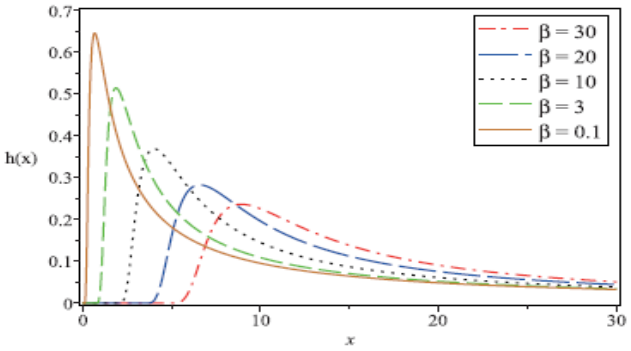

Figure 3. The HR function of the A distribution for different values of β.

5-طرائق التقدير :

5-1 طريقة الامكان الاعظم :

تعتبر هذه الطريقة من أهم الطرائق التقدير المهمة لما تحتويه من خواص جيدة ومنها الثبات ،كفاءة عالية واتساق في بعض الأحيان . افترض أن لدينا عددًا من المشاهدات من التوزيع بحجم عينة n من توزيع Inverse Gompertz. بعد ذلك ، نحصل على دالة الامكان بالشكل الاتي :

لنفترض $x_1, x_2, \dots, x_n$ تمثل عينة عشوائية بحجم n من التوزيع Inverse Gompertz فأن دالة لتوزيع الاحتمالي هي

$$\ell = \prod_{i=1}^{n} f_X(x_i;\beta)$$

$$\ell = \prod_{i=1}^{n} \frac{1}{x_i^2} \exp\left(\frac{1}{\beta}\left(1 - \exp\left(\frac{\beta}{x_i}\right)\right) + \frac{\beta}{x_i}\right)$$

$$LL = \beta \sum_{i=1}^{n} \frac{1}{x_i} - \frac{1}{\beta} \sum_{i=1}^{n} \left(\exp\left(\frac{\beta}{x_i}\right) - 1\right) - 2\sum_{i=1}^{n} \ln(x_i)$$

$$\frac{\partial LL}{\partial \hat{\beta}} = \sum_{i=1}^{n} \frac{1}{x_i} - \frac{1}{(\hat{\beta})^2} \sum_{i=1}^{n} \left(\frac{\hat{\beta}}{x_i} \exp\left(\frac{\hat{\beta}}{x_i}\right) - \exp\left(\frac{\hat{\beta}}{x_i}\right) + 1\right) = 0$$

2-5 طريقة كابلن - مير *Kaplan Meier method*:

وهي من الطرائق اللا معلمية التي اتبعها كابلن مير (1958) *Kaplan and Meier* لتقدير دالة البقاء فهناك طريقتان الأولى يتم فيها تقدير دالة الخطورة التجميعية $H(x)$ عن طريق تقدير دالة الخطورة $h(x)$ الطريقة الثانية إستخدام دالة الكثافة التجميعية أو دالة توزيع الفشل لتقدير دالة البقاء ودالة الخطورة.

1- أسلوب كابلن - مير الأول

- ترتيب أوقات الفشل (وقت البقاء) تصاعدياً وإعطاء كل فشل رتبة (*Rank*).
- حساب دالة الخطورة $h(x)$ ، حيث أن دالة الخطورة هي عبارة عن عدد ايام اوقات البقاء مقسوم على مقدار الفترة الزمنية $=\frac{k}{n-i+1}$

  $h(x)$, اذ أن k : تمثل عدد ايام اوقات البقاء , i : تمثل الرتبة , n : حجم العينة
- حساب $H(x)$ اذ أن $H(x)=[h(x_1)+ h(x_2)+\ldots+ h(x_n)]$
- حساب دالة البقاء $S_i(x)$, اذ ان $i=1,2$, $s_i(x) = \exp(-H_i(x))$

2- أسلوب كابلن - مير الثاني

- تقدير F(x) التي يعتمد تقديرها على البيانات اذ ان : $F(x) = \frac{i}{n}$ او $F(x) = \frac{i-0.5}{n}$ وهي ماتسمى بدالة الكثافة التراكمية أو $F(x) = \frac{i}{n+1}$ وهي ماتسمى برتبة الوسط الحسابي او $F(x) = \frac{i-0.3}{n+0.4}$ وهي ماتسمى برتبة الوسيط
- يمكن حساب دالة الخطورة وان دالة الفشل التجمعية حيث ان : $h_i(x) = \frac{F_{(x+1)} - F_x}{1-F_x}$
- ويمكن ايضا حساب دالة البقاء التي تساوي $S_i(x) = 1 - F_i(x)$
- ومنها نحصل على $\hat{s}(x)$ بطريقة كابلن – مير $\hat{s}_{i+1} = \prod_{i=1}^{n} s_{i+1}(x) \cdot \hat{s}_i$ اذ ان : $\hat{s}_i$ قيمة دالة البقاء المقدرة الاولى لكابلن مير

  $\hat{s}_{i+1}$ قيمة دالة البقاء المقدرة اللاحقة لكابلن مير

6- الجانب التجريبي :

تم استعمال اسلوب المحاكاة بطريقة مونت كارلو للمقارنة بين طرائق التقدير المختلفة حيث يتميز هذا الاسلوب بالمرونة ويوفر الكثير من التكليف عن طريق اخذ بنظر الاعتبار حجوم العينات المختلفة والقيم المختلفة لمعلمات التوزيع وتكرار التجربة في كل مرة ويتم في هذا الاسلوب توليد البيانات دون اللجوء الى البيانات الحقيقية مع عدم الاخلال بالدقة المطلوبة وتتلخص هذه الطريقة بالخطوات التالية :

1- تحديد القيم الافتراضية :حيث تم اختيار حجوم عينات مختلفة وهي (5,10,30,80,120) وكذلك تم استعمال قيم افتراضية لمعلمة النموذج وكما يأتي :

توليد البيانات:

1- اذ تم توليد المتغير العشوائي بطريقة التحويل العكسي كمايلي :

$$x_q = \frac{\beta}{\ln(1-\beta \ln q)}$$

2- ترتيب البيانات التي تم توليدها ترتيباً تصاعدياً $x_1 < x_2 < \cdots < x_i$

3- حل المعادلات التي تم الوصول اليها بالطرق العددية

4- تم تحديد الطريقة الافضل عن طريق مقياس المقارنة (*IMSE*) في حالة تقدير دالة البقاء والمخاطرة

$$IMSE(\hat{S}(x)) = \frac{1}{r}\sum_{i=1}^{r}\left[\frac{1}{n_x}\sum_{j=1}^{n_t}\left(\hat{s}_i(x_j) - s(x_j)\right)^2\right]$$

$$IMSE(\hat{h}(x)) = \frac{1}{r}\sum_{i=1}^{r}\left[\frac{1}{n_x}\sum_{j=1}^{n_t}\left(\hat{h}_i(x_j) - h(x_j)\right)^2\right]$$

اذ أن :

r : عدد تكرارات التجربة (1000) مرة

n_x : عدد البيانات المولدة لكل عينة

$\hat{s}_i(x_j), \hat{h}_i(x_j)$: مقدر دالة البقاء والمخاطرة على التوالي .

$S(x_j)$, $h(x_j)$: دالة البقاء والمخاطرة حسب القيم الابتدائية وعلى التوالي .

الجدول رقم (1) يبين قيم IMSE لتقدير دالة البقاء بجميع الطرائق وحجوم العينات ولجميع التجارب

model	n	MLE	KM	best
β=2.0	5	0.025349	2.44E-02	KM
	10	8.91E-03	8.79E-03	KM
	30	8.31E-03	8.29E-03	KM
	80	8.25E-03	8.20E-03	KM
	120	1.16E-03	1.19E-03	MLE
β=2.5	5	6.76E-02	6.20E-02	KM
	10	1.19E-02	1.13E-02	KM
	30	1.17E-02	0.01141	KM
	80	1.14E-02	1.01E-02	KM
	120	8.77E-03	8.80E-03	MLE
β=4.6	5	9 .81E-03	6.82E-03	KM
	10	7.30E-03	7.06E-03	KM
	30	7.21E-03	7.00E-03	KM

	80	5.80E-03	6.81E-03	MLE
	120	1.04E-03	1.09E-03	MLE
β=5.3	5	6.21E-03	6.18E-03	KM
	10	2.45E-03	2.40E-03	KM
	30	2.44E-03	2.33E-03	KM
	80	1.61E-03	1.77E-03	MLE
	120	1.45E-05	1.51E-04	MLE

من خلال النتائج في جدول (1) تبين مايلي :

1.عند متوسط مربعات الخطأ التكاملي ولحجوم العينات المختلفة (n=(5,10,30 يلاحظ وبصورة عامة إنفردت طريقة (كابلن مير) بالأفضلية على سائر طريقة الامكان الاعظم , وفي حجم عينة (n=120) ظهرت طريقة الامكان الاعظم(MLE) بالأفضلية في تقدير دالة البقاء .

2 . عند حجم عينة n=80 لنموذج الاول والثاني (β=2.0,2.5) ظهرت طريقة (كابلن مير) بالافضلية وعند نموذج الثالث والرابع (β=4.6,5.3) ظهرت طريقة الامكان الاعظم (MLE) بالأفضلية في تقدير دالة البقاء

الجدول رقم (2) يبين قيم IMSE لتقدير دالة المخاطرة بجميع الطرائق وحجوم العينات ولجميع التجارب

model	n	MLE	KM	best
β=2.0	5	4.29E-02	4.27E-02	KM
	10	4.22E-02	4.13E-02	KM
	30	0.041068	4.12E-02	MLE
	80	6.94E-04	4.95E-03	MLE
	120	5.22E-05	5.23E-04	MLE
β=2.5	5	6.65E-02	5.64E-02	KM
	10	6.52E-02	0.06402	KM
	30	6.42E-02	6.40E-02	KM
	80	0.0068594	6.86E-03	MLE
	120	7.53E-05	7.83E-04	MLE
β=4.6	5	0.380529	0.320761	KM
	10	0.279779	0.249545	KM
	30	0.233695	0.243841	MLE
	80	0.20355	0.233485	MLE
	120	0.020035	0.228505	MLE
β=5.3	5	0.297891	0.268753	KM
	10	0.268802	0.258384	KM
	30	0.225456	0.245317	MLE
	80	0.204796	0.215348	MLE
	120	0.0239918	0.029049	MLE

من خلال النتائج في جدول (2) تبين مايلي :

1.عند متوسط مربعات الخطأ التكاملي ولحجوم العينات المختلفة (n=(5,10 يلاحظ وبصورة عامة إنفردت طريقة (كابلن مير) بالأفضلية على سائر طريقة الامكان الاعظم , وفي حجم عينة (n=80,120) ظهرت طريقة الامكان الاعظم(MLE) بالأفضلية في تقدير دالة المخاطرة .
2.عند حجم عينة n=30 لنموذج الاول والثالث والرابع (β=2.0,4.6,5.3) ظهرت طريقة الامكان الاعظم (MLE) بالافضلية وعند نموذج الثاني (β=2.5) إنفردت طريقة (كابلن مير) بالأفضلية في تقدير دالة المخاطرة .

7- الاستنتاجات (Conclusions) :

من خلال النتائج جانب المحاكاة تبين مايلي :
1.عند متوسط مربعات الخطأ التكاملي ولحجوم العينات المختلفة (n=(5,10,30 يلاحظ وبصورة عامة إنفردت طريقة (كابلن مير) بالأفضلية على سائر طريقة الامكان الاعظم , وفي حجم عينة (n=120) ظهرت طريقة الامكان الاعظم(MLE) بالأفضلية في تقدير دالة البقاء .
2.عند حجم عينة n=80 لنموذج الاول والثاني (β=2.0,2.5) ظهرت طريقة (كابلن مير) بالافضلية وعند نموذج الثالث والرابع ( ) β=4.6,5.3 ظهرت طريقة الامكان الاعظم (MLE) بالأفضلية في تقدير دالة البقاء
3.عند متوسط مربعات الخطأ التكاملي ولحجوم العينات المختلفة (n=(5,10 يلاحظ وبصورة عامة إنفردت طريقة (كابلن مير) بالأفضلية على سائر طريقة الامكان الاعظم , وفي حجم عينة (n=80,120) ظهرت طريقة الامكان الاعظم(MLE) بالأفضلية في تقدير دالة المخاطرة .
4.عند حجم عينة n=30 لنموذج الاول والثالث والرابع (β=2.0,4.6,5.3) ظهرت طريقة الامكان الاعظم (MLE) بالافضلية وعند نموذج الثاني (β=2.5) إنفردت طريقة (كابلن مير) بالأفضلية في تقدير دالة المخاطرة .

أولاً :- المراجع العربية (Arabic References)

1- **العامري ,** سماح صباح (2021) **"تقدير دالتي البقاء والمخاطرة لتوزيع log-logistic بأستعمال الاحصاءات المرتبة مع تطبيق عملي"** رسالة ماجستير في الاحصاء مقدمة الى كلية الأدارة والأقتصاد في جامعة بغداد
2- الباقر , زينب محمد (2017) **"تقدير دالة المعولية لتوزيع بواسون مع تطبيق عملي"** رسالة ماجستير في الاحصاء مقدمة الى كلية الأدارة والأقتصاد في جامعة كربلاء
3- **صالح** , احمد علوان (2016) **"طرائق تقدير دالة المخاطرة لتوزيع Quasi- Lindely بحث مقارن مع تطبيق عملي"** رسالة ماجستير في الاحصاء مقدمة الى كلية الأدارة والأقتصاد في جامعة بغداد

ثانياً :- المراجع الأجنبية (Foreign References)

4- German, R." **Non-Parametric Estimation in Survival Models**",2005.
5- Horst, R. "**The Hazard Rate, Theory and Inference**", With supplementary MATLAB Programs. Justus Liebig University, Germany,2014.
6- R. Alshenawy (2020) **A new one parameter distribution: properties and estimation with applications to complete and type II censored data**, Journal of Taibah University for Science, 14:1, 11-18, DOI: 10.1080/16583655.2019.1698276
7- El-Bassiouny AH, EL-Damcese M, Mustafa A, Eliwa MS. **Exponentiated generalized Weibull-Gompertz distribution with application in survival analysis**. J Stat Appl Prob. 2017;6(1):7–16.
8- El-Bassiouny AH, EL-Damcese M, Mustafa A, Eliwa MS. **Characterization of the generalized Weibull-Gompertz distribution based on the upper record values**. Int J Math Appl. 2015;3(3):13–22.
9- El-Bassiouny AH, Tahir MH, Elmorshedy M, Eliwa MS. Univariate and multivariate double slash distribution: properties and application. J Stat Appl Prob. 2019. To appear.
10-El-Bassiouny AH, EL-Damcese M, Mustafa A, Eliwa MS. Mixture of exponentiated generalized Weibull-Gompertz distribution and its applications in reliability. J Stat Appl Prob. 2016a;5(3):1–14.
11-El-Morshedy M, Eliwa MS, Nagy H. A new two-parameter exponentiated discrete Lindley distribution: properties, estimation and applications. J Appl Stat. 2019a. doi:10.1080/02664763.2019.1638893.
12-Eliwa MS, El-Morshedy M, Afify AZ. The odd Chen generator of distributions: properties and estimation methods with applications in medicine and engineering. J Natl Sci Found Sri Lanka. 2019. To appear.
13-El-Morshedy M, Eliwa MS. The odd flexible Weibull-H family of distributions: properties and estimation with applications to complete and upper record data. Filomat. 2019;33(9). To appear.
14- Basheer AM. Alpha power inverse Weibull distribution with reliability application. J Taibah Univ Sci. 2019;13(1):423–432.
15- Eliwa MS, El-Morshedy M. Discrete flexible distribution for over-dispersed data: statistical and reliability properties with estimation approaches and applications. J Appl Stat. 2020b. To appear.

Solving Harmonic Equation by Implicit Method

Thabet Hasan Sultan

Department of Mathematics - Collage of Science - University of Maragheh -Iran

thabit1394@gmail.com

Solving Harmonic Equation by Implicit Method

Thabet Hasan Sultan

Department of Mathematics - Collage of Science - University of Maragheh -Iran

thabit1394@gmail.com

Abstract:

In this paper, we solving the harmonic equation by one of the differencing method which is the implicit numerical method the heat diffusion equation is one kinds of homogeneous harmonic equation. So, we solving this equation by this numerical method with the initial and boundary conditions. The results other method.

Keywords: Harmonic, Heat Diffusion Equation Numerical Method, Implicit Method.

1-1 Introduction:

The Partial Differential Equations (P. d. e) are used to expressing for many problems in many different Sciences, Fluid Mechanic, Physics, Chemical, Engineering, Elasticity, … etc.

One kinds of (P. d. e) is the Homogeneous Harmonic Equation, the general formula of this equation is

$$\frac{\partial^2 v}{\partial x^2}+\frac{\partial^2 v}{\partial y^2}=0 \quad \dots(1-1)$$

Or as the form

$$\nabla^2 v=0 \quad \dots(1-2)$$

The heat diffusion equation is one kind of this equation many researchers are solve this equation by the Numerical Method, in (2020), Adak is solving the general diffusion by Implicit and Explicit method [1] and Awni M. Gaftan in 2019 is used the $\theta-$ differencing

method for testing the effect the Isolating of some materials [2]. In (2004), Recktenwald is introduced the finite – differenced approximations to the heat equation [5] and in (2013), Thomas, J. W. is introduced the Numerical Partial differential equation with boundary –value problems [7].

1-2 The Implicit Method: [1] [2]

Is a numerical way of expressing the value of *v(x)* in the future time (t+Δt), depending on the future time (t + Δ t) and the present time

(t), and sometimes also about the past tense (t-Δt).)

The division is according to the explicit method into levels. After defining the initial conditions and boundary conditions, each level is divided into points.

They represent initial (primary) and boundary conditions.

We use the following equations to find the points in the levels:

1- The general form of the implicit method for the one-dimensional heat flow equation.

• One - dimension.

$$v_{i,j} = (1+2R)v_{i,j+1} - Rv_{i-1,j+1} - Rv_{i+1,j+1} \quad \dots(1-3)$$

whereas: - $\forall i = 1,2,3,\dots,n \ , \ \forall j = 0,1,2,3,\dots m$

$$R = \frac{k\Delta t}{h^2} \ , (\Delta x)^2 = h^2$$

2- The general form of the implicit method for solving the homogeneous harmonic equation.

$$v_{i-1,j+1} + v_{i+1,j-1} - 2v_{i+1,j} = 2v_{i,j+1} - 2v_{i+1,j+1} \quad \dots(1-4)$$

$\forall i = 1,2,3,\dots,n \ , \quad \forall j = 0,1,2,3,\dots,m$

And we express it as $v_{i,j+1}$ by $v_{i,j}$, we find that the time domain and the spatial domain are already represented in each time period, we write (j) (inner node),and the equations are solved simultaneously with the initial conditions and borderline

So the implicit method is easily as shown in the following figure [1], [2].

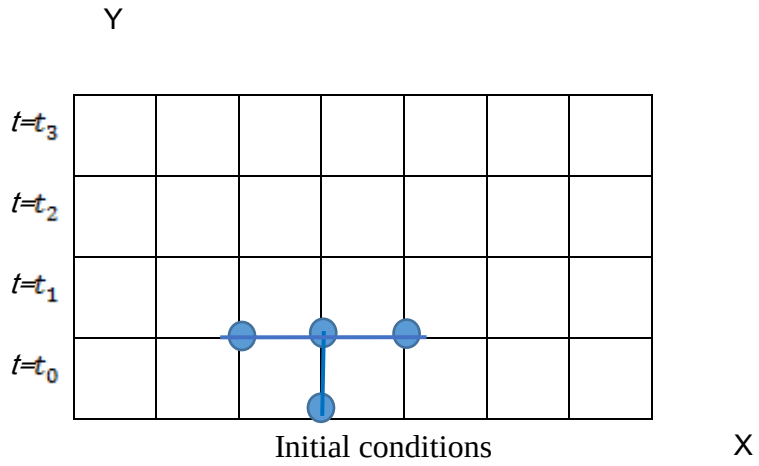

Figure (1 – 1)

1-3 Algorithm of Implicit Method:

1- We divide the solution area into several divisions that represent each level and are in the form of a rectangular grid, and we place the initial conditions, the right boundary conditions, and the left boundary conditions mentioned in the problem.

2 - Substitute values $(\forall i = 1,2,3, \dots, n, j = 0)$ into the general form of the equations, the implicit method (1 – 3)

3 - Substituting the values of the boundary conditions, the values of the initial conditions, and the value of R in the general formula, so we will get three general equations simultaneously with the addition of substituting the values of the initial conditions and the values of the boundary conditions.

4 - After the substitutions made in step (3) and solving the three equations, we get the unknown values $(v_{3,1}, v_{2,1}, v_{1,1})$ and by repeating the process on the previous steps when j=1.

5- Continuing to repeat the process in order to get the approximate solution that satisfies the condition.

1-4 Initial conditions: [5]

In order to solve a partial differential equation of the second degree, it is required to know the initial conditions of any harmonic and bi-harmonic equation. When we solve problems that appear in the harmonic and bi-harmonic equations, we have to know the initial conditions of the wave equation, which depends on two functions g and f as linear sinusoidal functions or as complex exponential functions

$$v(x,t)_{t=0} = f(x,0)$$

$$v(x,t) = v(x) \quad , \quad 0 < x < I$$

1-5 Boundary conditions and their types: [3] [8]

1- The boundary conditions of the harmonic and bi-harmonic equation consist of a set of types as follows

The boundary conditions of the harmonic and bi-harmonic equations are met according to the following mathematical formulas

$$v(t,0) = v_1(t) \quad , \quad 0 < x < I$$

$$v(t,I) = v_2(t) \quad , \quad 0 < x < I$$

This boundary condition is called the (Dirichlet Condition) in which the value of the function is known through each boundary point on the boundary of the solution region.

2 - While the boundary condition in the harmonic and bi-harmonic equation allocated within the borders of any region is in the following form

$$c\frac{\partial v}{\partial x}(t,0) = 0$$

It is called (Neumann Condition), where the value of the derivative of the used function is clear through every boundary point

3 - Robin Condition within the limits is in the form

$$c\frac{\partial v}{\partial x} + \mathrm{h}v(t,I) = g(t)$$

And this condition depends on the partial derivative of the function with the variable x

In conclusion, the three conditions that were mentioned earlier are used during the boundaries of the region by relying on knowing the value of the function once and knowing the value of its derivative within each region or on part of the boundaries

All conditions can be mixed, so we can get some values of the function or its derivatives through some boundary points. Therefore, the boundary conditions must be compensated once for the function itself and once for its derivatives.

1-6 Deriving the general formula for the implicit method for solving the one-dimensional heat equation: [2] [4] [7]

The one-dimensional heat equation is

$$\frac{\partial^2 \mathrm{v}}{\partial \mathrm{x}^2} = \left[\frac{1}{\mathrm{k}}\right]\frac{\partial v}{\partial t} \qquad \dots(1-5)$$

From equation (3 - 1) we have

$$v_{xx} = \frac{\partial^2 v}{\partial x^2}\ , \qquad v_t = \frac{\partial v}{\partial t}$$

In order to get the general form of the implicit method, we use the finite differences

$$v_{xx} = \frac{v_{i-1,j+1} - 2v_{i,j+1} + v_{i+1,j+1}}{(\Delta x)^2} \qquad \dots(1-6)$$

$$v_t = \frac{v_{i,j+1} - v_{i,j}}{\Delta t} \qquad \dots(1-7)$$

$$\forall i = 1,2,3,\dots,n\ , \qquad \forall j = 0,1,2,\dots,m$$

Where we substitute the differences ending (1 – 6) and (1 – 7) in equation (1 – 5) we get

$$\frac{v_{i-1,j+1} - 2v_{i,j+1} + v_{i+1,j+1}}{h^2} = \frac{1}{k}\left(\frac{v_{i,j+1} - v_{i,j}}{\Delta t}\right) \qquad \dots(1-8)$$

We multiply both sides of equation (1 – 8) by (k Δt) we get

$$\frac{k\Delta t}{h^2}\left(v_{i-1,j+1} - 2v_{i,j+1} + v_{i+1,j+1}\right) = v_{i,j+1} - v_{i,j} \qquad \dots(1-9)$$

Suppose that

$$R = \frac{k\Delta t}{h^2}$$

So equation (1 – 9) becomes as follows

$$R\left(v_{i-1,j+1} - 2v_{i,j+1} + v_{i+1,j+1}\right) = v_{i,j+1} - v_{i,j} \qquad \dots(1-10)$$

After simplifying equation (1 – 10) to its simplest form, we get the general formula for the implicit method, which is:

$$v_{i,j} = (1+2R)v_{i,j+1} - Rv_{i-1,j+1} - Rv_{i+1,j+1} \qquad \dots(1-11)$$

$$\forall i = 1,2,3,\dots,n \ , \qquad \forall j = 0,1,2,\dots,m$$

Whereas:

$$R = \frac{k\Delta t}{h^2}$$

1-7 Deriving the implicit method for the harmonic equation:

It is called the implicit method, since the solution for each level we walk through requires it to solve a system of linear equations with a dimension $(\mathrm{n} \times \mathrm{n})$and the points required to find the solution through the j+1 level are based on a known point in the level, and to find the point $\mathrm{v}_{\mathrm{i,j+1}}$ at the level we do the following: -

1- The general form of the homogeneous harmonic equation is:

$$\mathrm{v}_{\mathrm{xx}} + \mathrm{v}_{\mathrm{yy}} = 0 \quad \dots(1-12)$$

1- We use the following finite differences [5]

$$\mathrm{v}_{\mathrm{xx}} = \frac{\mathrm{v}_{\mathrm{i-1,j+1}} - 2\mathrm{v}_{\mathrm{i,j+1}} + \mathrm{v}_{\mathrm{i+1,j+1}}}{(\Delta \mathrm{x})^2} \qquad \dots(1-8)$$

$$\mathrm{v}_{\mathrm{yy}} = \frac{\mathrm{v}_{\mathrm{i+1,j-1}} - 2\mathrm{v}_{\mathrm{i+1,j}} + \mathrm{v}_{\mathrm{i+1,j+1}}}{(\Delta \mathrm{y})^2} \qquad \dots(1-13)$$

$\forall \mathrm{i} = 1,2,3,\dots,\mathrm{n} \ , \quad \forall \mathrm{j} = 0,1,2,3,\dots,\mathrm{m}$

knowing that: $(\Delta \mathrm{x})^2 = (\Delta \mathrm{y})^2 = \mathrm{h}^2$

2- We substitute equations (1 – 6) and (1 – 13) into equation (1 – 12) as shown below

$$\frac{\mathrm{v}_{\mathrm{i-1,j+1}} - 2\mathrm{v}_{\mathrm{i,j+1}} + \mathrm{v}_{\mathrm{i+1,j+1}}}{\mathrm{h}^2} + \frac{\mathrm{v}_{\mathrm{i+1,j-1}} - 2\mathrm{v}_{\mathrm{i+1,j}} + \mathrm{v}_{\mathrm{i+1,j+1}}}{\mathrm{h}^2} = 0 \qquad \dots(1-14)$$

By multiplying equation (1 – 14) by $(h^2)$for both sides and simplifying the equation, we get

$$v_{i-1,j+1} - 2v_{i,j+1} + 2v_{i+1,j+1} + v_{i+1,j-1} - 2v_{i+1,j} = 0 \qquad \dots(1-15)$$

And it can be formulated as follows as well

$$v_{i-1,j+1} + v_{i+1.j-1} - 2v_{i+1,j} = 2v_{i,j+1} - 2v_{i+1,j+1} \qquad \dots(1-16)$$

$$\forall i = 1,2,3,\dots,n \ , \qquad \forall j = 0,1,2,3,\dots,m$$

Whereas, equation (1 – 16) is the general form of the implicit method for solving the homogeneous harmonic equation.

Where the solution area is divided into levels and each level contains points that represent the initial conditions and the boundary conditions, where equation (1 – 16) is used to find the points in the levels and are solved simultaneously and with the frontier and initial conditions.

Example: - Use the implicit method to solve the one-dimensional heat flow equation

$v_t = v_{xx}$ on a rectangular plate, its dimensions are 4 * 2, applied on the x-axis and the y-axis at the center of the origin, according to the following data:

$$\Delta t = 4\,\text{sec} \quad , \quad \Delta x = 2 \quad , \quad k = 0.5$$

and primary conditions

$$v(x,t) = 0° \quad , \; 0 < x < 12 \quad , t = 0$$

and boundary conditions

$$v(0,t) = 5° \quad , \quad v(10,t) = 3°$$

Solution / We initially make a grid that contains nodal points and put the data in the issue in it and it is in the form

We write the general equation for the implicit method in solving the one-dimensional heat flow equation, namely

$$v_{i,j} = (1+2R)v_{i,j+1} - Rv_{i-1,j+1} - Rv_{i+1,j+1} \quad \ldots(1-11)$$

whereas: - $\forall i = 1,2,3,\ldots,n \;\; , \forall j = 0,1,2,3,\ldots m$

We find the value of R through the following mathematical formula

$$R = \frac{k\Delta t}{h^2} \quad , (\Delta x)^2 = h^2$$

$$R = 0.5\frac{4}{(2)^2} \quad \Rightarrow \quad R = 0.5$$

We start when $i = 1,2,3,4,5 \quad , j = 0$

$$i = 1 \; , \quad j = 0$$

$$v_{1,0} = (1+2R)v_{1,1} - Rv_{0,1} - Rv_{2,1} \quad \ldots(1-17)$$

$$i = 2 \ , \quad j = 0$$

$$v_{2,0} = (1 + 2R)v_{2,1} - Rv_{1,1} - Rv_{3,1} \qquad \dots (1 - 18)$$

$$i = 3 \ , \quad j = 0$$

$$v_{3,0} = (1 + 2R)v_{3,1} - Rv_{2,1} - Rv_{4,1} \qquad \dots (1 - 19)$$

$$i = 4 \ , \quad j = 0$$

$$v_{4,0} = (1 + 2R)\,v_{4,1} - Rv_{3,1} - Rv_{5,1} \qquad \dots (1 - 20)$$

$$i = 5 \ , \quad j = 0$$

$$v_{5,0} = (1 + 2R)v_{5,1} - Rv_{4,1} - Rv_{6,1} \qquad \dots (1 - 21)$$

We substitute the value of R = 0.5 and the values of the boundary conditions and initial conditions into equations (1 – 17), (1 – 18), (1 – 19), (1 – 20) and (1 – 21), and then we simplify and arrange the equations, we get

$$2.5 = 2v_{1,1} - 0.5v_{2,1} \qquad \dots (1 - 22)$$

$$0 = -0.5v_{1,1} + 2v_{2,1} - 0.5v_{3,1} \qquad \dots (1 - 23)$$

$$0 = -0.5v_{2,1} + 2v_{3,1} - 0.5v_{4,1} \qquad \dots (1 - 24)$$

$$0 = -0.5v_{3,1} + 2v_{4,1} - 0.5v_{5,1} \qquad \dots (1 - 25)$$

$$1.5 = -0.5v_{4,1} + 2v_{5,1} \qquad \dots (1 - 26)$$

By multiplying equation (1 – 23) by (4), we get

$$0 = -2v_{1,1} + 8v_{2,1} - 2v_{3,1} \qquad \dots (1 - 27)$$

We take the two equations (1 – 23) and (1 – 27) and solve them simultaneously (by the combination), so we get equation (1 – 28)

$$2.5 = 2v_{1,1} - 0.5v_{2,1} \qquad \dots (1 - 23)$$

$$0 = -2v_{1,1} + 8v_{2,1} - 2v_{3,1} \qquad \dots (1 - 27)$$

$$2.5 = 7.5v_{2,1} - 2v_{3,1} \qquad \dots (1 - 28)$$

By solving equations (1 – 24) and (1 – 28) simultaneously (by the combination), we get equation (1 – 29)

$$0 = -0.5v_{2,1} + 2v_{3,1} - 0.5v_{4,1} \quad \dots(1-24)$$

$$2.5 = 7.5v_{2,1} - 2v_{3,1} \quad \dots(1-28)$$

$$2.5 = 7v_{2,1} - 0.5v_{4,1} \quad \dots(1-29)$$

By multiplying equation (1 – 29) by (4), we get

$$10 = 28v_{2,1} - 2v_{4,1} \quad \dots(1-30)$$

By solving equations (1 – 25) and (1 – 30) simultaneously (by the combination), I get equation (1 – 31)

$$0 = -0.5v_{3,1} + 2v_{4,1} - 0.5v_{5,1} \quad \dots(1-25)$$

$$10 = 28v_{2,1} - 2v_{4,1} \quad \dots(1-30)$$

$$10 = 28v_{2,1} - 0.5v_{3,1} - 0.5v_{5,1} \quad \dots(1-31)$$

By multiplying equation (1 – 31) by (4), I get:

$$40 = 112v_{2,1} - 2v_{3,1} - 2v_{5,1} \quad \dots(1-32)$$

We take equations (1 – 26) and (1 – 32) and solve them simultaneously (by the combination) to obtain equation (1 – 33)

$$1.5 = -0.5v_{4,1} + 2v_{5,1} \quad \dots(1-26)$$

$$40 = 112v_{2,1} - 2v_{3,1} - 2v_{5,1} \quad \dots(1-32)$$

$$41.5 = 112v_{2,1} - 4v_{3,1} - 0.5v_{4,1} \quad \dots(1-33)$$

By multiplying equation (1 – 33) by (4), we get:

$$166 = 448v_{2,1} - 16v_{3,1} - 2v_{4,1} \quad \dots(1-34)$$

By solving equations (1 – 29) and (1 – 34) simultaneously (by subtraction), we get equation (1 – 35)

$$2.5 = 7v_{2,1} - 0.5v_{4,1} \quad \ldots(1-29)$$

$$166 = 448v_{2,1} - 16v_{3,1} - 2v_{4,1} \quad \ldots(1-34)$$

$$156 = 420v_{2,1} - 16v_{3,1} \quad \ldots(1-35)$$

By multiplying equation (1 – 28) by (8), we get

$$20 = 60v_{2,1} - 16v_{3,1} \quad \ldots(1-36)$$

By solving equations (1 – 35) and (1 – 36) simultaneously (by subtraction), we get

$$156 = 420v_{2,1} - 16v_{3,1} \quad \ldots(1-35)$$

$$20 = 60v_{2,1} - 16v_{3,1} \quad \ldots(1-36)$$

$$136 = 360v_{2,1}$$

$$\therefore v_{2,1} = 0.3777$$

Substitute the value of $v_{2,1} = 0.3777$ into equation (1 – 35)

$$156 = 420(0.3777) - 16v_{3,1}$$

$$16v_{3,1} = 2.6634$$

$$\therefore v_{3,1} = 0.1665$$

Substituting the value of $v_{2,1} = 0.3777$ into equation (1 – 22), we get

$$2.5 = 2v_{1,1} - 0.5(0.3777)$$

$$2v_{1,1} = 2.6885$$

$$\therefore v_{1,1} = 1.3444$$

Substitute the value of $v_{2,1} = 0.3777$ into equation (1 – 29)

$$2.5 = 7(0.3777) - 0.5v_{4,1}$$

$$0.5v_{4,1} = 0.1439$$

$$\therefore v_{4,1} = 0.2878$$

Substituting the value of $v_{4,1} = 0.2878$ into equation (1 – 26), we get the following

$$0 = -0.5(0.2878) + 2v_{5,1} - 1.5$$

$$2v_{5,1} = 1.6439$$

$$\therefore v_{5,1} = 0.82195$$

In the same way as the solution when applied to the other levels, you will get the following point values.

$$v_{1,2} = 2.12284$$

$$v_{2,2} = 0.82557$$

$$v_{3,2} = 0.41829$$

$$v_{4,2} = 0.51458$$

$$v_{5,2} = 1.28962$$

$$v_{1,3} = 2.62751$$

$$v_{2,3} = 1.25287$$

$$v_{3,3} = 0.73283$$

$$v_{4,3} = 0.84186$$

$$v_{5,3} = 1.60528$$

Reference

[1] Adak, M. (2020). "Comparison of explicit and implicit finite difference schemes on diffusion equation," in Springer Proceedings in Mathematics and Statistics, vol. 320, pp. 227–238. doi: 10.1007/978-981-15-3615-1_15

[2] Gaftan, A. M. (2019). "θ-Differencing Method for testing the Isolating Qualification of Some Materials,". [Online]. Available: http://pjrpublication.com/

[3] Gakhov, F. D. (1990). Boundary value problems. Courier Corporation.

[4] Morton, K. W., & Mayers, D. F. (2005). Numerical solution of partial differential equations: an introduction. Cambridge university press.

[5] Recktenwald, G. W. (2004). Finite-difference approximations to the heat equation. Mechanical Engineering, 10(01).

[6] Sukhatme, S. P. (2005). A textbook on heat transfer. Universities Press.

[7] Thomas, J. W. (2013). Numerical partial differential equations: finite difference methods (Vol. 22). Springer Science & Business Media.

[8] Zill, D. G., & Cullen, M. R. (2009). Differential equations with boundary-value problems. 7thEdn. United States: Brooks/Cole.

[9] Zill, D. G., Cullen, M. R., & Wright, W. S. (1997). Differential Equations with Boundary-Value Problems, Brooks.